

**e-ISSN : 2320-0847**  
**p-ISSN : 2320-0936**



# **American Journal of Engineering Research (AJER)**

**Volume 4 Issue 11– November 2015**

**[www.ajer.org](http://www.ajer.org)**

**[ajer.research@gmail.com](mailto:ajer.research@gmail.com)**

## Editorial Board

### American Journal of Engineering Research (AJER)

**Dr. Moinuddin Sarker,**

Qualification :PhD, MCIC, FICER,  
MInstP, MRSC (P), VP of R & D  
Affiliation : Head of Science / Technology  
Team, Corporate Officer (CO)  
Natural State Research, Inc.  
37 Brown House Road (2nd Floor)  
Stamford, CT-06902, USA.

**Dr. Jonathan Okeke  
Chimakonam**

Qualification: PHD  
Affiliation: University of Calabar  
Specialization: Logic, Philosophy of  
Maths and African Science,  
Country: Nigeria

**Dr. ABDUL KAREEM**

Qualification: MBBS, DMRD, FCIP, FAGE  
Affiliation: UNIVERSITI SAINS Malaysia  
Country: Malaysia

**Dr. sukhmander singh**

Qualification: Phd  
Affiliation: Indian Institute Of  
Technology, Delhi  
Specialization : PLASMA PHYSICS  
Country: India

**Dr. Nwachukwu Eugene Nnamdi**

Qualification: Phd  
Affiliation: Michael Okpara University of  
Agriculture, Umudike, Nigeria  
Specialization: Animal Genetics and  
Breeding  
Country: Nigeria

**Dr. June II A. Kiblasan**

Qualification : Phd  
Specialization: Management, applied  
sciences  
Country: PHILIPPINES

**Dr. Narendra Kumar Sharma**

Qualification: PHD  
Affiliation: Defence Institute of Physiology  
and Allied Science, DRDO  
Specialization: Proteomics, Molecular  
biology, hypoxia  
Country: India

**Prof. Dr. Shafique Ahmed Arain**

Qualification: Postdoc fellow, Phd  
Affiliation: Shah abdul Latif University  
Khairpur (Mirs),  
Specialization: Polymer science  
Country: Pakistan

**Dr. Alcides Chaux**

Qualification: MD  
Affiliation: Norte University, Paraguay,  
South America  
Specialization: Genitourinary Tumors  
Country: Paraguay, South America

**Dr. Md. Nazrul Islam Mondal**

Qualification: Phd  
Affiliation: Rajshahi University,  
Bangladesh  
Specialization: Health and Epidemiology  
Country: Bangladesh

<b>S.No.</b>	<b>Manuscript Title</b>	<b>Page No.</b>
<b>01.</b>	Design Analysis of a Locally Fabricated Palm Kernel Shells Grinding Machine F. I. Apeh    B. S. Yahaya    F. Achema    M. O. Fabiyi    E. S. Apeh	01-07
<b>02.</b>	Mechanical and Microstructural Properties of TiO <sub>2</sub> doped Zirconia Toughened Alumina (ZTA) Ceramic Composites at different TiO <sub>2</sub> contents Sajib Aninda Dhar    Shoumya Nandy Shuvo    A.K.M.B. Rashid	08-12
<b>03.</b>	Optimization of the Production Mixture of Selected Raw Material for Plastic Production: A Case Study of Louis Carter Plastic Manufacturing Industry Okolie Paul Chukwulozie    Chukwuneke Jeremaih Lekwuwa    Okoli Ndubuisi Celestine   Azaka Onyemazuwa Andrew	13-25
<b>04.</b>	Currency Recognition System Using Image Processing S. M. Saifullah    AnikaRahmanAnanna    Md. Shakhawat Hossain    Md. Jaouad Hossain   Md. SaniatRahman Zishan	26-32
<b>05.</b>	Effects of Waste Glass (WG) on the Strength Characteristics of Cement Stabilized Expansive Soil I.A.Ikara    A.M.Kundiri    A.Mohammed	33-41
<b>06.</b>	Studies on Shelf-Life of Six Promising Mango (Mangiferindica L.) Cultivars under Favorable Condition K. Venkat Reddy	42-46
<b>07.</b>	Mechanical Behaviour and Microstructural Characterization of Carbon Steel Samples from Three Selected Steel Rolling Plants P. O. Atanda    A. A. Abioye    A. O. Iyiola	47-56
<b>08.</b>	Measurement of the viscosities of He, Ne and Ar for the determination of their gas – kinetic diameters. P.N. Ekemezie    E.E. Enekeuchi    Odinma S.C	57-62
<b>09.</b>	Development and Application of Geneva Mechanism for Bottle Washing. Ujam, A. J    Ejeogo, G    Onyeneho, K. C	63-73
<b>10.</b>	Transport and Mechanical Characteristics of Corrosion-Inhibited High- Strength Self-Compacting Concrete Marva Blankson    Savaş Erdem    Ezgi Gürbüz	74-78
<b>11.</b>	Design and Simulation of a Banking Network System Abdul Hannan   M.A.Jobayer Bin Bakkre    Rajib Chandra Ray    Md.Selim Hossain	79-91
<b>12.</b>	An Intelligent Line Follower Using Ldr Sensor Abdul Hannan    M.A. Jobayer Bin Bakkre    Md. Selim Hossain    Rajib Chandra Ray	92-102

## CONTENTS

13.	Cultivating Technological Innovation in the Mind PROF ANYATA BENEDICT U.    AKPAN PAUL P.    UNEKE LOUIS A.	103-108
14.	Comparative Study of Path Loss Models for Wireless Communication in Urban and Sub-urban Environment for Port Harcourt, Nigeria Akujobi Ekeocha    Nosiri Onyebuchi    Achumba Ifenyinwa	109-115
15.	Hybridised Single-Phase Cascaded Multilevel Inverter Topology Using Reduced Number of Power Switches G. C. Diyoke    O. A. Nwaorgu    I. K. Onwuka	116-127
16.	Minimizing Corona on Power Distribution Lines Using Optimization by Graphical Method Osita Oputa	128-134
17.	Sequential Extraction Analysis of Cu, Pb, Ni and Zn in Cereals and Soils Mohammed, S.S.    Abdullahi, M.A.    Imam, M. M.	135-139
18.	Assessment of Ni and Cd Bioavailability in soils around selected Automobile Workshops of Kaduna, Nigeria. Mohammed, S.S.    Abdulmalik, I. A.    Yusuf, H.	140-142
19.	Secure SMS Mobile Transaction with Peer to Peer Authentication Design for Mobile Government Mohammad Khalaf Rahim Al-juaifari	143-149
20.	Use of Coke Oven Gas during shutdown period of Direct Reduced Iron Plant for Steam Generation: Experimentation and Optimization Harish C. Dalai    Dr. N.C.Nayak	150-154
21.	Text Detection in Video Using Haar Wavelet Transformation and Morphological Operator Dinesh AnnajiKene    Dr. D. J. Pete	155-162
22.	Strain Based Finite Element for Cylindrical Shell under Sinusoidal Loads A. Mousa    Ahmed E. Al-Juaidi	163-170
23.	A study of propagation path-loss models Nwaokoro Amaka Ann    Emerole Kelechi Chukwunonyerem	171-175
24.	Status and Perceptions of the Application of Building Information Modeling for Improved Building Projects Delivery in Nigeria S.C Ugochukwu    S.C Akabogu    K.C Okolie	176-182



## Design Analysis of a Locally Fabricated Palm Kernel Shells Grinding Machine

F. I. Apeh, B. S. Yahaya, F. Achema, M. O. Fabiyi and E. S. Apeh

Engineering Materials Research Department, Nigerian Building and Road Research Institute, KM 10 Idiroko Road, Ota, Ogun State, Nigeria

**ABSTRACT :** The technological advancement of any nation have been influenced and uplifted by the extent to which it can usefully harness and convert its mineral and local resources into household products and as such, the need to design an implements for their production. Design analysis of a fabricated palm kernel shells grinding machine using locally sourced materials was carried out. The machine was designed and fabricated from locally available materials for grinding palm kernel shell and likely limestone as well as animal bones into small particle size of less  $425\mu\text{m}$  or greater than. The grinding process was achieved by the use of hammers in the grinding chamber with a three phase 75hp motor as prime mover. The design analysis carried out on the palm kernel shells grinding machine showed that the machine has a grinding efficiency of 97.9%, grinding capacity of 625kg/hr., percentage recovery of the material (palm kernel shell) is 92.6% and fineness modulus of 0.39.

**Keywords -** Design Analysis, Fine Particles, Grinding Efficiency, Grinding Machine, Palm Kernel Shell

### I. INTRODUCTION

A grinding machine is a complex mechanism designed to break a solid material into smaller pieces or to the required sizes. There are different types of grinding machines for various materials processing. Historically, grinding mills or grinding machines were powered manually (mortar and pestle), or by using working animal (horse mill), wind (wind mill) or water (water mill), but in the recent time, it is been powered by A.C or D.C power supply. Grinding of solid matters occurs under mechanical forces that trench the structure by overcoming the interior bonding forces. After grinding, the state of the solid is changed; the grain size, the grain size disposition and of which the grain shape are also affected [1].

Palm kernel shells (PKS) are fibrous, tough and hard material that covers the palm nut after the removal of oil rich outer cover. It has been found that, the shell contains some chemical, physical and mechanical properties that make it very useful in some other areas of applications [2]. The ash generated from burning off palm kernel shells has been found to be a good binder when mixed with appropriate ratio to ordinary Portland cement [3]. Palm kernel shells are also used as bio-carbon in water treatment plant [4]. A typical palm kernel shell has the following chemical and physical properties: the chemical properties are; Calcium Oxide (CaO)-8.786%, Silicon Oxide ( $\text{SiO}_2$ )- 54.81%, Potassium Oxide ( $\text{K}_2\text{O}$ )- 6.254%, Magnesium Oxide ( $\text{MgO}$ )-6.108%, Iron oxide ( $\text{Fe}_2\text{O}_3$ ) - 0.362%, Alumina ( $\text{Al}_2\text{O}_3$ )-11.40% and the physical properties are; moisture content - 6.11%, ash content - 8.6%, bulk density{(wet and dry),-  $7.40\text{kg/m}^3$  and -  $9.24\text{kg/m}^3$  respectively}, porosity {(wet and dry) - 28% and - 65% respectively}[5,6]. Palm kernel shell has been found to have a calorific value of 5.2MWh/MT [7]. The desire to design and fabricate PKS grinding machine was borne out of the needs to develop indigenous technological innovation for processing of semi raw materials. The PKS grinding machine was designed for processing or grinding palm kernel shells into the required particle size. The main aim of this work is to grind palm kernel shells so that it can be mixed with clay (powder) during nodulization process for the production of pozzolana cement. During the process, the PKS serves as fuel and subsequently became binder after ball milling. The machine is of hammer mill type of which the hammers are mounted on a shaft in the chamber for the milling operation. The hammers revolve at high speed in the chamber and as the hummers hit the dry shells repeatedly, the materials are reduced to the required particle size. The machine is incorporated with an adjustable separator for possible regulation of the PKS particle size during the operation. It is powered with 75hp electric motor of 1,440 rpm. The design and fabrication of this machine tend to solve and encourage the use of locally available raw materials and boost capacity building in the area of machine construction for their application in relevant field.

## II. METHODOLOGY

### 2.1 Design Analysis

In carrying out the design, all the various components that require proper calculation were considered. Some of these component parts are: the shaft, belt length, hammer's shaft diameter, etc. The main shaft is a rotating component that operates within a cylinder or housing. The speed of the shaft is an important factor that determines the performance of the machine. The shaft speed is derived as shown below:

Let the velocity of belt =  $V$  m/s (1)

Let the velocity of belt at the point of contact with wheel =  $V$  m/s (2)

and the relationship between angular and linear velocity is  $V = \pi ND$  [8] (3)

Since, the velocity is the same on the large pulley and small pulley, then equation (4) below can be derived,

$$\begin{aligned} V_1 &= V_2 \\ \pi N_1 D_1 &= \pi N_2 D_2 \end{aligned} \quad (4)$$

from here, it implies that,

$$\frac{D_1}{D_2} = \frac{N_2}{N_1} \quad (5)$$

where,  $N_1$  = revolution of the smaller pulley (rpm),  $N_2$  = revolution of the larger pulley (rpm),  $D_1$  = diameter of the small pulley (mm),  $D_2$  = diameter of the large pulley (mm). The exact shaft speed is only obtained when there is no slip condition of the belt over the pulley. When slip and creep condition is present, the value of the rotational speed is reduced by 4% [9].

### 2.2 Determination of the Length of the Belt

The combination of pulleys and belts have two uses, that is, to increase or reduce speed or torque or to transfer power from one shaft to another. If the transfer of power is what is required, then two pulleys of the same diameter will do the work, but most of the time, the speed can be increased and or reduce the torque or vice versa. In this design, the speed of the system was increased while the torque reduces. This is done by using pulleys of different diameters. The belts were employed to transfer power through rotational motion from one shaft to another. The centre to centre distance between the large pulley and small pulley used in this design was measured and is equal to 117mm. The length of the desired belt is given by [10], equation (6)

$$L = 2C + 1.57(D_2 + d_1) + \frac{d_1 + D_2}{4C} \quad (6)$$

where,  $L$  = length of the belt, mm,  $C$  = the centre to centre distance between large pulley and the small pulley,  $d_1$  = diameter of the small pulley and  $D_2$  = diameter of large pulley, mm.

**Table 1:** Dimensions of standard V-belts [11]

Types of belt	Power ranges [kw]	Minimum pitch diameter of pulley, D[mm]	Top width, b[mm]	Thickness, t[mm]
A	0.7-3.7	75	13	8
B	2-15	125	17	11
C	7.5-75	200	22	14
D	20-150	355	32	19
E	30-350	500	38	23

### 2.3 Determination of the Belt Contact Angle, ( $\beta$ )

Belt drives depend on friction between itself and the pulley. Excessive friction leads to wastes of energy and rapid wears of the belt [12]. There are some factors that affect belt friction, which include tension, contact angle and the materials used for the production of the belt and pulley. In order to minimize excessive friction in any machine, a smaller belt contact angle is required, because the smaller the belt contact angle the lower the heat generated between the pulleys and the belts. Belt contact angle is given by [12], equation (7):

$$\beta = \sin^{-1} \frac{D-d}{C} \quad (7)$$

where,  $D$  = diameter of the large pulley, mm,  $d$  = diameter of the small pulley, mm, and  $C$  = the centre to centre distance between large pulley and the small pulley, mm

The angles of wrap for the pulleys which is used to determine the governing pulley is given by [8], equation (8) and equation (9):

$$\alpha_1 = 180 - \sin^{-1} \left( \frac{D-d}{C} \right) \quad (8)$$

$$\alpha_2 = 180 + \sin^{-1} \left( \frac{D-d}{C} \right) \quad (9)$$

where,  $\alpha_1$  = angle of wrap for the smaller pulley, degree,  $\alpha_2$  = angle of wrap for the larger pulley, degree.

## 2.4 Determination of the Belt Tension

This is to determine how much load a belt can carry before it slips and this depends on a lot of factors, which have been discussed earlier. The most important among them is the initial tension i.e., the force pulling the pulley(s) toward each other when at rest. When the belt is slack, little initial tension will result in slipping of the belt, and when it is too tight, it will lead to unnecessarily stresses and subsequently wearing the bearings. The belt tension is calculated [13], using equation (10):

$$T_2 = \frac{(T_1 - mv^2)}{\exp\left[\frac{\mu\alpha}{\sin\theta}\right]} \quad (10)$$

where,  $T_1$  = the tension in the tight side of the belt ( $T_1 = SA$ ),  $T_2$  = the tension in the slack side of the belt,  $S$  = the maximum permissible belt stress,  $A$  = area of belt,  $m$  = mass per unit length of belt,  $v$  = linear velocity of the belt ( $mv^2$  = centrifugal force acting on the belt),  $\mu$  = constant = 0.25,  $\alpha$  = angle of wrap, degree,  $\theta = 40^\circ$ .

## 2.5 Determination of the Power been Transmitted to the Shaft, Torque and Elastic Creep

Power transmission is the movement of energy from its place of generation to a location where it is applied to perform a useful work. While Torque is a measure of how much force acting on an object causes that object to rotate. The power transmitted to the shaft is determined by considering the tension in the slack and tight side of the belt and the velocity of the belt.

Let  $T_1$  be the tension in the tight side,  $T_2$  the tension in the slack side and  $V$ , the velocity of the belt in m/s. Power transmission to the shaft is derived by [8], equation (11) which involves mechanical power and is the product of force and velocity [8], so,

$$P = F \times v \quad (11)$$

where,  $P$  = the power,  $F$  = is the force,  $v$  = is the velocity and is equal to  $\pi ND$ ,  $N$  = the number of revolution per minute,  $D$  = the diameter of the pulley.

In the design, there is a force pulling in opposition to the other, hence, the net power transmitted is:

$$P = (T_1 - T_2)v \quad (12)$$

$$P = \pi ND(T_1 - T_2) \quad (13)$$

The presence of friction between pulley and belt causes differential tension in the belt. This differential tension causes the belt to elongate or contract and create a relative motion between the belt and the pulley surface. This relative motion between the belt and the pulley surface is created due to the phenomena known as elastic creep. The belt always has an initial tension when installed over the pulleys. This initial tension is the same throughout the belt length when there is no motion. During rotation of the drive, tight side tension is higher than the initial tension and slack side tension is lower than the initial tension. When the belt enters the driving pulley it is elongated and while it leaves the environment it contracts. The average belt velocity on the driving pulley is slightly lower than the speed of the pulley surface [8].

The equations below express the magnitude of the initial tension in the belt [8]:

$$\text{Tight side elongation} \propto (T_1 - T_i) \quad (14)$$

$$\text{Slack side contraction} \propto (T_i - T_2) \quad (15)$$

where,  $T_i$  is the initial belt tension.

Since belt length remain the same i.e., elongation is the same as the contraction,

$$T_i = \frac{T_1 + T_2}{2} \quad (16)$$

Torque ( $\tau$ ) at the main shaft is calculated by considering the tension in the tight side of the belt ( $T_1$ ), as well as tension in the slack side of the belt ( $T_2$ ) and the radius of the main shaft ( $R$ ) [8], equation (17):

$$\tau = (T_1 - T_2)R \quad (17)$$

The force exerted on the main shaft of the machine is determined by calculating the weight of individual hammers. The weight ( $W_h$ ) of each hammer is calculated by the relation below:

$$W_h = m_h g \quad (18)$$

where,  $m_h$  is the mass of one hammer (kg),  $g$  is constant, that is, acceleration due to gravity ( $10\text{m/s}^2$ ). The total force ( $F_t$ ) to be exerted on the main shaft is calculated by multiplying the weight of each hammer ( $W_h$ ) by the total number of hammers weight, equation (19):

$$F_t = W_\Sigma \times g = 284.2\text{N} \quad (19)$$

where,  $W_\Sigma$  = total weight of the hammers, Kg,  $g$  = acceleration due to gravity ( $10\text{m/s}^2$ ).

## 2.6 Determination of Centrifugal Forces on the Hammers

The centrifugal force ( $F_c$ ) that may be exerted by the hammers on the main shaft of the machine is determined by considering the mass ( $m$ ) of the main shaft, radius of the main shaft ( $r$ ) and the velocity ( $v$ ) of the main shaft, equation (20):

$$F_c = \frac{mv^2}{r} \quad (20)$$

## 2.7 Determination of the Hammer Shaft Diameter

In order to come up with the shaft diameter the bending moment needed to be considered. The bending moment ( $m_b(max)$ ) on the shaft is given by [14], equation (21):

$$m_b(max) = \frac{wl^2}{8} \quad (21)$$

Since the bending moment ( $m_b$ ) of a beam is a measure of the strength of such beam, it hence depends upon the loading and resultant reactions ( $l/y\mu a\theta$ ) [14], the allowable stress ( $\sigma_s$ ) of a beam is equal to:

$$\sigma_{s(allowable)} = \frac{m_b Y_{max}}{I} \quad (22)$$

$$Z = \text{section modulus of the beam} = \frac{I}{Y_{max}},$$

therefore,

$$\sigma_{s(allowable)} = \frac{m_b}{Z} \quad (23)$$

where  $Y_{max}$  = distance from neutral axis to outer fibers,  $I$  = moment of inertia,  $Z$  = Section modulus,  $m_b$  = bending moment. For a solid round bar  $I$  and  $Z$  is given as [12]:

$$I = \frac{\pi d^4}{64} \quad (24)$$

and

$$Z = \frac{\pi d^3}{32} \quad (25)$$

The schematic diagram of the PKS grinding machine is as shown in Figure 1 below.

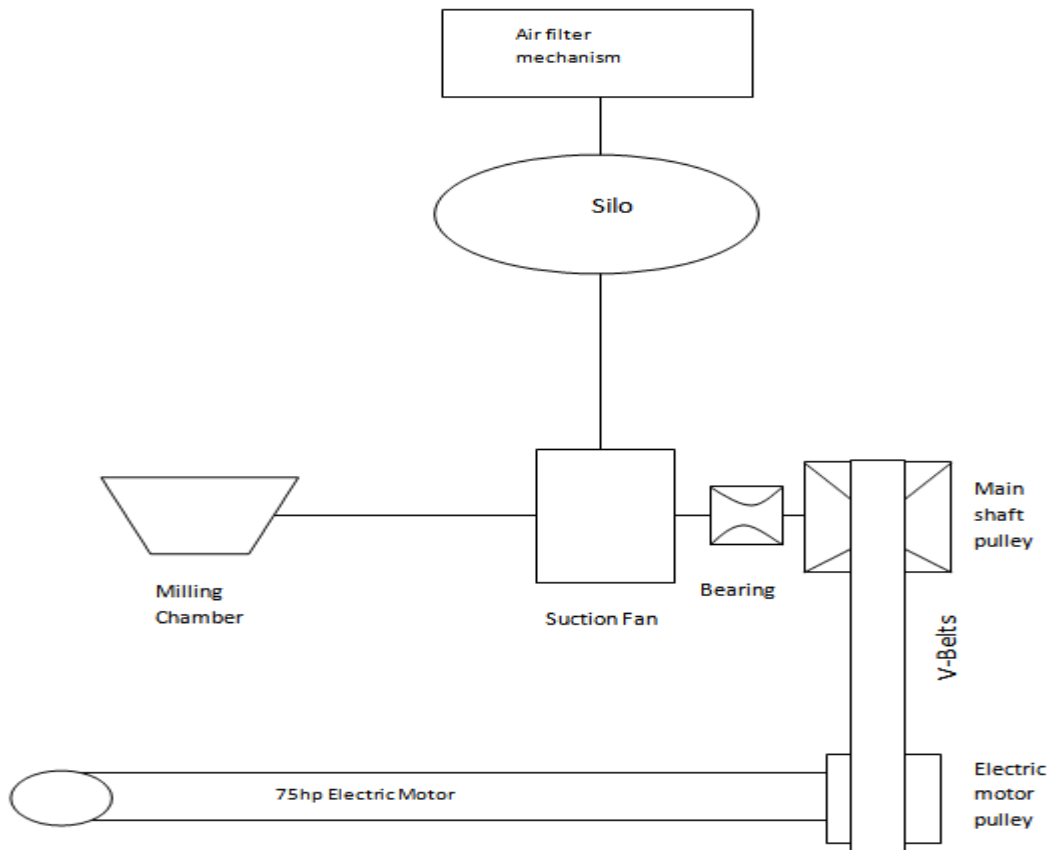


Figure 1: Schematic Diagram of the Fabricated PKS Grinding Machine



## 2.8 Determination of the main Shaft Diameter

The American Society of Mechanical Engineers (ASME) code equation for a solid shaft having little or no axial loading is [10]:

$$d^3 = \frac{16}{\pi \sigma_s} \sqrt{(K_b m_b)^2 + (K_t m_t)^2} \quad (26)$$

where,  $d$  = diameter of shaft,  $\sigma_s$  = allowable stress (55MN/m<sup>2</sup> for shaft without keyway and 40MN/m<sup>2</sup> for shaft with keyway),  $K_b$  = factor for gradually applied load = 1.5,  $K_t$  = factor for suddenly applied load = 1.5. The result of the calculations are tabulated in Table 2

## 2.9 Construction Details of the Major Parts

**Main Shaft:** A 100 mm diameter x 480 mm length rod of tool steel was used for the shaft. The shaft was faced and center drilled which was stepped turned to 90 and 80 mm at the hammer side and 90mm, 80mm and 70mm at the suction fan side. The keyway was milled out using milling machine.

**Beater Shaft:** 15 mm diameter rod was cut, faced and turned to 12 mm diameter. The length of the shaft used was 70 mm.

**Hammer:** 20 numbers of spring steel hammers were cut into 280mm by 108mm. A hole of 40 mm was drilled at the bottom of each hammer, using twist drill to enable it fit into the hammer shaft.

**Hopper:** It is pyramidal in shape and it was made from a mild steel sheet of 1.5mm thick plate. It was dimensioned 204 x 204 mm top opening, 50 x 50 mm base opening and height 240 mm. The plate was marked and cut to sizes and then welded together using arc welding.

**Grinding Chamber:** A 10mm thick mild steel cylindrical drum of 1000mm by 800mm was cut into two of equal halves. The base layer of the cylindrical drum was lined with 10mm thick mild steel sheet while 8mm thick mild steel sheet was used to lined the upper layer of the chamber. Hinges and bolts brackets were welded to the edge of the upper and base layer of the cylinder drum to form the grinding chamber. The chamber houses the hammers, hammer shaft, suction fan, separator, and the main shaft.

## 2.10 Testing

Testing is a vital step in the process of machine development after the design and construction and this is necessary in order to:

- determine the performance of the machine;
- expose defect and area of possible improvement; and
- appreciate the level of success in the research carry out.

The resultant of the above is to determine the workability and efficiency of the machine.

## 2.11 Testing of Palm Kernel Shell Grinding Machine

In carrying out the test, the machine was on and allowed to operate for few minutes before loading in the dry PKS (50kg) through the hopper. The grinding time was noted and recorded. This operation was repeated for three times and the average was used for the calculation. After the testing, the machine was used for continuous loading and the materials grinded and sucked into the silos prior to discharging.

# III. RESULTS AND DISCUSSION

## 3.1 Results

The result of the calculations made and performance analysis carried out on the machine is shown in Table 2 and Table 3 below.

**Table 2:** Calculated Parameters

Parameters	Symbol	Value	Unit
Shaft Speed	$N_2$	1800	Rpm
Length of Belt	$L$	800	Mm
Belt Velocity	$V_b$	15.07	m/s
Belt Contact Angle	$B$	19.99	Degree
Angle of wrap for smaller pulley	$\alpha_1$	160.01	Degree
Angle of wrap for larger pulley	$\alpha_2$	199.99	Degree
Tension in the slack side of belt	$T_2$	1183.34	N
Tension in the tight side of belt	$T_1$	4895.05	N
Initial Tension of the Belt	$T_i$	3039.20	N
Torque at the hammer shaft	$\tau_h$	296.88	Nm

Torque at the main shaft	$\tau_m$	371.17	Nm
Power transmitted to the shaft	P	55935.47	W
Weight of hammer	$W_h$	14.21	N
Centrifugal force exerted by the hammer	C.F	3710.71	N
Diameter of hammer shaft	d	12	mm
Diameter of main shaft	D	200	mm

**Table 3:** Performance Result of the PKS Machine

Test	Quantity (Kg)	Obtained (Kg)	Product	Loss	Percentage Recovery (%)	Percentage Loss (%)
1	50	48.25		1.75	96.5	3.5
2	50	47.70		2.30	95.4	4.6
3	50	48.30		1.70	96.6	3.4

$$\text{Average Percentage Recovery} = \frac{96.5+95.4+96.6}{3} = 96.2 \% \quad (27)$$

### 3.2 Discussions

In this project, a PKS grinding machine was design and fabricated with an adjustable separator for easy control of grain size. The test results show that, the fabricated PKS grinding machine has satisfactory performance in productivity, the grinded materials has low product temperature, which is very good for feed quality.

To select the right type of belt after the required belt length has been determined; power range, minimum pitch diameter, top width and thickness of the pulley were considered. V-belts were considered based on the calculation and that, they transfer torque effectively notwithstanding that they loose a bit of speed as the belt stretches under load. From Table 1, a standard V-belt of designation C115 was selected based on the power range.

From Table 2, it was observed that the value of  $T_1$  is greater than that of  $T_2$  which shows that the slack side of the belt is in the upper side and the tight side of the belt is in the lower side, which gives rise to the low value of the belt contact angle as required. Shaft size is dictated by torque but changes in horsepower and speed (RPM) affect torque [15] and this explains the variation between the value of the main shaft and the hammer shaft with their respective torque values as shown in Table 2. From the calculation in equations (8 and 9), it was discovered that the figure obtained for the small pulley is smaller, hence it governs the drive. From the expression in equation (16), increase in initial tension will lead to power transmission increase. If initial tension is gradually increased then  $T_1$  will also increase and at the same time  $T_2$  will decrease. Thus, if it happens that  $T_2$  is equal to zero, then  $T_1 = 2T_1$  (16) and from there maximum power transmission will be achieved [8].

It has been observed from the result of the tests that, the grinding efficiency of the machine was found to be 97.7% and production capacity was 625 Kg/hr of the dry PKS. It is clear from the grinding capacity and efficiency as enumerated above that, the performance of the machine is excellent. The average percentage recovery was 96.2%. The loss in the materials grinded as obtained from the original quantity fed into the machine was due to the sticking of the powdery materials to the wall of the grinding chamber and escape of powdery materials through some tiny holes along the line of discharge during production.

## IV. CONCLUSION

The design and fabrication of palm kernel shell grinding machine was based on the need to develop indigenous technology for processing of raw materials. Detailed calculations made and the use of locally available raw materials for the fabrication of the machine has significant technological benefit. From the design consideration and analysis; reliability, safety, serviceability and cost of construction were given due consideration. From the design analysis on the fabricated palm kernel shell grinding machine the following can be established:

- Grinding Efficiency = 97.7%;
- Grinding Capacity = 625 Kg/hr; and
- Percentage Recovery = 96.2%.

The adjustable separator screen attached to the suction outlet gives room for sizing of the various grain sizes needed for different production purposes and based on the above, the design analysis was successful carried out.

## REFERENCES

- [1] [Http://en.wikipedia.org/wiki/Crusher](http://en.wikipedia.org/wiki/Crusher), accessed on the 14/4/ 2014.
- [2] Omange G. N., Palm kernel shells as road building materials, *Technical Transactions of the Nigerian Society of Engineers*, 36(1), pp. 17-25. 2001
- [3] Uviasah M. O., *Properties of Palm kernel shells and Fibre as aggregates for making concrete*, Unpublished Bachelor of Engineering Thesis, Department of Civil Engineering, University of Benin, Benin, Nigeria. 1976
- [4] Neville A. M., *Properties of concrete* (Pearson Education, Asia Pte Ltd, Edingburg, Scotland, 1995) pp. 108-176.
- [5] Akpe, E., *Characteristics Strength of Concrete using Palm kernel shells as light weight aggregate*, Unpublished Technical Report, Department of Civil Engineering, Edo State University, Ekpoma, Nigeria. 1997
- [6] Festus A. Olutoge, Habeeb A. Quadri, and Oladipupo S. Olafusi, Investigation of the Strength Properties of Palm Kernel Shell Ash Concrete, *ETASR - Engineering, Technology & Applied Science Research Vol. 2, No. 6*, 2012, pp315-319.
- [7] Dagwa, I. M, and Ibhadode, A. O, Some physical and Mechanical properties of palm kernel shell (PKS), *Botswana Journal of Technology, Vol. 17, No. 2*, 2008, pp 10-16.
- [8] Khurmi, R.S. and Gupta J. K., *Text book on Machine Design* (Eurasia Publishing House, New Delhi. 2008)
- [9] Spolt, M. F., *Design of Machines Element* (6<sup>th</sup> ed. Prentice Hall, New Delhi, India. 1988)
- [10] John, H., and Stephens, R. C., *Mechanic of Machines* (4<sup>th</sup> ed., 24, Edward, London, England, 1984)
- [11] Khurmi, R. S. and Gupta, J. K., *Shaft, V-belt and Rope Drives: A Textbook of Machine Design*. 13<sup>th</sup> Edition. (S. Chand and Co. Ltd., New Delhi, 2004) pp: 456-498, 657-659.
- [12] Jimoh, M. O. and Olukunle, O. J., Design of an effective automated machine for quality palm kernel production, *IOSR Journal of Mechanical and Civil Engineering (IOSR-JMCE) e-ISSN: 2278-1684 Volume 6, Issue 1*, 2013, PP 89-97.
- [13] Maitra, G. M., and Prasad, L.V., *Handbook of Mechanical Design* (McGraw Hill, New Delhi, India, 1985) pp. 89-108.
- [14] Ryder, G. H, *Strength of Material* (3<sup>rd</sup> ed. Catalogue 300E/EB 666, SKF General Catalogue Macmillan, New York, USA. 1969)
- [15] <http://www.pumpsandsystems.com/topics/motors/relationship-torque-and-shaft-size-0#sthash.5us0UciZ.dpuf>, accessed on the 13/3/ 2015.

## Mechanical and Microstructural Properties of TiO<sub>2</sub> doped Zirconia Toughened Alumina (ZTA) Ceramic Composites at different TiO<sub>2</sub> contents

Sajib Aninda Dhar, Shoumya Nandy Shuvo, A.K.M.B. Rashid

*Department of Materials and Metallurgical Engineering*

*Bangladesh University of Engineering and Technology (BUET), Dhaka-1000, Bangladesh*

**ABSTRACT:** Zirconia-Toughened Alumina (ZTA) is a glistening name for new generation of toughened ceramics for the past decade. In this experiment, microstructural and mechanical properties of ZTA ceramic were modified with TiO<sub>2</sub> as an additive which were constructed using a solid-sintering route. For various weight percents of TiO<sub>2</sub> (i.e. 0 wt%, 2 wt%, 3wt%, 4 wt%, 6 wt% and 8 wt%), corresponding constructed samples were dry mixed, uniaxially pressed and sintered at 1600°C for 1 hour in a pressureless condition. Properties like density, porosity, flexural strength, fracture toughness and Vickers hardness were measured for each sample. The grain growth was observed by using Scanning Electron Microscope (SEM). It was found that the flexural strength, fracture toughness and hardness have gradually increased with TiO<sub>2</sub> additions, reaching its maximum value at 4 wt.% and then decreased upon further addition of TiO<sub>2</sub>. Scanning Electron Microscopy showed that the grain growth of Al<sub>2</sub>O<sub>3</sub> was hindered significantly with the addition of 4 wt% TiO<sub>2</sub>, but increased in size with further addition of TiO<sub>2</sub>. Hardness and bulk density have also improved from 0wt% to 4wt% due to the fine microstructure, thus enhancing its properties.

**Keywords:** Fracture toughness, ZTA, TiO<sub>2</sub>, sintering, microstructure, Flexural Strength

### I. Introduction

Ceramics, the wonder materials are becoming an essential part of today's materials due to the advantages such as low density, strength, hardness and its inertness at high temperature [1]. They are extensively used as materials in making aircraft structures, electronic packaging to medical equipment, and space vehicle to home building. Regardless of their advantages, ceramic materials exhibit very low toughness which eventually limits their overall applications [2–6]. The challenge of increasing the toughness of ceramic based materials has been a key motivation in the field of ceramic research [6–8]. In this pursuit of improving toughness, Al<sub>2</sub>O<sub>3</sub> based materials are often used as the benchmark due to its abundance, relative cheapness and excellent mechanical properties [9–11]. The introduction of the yttria stabilized zirconia (YSZ) toughening agent further increased the toughness of the zirconia toughened alumina (ZTA) ceramic composite [12]. Additionally, the use of additives was also introduced to reduce the sintering temperature, customise the microstructure as well as improve the product properties. It has been reported that the addition of TiO<sub>2</sub> promotes the sintering and grain growth of Al<sub>2</sub>O<sub>3</sub> [13–15]. This advantage has been considered to be a result of the enhanced diffusivity due to the increasing concentration of the Al<sup>3+</sup> vacancies which is generated by the Ti<sup>4+</sup> substituting for Al<sup>3+</sup>. As the quantity of additive approaches 0.15 – 0.35 mol%, i.e. the solubility limit, a further increase in the densification rate and grain growth can be observed. Nevertheless, beyond its solubility limit, the contrary trend of decreasing densification and grain growth may be due to the pinning effect at the grain boundaries of the second phase, Al<sub>2</sub>TiO<sub>5</sub> [15]. The grain growth of the Al<sub>2</sub>O<sub>3</sub> and ZTA is encouraged by TiO<sub>2</sub> which is an important sintering additive, bringing about a completely dense and finer homogeneous structure. The authors' previous works investigated MgO, Cr<sub>2</sub>O<sub>3</sub>, CeO<sub>2</sub> and CaCO<sub>3</sub> for improving the mechanical properties of ZTA without diminishing properties of ZTA [3–6,16,17]. The current research has been done to understand the role of TiO<sub>2</sub> in ZTA ceramic composites. The amounts of TiO<sub>2</sub> were varied from 0 wt % to 8 wt % with fixed amount of ZTA as the matrix. Hence, this study aims to investigate the mechanical and microstructural properties of TiO<sub>2</sub> doped Zirconia Toughened Alumina (ZTA) Ceramic Composites.



## II. Methodology

The raw materials used for this research were  $\text{Al}_2\text{O}_3$  (Martinswerk, 99% purity), YSZ (Goodfellow, 5.4 mole%  $\text{Y}_2\text{O}_3$  as stabilizer, >96% purity) and Anatase- $\text{TiO}_2$  (Fluka, 99% purity, grain size: < 25nm). The initial mixture was 80 wt%  $\text{Al}_2\text{O}_3$  and 20 wt% YSZ and was mixed with different amounts of  $\text{TiO}_2$ , whilst maintaining the ratio of  $\text{Al}_2\text{O}_3$  to YSZ at 4:1. The mixtures were wet mixed using Ball Mixer Mill with  $\text{ZrO}_2$  balls. The slurry was then dried for 24 h at  $100^\circ\text{C}$  in an Electrotherm oven, following which the dried cake was crushed and passed through a  $100\ \mu\text{m}$  sieve. The powders were then hydraulically pressed at 250 MPa for 120 sec into pellets of 14 mm diameter and 4 mm thickness without binder. The pellets were sintered at  $1600^\circ\text{C}$  for 1 hour at a heating rate of  $5^\circ\text{C}/\text{minute}$  in a pressureless condition.

Flexural strength of the samples were measured using three point bend test, where the dimensions of the samples were  $50\text{mm} \times 30\text{mm} \times 25\text{mm}$ , keeping span length of 40mm and crosshead speed of 1mm/min. To measure the Vickers hardness and fracture toughness of the sintered samples, the Vickers indentation technique was used. With the *Hardness Tester Mitutoyo-model HV-114*, the Vickers hardness was measured by taking the average of five different readings for each sample. The polished sintered samples were subjected to HV 30 kgf for 15 sec while the bulk density of the samples were calculated based on the Archimedes principle.

A Field Emission Scanning Electron Microscope (FE SEM) was used to observe microstructures of the samples and their grain growth. The electrical conductivities of all test samples used in this research project were usually poor. To avoid this, the surfaces of all samples were coated by gold sputtering technique. The samples were bonded with conductive carbon tape on an aluminium stub. Then the stub and surface was further connected with highly conductive copper foil. For SEM analysis, 5 kV accelerating voltage was used. Under FE-SEM, various grain growths were observed and they were photographed.

## III. Result and Discussion

Figure 1 shows the flexural strength of ZTA- $\text{TiO}_2$  ceramic composite with different  $\text{TiO}_2$  contents. As shown in the bar chart, flexural strength gradually increases from 519.3 MPa (0 wt%) to 891.8 MPa (4 wt%), where flexural strength is the highest, and then decreases with further addition of  $\text{TiO}_2$  content. This increase in flexural strength may be attributed to the fact that  $\text{TiO}_2$  increases the pinning effect in the microstructure, therefore increasing the amount of stress required to bend the samples to rupture, and also due to the refinement of microstructure as shown in figure 2(d).

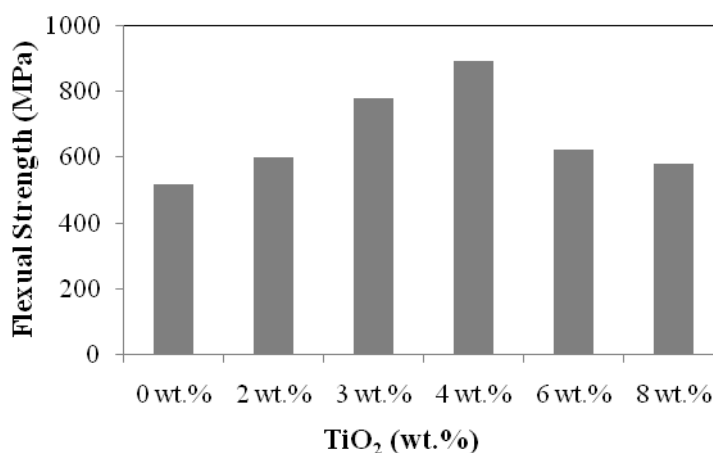


Fig. 1: Flexural strength of ZTA- $\text{TiO}_2$  ceramic composite with different  $\text{TiO}_2$  contents.

Figures 2(a), 2(b), 2(c), 2(d), 2(e) and 2(f) show the Scanning Electron Microscope images of ZTA- $\text{TiO}_2$  ceramic composite samples with 0wt.%, 2wt.%, 3wt.%, 4wt.%, 6wt.% and 8wt.%  $\text{TiO}_2$  respectively. According to the micrographs, it can be clearly observed that  $\text{TiO}_2$  has influenced the grain growth of the ZTA- $\text{TiO}_2$  ceramic composites. The figures illustrate that as  $\text{TiO}_2$  content was increased grain growth was hindered and at 4 wt.%  $\text{TiO}_2$  grain size and grain growth was minimum, therefore successfully refining the microstructure. This observation also supports the fact that at 4wt.%  $\text{TiO}_2$ , flexural strength of the composite is maximum as shown in figure 1. Upon further addition, excess  $\text{TiO}_2$  was no longer able to prevent the grain growth of the composites. According to Manshor *et al.* [18], excess  $\text{TiO}_2$  will start to react with  $\text{Al}_2\text{O}_3$  and form  $\text{Al}_2\text{TiO}_5$  which in turn increases the grain size of the ZTA- $\text{TiO}_2$  ceramic composites.

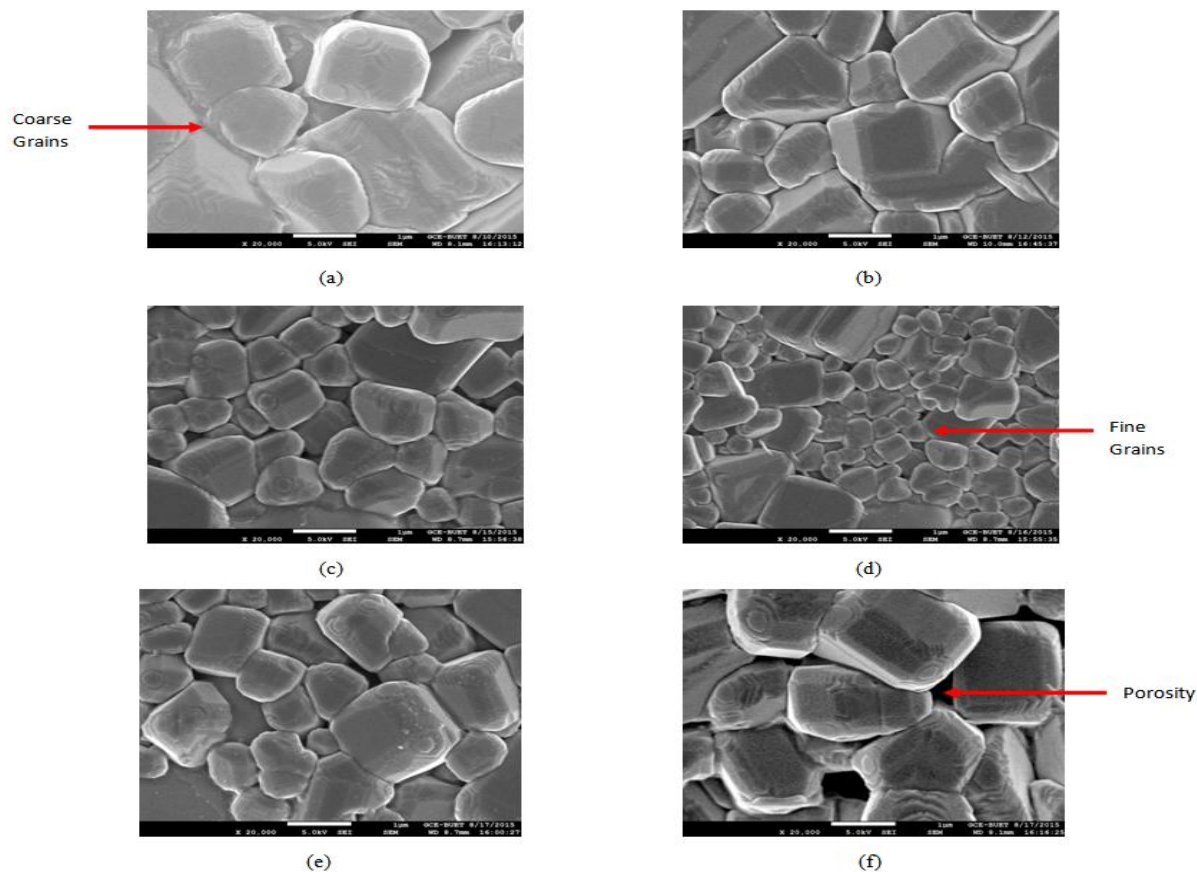


Fig. 2(a): SEM image of ZTA-TiO<sub>2</sub> ceramic composite with 0 wt.% TiO<sub>2</sub>.  
 Fig. 2(b): SEM image of ZTA-TiO<sub>2</sub> ceramic composite with 2 wt.% TiO<sub>2</sub>.  
 Fig. 2(c): SEM image of ZTA-TiO<sub>2</sub> ceramic composite with 3 wt.% TiO<sub>2</sub>.  
 Fig. 2(d): SEM image of ZTA-TiO<sub>2</sub> ceramic composite with 4 wt.% TiO<sub>2</sub>.  
 Fig. 2(e): SEM image of ZTA-TiO<sub>2</sub> ceramic composite with 6 wt.% TiO<sub>2</sub>.  
 Fig. 2(f): SEM image of ZTA-TiO<sub>2</sub> ceramic composite with 8 wt.% TiO<sub>2</sub>.

Figure 3 presents the results of Vickers hardness for ZTA-TiO<sub>2</sub> ceramic composite with different TiO<sub>2</sub> contents. Vickers hardness was observed to gradually increase from 1503 HV (0 wt% TiO<sub>2</sub>) to 1610 HV (4 wt% TiO<sub>2</sub>), indicating an improvement of approximately 7 %. The results of Vickers hardness are directly related to the results of the bulk density, as shown in figure 4. The highest value of Vickers hardness, 1610 HV (4 wt% TiO<sub>2</sub>), also coincides with the highest density value (4.18 g/cm<sup>3</sup>). The increase in hardness with the increasing TiO<sub>2</sub> content is attributed to an increase in densification. The Vickers hardness and bulk density both decrease with further addition of TiO<sub>2</sub>. This is believed to be due to the presence of the secondary phase i.e. Al<sub>2</sub>TiO<sub>5</sub> as indicated by Manshor *et al.* [18].

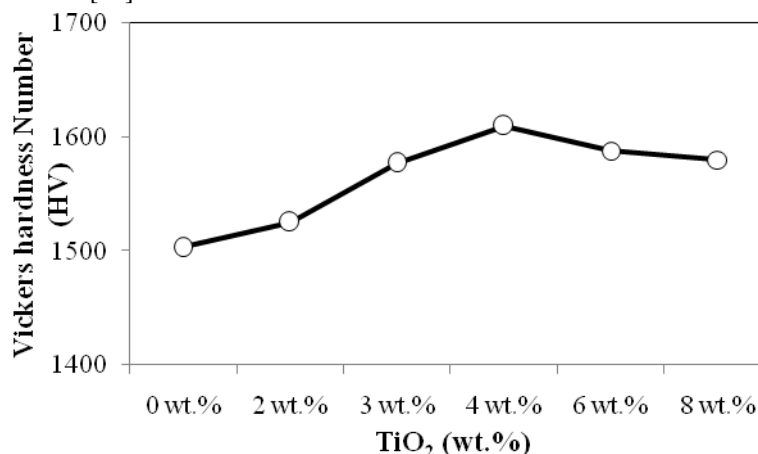


Fig. 3: Vickers hardness of ZTA-TiO<sub>2</sub> ceramic composite with different TiO<sub>2</sub> contents.

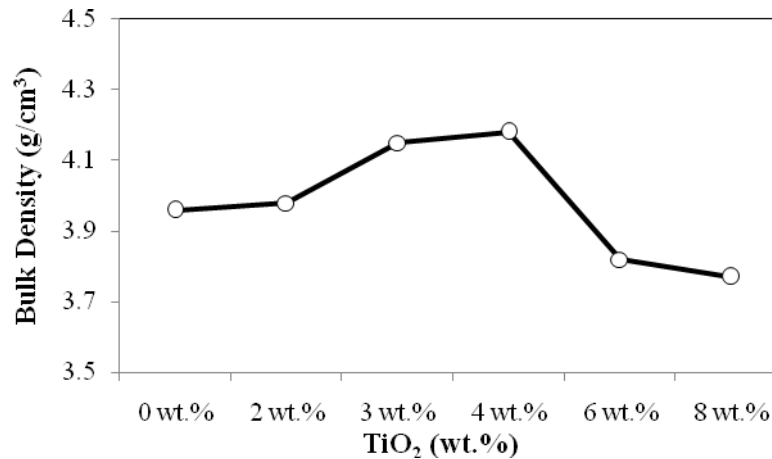


Fig. 4: Bulk Density of ZTA-TiO<sub>2</sub> ceramic composite with different TiO<sub>2</sub> contents.

Figure 5 shows the results of the fracture toughness for ZTA- TiO<sub>2</sub> ceramic composite. The fracture toughness gradually increased from 5.46 MPa.m<sup>1/2</sup> (0 wt% TiO<sub>2</sub>) to 5.81 MPa.m<sup>1/2</sup> (4 wt% TiO<sub>2</sub>), and then only had a minor increment after further addition of TiO<sub>2</sub>.

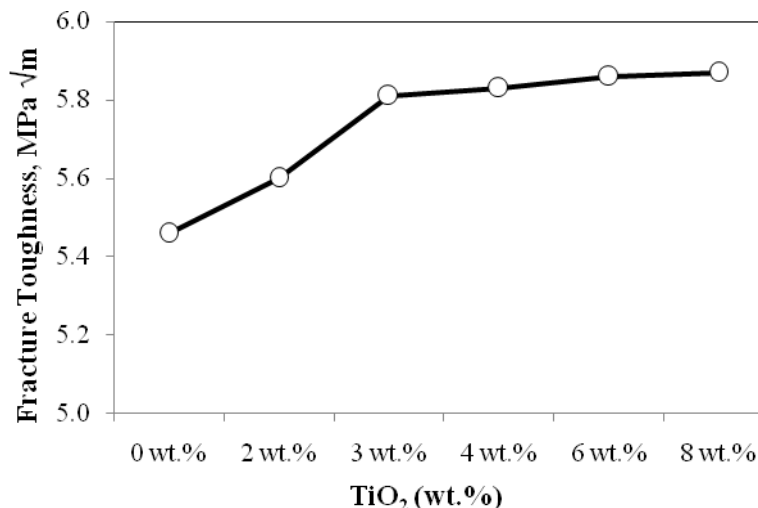


Fig. 5: Fracture toughness of ZTA-TiO<sub>2</sub> ceramic composite with different TiO<sub>2</sub> contents.

According to Wang *et al.*, [15], the TiO<sub>2</sub> addition to the ultrafine Al<sub>2</sub>O<sub>3</sub> demonstrated that the toughness was reliant on the Al<sub>2</sub>O<sub>3</sub> grain size, whereby the toughness raised from 4.4 to 5.2 MPa.m<sup>1/2</sup> as grain size increased from 0.6 to 2.44 μm due to the effect of TiO<sub>2</sub> additive.

#### IV. Conclusion

This experiment demonstrates the effects of TiO<sub>2</sub> particles on the mechanical and microstructural properties of ZTA-TiO<sub>2</sub> ceramic composites. The flexural strength of the composite was found to gradually increase when TiO<sub>2</sub> was added from 0 wt.% to 4 wt.%, reaching the maximum flexural strength at 4 wt.%, and then declines with further addition of TiO<sub>2</sub>. According to the Scanning Electron Micrographs, grain growth is hindered maximum at 4 wt.% TiO<sub>2</sub>, and grain size increases when TiO<sub>2</sub> content is greater than 4 wt.%, which is thought to be due to the formation of a secondary phase Al<sub>2</sub>TiO<sub>5</sub>. Hardness and bulk density were found to be the highest at 4 wt.% TiO<sub>2</sub>, whereas fracture toughness tend to gradually increase from 0 wt.% TiO<sub>2</sub> to 4 wt.% TiO<sub>2</sub> and then shows no significant increase or decrease upon further addition.

#### Reference

- [1] Y. Ye, J. Li, H. Zhou, J. Chen, Microstructure and mechanical properties of yttrium-stabilized ZrO<sub>2</sub>/Al<sub>2</sub>O<sub>3</sub> nanocomposite ceramics, *Ceram. Int.* 34 (2008) 1797–1803. doi:10.1016/j.ceramint.2007.06.005.
- [2] A.Z.A. Azhar, M.M. Ratnam, Z.A. Ahmad, Effect of Al<sub>2</sub>O<sub>3</sub>/YSZ microstructures on wear and mechanical properties of cutting inserts, *J. Alloys Compd.* 478 (2009) 608– 614. doi:10.1016/j.jallcom.2008.11.156.

- [3] G. Magnani, A. Brillante, Effect of the composition and sintering process on mechanical properties and residual stresses in zirconia–alumina composites, *J. Eur. Ceram. Soc.* 25 (2005) 3383–3392. doi:10.1016/j.jeurceramsoc.2004.09.025.
- [4] N.A. Rejab, A.Z.A. Azhar, M.M. Ratnam, Z.A. Ahmad, The effects of CeO<sub>2</sub> addition on the physical, microstructural and mechanical properties of yttria stabilized zirconia toughened alumina (ZTA), *Int. J. Refract. Met. Hard Mater.* 36 (2012) 162–166. doi:10.1016/j.ijrmhm.2012.08.010.
- [5] Z.D.I. Sktani, A.Z.A. Azhar, M.M. Ratnam, Z.A. Ahmad, The influence of in-situ formation of hibonite on the properties of zirconia toughened alumina (ZTA) composites, *Ceram. Int.* 40 (2014) 6211–6217. doi:10.1016/j.ceramint.2013.11.076.
- [6] A.Z.A. Azhar, L.C. Choong, H. Mohamed, M.M. Ratnam, Z.A. Ahmad, Effects of Cr<sub>2</sub>O<sub>3</sub> addition on the mechanical properties, microstructure and wear performance of zirconia-toughened-alumina (ZTA) cutting inserts, *J. Alloys Compd.* 513 (2012) 91–96. doi:10.1016/j.jallcom.2011.09.092.
- [7] B. Smuk, M. Szutkowska, J. Walter, Alumina ceramics with partially stabilized zirconia for cutting tools, *J. Mater. Process. Technol.* 133 (2003) 195–198. doi:10.1016/S0924-0136(02)00232-7.
- [8] B. Basu, J. Vleugels, O. Van der Biest, Toughness tailoring of yttria-doped zirconia ceramics, *Mater. Sci. Eng. A.* 380 (2004) 215–221. doi:10.1016/j.msea.2004.03.065.
- [9] D. Wang, N.F. Ismail, N.A. Badarulzaman, Effect of MgO Additive on Microstructure of Al<sub>2</sub>O<sub>3</sub>, *Adv. Mater. Res.* 488–489 (2012) 335–339. doi:10.4028/www.scientific.net/AMR.488-489.335.
- [10] Y. Zu, G. Chen, X. Fu, K. Luo, C. Wang, S. Song, et al., Effects of liquid phases on densification of TiO<sub>2</sub>-doped Al<sub>2</sub>O<sub>3</sub>–ZrO<sub>2</sub> composite ceramics, *Ceram. Int.* 40 (2014) 3989–3993. doi:10.1016/j.ceramint.2013.08.049.
- [11] S. Maitra, S. Das, a. Sen, The role of TiO<sub>2</sub> in the densification of low cement Al<sub>2</sub>O<sub>3</sub>–MgO spinel castable, *Ceram. Int.* 33 (2007) 239–243. doi:10.1016/j.ceramint.2005.09.007.
- [12] C. Ortmann, T. Oberbach, H. Richter, P. Puhlfürß, Preparation and characterization of ZTA bioceramics with and without gradient in composition, *J. Eur. Ceram. Soc.* 32 (2012) 777–785.
- [13] R.D. Bagley, I.B. Cutler, D.L. Johnson, Effect of TiO<sub>2</sub> on Initial Sintering of Al<sub>2</sub>O<sub>3</sub>, *J. Am. Ceram. Soc.* 53 (1970) 136–141. doi:10.1111/j.1151-2916.1970.tb12055.x.
- [14] A. Rittidech, R. Somrit, T. Tunkasiri, Effect of adding Y<sub>2</sub>O<sub>3</sub> on structural and mechanical properties of Al<sub>2</sub>O<sub>3</sub>–ZrO<sub>2</sub> ceramics, *Ceram. Int.* 39 (2013) S433–S436. doi:10.1016/j.ceramint.2012.10.108.
- [15] C.-J. Wang, C.-Y. Huang, Effect of TiO<sub>2</sub> addition on the sintering behavior, hardness and fracture toughness of an ultrafine alumina, *Mater. Sci. Eng. A.* 492 (2008) 306–310. doi:10.1016/j.msea.2008.04.048.
- [16] A.Z.A. Azhar, H. Mohamad, M.M. Ratnam, Z.A. Ahmad, The effects of MgO addition on microstructure, mechanical properties and wear performance of zirconia-toughened alumina cutting inserts, *J. Alloys Compd.* 497 (2010) 316–320. doi:10.1016/j.jallcom.2010.03.054.
- [17] N.A. Rejab, A.Z.A. Azhar, K.S. Kian, M.M. Ratnam, Z.A. Ahmad, Effects of MgO addition on the phase, mechanical properties, and microstructure of zirconia-toughened alumina added with CeO<sub>2</sub> (ZTA–CeO<sub>2</sub>) ceramic composite, *Mater. Sci. Eng. A.* 595 (2014) 18–24. doi:10.1016/j.msea.2013.11.091.
- [18] H. Manshor, S. Md. Aris, A. Z. A. Azhar, E. C. Abdullah, Z. A. Ahmad, Effects of TiO<sub>2</sub> addition on the phase, mechanical properties, and microstructure of zirconia-toughened alumina ceramic composite, *Ceramics International* Volume 41, Issue 3, Part A, April 2015, Pages 3961–3967, doi:10.1016/j.ceramint.2014.11.080.



## Optimization of the Production Mixture of Selected Raw Material for Plastic Production: A Case Study of Louis Carter Plastic Manufacturing Industry

<sup>1</sup>Okolie Paul Chukwulozie\*, <sup>1</sup>Chukwuneke Jeremaih Lekwuwa, <sup>2</sup>Okoli Ndubuisi Celestine, <sup>1</sup>Azaka Onyemazuwa Andrew

<sup>1</sup>Mechanical Engineering Department, Nnamdi Azikiwe University, Awka

<sup>2</sup>Industrial Production Engineering Department, Nnamdi Azikiwe University, Awka

Corresponding Author Email\*- [pc.okolie@unizik.edu.ng](mailto:pc.okolie@unizik.edu.ng)

**Abstract-** Statistical experiment design and analysis tools for the production have being developed specifically for the purpose of optimizing mixes, such as plastic products, in which the final product properties depend on the relative proportions of the components rather than their absolute amounts. Although mixture methods have been used in industries to develop products such as gasoline, metal alloys, detergents and foods, they have seen little application in the plastic industry. This paper describes an analysis in which a statistical mixture design tool called response surface design optimization tool was used to optimize the six mixture components of 25mm waste pipe, in order to obtain the optimal mixture ratio and their corresponding product yield. The results obtained show an optimal mixture ratio of PVC (45442.820), Stabilizer (1514.760), Calcium carbonate (0.0), Steric acid (151.480), Titanium (12.120), and Pigment (1.4079) for 25mm waste pipe. The optimal yield and composite desirability for 25mm waste pipe are 51990kg and 0.99990. The objective of the study from the result above was to reduce the wastage of raw materials, so as to increase the profitability of the final products. In addition, the model in use is recommended to the case company for effective utilisation of their various raw material mixes so as to obtain various optimal solutions of their raw materials mix and their various production yields.

### I. INTRODUCTION

For many manufacturers the task of meeting the ever rising demand and customer expectations and lowering production costs in an environment of more products, more complexity, more choice and competition is placing great stress on the effectiveness of the production mixture ratio of the different chemicals used in the production of their different product and the quantity of the products gotten from the mixture. Organizations have already adopted solutions with varying degree of production mixture ratios, operations executive acknowledged that this mixture ratio does not give an optimum yield as a result of wastes encountered during the production.

Loius carter plastic industry limited is one of the impending plastic industries in Nigeria, the work within the market of different plastic product like extrusion product for both domestic and industrial use, sales of their product carry a sturdy seasonality effect; the peak is during the dry season and the raining season is the period of building inventory. Products are customer correlated, so that no production to inventory occurs without an explicit manufacturing authority from customers. Because of this, it is expedient for the company to know how much number of products is expected to be achieved from a given quantity of raw material mix in order to be able to react to customers' needs as at when needed and hence optimization of the raw material mix.

Taha (1992) exemplified how linear programming was applied to determine the feed mix to maintain a balanced ratio that includes calcium, protein, and fibre in the right proportion by the Ozark Poultry Farm. Kareem and Aderoba (2008) attempted to show the effectiveness of adopting the linear programming model in maintenance and manpower planning using data from a cocoa processing industry in Akure, Ondo State of Nigeria. Their result shows that only four maintenance crew out of the 19 employees are needed in that section to effectively

carry out maintenance jobs in the industry. But in their own contributions, Nedim et al (2002) tried to reveal that risk analysis is necessary in order to maximize resources allocation efficiency and minimize the effects of risk environment. They used data from a sample of a company's products taking risk into account as the objective function. The result proposed that producing 5 units of  $X_1$  generates 36% loss possibility. If decision makers aim risk not to exceed certain limits, then, variances should be used as constraints. The model recommends that producing 3 units of  $X_1$  will decrease the objective function from \$432 to \$287. Benedict et al (2012) in their work Optimized Profit with the Linear Programming Model: A Focus on Golden Plastic Industry Limited, Enugu, Nigeria. They determined the product mix of Golden Plastic Industry Limited, Emene. In the process, they established optimal quantities of the various PVC pipes to be produced within the study period in order to maximize profit. Also the status of the resources and the unit worth of each resource to the objective function were known. Michelle Leung (2009) in his work on Production Scheduling Optimization of a Plastics Compounding Plant with Quality Constraints where the scheduling of parallel production units was considered. A mixed integer program was developed and implemented in GAMS. The model allows that jobs performed on different units may be shifted or resequenced according to the quantity of demand and the product the job performs. Ezeliara et al (2013) in their work Moving Average Analysis of Plastic Production Yield in a Manufacturing Industry states that a close examination of the production pattern and the behavior of the production system based on the data analyses shows that the production industry is organizing production with a clear focus to meet the customers' requirements and stiff competitors in the plastic manufacturing industry. However, greater percentages of the customers are not served as and when due leading to queues and waiting before customers are served. However, the tool developed can help the company to remedy this situation.

This study intends to examine Loius Carter Plastic Industry Limited, to analyse the opportunity of adopting response surface design and its optimization tool in determining the quantity of products to have been produced over a given period of time from a given quantity of raw material mix. It is one of the most important industrial sites in Nigeria because of its strategic location with a cluster of industries. The choice of response surface design and its optimization tool is informed by the ability of the technique to solve problems relating to quantity of products that is to be achieved by a given quantity of raw material mix over a given period of time, and it is in a better position to determine waste over that period of time. The aim of the study is to optimize the production extent of products from a given quantity of raw material mixture over a given period of time, determining the accurate mixture ratio of the respective components of the raw material to be mixed in order to give optimum production. The objective function of this project is to determine the optimal number of products that can be gotten from a given quantity of raw material mix. With this value, the case study company can determine whether or not it has been operating within this optimal range and if not, plan for a way to increase their production yield by reducing waste of their raw material.

## II. RESEARCH METHODOLOGY

### 2.1 Data Collection and Regression Model

The production mixture data of Louis carter Plastic Industry Limited were collected. Regression analysis was used to statistically investigate the relationships between variables. Regression analysis is widely used for prediction and forecasting, where its use has substantial overlap with the field of machine learning. Regression analysis is also used to understand which among the independent variables are related to the dependent variable, and to explore the forms of these relationships. In restricted circumstances, regression analysis can be used to infer causal relationships between the independent and dependent variables. However this can lead to illusions or false relationships, so caution is advisable; (Armstrong et al 2012) for example, correlation does not imply causation.

Many techniques for carrying out regression analysis have been developed. Familiar methods such as linear regression and ordinary least squares regression are parametric, in that the regression function is defined in terms of a finite number of unknown parameters that are estimated from the data.

Nonparametric regression refers to techniques that allow the regression function to lie in a specified set of functions, which may be infinite-dimensional. The performance of regression analysis methods in practice depends on the form of the data generating process, and how it relates to the regression approach being used. Since the true form of the data-generating process is generally not known, regression analysis often depends to some extent on making assumptions about this process. These assumptions are sometimes testable if a sufficient quantity of data is available. Regression models for prediction are often useful even when the assumptions are moderately violated, although they may not perform optimally. However, in many applications, especially with small effects or questions of causality based on observational data, regression methods can give misleading results. (David et al 2005), (Dennis et al 1982).

Regression models involve the following variables: The unknown parameters, denoted as  $\beta$ , which may represent a scalar or a vector.

The independent variables,  $X$ .

The dependent variable,  $Y$ .

In various fields of application, different terminologies are used in place of dependent and independent variables. A regression model relates  $Y$  to a function of  $X$  and  $\beta$ .

$$Y \approx f(X, \beta) \quad (3.1)$$

The approximation is usually formalized as  $E$

$(Y | X) = f(X, \beta)$ . To carry out regression analysis, the form of the function  $f$  must be specified. Sometimes the form of this function is based on knowledge about the relationship between  $Y$  and  $X$  that does not rely on the data. If no such knowledge is available, a flexible or convenient form for  $f$  is chosen.

Assume now that the vector of unknown parameters  $\beta$  is of length  $k$ . In order to perform a regression analysis the user must provide information about the dependent variable  $Y$ : If  $N$  data points of the form  $(Y, X)$  are observed, where  $N < k$ , most classical approaches to regression analysis cannot be performed: since the system of equations defining the regression model is underdetermined, there are not enough data to recover  $\beta$ . If exactly  $N = k$  data points are observed, and the function  $f$  is linear, the equations  $Y = f(X, \beta)$  can be solved exactly rather than approximately. This reduces to solving a set of  $N$  equations with  $N$  unknowns (the elements of  $\beta$ ), which has a unique solution as long as the  $X$  are linearly independent. If  $f$  is nonlinear, a solution may not exist, or many solutions may exist. The most common situation is where  $N > k$  data points are observed. In this case, there is enough information in the data to estimate a unique value for  $\beta$  that best fits the data in some sense, and the regression model when applied to the data can be viewed as an over determined system in  $\beta$ . In the last case, the regression analysis provides the tools for: (i) Finding a solution for unknown parameters  $\beta$  that will, for example, minimize the distance between the measured and predicted values of the dependent variable  $Y$  (also known as method of least squares), and (ii) Under certain statistical assumptions, the regression analysis uses the surplus of information to provide statistical information about the unknown parameters  $\beta$  and predictors predicted values of the dependent variable  $Y$ .

## 2.2 Response Surface Methodology

Response surface methodology is an empirical statistical approach for modeling problems in which several variables influence a response of interest. In RSM, an approximate relation between a single response and multiple variables is modeled as a polynomial equation obtained through regression analysis. The equation is called a response surface and is generally represented graphically on a contour plot for analyzing an optimal solution. Usually, a low-order polynomial in some regions of variables is used (Montgomery 2001). Assume that  $y$  denotes the response and  $x_g$  denotes the variables,  $g = 1, \dots, N$ . When a linear function of variables can effectively model a response, then the response surface is a first-order model, as follows.

$$\hat{y} = \hat{\beta}_0 + \hat{\beta}_1 x_1 + \hat{\beta}_2 x_2 + \dots + \hat{\beta}_N x_N \quad (3.2)$$

where  $\beta_g$  is the regression coefficients,  $g = 1, \dots, N$ .

When specifying curvature of a response surface, a polynomial of a high order is appropriate for the response surface. For instance, a second-order model of the response surface is

$$\hat{y} = \hat{\beta}_0 + \sum_{g=1}^N \hat{\beta}_g x_g + \sum_{g=1}^N \hat{\beta}_{gg} x_g^2 + \sum_{g < f} \sum \hat{\beta}_{gf} x_g x_f \quad (3.3)$$

The fitted response surface is an adequate approximation of the true response function when an appropriate model is selected. Furthermore, model parameters are estimated effectively when proper experimental designs are used to obtain experimental data. Details of experimental designs for fitting response surfaces are found in (Khuri 1987) and Montgomery (Montgomery 2001).

## III. DATA PRESENTATION AND ANALYSIS

**Table 1: Presentation of 2010-2011 Monthly Data on Production Output**

Year	Month	M. Units	25mm Waste pipe (units)
2010	Jan	1	0
	Feb	2	47,303.00
	Mar	3	37,413.00
	April	4	33,641.00

	May	5	27,374.00
	June	6	38,750.00
	July	7	50,588.00
	Aug	8	61,203.00
	Sept	9	70,105.00
	Oct	10	75,209.00
	Nov	11	5,964.00
	Dec	12	93693
2011	Jan	13	77,964.00
	Feb	14	65,755.00
	Mar	15	62,349.00
	April	16	8,885.00
	May	17	79,724.00
	June	18	36,343.00
	July	19	55,114.00
	Aug	20	85,009.00
	Sept	21	69,522.00
	Oct	22	29,138.00
	Nov	23	25,063.00
	Dec	24	0

Source: Louis Carter grouped data

$X_1$ = 32mm Pressure pipe,  $X_2$ = 25mm Waste pipe

### 3.1 Method of data analysis

Response Surface Design and optimization methods were used to model, design and to optimize the production mixture of Louis Carter manufacturing industry to observe the optimum production output of the raw materials.

**Table 2: Presentation of 2010-2011 Monthly Data on Production Output of 25mm Waste Pipe**

25mm Waste Pipe (units)	25mm Waste Pipe(0.9kg)	PVC	Stabilizer	Calcium Carbante	Steric acid	Titanium dioxide	Pigment
0	0	0	0	0	0	0	0
31535	28381.8	22942.82	764.7607	4588.564	76.47607	6.118086	3.059043
24942	22447.8	18145.99	604.8664	3629.198	60.48664	4.838931	2.419465
22427	20184.6	16316.5	543.8834	3263.3	54.38834	4.351067	2.175534
18249	16424.4	13276.89	442.5631	2655.378	44.25631	3.540504	1.770252
25833	23250	18794.46	626.482	3758.892	62.6482	5.011856	2.505928
33725	30352.8	24536.11	817.8702	4907.221	81.78702	6.542962	3.271481
40802	36721.8	29684.58	989.4859	5936.915	98.94859	7.915887	3.957944
46737	42063	34002.21	1133.407	6800.442	113.3407	9.067256	4.533628
50139	45125.4	36477.74	1215.925	7295.549	121.5925	9.727398	4.863699
3976	3578.4	2892.649	96.42164	578.5299	9.642164	0.771373	0.385687
62462	56215.8	45442.82	1514.761	9088.564	151.4761	12.11809	6.059043
51976	46778.4	37813.97	1260.466	7562.794	126.0466	10.08372	5.041862
43837	39453	31892.38	1063.079	6378.476	106.3079	8.504635	4.252317
41566	37409.4	30240.41	1008.014	6048.081	100.8014	8.064109	4.032054
5923	5331	4309.388	143.6463	861.8776	14.36463	1.14917	0.574585
53149	47834.4	38667.6	1288.92	7733.52	128.892	10.31136	5.15568
24229	21805.8	17627.02	587.5674	3525.404	58.75674	4.700539	2.350269
36743	33068.4	26731.3	891.0433	5346.26	89.10433	7.128347	3.564173
56673	51005.4	41230.92	1374.364	8246.185	137.4364	10.99491	5.497456
46348	41713.2	33719.44	1123.981	6743.889	112.3981	8.991852	4.495926
19425	17482.8	14132.46	471.0821	2826.493	47.10821	3.768657	1.884329
16709	15037.8	12156.01	405.2005	2431.203	40.52005	3.241604	1.620802
0	0	0	0	0	0	0	0

Source: Louis Carter grouped data



## IV. DATA ANALYSIS AND DISCUSSION

## 4.1 Response Surface Regression: 25mm Waste Pipe versus PVC, Stabilizer, ...

Estimated Regression Coefficients for 25mm Waste Pipe(kg)

Term	Coef	SE Coef	T	P
Constant	28108	0.213266	E+07	
0.000				
PVC	26462	757	34.961	0.000
Stabilizer	-294	189	-1.556	0.195
Calcium Carbamate	1875	759	2.471	0.069
Steric acid	72	24	2.956	0.042
Titanium dioxide	-4	3	-1.496	0.209
Pigment	-2	1	-3.165	0.034
PVC*PVC	-421734	272759	-1.546	0.197
Stabilizer*Stabilizer	558404	289984	1.926	0.126
Calcium Carbamate*Calcium Carbamate	4221	872	4.839	0.008
Steric acid*Steric acid	-159551	35662	-4.474	0.011
Titanium dioxide*Titanium dioxide	-11103	7518	-1.477	0.214
Pigment*Pigment	-1364	853	-1.599	0.185
PVC*Titanium dioxide	760032	459022	1.656	0.173
PVC*Pigment	73819	183598	0.402	0.708
Stabilizer*Titanium dioxide	-1004598	502670	-1.999	0.116
Stabilizer*Pigment	111146	172388	-0.645	0.554
Steric acid*Titanium dioxide	272964	58484	4.667	0.010
Steric acid*Pigment	46242	19363	2.388	0.075
Titanium dioxide*Pigment	-6187	3091	-2.002	0.116

S = 0.00116064

PRESS = 0.00186542

R-Sq = 100.00%

R-Sq(pred) = 100.00%

R-Sq(adj) = 100.00%

$$25\text{mm Waste pipe (kg)} = \beta_0 + \beta_1 X_1 + \beta_2 X_2 + \beta_3 X_3 + \beta_4 X_4 + \beta_5 X_5 + \beta_6 X_6 + \beta_7 X_1^2 + \beta_8 X_2^2 + \beta_9 X_3^2 + \beta_{10} X_4^2 + \beta_{11} X_5^2 + \beta_{12} X_6^2 + \beta_{13} X_1 X_5 + \beta_{14} X_1 X_6 + \beta_{15} X_2 X_5 + \beta_{16} X_2 X_6 + \beta_{17} X_4 X_5 + \beta_{18} X_4 X_6 + \beta_{19} X_5 X_6 \quad \text{..(4.2)}$$

PVC =  $X_1$ Stabilizer =  $X_2$ Calcium Carbamate =  $X_3$ Steric acid =  $X_4$ Titanium dioxide =  $X_5$ Pigment =  $X_6$ Constant =  $\beta_0$ Coefficient =  $\beta$

Results for Table 2:

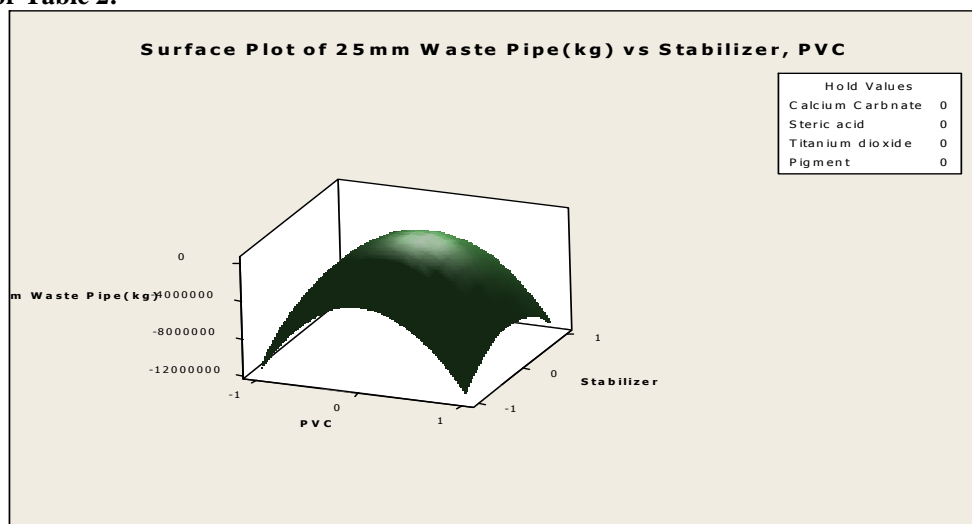


Fig 4-19: Surface Plot of 25mm Waste Pipe(kg) vs Stabilizer, PVC

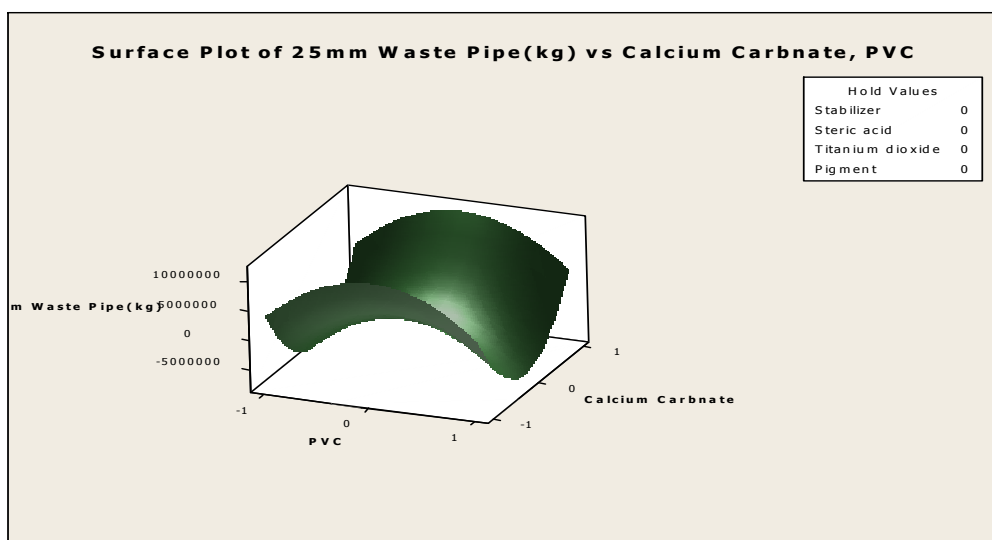


Fig 4-20: Surface Plot of 25mm Waste Pipe(kg) vs Calcium Carbamate, PVC

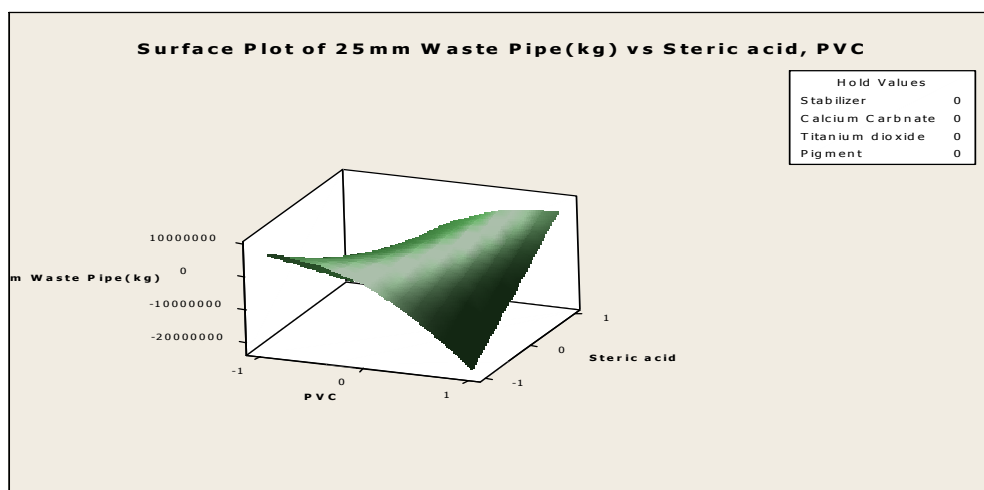


Fig 4-21: Surface Plot of 25mm Waste Pipe(kg) vs Steric acid, PVC

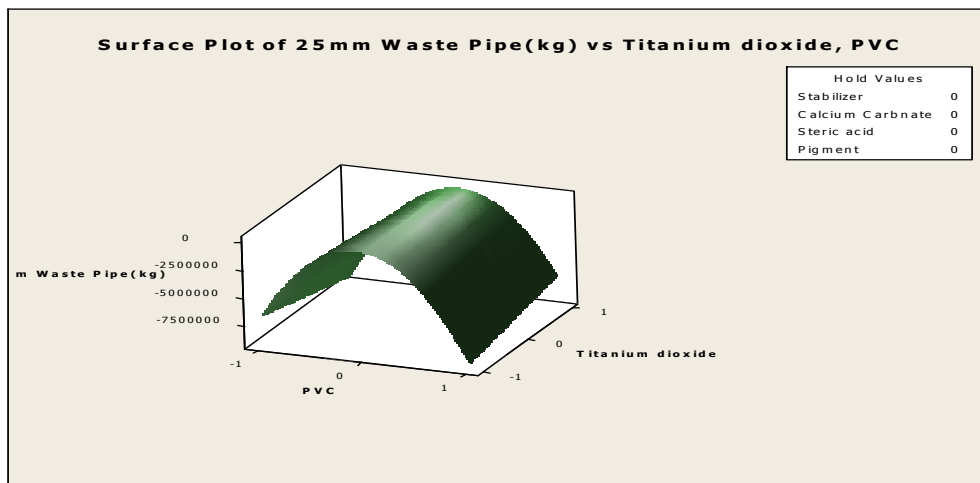


Fig 4-22: Surface Plot of 25mm Waste Pipe(kg) vs Titanium dioxide, PVC

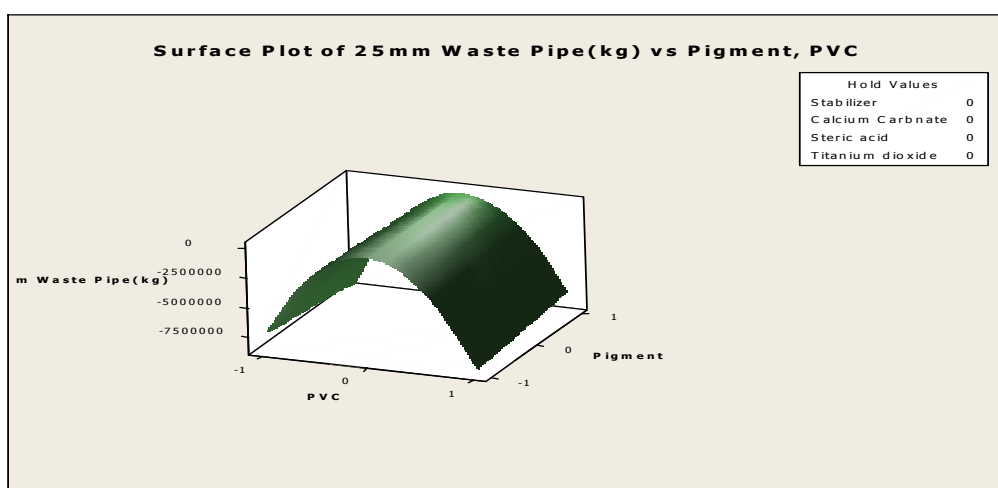


Fig 4-23: Surface Plot of 25mm Waste Pipe(kg) vs Pigment, PVC

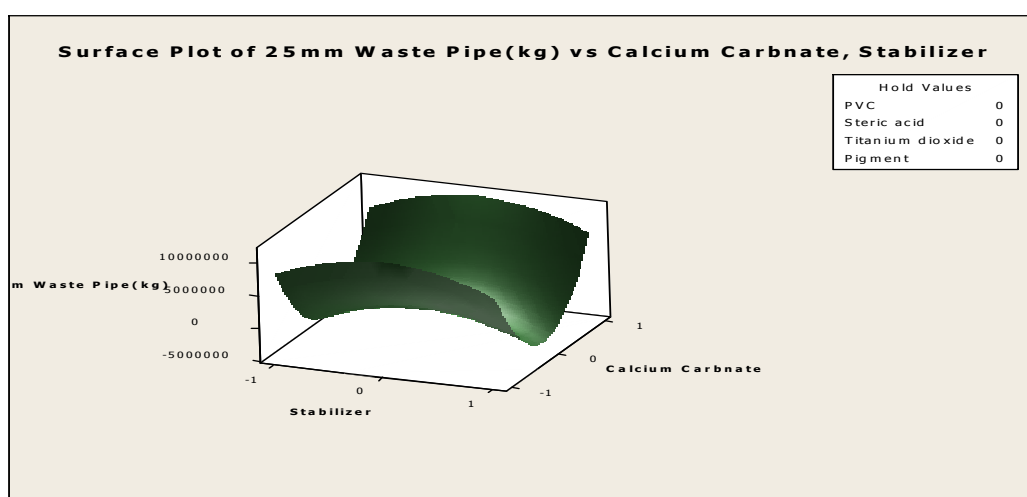


Fig 4-24: Surface Plot of 25mm Waste Pipe(kg) vs Calcium Carbamate, Stabilizer

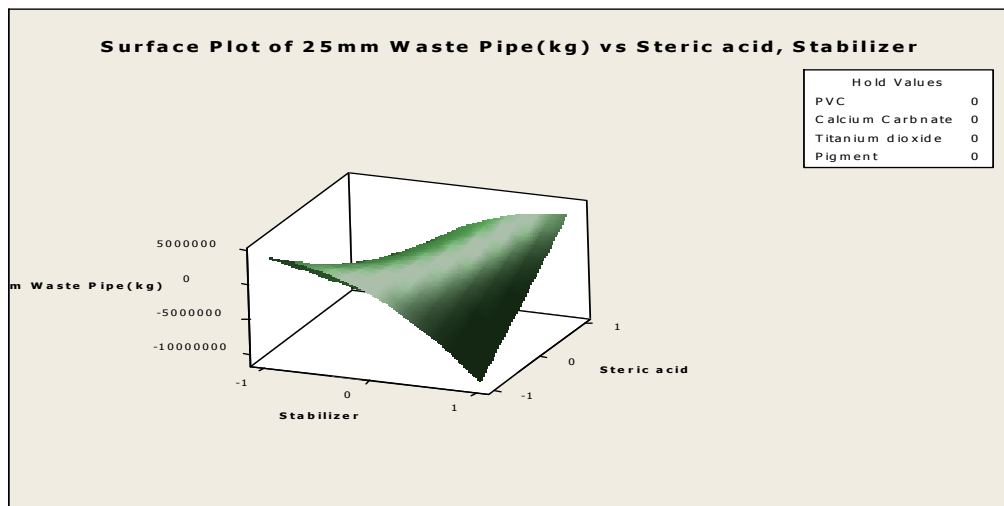


Fig 4-25: Surface Plot of 25mm Waste Pipe(kg) vs Steric acid, Stabilizer

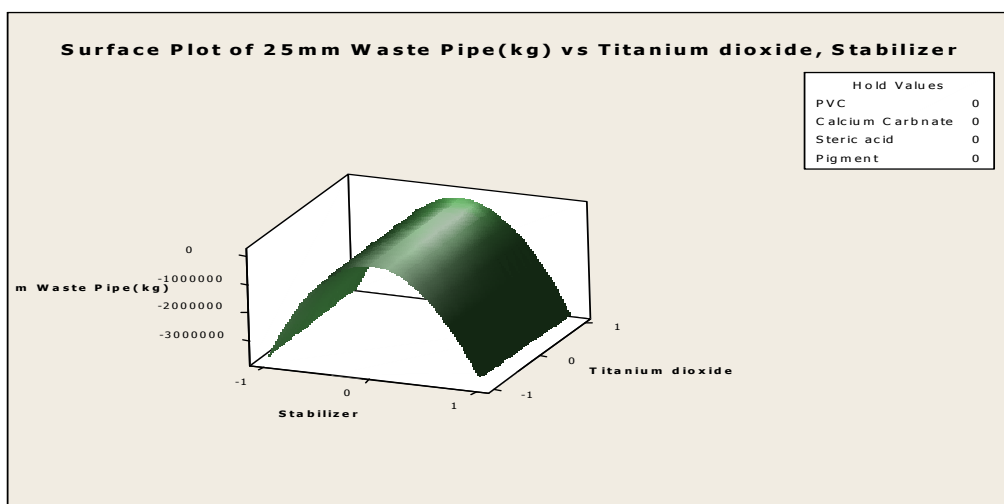


Fig 4-26: Surface Plot of 25mm Waste Pipe(kg) vs Titanium dioxide, Stabilizer

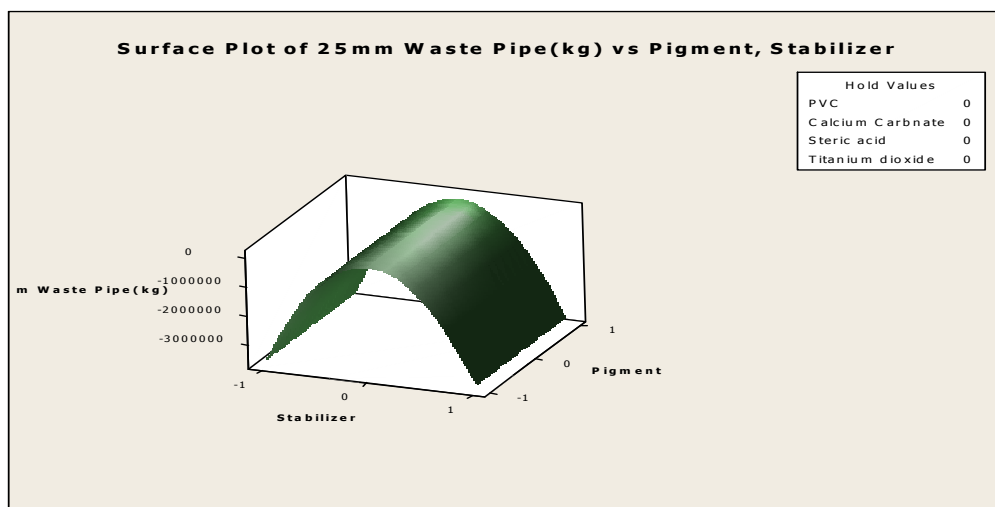


Fig 4-27: Surface Plot of 25mm Waste Pipe(kg) vs Pigment, Stabilizer

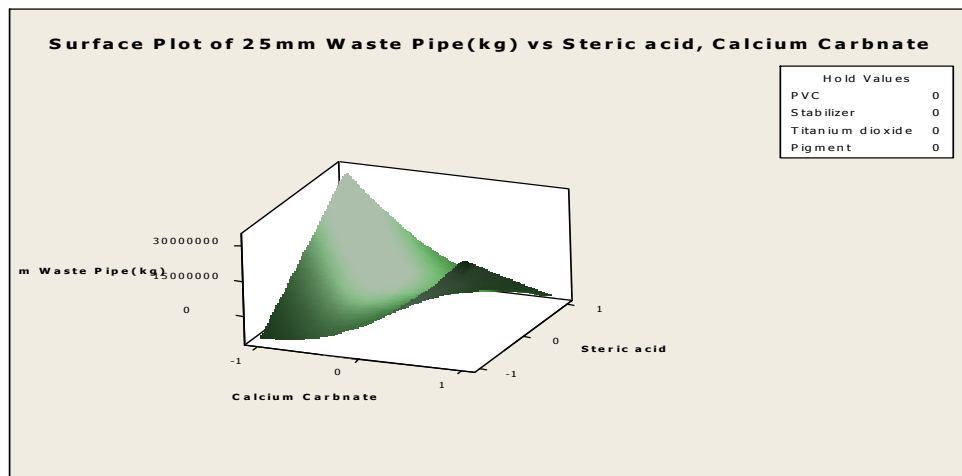


Fig 4-28 Surface Plot of 25mm Waste Pipe(kg) vs Steric acid, Calcium Carbamate

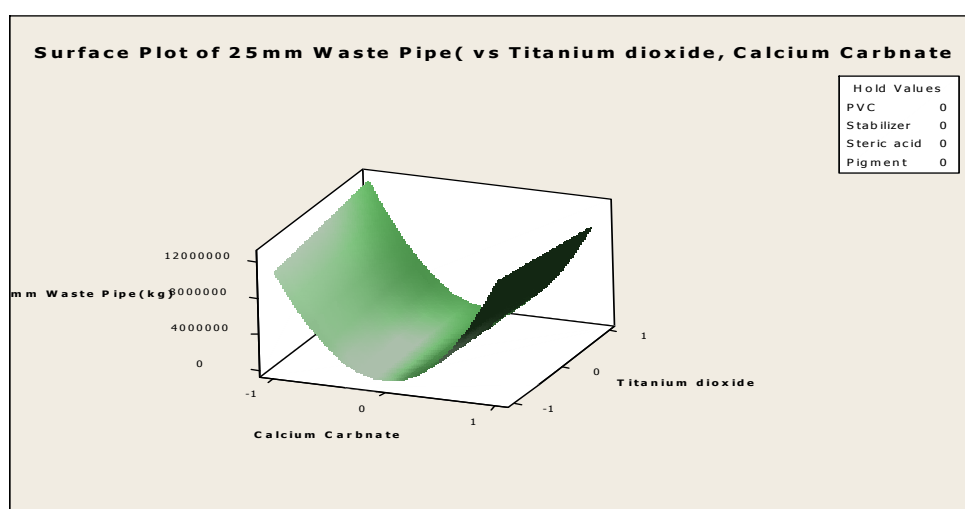


Fig 4-29: Surface Plot of 25mm Waste Pipe(kg) vs Titanium dioxide, Calcium Carbamate

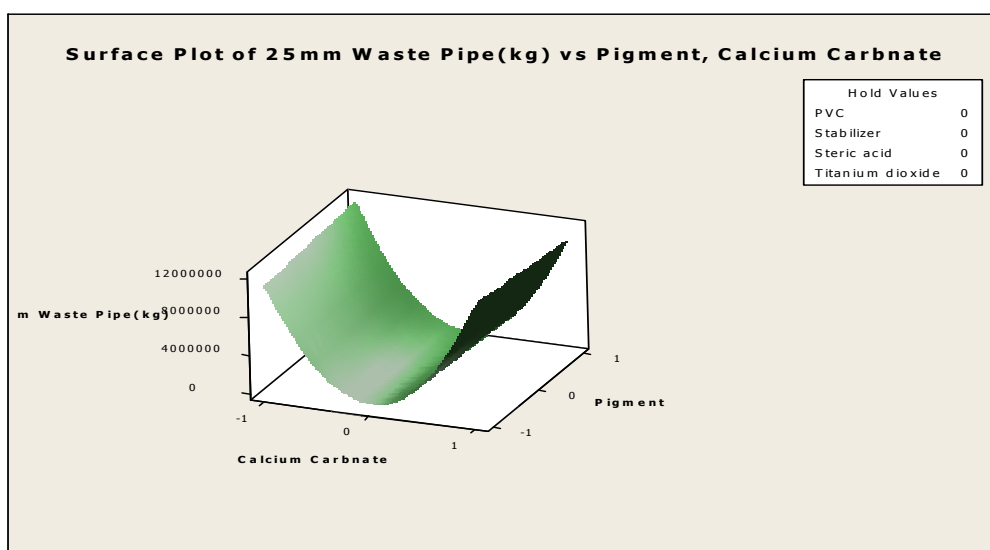


Fig 4-30: Surface Plot of 25mm Waste Pipe(kg) vs Pigment, Calcium Carbamate



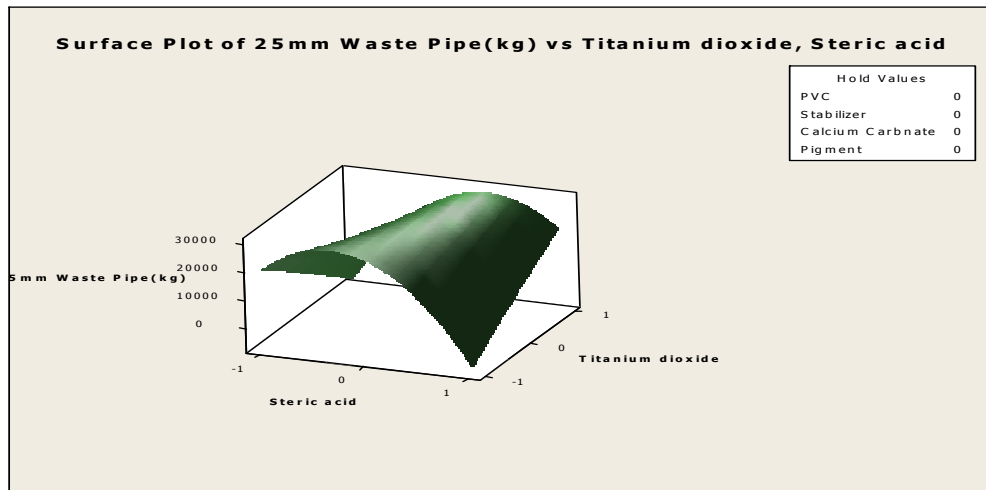


Fig 4-31: Surface Plot of 25mm Waste Pipe(kg) vs Titanium dioxide, Steric acid

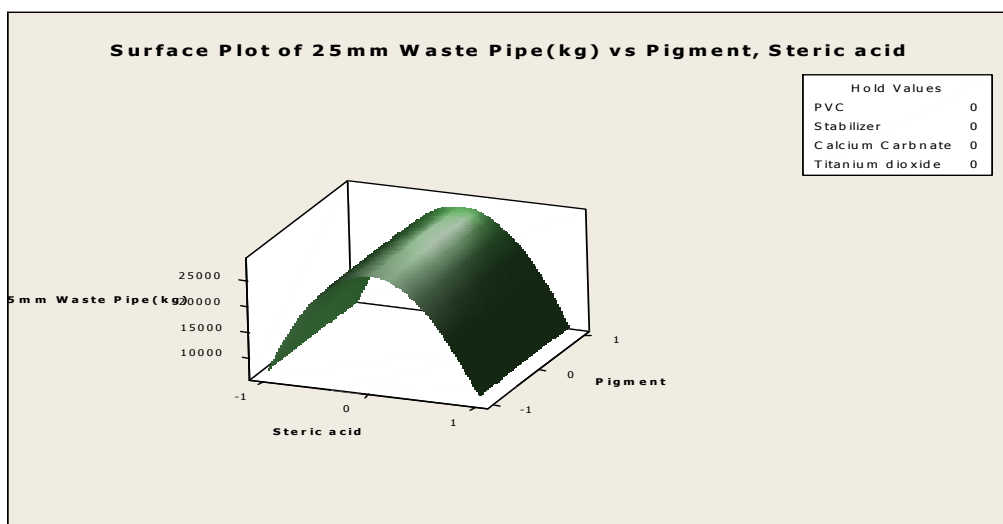


Fig 4-32: Surface Plot of 25mm Waste Pipe(kg) vs Pigment, Steric acid

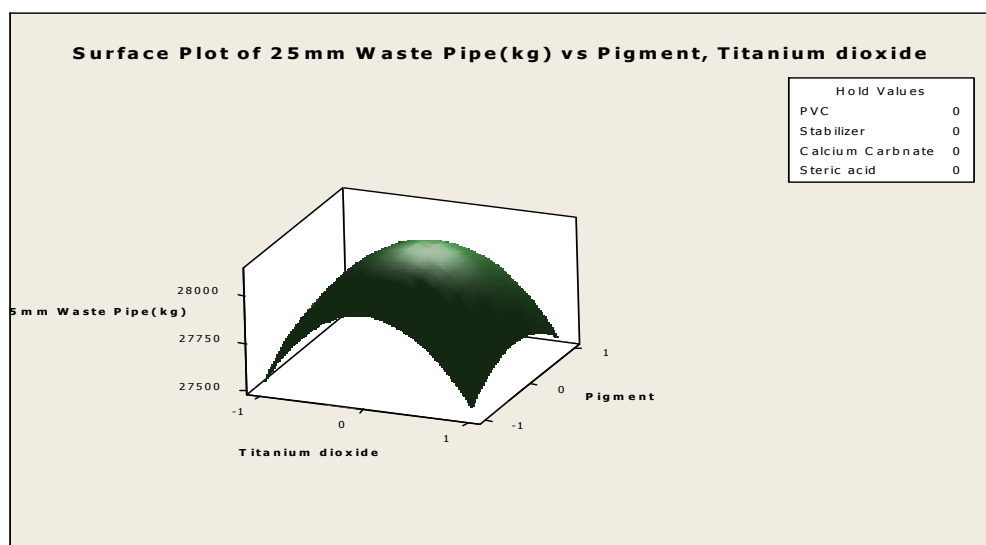


Fig 4-33: Surface Plot of 25mm Waste Pipe(kg) vs Pigment, Titanium dioxide

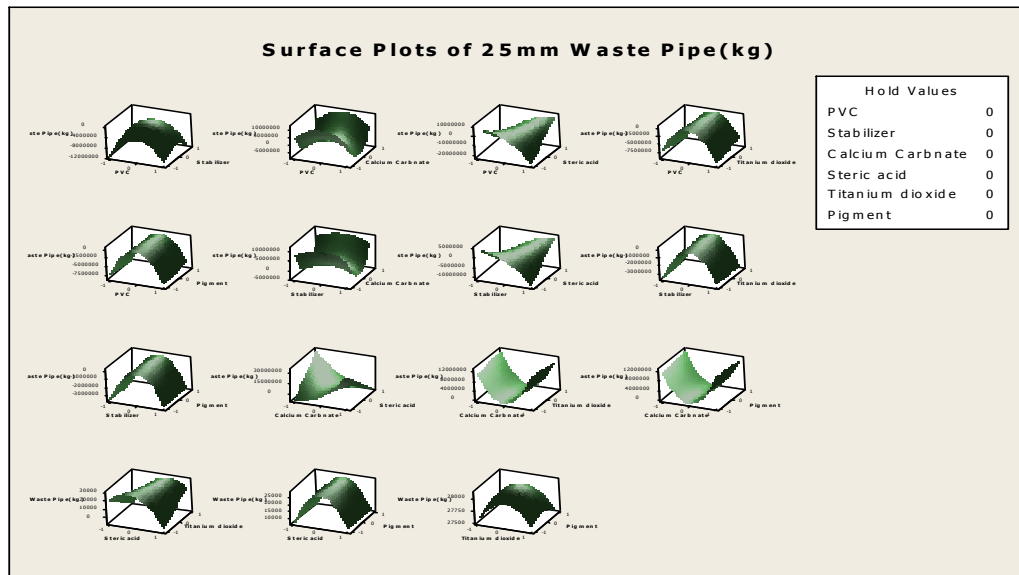


Fig 4-34: Surface Plots of 25mm Waste Pipe(kg)

## 4.2 Response Optimization

### Parameters

25mm waste Pipe	Goal	Lower	Target	Upper	Weight	Import
	Target	1000	52000	100000	1	1

### LOCAL SOLUTIONS TABLE

S/N	PVC	STABILIZER	CALCIUM CARBONATE	STERIC ACID	TITANIUM DIOXIDE	PIGMENT
1	45442.8	1514.76	0	151.48	12.12	1.40788
2	45442.8	1514.76	9088.55	151.097	11.6424	0
3	45442.8	1514.76	0.0001670	151.480	12.1200	60.5738
4	45442.8	1514.76	9088.56	151.480	12.1200	6.05685
5	45442.8	0	9088.56	151.459	12.12	0.0703254
6	45442.8	0	0	151.457	12.12	0.0743382
7	45442.8	0.0025821	0.0004172	151.479	12.1200	6.00280
8	45442.8	0.0026424	9088.56	151.479	12.1200	5.99895
9	22721.4	757.38	4544.28	75.74	6.06	3.02937
10	0.0002108	1514.76	9088.56	0	0	0
11	0.0003063	1514.76	0	0	0	0
12	0.0070180	0.0005276	9088.56	0.0052626	0	
13	1079.88	0	0	0	0	0
14	0	0	9088.56	2.73378	0	3.31244
15	0	0	0	5.23173	2.19678	2.81976
16	0	1514.76	9088.56	1.13804	0	2.30648
17	0	1514.76	0	1.34309	0	1.63020
18	45442.8	0	9088.56	150.789	2.06027	6.06
19	45442.8	0	0	150.613	2.50444	6.06
20	45442.8	1514.76	9088.56	150.482	2.88153	6.06
21	45442.8	1514.76	0	150.415	3.07537	6.06
22	45442.8	1514.76	9088.56	150.150	3.36754	0.485057
23	45442.8	1514.76	0	150.076	3.55214	0.511846
24	45442.8	0	9088.56	150.053	3.61434	1.05102
25	45442.8	0	0	149.982	3.79266	1.10610
26	0	1514.76	9088.56	2.96286	3.84594	0
27	0	1514.76	0	3.15960	3.35380	0
28	0	0	9088.56	3.87216	1.70613	0.0571311
29	0.0009029	0	0	5.88235	2.48085	2.20986
30	0	0	9088.56	4.49556	2.04860	4.54440
31	0	0	0	5.00512	1.30813	4.41359
32	0	1514.76	9088.56	4.19395	2.38954	2.31145
33	0	1514.76	0	4.50495	1.87758	1.87799
34	45442.8	1514.76	0	151.48	12.12	1.40788

TABLE OF PREDICTED RESPONSES

S/N	25mm WASTE PIPE	DESIRABILITY	COMPOSITE DESIRABILITY
1	51994.8	0.999898	0.999898
2	53235.4	0.974263	0.974263
3	53744.2	0.963662	0.963662
4	56215.8	0.912171	0.912171
5	47033.4	0.902615	0.902615
6	44575.8	0.854428	0.854428
7	60728.5	0.818157	0.818157
8	63191.4	0.766846	0.766846
9	28107.9	0.531527	0.531527
10	8931.38	0.155517	0.155517
11	6459.81	0.107055	0.107055
12	2471.57	0.028854	0.028854
13	2000.01	0.019608	0.019608
14	2883.76	0.03637	0.036937
15	2458.30	0.028594	0.028594
16	3728.61	0.053502	0.053502
17	2906.71	0.037386	0.037386
18	2000.01	0.019608	0.01906
19	5689.19	0.091945	0.091945
20	5953.29	0.097123	0.097123
21	5916.80	0.096408	0.096408
22	5896.38	0.096007	0.096007
23	5849.03	0.095079	0.095079
24	5831.77	0.094741	0.04741
25	5776.23	0.093652	0.093652
26	4338.62	0.065463	0.065463
27	3745.99	0.053843	0.0543843
28	3230.40	0.043733	0.043733
29	2867.81	0.036624	0.036624
30	4021.64	0.059248	0.059248
31	2611.93	0.031606	0.031606
32	4677.16	0.072101	0.072101
33	399074	0.058642	0.058642
34	51994.8	0.999898	0.999898

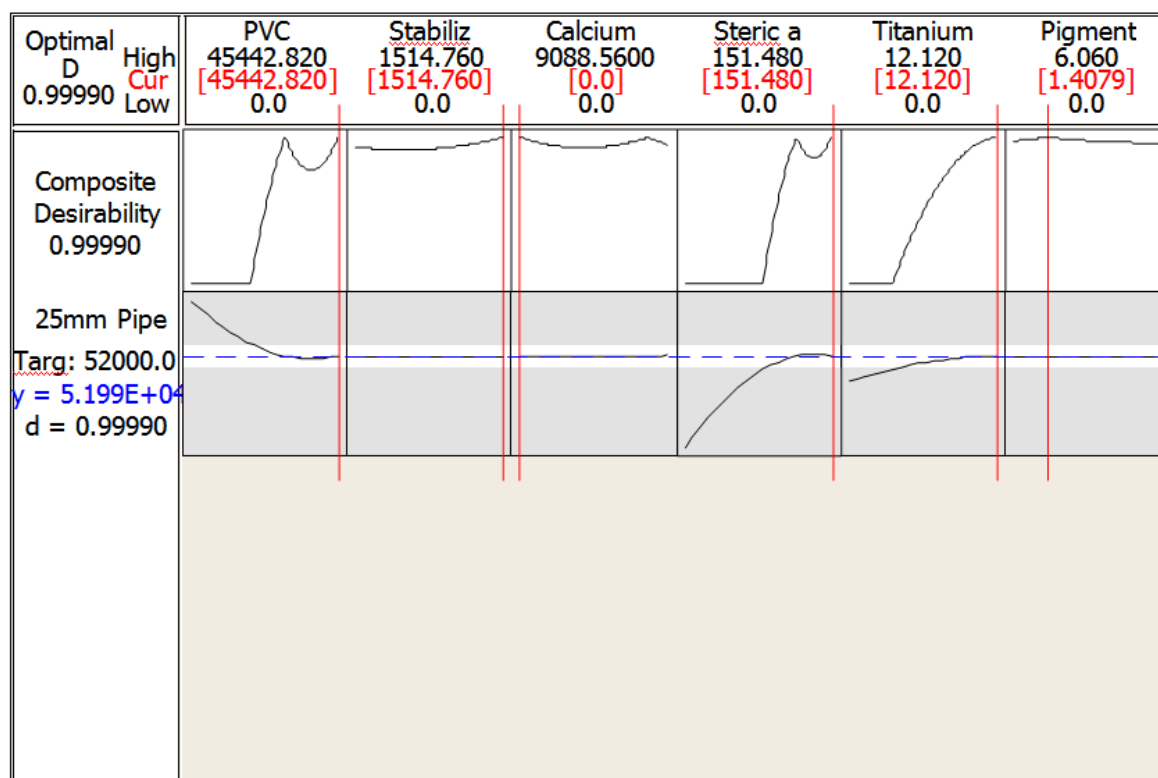


Fig 4-35: Optimization Plot

### 4.3 Discussion

These results express the optimal production mix of the raw materials in the selected products. The use of response surface model was applied to show the optimal production of the products over the month. The models show that there is a good relationship between the dependent variables and the independent variables and the coefficient of the relationships of the models (R-Sq) is 100%. It also shows from the surface plot, the relationship between the selected products and two different raw materials. The 25mm waste pipe vs Stabilizer, PVC shows increase in the product increases the PVC, then decreases at some point, and increases the Stabilizer, and finally in the 25mm waste pipe vs Steric acid, PVC shows that increase in the product decreases the PVC, and increases the Steric acid. However, the optimal solution of the 25mm waste pipe above shows an optimal production of 51990kg for the monthly production of the products. The company can achieved the results if the case study will be mindful of their wasted raw materials during production. The model is therefore recommended to the case study company for its applicability for the production of their products in other to achieve its optimal production mixture for the raw materials.

### V. Conclusion

The study has successfully determined the product mix of the raw material of Louis carter Plastic Industry Limited for 25mm waste pipe. This was done using response surface design and its optimization tool. In the process, the optimal quantities of the various PVC raw materials to be mixed within the study period in order to maximize profit were established. This is the advantage of going beyond mere knowledge of existing decision making tools of using wishful mental analysis to actual practical utilization of good engineering powerful tools in decision making of industries. Another issue becomes how the managerial cadre of the case study company could employ this technique in arriving at the objective function of the study. This can go a long way to assisting the management, at least, in the short run. However, in the long run, the case study company would probably gain more from having more permanent employees who can suggest opportunities to utilize these new techniques. There should be people not just one person who can effectively and efficiently interpret the results of mathematical analysis in the company's particular context, as well as possess the necessary competence in the utilization of computers for easy handling of the complex mathematical techniques involved. From the discussion of the study above, it can be seen that response surface model was used to optimize the production mix of the raw materials of selected products and this shows that the case study company wastes some of their raw materials. For this reason, we are recommending this model for the Case Study Company and also advises the company to look into their production system in order to reduce this wastage if they must optimize profit which is the objective function of every enterprise.

### REFERENCES

- [1] Benedict I. Ezema (2012), Optimizing Profit with the Linear Programming Model, Interdisciplinary Journal of Research in Business, Vol. 2, Issue. 2, pp.37- 49
- [2] David L. Kurtz, Louis E. Boone (1992), "Principles of Management", McGraw-Hill Inc., USA, p.28.
- [3] Kareem, B. and A. Aderoba, (2008), "Linear Programming based Effective Maintenance and Manpower Planning Strategy", *International Journal of the Computer, the Internet and Management*, vol.16 pp.26-34.
- [4] Khuri, A. I. and Cornell, J. A. (1987), "Response Surfaces: Designs and Analyses", pp50-56
- [5] Michelle Leung, Production Scheduling Optimization of a Plastics Compounding Plant with Quality Constraints, MSc thesis University of Waterloo, Ontario, Canada, 2009
- [6] Montgomery, D. C. (2001), *Design and Analysis of Experiments*, John Wiley and Sons, New York, NY, p30.
- [7] Nedim M. Sirakaya, Alemdar, and Sibel (2002), "A sample of Determination of Product combination with Linear Programming in Risk Environment", *European Journal of Economics, Finance and Administrative Sciences*, p 30.
- [8] Okolie, P.C, Ezeliora, C.D, Iwenofu, C.O, and Sinebe, J.E. (2014), "Optimization of a Soap Production mix using Response Surface Modelling: A case of Niger Bar Soap Manufacturing Industry Onitsha, Anambra State" *International Journal of Scientific and Technology Research* 3(9), pp.346-352
- [9] Taha, H., (2008), "Operations Research: An Introduction", 110001 PHI Learning Private Limited, New Delhi, p25.

## Currency Recognition System Using Image Processing

S. M. Saifullah<sup>1</sup>, AnikaRahmanAnanna<sup>2</sup>, Md. Shakhawat Hossain<sup>3</sup>, Md. Jaouad Hossain<sup>4</sup>, Md. SaniaRahman Zishan<sup>5</sup>

<sup>1, 2, 3, 4, 5</sup>(Electrical and Electronic Engineering, American International University-Bangladesh, Bangladesh)

**ABSTRACT :** In the last few years a great technological advances in color printing, duplicating and scanning, counterfeiting problems have become more serious. In past only authorized printing house has the ability to make currency paper, but now a days it is possible for anyone to print fake bank note with the help of modern technology such as computer, laser printer. Fake notes are burning questions in almost every country. Like others country Bangladesh has also hit really hard and has become a very acute problem. Therefore there is a need to design a currency recognition system that can easily make a difference between real and fake banknote and the process will time consuming. Our system describes an approach for verification of Bangladeshi currency banknotes. The currency will be verified by using image processing techniques. The approach consists of a number of components including image processing, image segmentation, feature extraction, comparing images. The system is designed by MATLAB. Image processing involves changing the nature of an image in order to improve its pictorial information for human interpretation. The image processing software is a collection of functions that extends the capability of the MATLAB numeric computing environment. The result will be whether currency is real or fake.

**Keywords** -Image pre-processing, Conversion, segmentation, Feature extraction, Currency recognition.

### I. INTRODUCTION

It's very difficult for the people to differentiate the real and the fake currencies. In Bangladesh, fake notes are available. In fact, the bank workers cannot distinguish the difference between the real and the fake currencies because they check the notes in bare eyes and so their perception can be wrong sometimes. For this ordinary people can be cheated anytime. And also this causes an increment of doing many criminal offences. To solve this major problem, a system is developed that will detect the currency whether it is fake or real. For example, Bangladeshi currency is used for analysis.

The system presents the image processing system containing all the necessary processes such as image scanning and reading, image pre-processing, segmentation, feature extraction etc. along with a code that is done in MATLAB software. So this system is represented as an identifier of the fake and real currencies. MATLAB is the computational tool of choice for research development and analysis. The image formats supported by BMP, HDF, JPEG, PCX, TIFF, XWV, PNG and so on.

### II. METHODOLOGY OF RECOGNIZING BANGLADESHI CURRENCY

A block diagram is given below that represents the processes is done for our currency recognition system. All the processes are shown afterwards in the block diagram.



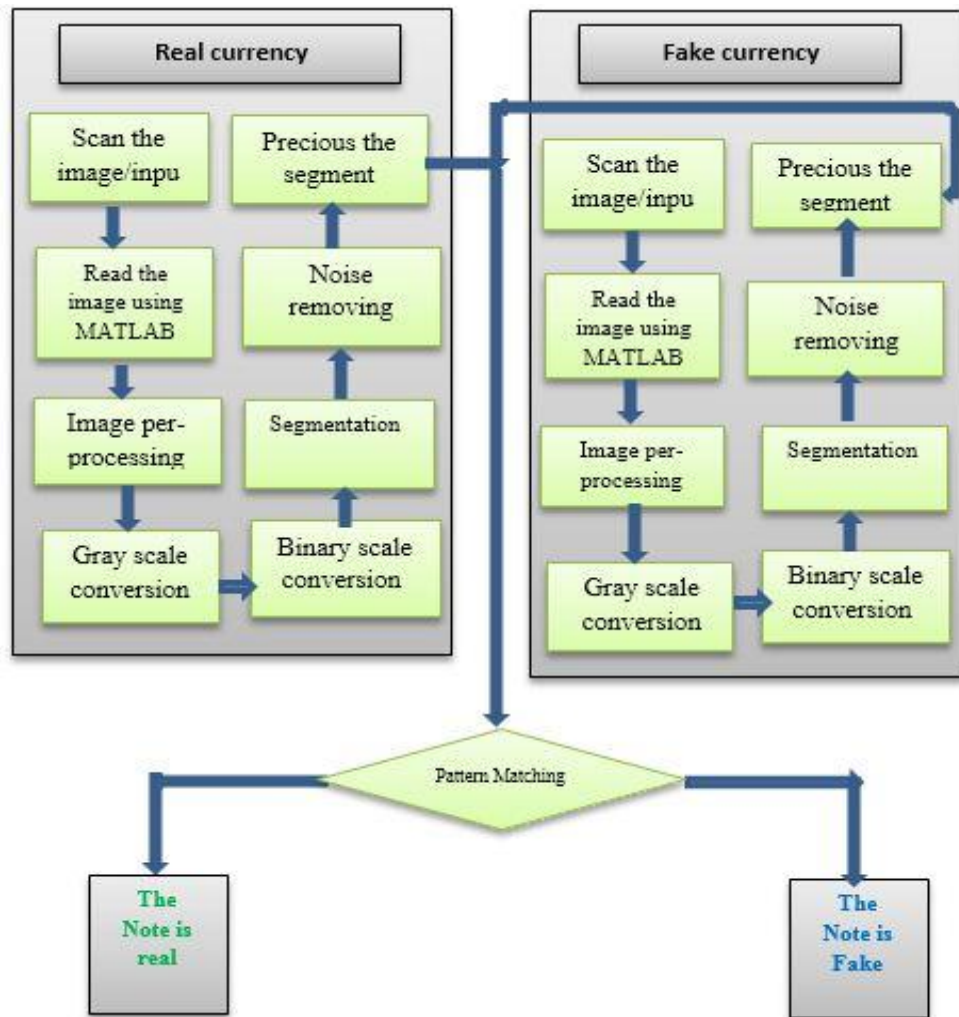


Figure 1: Block Diagram of the system.

### Image Scanning and Reading:

The image we get from scanner is formatted by JPEG. JPEG (Joint Photographic Experts Group) is a standard for destructive or loss compromising for digital images. When you save the image as JPEG, the image will lose some information, and this cannot be recovered. And after that the JPEG image is read using MATLAB code. [1]

#### A. Image Smoothing:

While performing image transfers, some noise may appear on the image. Removing the noise is an important step when image processing is being performed. However noise may affect segmentation and pattern matching. Mask values can be used to determine the degree of smoothing and to reduce noise. Higher is the size of mask, more is the smoothing. [2]

#### B. Conversions:

There are two types of conversion happened in our system. One is Gray scale and other is Binary scale conversions.

- **Gray Scale Conversion:**

Gray describes the colors ranging from black to white. Gray paints are created by mixing the two colors. We convert RGB to gray. [3]

- **Binary Scale Conversion:**

A binary image is a digital image that has only two possible values for each pixel. Typically the two colors used for a binary image are black and white. We use binary conversion for proper segmentation. [4]

### C. Image segmentation:

The result of image segmentation is a set of segments that collectively cover the entire image, or a set of contours extracted from the image. Each of the pixels in a region is similar with respect to some characteristic or computed property, such as color, intensity, or texture. Adjacent regions are significantly different with respect to the same characteristic. [5]

### D. Feature Extraction:

The feature extraction includes the extraction of features of serial numbers of currency notes. During this process, the dimensionality of data was reduced. Feature extraction or selection was a pivotal procedure considerably for currency recognition, which effects on design and performance of the classifier intensively. Basically, at first instance, people may not pay attention to the details and exact characteristics of banknotes for their recognition, rather they consider the common characteristics of banknotes such as the size, the background color (the basic color), and texture present on the banknotes. [6]

### E. Pattern Matching:

Pattern Matching is the process after segmentation where the difference between the real and the fake notes can be identified in an accurate way.

## III. SIMULATIONS AND ANALYSIS OF THE RESULTS

MATLAB simulation tool is used for image processing and for analyzing the simulated results. Analysis of the simulated results are discussed in the below sections.

### A. Scanned Image:

A digital image scan takes a similar approach to the second type of photo sensor, but instead of using one matrix for each component, it uses one array per component. A scanner is needed to scan the currency both of real and fake.



Figure 2: Scanned RGB image for 100 taka real.



Figure 3: Scanned RGB image for 100 taka fake.

### B. Read the Image Using MATLAB:

After scanning, the images are converted in JPG format. Then both images are inserted in MATLAB. Two types of 100-taka currency (BANGLADESHI) are used in this experiment, one is real and other is fake.



Figure 4: MATLAB input Image for 100 taka real.



Figure 5: MATLAB input Image for 100 taka fake.

### C. Gray Scale Conversion:

After step B, the RGB image is converted to gray and then gray image.



Figure 6: Gray scale image for 100 taka real.



Figure 7: Gray scale image for 100 taka fake.

### D. Segmentation for Black Line:

From the gray scale image segmented part of backlines for both real and fake currency are selected.



Figure 8: Gray segmented image for 100taka real.



Figure 9: Gray segmented image for 100 taka fake.

### E. Binary Scale Image for Segmented Image:

Then binary scale image is converted from the gray scale image for the segmentation.



Figure 10: Binary Scale Image for 100 taka real.



Figure 11: Binary Scale Image for 100 taka fake.

### F. Open area image:

Open area performs morphological opening on the binary image with the structuring. The morphological open operation is erosion followed by dilation, using the same structuring element for both operations



Figure12: Open area image for 100 taka real.



Figure13: Open area image for 100 taka fake.

### G. Post Analysis for Segmented Open Area Image:

Post analysis means that the segmented image is needed to be more precious. From the below figure difference between real and fake can be visually seen.



Figure 14: Open area Image for 100 taka real.



Figure 15: Open area Image for 100 taka fake.

### H. Image for black line:



Figure 16: Image of black line for real 100 taka.



Figure 17: Image of black line for fake 100 taka.

### I. Graph for black line:

The graph of the black line was plotted for both real and fake currency by using MATLAB. The difference between real and fake notes can be determined now.



Figure 18: Graph for No of backline for 100 taka real



Figure 19: Graph for No of backline for 100 taka fake

**J. Black strip:**

Every currency has some unique characteristic. Every Bangladeshi currency has black strip. And it's one of the unique characters of money. Image of the black strip of 100 taka is given below both real and fake.

Real Currency

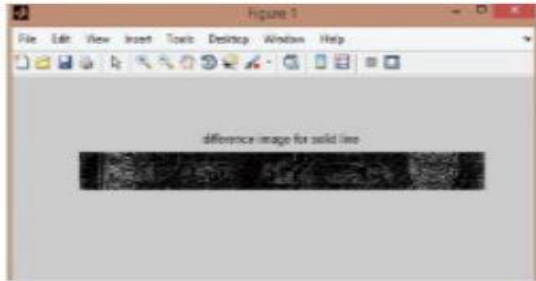


Figure 20: Image for No of back strip for 100 taka real.

Fake Currency

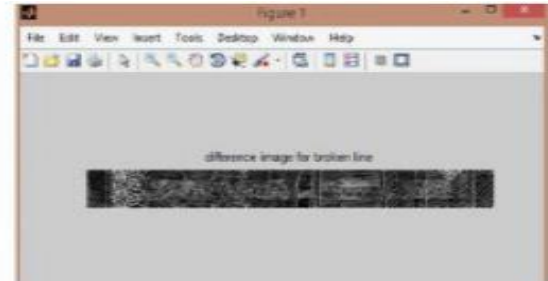


Figure 21: Image for No of back strip for 100 taka fake.

**K. Graph for Black Strip:**

The graphs of the black line for both real and fake notes are simulated by using MATLAB. The differences between real and fake notes are visible in the graph.

Real Currency

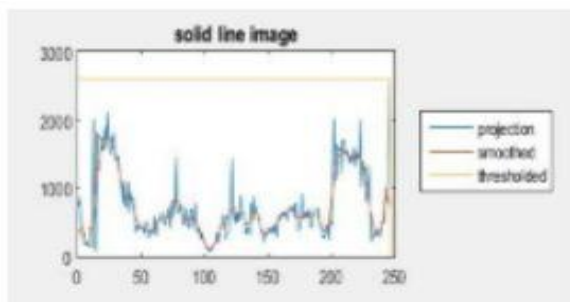


Figure 22: Graph for No of back strip for 100 taka real .

Fake Currency

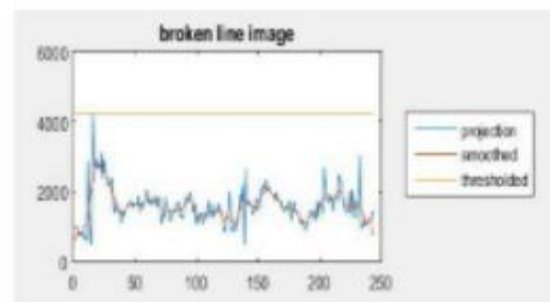


Figure 23: Graph for No of back strip for 100 taka fake.

**L. No of Black line:**

The last step is to simply count the number of black lines in each image. If there is just 1, this denotes that the bank note is fake, while if there is more than 1, this denotes that the bank note is fake.[8]

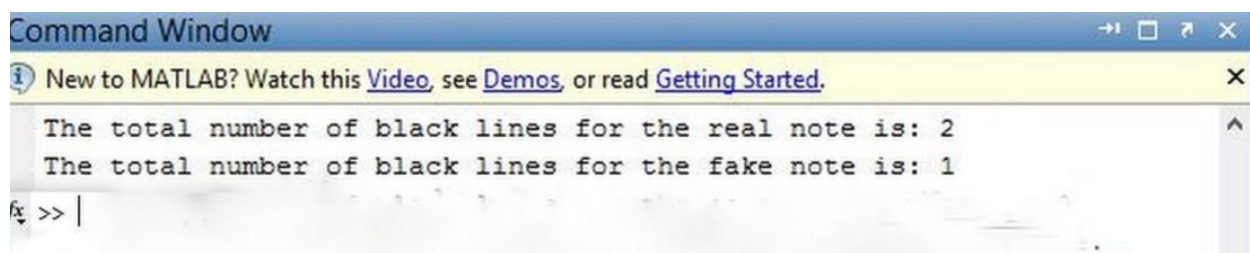


Figure 24: No of black line shown in command window.

**IV. CONCLUSION**

This paper discussed the currency recognition system with a digitalized image processing system. This system can work for assisting visually impaired people to correctly determine the denomination of the currency notes. It can help to distinguish the original note from counterfeit currency. If the image exhibit information loses such as surface damage, noise level, sharpness issues and so on, the recognition may fail and the user has to do the processing again. The system had been programmed by using MATLAB and it will include a user-friendly interface.



## V. Acknowledgements

First of all, we would like to thank Almighty Allah for completing the paper successfully. We would like to thank our beloved elder brothers Md. Moidul Islam, and Md. Mostafizur Rahman, who encouraged and supported us throughout to produce a good research and also a good paper.

## REFERENCES

- [1] Math Works Website Available at <http://www.mathworks.com/products/scan/image/>
- [2] Proakis and Manolakis. [Digital Signal Processing \(4<sup>th</sup> ed.\)](#) [Online]. Available: <http://www.code.google.com>
- [3] RubeenaMirza, Vinti Nanda, "Paper Currency Verification System Based on Characteristic Extraction Using Image Processing", IJEAT, February 2012, pp 2249 – 8958
- [4] KishanChakraborty, Jordan Basumatary,DebasmitaDasgupta, Jagadish Chandra Kalita,,Subra Mukherjee , "RECENT DEVELOPMENTS IN PAPER CURRENCY RECOGNITION"SYSTEM, IJRET, 2012, pp2321-7308
- [5] (2015) mathworks website [online] Available: <http://www.mathworks.com/products/Security>
- [6] Yaojia Wang Siyuan Lin, Siyuan Lin, "a currency recognition system," International Journal of Engineering and Advanced Technology (IJEAT), February 2012. Pp 2249 – 8958.
- [7] Amol A. Shirsath<sup>1</sup> and S. D. Bharkad<sup>2</sup>"IJRET "A currency recognition system" International Journal of Research in Engineering and Technology ,2013 pp 2321-7308.
- [8] MathWorksWebsite . [online] : Available: <http://www.mathworks.com/help/matlab/ref/im2bw.htm>

## Effects of Waste Glass (WG) on the Strength Characteristics of Cement Stabilized Expansive Soil

I.A.Ikara<sup>1\*</sup>, A.M.Kundiri<sup>2</sup> and A.Mohammed<sup>1</sup>

<sup>1</sup> (Department of Civil Engineering, Abubakar Tafawa Balewa University, Bauchi State, Nigeria)

<sup>2</sup> (Department of Civil and Water Resource Engineering, University of Maiduguri, Borno State, Nigeria)

**Abstract:** The study investigates the suitability of using waste glass (WG) as admixture to cement stabilized black cotton soil (BCS) for roads, fills and embankment. The soil was classified as A-7-5 and CH according to the American Association of State Highway and Transport Officials (AASHTO) and the Unified Soil Classification System (USCS) Classifications. Chemical analysis revealed that WG is rich in main oxides such as Silicon Oxide (69.2), Aluminium Oxide (2.29), Iron Oxide (1.57), Calcium Oxide (15.1) and Sodium Oxide (8.75). The soil was stabilized with 0, 2, 4, 6 and 8% cement and 0, 5, 10, 15 and 20% WG by weight of the dry soil. Laboratory tests were carried out using the Standard Proctor (SP) compactive efforts, California Bearing Ratio (CBR), Unconfined Compressive Strength (UCS), and compaction characteristics tests to evaluate the effectiveness of WG on Ordinary Portland cement (OPC) stabilized BCS. The results obtained showed a decrease in the plasticity index (PI), liquid limit (LL), plastic limit (PL) and increase Maximum Dry Density (MDD) with increase in WG content in all cement proportions used and as compared to the values obtained for the natural soil. The peak 7 days UCS values of 1152kN/m<sup>2</sup> was obtained at 8% OPC and 20% WG. Similarly, highest CBR value of 53.8% was obtained at an optimum blend of 8% OPC/20%WG. The results indicate that there is a potential in the use of WG as admixture to strengthen Black cotton soils.

**Keywords:** Black cotton soil, Waste Glass, Ordinary Portland cement

### I. Introduction

Black cotton soils (BCS) are clays or very fine silts that have a tendency for volume changes, to swell and soften or shrink and dry-crack, depending on the increase or decrease in moisture content. Black cotton soils (BCS) are found predominantly in the North-Eastern part of Nigeria, lying within the Chad Basin and partly within the Benue trough (Ola, 1981; NIBBRI, 1983; Osinubi et al, 2009).

The swell-shrink movements in expansive soils have historically caused frequent problems because of the unpredicted upward movements of structures or cracks in pavements resting on them. In addition, they also affect the serviceability performance of lightweight structures supported on them. These soils increase in volume on absorbing water during rainy seasons and decrease in volume when the water evaporates from them (Chen, 1988). The volume increase (swell) if resisted by any structure resting on it; then vertical swelling pressure is exerted by the soil on the structure. This pressure if not controlled, may cause uplifting and distress in the structure (Shelke and Murthy 2010). The strength loss on wetting is another severe problem with such soils. Due to this peculiar behaviour many civil engineering structures constructed on expansive soils get severely distressed. Pavements are in particular, susceptible to damage by expansive soils because they are lightweight and extend over large areas. Dwelling houses transferring light loads to such soils are also subjected to severe distress. Similarly, earth structures such as embankments, canals built with these soils suffer slips and damages (Mishra et al., 2008). The swelling and shrinking of the soil generate depressions, cracks and swelling of pavement constructed on it. Noticeable cracks which may result to failure are witnessed on buildings constructed on this type of soil, Costa and Baker (1981) reported that the damaging effect of these cracks is as high as 0.16 to 0.6 MN/m<sup>2</sup>. It is therefore necessary to upgrade the engineering properties of deficient soils before they are put to use in construction.

Despite the proven performance of lime and Portland cement in the modification of the engineering and allied properties of problematic soils, the cost of blending soils with these stabilizers is usually prohibitive. In order to abate the cost of road base stabilization, one reasonable alternative is to mix the soil-lime or soil-cement blends with requisite amount of admixture (Matawal, et-al, 2006).

Glass is a hard material normally fragile and transparent common in our daily life. It is composed mainly of sand (silicate) and an alkali. It does not harm the environment in any way because it does not give off pollutants but it is non-biodegradable, once it is broken it can harm humans as well as animals if not dealt with carefully. It is regarded as useless and so discarded, littering the environment and constituting a nuisance in the community. The physical properties of the crushed glass are that they exhibit high permeability, high crushing resistance, small strain stiffness, and these properties could enhance its usage in geotechnical engineering works for soil stabilization, embankment constructions etc.

Ideally, most waste glass would be recycled into new glass. However, since only colour sorted and contamination-free waste glass is feasible for reuse in the glass industry, there is a surplus of waste glass which cannot be reused by glass manufacturers. The increased amount of such waste being collected, which is surplus to current requirement will also need alternative uses. These portions deserve attention as the beneficial reuse of broken/crushed glass will reduce the space it takes up in our landfills enhancing our efforts to protect our environment.

Previous research work on waste glass had focused its use in concrete or asphalt paving materials (Shayan and Xu, 2004; Wu et al., 2003; Bignozzi et al., 2009; Byars et al., 2004; Nwaubani, 2013). Some researchers have studied the engineering properties of soil-crushed waste glass blend (Dennis et al., 2006; Grubb et al., 2006; Eberemu et al., 2012;) suggesting its suitability as an additive and as an admixture when used with standard stabilizers for highway pavement works; not much is known in literature about the geotechnical behavior of cement stabilized black cotton soil with waste glass admixture, hence the need for this study.

## II. Materials

The Black cotton soils is obtained from Baurein village Yamaltu-Deba local government area of Gombe state, Nigeria. The waste glass (WG) used in this study was sourced from post-consumer waste, the glass was finely grinded, and an average particle size of  $< 300 \mu\text{m}$  was used. The BCS was classified as A-7-5 (AASHTO 1986) and CH (ASTM 1992). The properties of BCS is given in Table 1. The ordinary Portland cement (OPC) Ashaka brand, was obtained from the market, the chemical composition of the BCS, WG and OPC compositions is presented in Table 2.

## III. Experimental Methods

Laboratory tests were conducted in accordance with BS standard. The Atterberg limit tests, Standard proctor tests (SP), California bearing ratio tests (CBR) and unconfined compressive strength tests (UCS) were conducted in accordance with BS 1377(1990) and BS 1924 (1990). Compaction tests were conducted on BCS with varying percentages of OPC from 0%, 2%, 4%, 6% 8% and optimum mixes were obtained. After obtaining the optimum mix proportion, varying percentages of WG was added to the optimum mix of BCS-OPC from 5% - 20% at an increment of 5% by dry weight of the soil. The California Bearing Ratio (CBR) test was conducted on the BCS and OPC/WG stabilized BCS mixtures, the samples were compacted at their respective optimum moisture content in the CBR mould. Two sets of each sample were prepared and subjected to un-soaked and soaked CBR test. The soaking was done for 48 hours. Unconfined compressive strength test was carried out on OPC/WG stabilized BCS samples, the samples were compacted at optimum moisture content using the SP energy level. Tests specimen are of specified height to diameter ratio in accordance with BS 1377, the cylindrical specimens used in this test are of diameter 38 mm and height 76 mm. After compaction, the OPC/WG stabilized BCS was extruded from the mold and sealed with double wrappings in polythene bags that were kept at a constant temperature of  $25 \pm 2^\circ\text{C}$ . This was done for various periods to allow for uniform moisture distribution and curing. After curing, specimens were placed in a load frame machine driven strain controlled at 0.10 %/min and crushed until failure occurred. Specimens were cured for 7, 14 and 28 days. The durability assessment of the soil stabilized specimens was carried out by immersion of 7 days cured UCS specimen in water for the measurement of resistance to loss in strength rather than the wet-dry and freeze-thaw tests highlighted in ASTM (Annual 1992). The resistance to loss in strength was determined as a ratio of the UCS values of sealed cellophane-cured specimens of 7 days, unsealed, and later immersed in water for another 7 days to the UCS values of 14 days cellophane –cured specimens.

## IV. Results and Discussions

### Atterberg limit

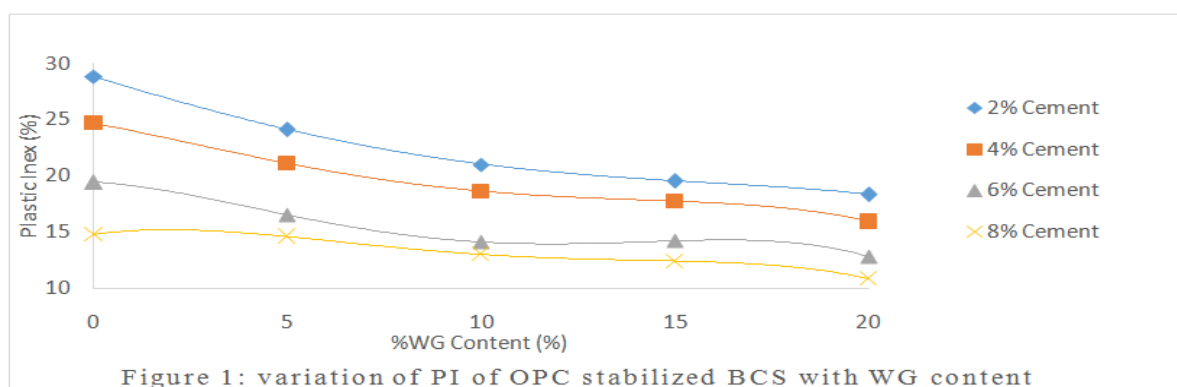
The liquid limit (LL) and plastic limit (PL) of the OPC/WG stabilized BCS have been determined in the laboratory in accordance with BS 1377 (1990). Figure 1 shows the variation of OPC/WG blend on the PI of the soil. It was observed that the PI decreased for a combination of OPC/WG blend up to 20% WG. The highest decrease from 30.6% to 10.8% was recorded at 8% OPC / 20% WG blend. Similar trends for glass cullet dredged material blend was reported by Dennis et al., (2006) and Grubb et al., (2006).

**Table 1: Properties of the Natural Soil**

Natural moisture content (%)	24.43
Liquid limit (%)	65.5
Plastic limit (%)	34.9
Plasticity index (%)	30.6
Specific gravity	2.65
Percentage passing BS No. 200 sieve	80.2
Percentage Sand fraction	74
Percentage Silt fraction	16
Percentage Clay fraction	10
Activity	3.06
Maximum dry density ( $\text{Mg/m}^3$ )	1.4
Optimum moisture content (%)	27.7
Unconfined compressive strength ( $\text{kN/m}^2$ )	190
Soaked California bearing ratio (%)	9.4
Un-Soaked California bearing ratio (%)	10.6
Colour	Dark gray
AASHTO classification	A-7-5(13)
Group Index	13
USCS classification	CH
NBRRI classification	Medium swell

**Table 2: XRF results of the BCS and WG**

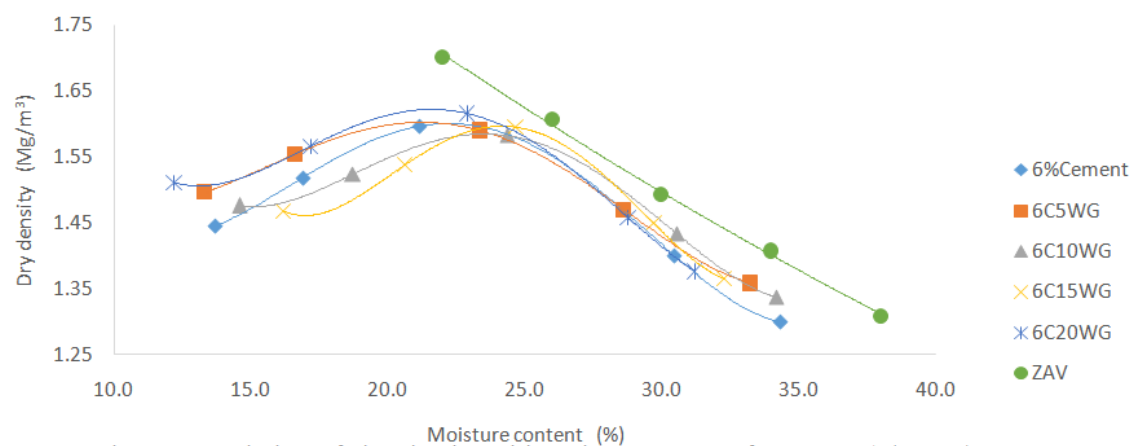
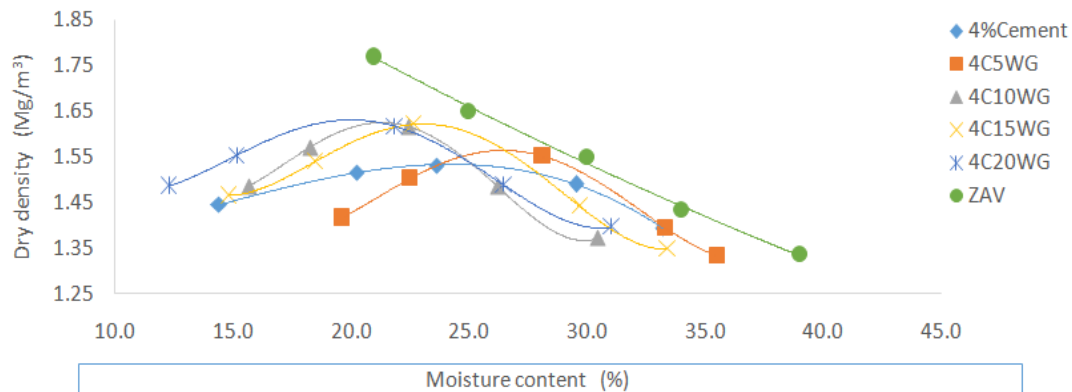
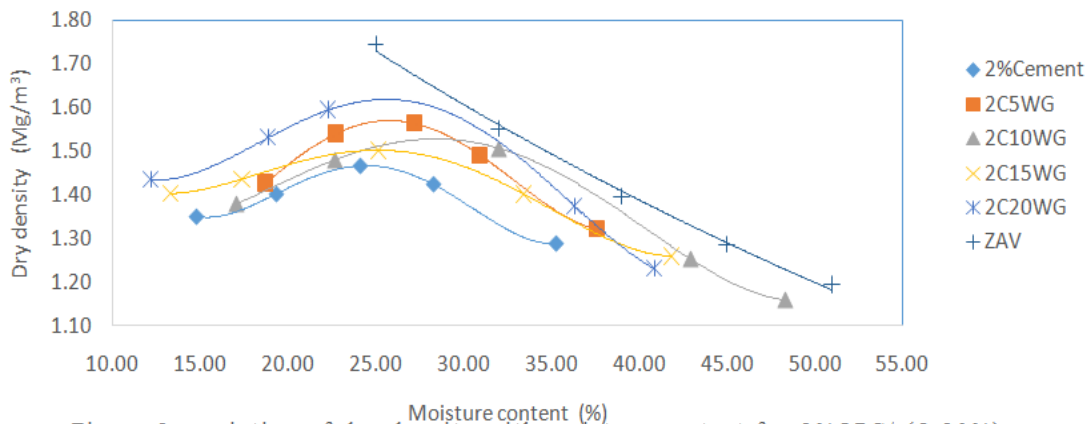
Compound	Concentration (%)	
	Soil	WG
Aluminium, Al	16.58	2.29
Silicon, Si	60.79	69.2
Potassium, K	1.39	1.10
Calcium, Ca	1.37	15.1
Manganese, Mn	0.08	0.02
Iron, Fe	6.13	1.57
Sodium, Na	0.16	8.75
Magnesium, Mg	1.17	0.49



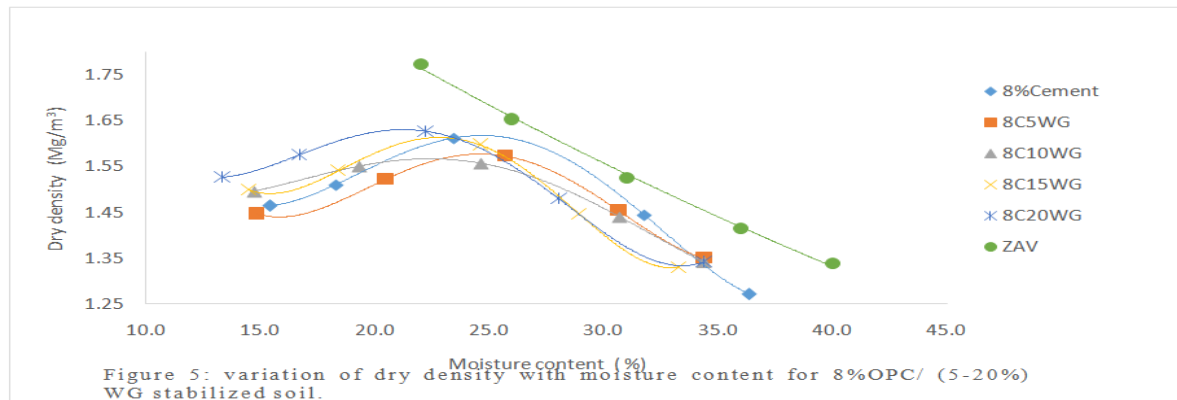
### Compaction characteristics

#### Effect of Compaction Condition on Dry Density and Water Content

The results obtained on the dry densities for the soil and soils treated with OPC and OPC/WG, showed that as the replacement levels of OPC and WG increase, the dry densities increase with the maximum value achieved at 20% replacement level for WG and at 8% replacement level for OPC. These behaviour are depicted in Figures 2 – 5 and showed that maximum dry densities for soil treated with 2-8% OPC is  $1.61 \text{ Mg/m}^3$ , while that of 2% OPC (5-20% WG), 4% OPC (5-20% WG), 6% OPC (5-20% WG) and 8% OPC (5-20% WG) is 1.62, 1.62, 1.62 and  $1.63 \text{ Mg/m}^3$  respectively. The effects of the various replacement levels on the moisture contents, showed a divergent behaviour. As the replacement levels are increasing, the moisture content decrease which is an indication of better performance achieved at 20 % replacement level.

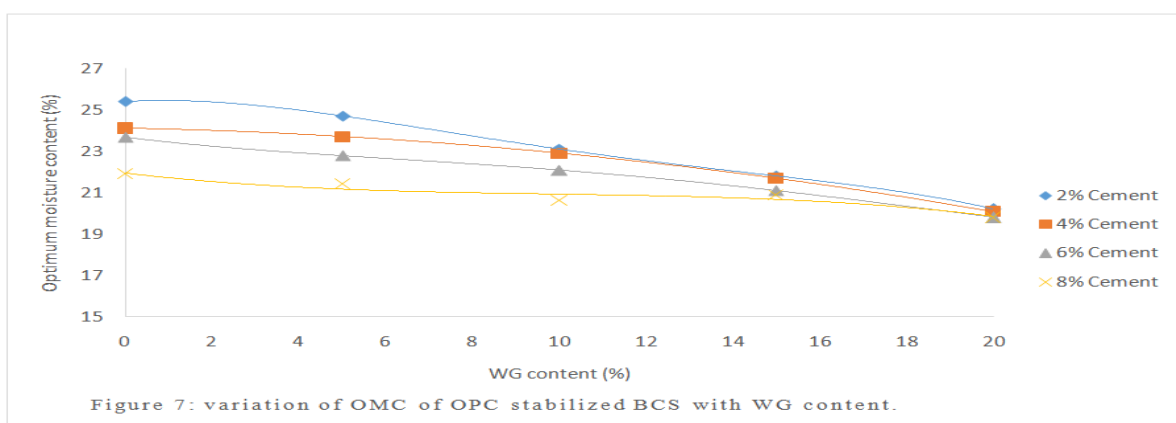
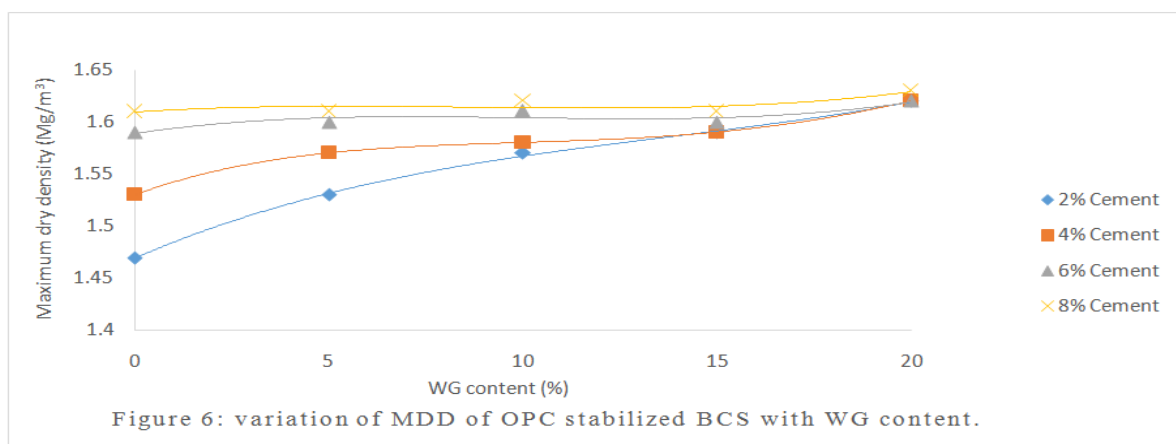






### Effect of OPC/WG on maximum dry density and Optimum moisture content

On addition of WG to the soil/OPC mixture, an increase in MDD was observed with WG content. The increase in MDD was attributed to the formation of new compounds, increase in surface area of particles at higher dosage of OPC/WG blend, as well as improved workability of the soil due to the increase in the percentage of CaO in the mixture and the desiccating property of WG. Figure 6 shows the effects of OPC/WG blend on the MDD of the soil. Also, the addition of water causes the bulking phenomenon in the stabilized soil. The fine cement particles influenced the compatibility of soil-cement material as such the soil-cement interaction resulted in the cementitious products and it gained strength. This trend is in order and agrees with Arabani et al., 2012 who reported that increase in MDD is due to the basic fact that soil-cement mix might have difference in specific gravity than the original soil. The variations of OMC is shown in Figures 7. The OMC decreased with increase in OPC/WG blend, this may be attributed to the fact that the OPC/WG dosage increased the surface area of soil particles due to the alkali ( $\text{Na}_2\text{O}$ ) content of WG in the formation of calcium silicate hydrates (C-S-H) for strength development of the treated soil, Khmiri et al., (2013).

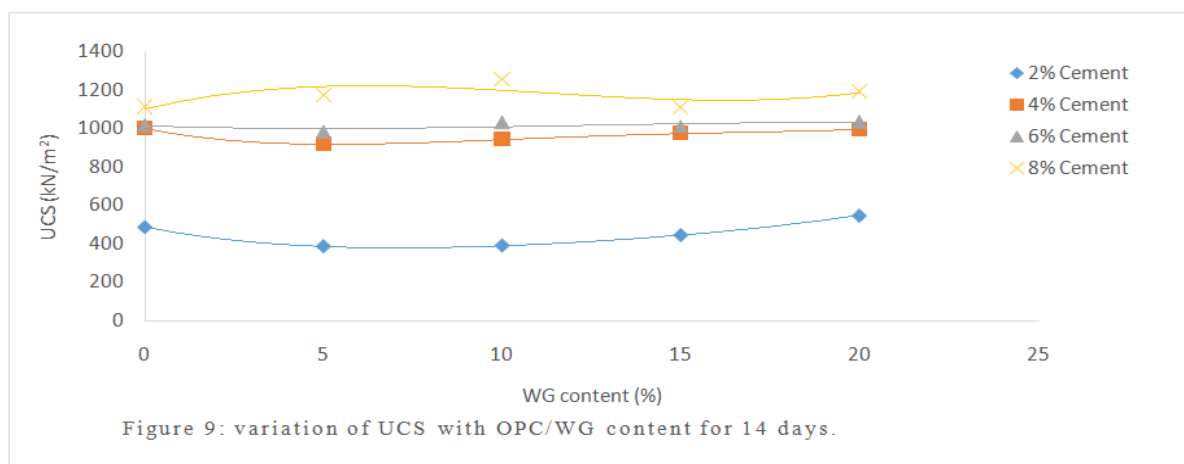
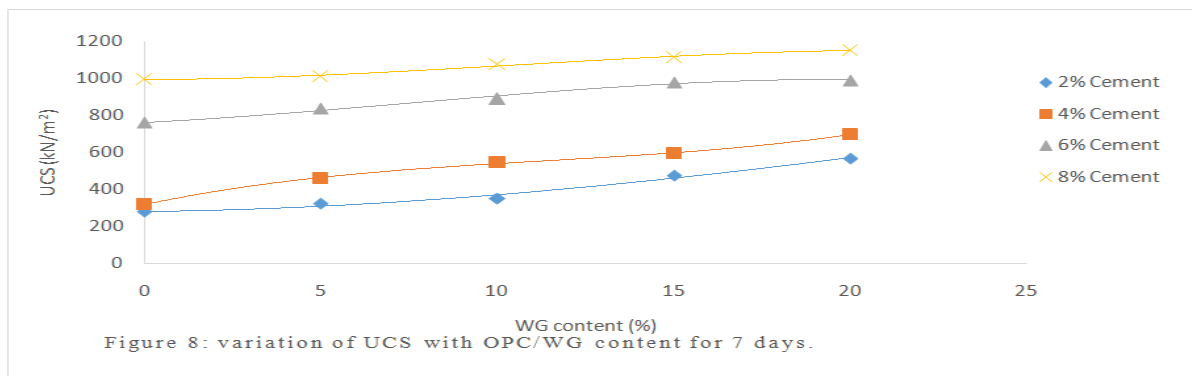


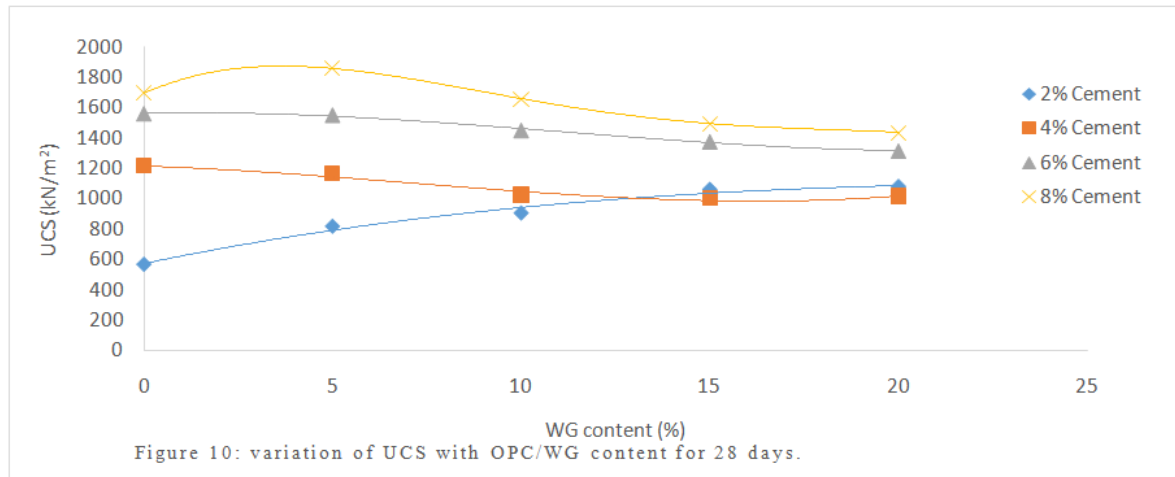
### Unconfined Compressive Strength

The variation of UCS with various percentages of OPC / WG blend after compacting the specimens at OMC for 7 days showed that compressive strength improved significantly after 7 days of curing. However, the peak 7-day UCS value of  $1152 \text{ kN/m}^2$  was recorded at 8% OPC / 20% WG blend, as shown in figure 8. The TRRL (1977) specified  $1720 \text{ kN/m}^2$  as criterion for adequate stabilization using OPC. The influence of compactive effort on the compressive strength of the 7 days cured specimens is well pronounced for each of the blend tested.

The variations of UCS for the samples cured for a period of 14 days is shown in Figure 9, the influence of WG admixture on the compressive strength has a long-term effect which may be attributed to the slow pozzolanic chemical reaction with WG and calcium hydroxide (CH) of cement when compared with OPC hydration. This agreed with the assertion of Dyer and Dhira (2001). The long-term chemical reaction progressively increases the strength of the mix. The UCS value of  $1257 \text{ kN/m}^2$  obtained for a combination of 8% OPC/10% WG was noticeably higher than the UCS values obtained for "OPC alone" treated specimens. It could therefore be inferred that the compressive strength increased linearly by fixing the OPC content and varying WG content from 5-20%. The increase in the compressive strength may be attributable to the concentration of OPC in this range, which reduces plasticity, thereby improving cementitious properties of the soil. It is evident that the OPC/WG content, curing age, as well as the rise in the pH level of the soil gives rise to strength development of the specimens. Figure 10 shows the specimen cured for 28 days. The results illustrated that at 4, 6 and 8% OPC the compressive strength decreased with higher dosage of WG admixture. However, at 2% OPC content the strength increase with higher concentration of WG. Which agreed with Ingles and Metcalf (1972). Higher strength was achieved at 8% OPC / 5% WG blend, this may be due to pozzolanic reaction, which progressively enhances the strength of the treated soil. The development of high UCS values at the 28-day curing period is attributed to the effect of OPC which promotes the production of alkaline compounds that increases the pH value of the soil and promotes the self-hardening characteristics of the WG admixture.

By Comparing the 28 days strength with those obtained at 7 and 14 days, it is obvious that the lower values obtained at 7 and 14 days were as a result of premature failure of the specimens (splitting of ends and spalling of the surface). Also, Wartman et al. (2004) suggested that the impact of WG on strength of fine grained soils may be delayed until WG particles cease floating in the fine grained matrix and develop particle to particle interactions which subsequently dominate the strength behaviour.





### California Bearing Ratio

Figure 11 shows the variation of un-soaked CBR with various percentages of OPC/WG blend. The CBR value of the specimen treated with OPC only increased with increase in OPC content, with the addition of WG, the CBR value increased at higher percentage of WG. This may be attributed to the increase in the contact area and adhesion between OPC and soil by WG which will create a dense network of interconnected particles, an increase of about 407.5% in the CBR value was noticed at 8% OPC/20% WG blend.

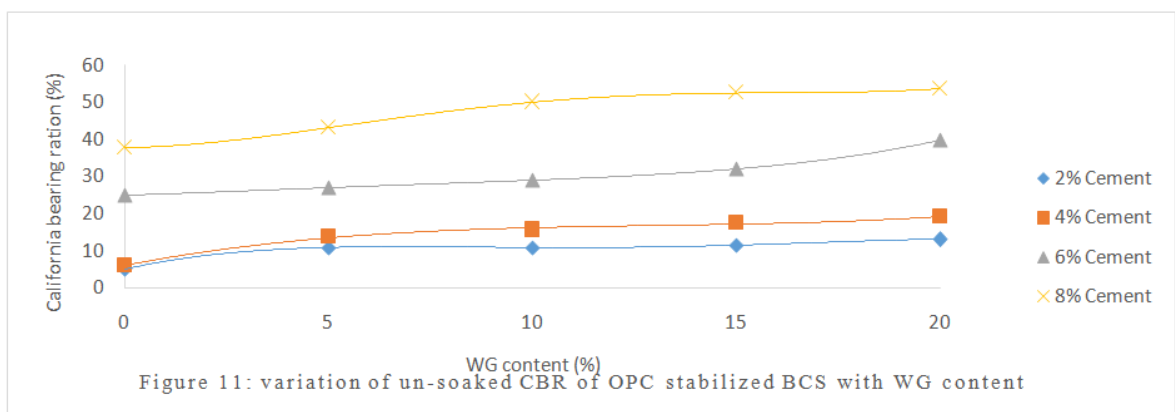
Arabani et al., (2012), in their study of cement stabilized with crushed glass sand blends reported that the cementitious reaction between cement and blends took place as a primary process. The hydration of the cement was regarded as primary reaction and formed the normal hydration products that bound particles together. The increase in the CBR value may be due to the shear transfer mechanism between the soil and WG, and the improvement in the strength might be due to the pozzolanic action of WG/OPC mix. Furthermore, the peak CBR value of 39%, with 0% WG content did not meet the 180% CBR value criterion recommended by the Nigerian General Specification (1997) for OPC stabilized soil. This is attributed to the high content of montmorillonite in the soil, which seems to negate the effectiveness of OPC.

However, specimens treated with 8% OPC/ (5-20%) WG meet the requirement of 30% CBR of the Nigerian General Specification (1997) for use of the soil material for sub-base in roads, other mixes also met this requirement, and they include 6% OPC / (5-20%) WG, 4% OPC /20% WG compacted at MP energy level and 6% OPC / (15-20%) WG compacted at SP energy level

However, at 2, 4 and 6% OPC with varying proportions of WG compacted with both compactive effort did not meet the requirement for good quality base or sub-base for road pavement, it however, suffices for use as a sub-grade material.

### Durability of CBR Specimens

The variation of soaked CBR with WG is shown in figure 12. It is observed that 48 hours soaking period did reduce the CBR values, but the soil may not be suitable for use as a base or sub-base material. This could imply that prolong soaking of the specimens might give lower CBR values.



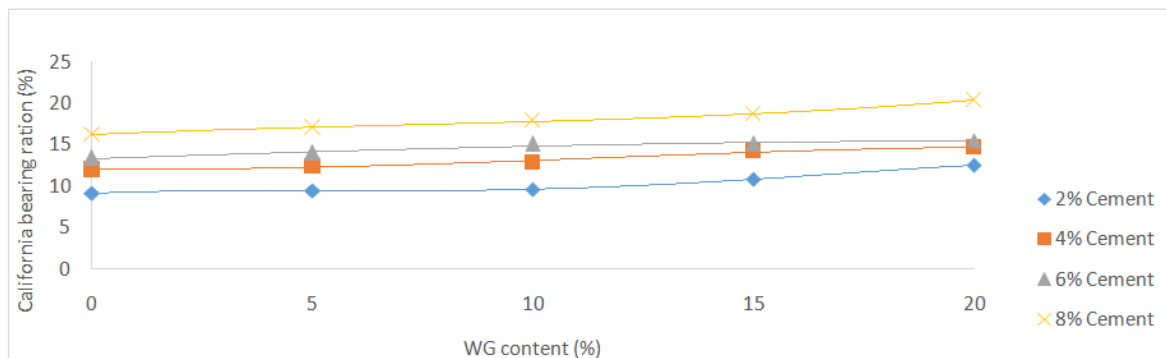


Figure 12: variation of soaked CBR of OPC stabilized BCS with WG content

## Conclusions

From the experimental results of the investigations, the following conclusions can be made:

- The addition of WG resulted in the reduction of plasticity index, thus given rise to greater workability when compared to untreated clays.
- The addition of WG resulted in a reduction in Optimum Moisture Content and increased the Dry Density of cement stabilized BCS with WG content for Standard and Modified compactive efforts.
- The results also showed that WG may be substantially used to improve the Unconfined Compressive Strength (UCS) of treated soils.
- The CBR values obtained for the OPC/WG stabilized soils gave higher values obtained for the untreated soil.

## References

- AASHTO. (1986). Standard specification for transportation materials and methods of sampling and testing, 14<sup>th</sup> Ed., Washington, D.C.
- Arabani, M., Sharafi, H., Habibi, M.H. and Haghsheenas, E. (2012). "Laboratory evaluation of cement stabilized crushed glass-sand blends". Electronic Journal of Geotechnical Engineering (EJGE), Vol. 17, pp 1777-1792.
- ASTM. (1992). Annual book of ASTM standards, Vol. 04.08, Philadelphia.
- Bignozzi, M. C., Saccani, A., and Sandrolini, F. M. (2009), waste glass from glass separated collection: An eco-sustainable addition to new building materials. Waste Management. 29, pp. 329-334.
- BS 1377 (1990). Methods of Testing Soils for Civil Engineering Purposes. British Standard Specification. London.
- BS 1924 (1990). Methods of Tests for Stabilized Soils. British Standard Specification. London.
- Byars, E.A, Morales, B., and Zhu, H.Y. (2004a), ConGlassCrete I. [Online] Centre of Cement and Concrete. University of Sheffield. Published by: The Waste and Resources Action Programme. Available at: <http://www.wrap.org.uk/downloads/ConGlassCreteIFinalBody.c242a657.445.pdf>
- Chen, F.H. (1988). "Foundations on Expansive Soils." Developments in Geotechnical Engineering. Vol.54, Amsterdam: Elsevier Science Publishing.
- Costa, J.K. and Baker, V.R. (1981). Surficial Geology, "Building with the Earth" John Wiley, New-York.
- Dennis, C.G., Patricia, M.G., Wartman, J., Liu, Y. and Carnivale, M. (2006). "Laboratory Evaluation of Crushed Glass-Dredged Material". Journal of Geotechnical Engineering, ASCE 562-590.
- Dyer, T.D. and Dhir, R.K. (2001). "Chemical Reactions of Glass Cullet used as Cement Component" Journal of Materials in Civil Engineering, 13(6), pp. 412-417.
- Eberemu, Adrian O., Amadi, Agapitus.A., and Lawal Mohammed, (2012) "The Geotechnical properties of black cotton soil treated with crushed glass cullet." Nigerian Journal of Technological Research
- Grubb, D. G., Davis, A., Sands, S. C., Carnivale, M., III, Wartman, J., Gallagher P. M. and Yigang Liu (2006) Laboratory Evaluation of Crushed Glass-Dredged Material Blends. Journal of Geotechnical and Geo-environmental Engineering, 132:5\_562\_576.
- Ingles, O.G. and Metcalf, J. B. (1972). Soil stabilization principles and practice. Burtterworths, Sydney, 103-144.
- Khmiri, A., Chaabouni, M. and Samet, B., (2013). "Chemical behaviour of ground waste glass when used as partial cement replacement in mortars". Construction and building materials, 44, pp. 74-80.
- Matawal, D. S., Umar, S. Y. and Bala, Y. U. (2006). Effect of Oil Palm Ash (OPA) on Cement Stabilized Soil. Journal of Civil Engineering, Nigerian Institution of Civil Engineers, Vol. 5, No. 3, pp. 5 – 12.
- Mishra, A. K., Dhawan, S. and Rao, M. S. (2008). "Analysis of swelling and shrinkage behavior of compacted clays". Geotechnical and Geological Engineering, 26(3), 289–298
- NBRRI, (1983). Engineering properties of black cotton soil of Nigeria and related pavement design. Nigerian building and road research institute, research paper No. 1-20.
- Nigerian general specification-Roads and bridges. (1997). Federal Ministry of Works, Lagos
- Nwaubani, S.O. (2013). Fineness of Waste Glass Powder and the Influence on Properties of Cement Mortars. International Journal of Civil Engineering and Building Materials, Vol. 3, No. 3, pp. 106-114.
- Ola, S.A. (1981). Stabilization of Maiduguri black cotton soils of Nigeria with sands. Bulletin of the International Association of Engineering Geology, No.24, Page 145-150. AACHEN/ESSEN 1981.

- [22]. Osinubik.j., Ijimdiya T.S., Nmadu I, (2009). 'Lime Stabilization of Black Cotton Soil Using Bagasse Ash as Admixture.' *Advanced Materials Research*, Volumes 62 - 64, pp.3-10. In: *Advances in Materials and Systems Technologies II*. On line <http://www.scientific.net/AMR.62-64.3>. Trans Tech Publications, Switzerland.
- [23]. Shayan, A., Xu, A. (2004). Value-added utilization of waste glass in concrete. *Cement and Concrete Research* 34 (1), 81–89.
- [24]. Shelke, A.P. and Murthy, D.S. (2010). "Reduction of Swelling Pressure of Expansive Soils Using EPS Geofom." *Indian Geotechnical Conference* (2010).
- [25]. TRRL (1977), "A guide to the structural design of Bitumen surfaced Roads in tropical and Sub – Tropical countries", Transport and Road Research Laboratory, Road Note 31, H. M. S. O. London.
- [26]. Wartman, J., Grubb, D. G. & Strenk, P. (2004). Engineering properties of crushed glass soil blends. *Geotechnical engineering for transportation projects*. ASCE, New York, pp. 732-739.
- [27]. Wu, S., Yang, W. and Xue, Y. (2003). *Preparation and Properties of Glass-asphalt Concrete*, Key Laboratory for Silicate Materials Science and Engineering of Ministry of Education, Wuhan University of Technology, Wuhan 430070, P.R China.

## Studies on Shelf-Life of Six Promising Mango (*Mangiferindica* L.) Cultivars under Favorable Condition

\*K. Venkat Reddy

Research scholar, Management Science, JNTU, Hyderabad

**ABSTRACT:** Six mango hybrids, Amrapali, Mallika, Neeleshan, Prabhashankar, Ratna, Sabri and Langra were taken as local check to study their shelf life. The PLW and spoilage of fruit increased with prolongation of storage period, regardless of cultivars. On termination day of storage (10<sup>th</sup> day) the minimum PLW (16.65%) and spoilage (28.36%) was noted in Mallika while highest PLW (32.85%) and spoilage (42.67%) were obtained in check variety Langra. TSS content in fruits increased up to 8<sup>th</sup> day and further extension in storage period it declined in other cultivars. On concluding day of experiment (8<sup>th</sup> day) the maximum TSS was noted in Mallika (23.02°Brix) while the lowest was obtained in Langra (18.12°Brix). Total sugar enhanced gradually up to 8<sup>th</sup> day of storage, except in Mallika which showed increasing trend up to 10<sup>th</sup> day. On last day of storage the maximum total sugars was noticed in Mallika (14.98%) however, the lowest was recorded in Langra (11.74%). On 8<sup>th</sup> day of storage Mallika was organoleptically rated as excellent. On last day of storage, Amrapali, Mallika were fair while rest of the cultivars were under poor grade quality. The keeping quality of Mallika, Ratna and Amrapali were better than other hybrids and check variety Langra. Especially fruits of Mallika can be stored for longer period at ambient conditions.

### I. INTRODUCTION

Mango (*Mangifera indica* L.) is a diffuse-porous species and one of the most important tropical tree crops (Lu et al., 2000) belongs to the family Anacardiaceae (Morton, 1987). Mango fruits have increasing commercial importance throughout the world and are a valued source of income in all mango producing countries (Siddiqui, 2008; Siddiqui et al., 2014). It is an important fruit crop of India acknowledged as “King of fruits” and the “national fruit of India”. Mango is widely grown for its special features like high nutritive value, high productivity, Processing potential, delicious taste and suitability to be grown in widely ecological amplitude. Reputed as fruit for excellence, mango has assumed a leading position among commercial fruits (Singh, 2004). In India, mango accounts approximately 2.70 million hectare area and 18.30 million tonnes production (NHB, 2013) having superior position in the world market. Apart from the use of ripe mango, young and unripe fruits are utilized for culinary purposes as well as for preparing pickles, chutneys and amachur. Like all other fresh commodities, the potential market of mango is directly correlated with the quality of the fruits. To facilitate access to the domestic and offshore markets, mango fruit storage potential and fruit quality consistency needs to be improved (Simmons et al., 1997). Further keeping quality of fruits is also an important criteria during the selection of varieties to a particular region. Most of the present day cultivars appeared to have been selected for characters like size, quality and period of maturity. An increase in the storage life and improvement of mango fruits quality is really desirable to prevent these gluts in the market and to curtail the post-harvest losses (Siddiqui et al., 2014a). So during the selection of a variety, high yield potential with longer shelf life are important aspects to fulfill the demand of the day. Keeping all the above facts under considerations the present investigation was carried out with eleven released hybrids from different parts of the country with local check variety Langra.

### II. MATERIALS AND METHODS

#### Mango Hybrids for Experiment

The experiment was carried out on fruits from the 15 years old healthy plants of six hybrids of mango as well as the most important variety of this region Langra was also included as check. Selected hybrids were Amrapali, Mallika, Neeleshan, Prabhashankar, Ratna, Sabri, and Langra (check) and used as treatments T1, T2, T3, T4, T5, T6 and T7 respectively. All the 6 treatments were replicated thrice times.



**Evaluation of shelf life of fruits**

All the observations of the fruits under storage were determined at 2 days interval starting from the date of harvesting till the end of storage. The standard methods for the estimation of physico-chemical parameters are described here.

**Physiological loss in weight (PLW)**

To estimate the PLW, initial weight of fruits under each treatment was measured replication wise at the time of storage and final weight was also measured at end of storage. PLW was computed in terms of percentage of initial weight basis.

**Spoilage loss of fruits**

The spoiled fruits on each day of observations were separated out from all the treatments and weighed separately. The percentage of spoiled fruits on each day of observation from each treatment was calculated.

**Changes in Total Soluble Solids (TSS)**

The Total Soluble Solids of fruits was recorded with the help of a hand refractometer (Rangana, 2010). It was determined by applying 2 drops of homogenized juice on the prism of hand refractometer. TSS (°Brix) was noted directly from the digital screen at room temperature ( $30^{\circ}\text{C} \pm 2$ ).

**Organoleptic evaluation**

To assess the acceptability of consumer studies on organoleptic evaluation were conducted by score card system with a panel of five semi trained judges. They evaluated the colour, flavour, taste, appearance and overall acceptability of fruits on the basis of 9-point Hedonic scale (Amerine et al., 1965). The observations were conducted when the 75 per cent fruits ripened. Sensory evaluation of mango fruits of different cultivars during storage was recorded from 6th day of storage at three days intervals.

**Statistical methods**

Observations recorded during the investigation were subjected to analysis of variance using completely randomized design as described by Cooharan and Cox (1975) and the significance of different source of variation was tested by error mean square by 'F' test.

### III. RESULTS

The physiological loss in weight (PLW) of fruits during storage was recorded at four day interval. It is evident from the Table-1 that in all the cultivars as the day of storage increased the PLW gradually and significantly increased till the last day of storage. At the last day of storage (10th day) Mallika gave lowest PLW (16.65%) and proved its superiority over remaining cultivars. The highest PLW (40.85%) was observed in check variety Langra followed by Ratna (31.60%) and Sabri (30.96%).

**Spoilage loss of fruits (per cent)**

The spoilage losses during storage of different cultivars are presented in Table-2. At the 16th day of storage the minimum spoilage loss (28.36%) was also observed in cultivar Mallika, however, it was found uneconomical due to more than 12% spoilage while the highest spoilage loss (52.67%) was recorded in check variety Langra followed by Ratna (54.51%) and Sabri (51.34%).

**Changes in Total soluble solids (°Brix) during storage**

The data regarding to total soluble solids (TSS) content of the stored fruits are given in Table-3. The TSS content of mango fruits increased with advancement of storage period up to 8th day of storage, irrespective of cultivars and thereafter it declined on last day of storage (10th day). However, in case of Amrapali and Langra it was declined after 8th day. At the termination day (10th day) of experiment the highest TSS (25.02 °Brix) was noticed in Mallika. While the lowest TSS (14.180°Brix) was recorded in check variety Langra followed by Neeleshan (19.960°Brix) and Sabri (20.120°Brix).

**Organoleptic evaluation of fruits**

Organoleptic scores (Table-4) increased gradually up to 6th day of storage, irrespective of cultivars except Mallika which showed increasing trend up to 8th day of storage. The maximum organoleptic score (96.64) was obtained on 6th day in check variety Langra and considered as excellent grade which was statistically similar to Amrapali (96.24) followed by Sabri (90.64) while remaining cultivars are organoleptically rated as good. On 8th day of storage organoleptically excellent rating was obtained only in Mallika (91.33). The cultivars Amrapali

(82.42) were organoleptically rated as good and rest of the cultivars showed either fair or poor grade. On termination of experiment (10th day) none of the cultivars organoleptically rated either as excellent or good grade. Organoleptically fair grade was obtained in Mallika (78.46), Amrapali (74.20) whereas remaining cultivars showed poor grade.

#### IV. DISCUSSION

##### Physiological loss in weight (PLW)

During the course of investigation it was observed that physiological loss in weight (PLW) increased significantly with the increasing period of storage, irrespective of cultivars. Similar results were obtained in the work done on banana (Parmar and Chundawat, 1984, Emerald and Sreenarayanan, 1999), Sapota (Siddiqui et al., 2014b, Gautam and Chundawat, 1990, Sarkar et al., 1995) and mango (Singh et al, 1993 and Singh et al., 1998). The lowest PLW was noted in Mallika which showed superiority over remaining cultivars while the maximum PLW was obtained in check variety Langra. The higher rate of PLW in Langra might be due to early ripening consequently enhanced rate of various physiological and degradative metabolic processes during storage. These results get support from the work of Singh et al., (2004) and Gill and Dhillon (2008) in mango. The higher weight loss in mango fruits might be due to greater loss of moisture owing to higher rate of evapo-transpiration and respiration through uninterrupted atmospheric column under higher temperature and low relative humidity. The thinner skinned fruits with less waxy coating may show more PLW while the reverse is true with thick-skinned fruits.

##### Spoilage of fruits

The spoilage of fruits increased successively with the prolongation of storage period, irrespective of cultivars. The cultivar Mallika gave the lowest spoilage loss during storage at all the days and check variety Langra produced the highest spoilage loss. Similar increase in rotting of fruit with the decline in acid content is at least impart due to utilization of organic acids in energy production and alcoholic fermentation (Purvis, 1933). Delayed ripening, slower rate of physiological events and reduced biochemical degradation might be responsible for high acid in cultivar Mallika. Decline in titratable acidity during storage as a result of conversion of acids into salts and sugars have also been obtained by Gill and Dhillon (2008), Kumar et al. (1992) and Joshi and Roy (1985) in mango.

##### The total soluble solids

The total soluble solids of the mango fruits enhanced gradually and significantly upto 12th day, regardless of cultivars. However in case of Amrapali and Langra it declined after 8th day of storage. During storage TSS of mango fruits increased with the advancement of storage period was also reported by Joshi and Roy (1985), Tirmazi and Wills (1981) and Kumar et al. (1992). According to Stahl and Cambell (1936) the conversion of cell wall materials such as pectin and hemicellulose in reducing substances during storage are responsible for increasing TSS in fruits. The increase in TSS may be accounted to the moisture loss, hydrolysis of polysaccharides and conversion of organic acids into sugars. The decrease in TSS on prolonged storage could be due to greater utilization of reserved sugars in respiration process during prolonged storage. Slow and gradual increase in TSS in cultivar Mallika might be due to delay in ripening. These findings elucidate the reports of Garget et al. (1976), Singh (1988) and Khader (1989), Dutta et al. (2008) and Gill and Dhillon (2008) in mango.

##### Organoleptic qualities

The majority of the factors rated good up to 8th day of storage to all the cultivars however Amrapali and Mallika fruits rated good up to 12th day of storage. The faster rate of senescence might be responsible for the deterioration in the qualities of fruits. The texture becomes soft due to solubilization of pectic substances from the middle lamella whereas loss of the flavour might be due to disintegration of flavouring substances like ketones and aldehydes. The deterioration in shape, colour and general appearance might be due to physiological changes and shrinkage caused by loss of moisture from the tissues of fruits. Kapse et al. (1985), Ranjan (1992) and Gill and Dhillon (2008) also found more or less similar trend of deterioration in mango fruits during storage.

Table 1: Changes in physiological loss in weight (%) during storage

Treatment	Cultivar	Days of storage						Mean
		0	2	4	6	8	10	
T1	Amrapali	0.00	2.85 (9.72)	5.76 (19.89)	8.62 (17.07)	15.12 (22.88)	26.17 (30.76)	11.70 (18.86)
T2	Mallika	0.00	2.06 (8.25)	3.98 (11.51)	5.65 (14.94)	10.17 (18.59)	18.65 (25.58)	8.10 (16.65)
T3	Neeleshan	0.00	4.10 (11.68)	6.87 (15.19)	12.64 (20.82)	21.16 (27.38)	30.15 (33.30)	14.98 (21.68)
T4	Prabhashankar	0.00	3.49 (10.77)	6.38 (14.63)	11.23 (19.58)	17.26 (24.54)	26.18 (30.77)	12.91 (20.06)
T5	Ratna	0.00	2.12 (8.37)	6.00 (14.18)	10.82 (19.20)	15.31 (23.03)	22.35 (28.21)	11.32 (18.60)
T6	Sabri	0.00	4.30 (11.97)	7.84 (16.26)	14.16 (22.10)	22.10 (28.04)	30.96 (33.80)	15.87 (22.43)
T7	Langra (check)	0.00	5.61 (13.70)	8.12 (16.55)	16.32 (23.82)	24.81 (29.87)	34.85 (36.18)	17.94 (24.03)
C.D. at 5% CV	T = 1.38 5.54%							

Table 2: Spoilage Loss (%) in fruits during storage

Treatment	Cultivar	Days of storage						Mean
		0	2	4	6	8	10	
T1	Amrapali	0.00	0.00	3.16 (10.24)	10.24 (18.66)	18.54 (25.50)	39.26 (38.79)	14.24 (18.64)
T2	Mallika	0.00	0.00	2.08 (8.29)	5.64 (13.74)	10.16 (18.58)	22.36 (28.22)	8.05 (13.77)
T3	Neeleshan	0.00	0.00	5.16 (13.13)	13.12 (21.23)	24.10 (29.40)	45.28 (42.29)	17.53 (21.21)
T4	Prabhashankar	0.00	0.00	5.46 (13.51)	11.89 (20.17)	21.76 (27.80)	41.82 (40.29)	16.19 (20.35)
T5	Ratna	0.00	0.00	3.74 (11.15)	8.24 (16.68)	16.48 (23.95)	32.54 (34.78)	12.20 (17.31)
T6	Sabri	0.00	0.00	6.14 (14.34)	17.26 (24.54)	27.35 (31.53)	51.34 (45.77)	20.42 (23.24)
T7	Langra (check)	0.00	0.00	7.24 (15.61)	18.46 (25.44)	30.42 (33.47)	58.67 (50.00)	22.96 (24.90)
C.D. at 5% CV	T = 0.59 8.94%							

Table 3: Changes in TSS contents of fruit during storage

Treatment	Cultivar	Days of storage						Mean
		0	2	4	6	8	10	
T1	Amrapali	16.28	19.35	21.74	24.22	22.96	21.45	21.00
T2	Mallika	11.24	14.65	16.84	19.54	23.56	23.02	18.14
T3	Neeleshan	11.84	12.70	17.95	20.68	21.18	19.96	17.39
T4	Prabhashankar	10.88	12.96	16.88	20.72	22.16	20.65	17.38
T5	Ratna	11.24	16.48	19.35	22.64	23.78	21.06	19.09
T6	Sabri	13.20	15.64	18.84	21.45	22.10	20.12	18.56
T7	Langra (check)	13.75	17.14	19.34	20.84	19.46	18.18	18.12
C.D. at 5% CV	T = 0.52 2.90%							

**Table 4: Changes in organoleptic quality of fruits during storage**

Treatment	Cultivar	Days of storage				Mean
		4	6	8	10	
T1	Amrapali	94.35	96.24	82.42	74.20	86.80
T2	Mallika	76.30	85.28	91.33	78.46	82.84
T3	Neeleshan	73.68	80.31	77.49	61.37	73.21
T4	Prabhashankar	72.32	81.48	76.26	60.17	72.56
T5	Ratna	74.40	82.55	72.42	64.28	73.41
T6	Sabri	78.00	90.64	62.10	58.25	72.25
T7	Langra (check)	90.27	96.46	60.21	40.46	71.85
C.D. at 5%	T = 1.52					
CV	7.58%					

## V. CONCLUSION

On the basis of physiological attributes of fruits it can be concluded that the keeping quality of Mallika, Ratna and Amrapali were better than other hybrids and check variety Langra. Fruits of Mallika can be stored for a longer period of storage at ambient conditions. Results clearly indicated that PLW, Spoilage, TSS total sugars were increased however, organoleptic quality reduced during storage period of mango hybrids. It be inferred that cultivars Mallika maintained organoleptically excellent grade up to 8th day of storage while Amrapali rated as good grade. Post-harvest life of all the hybrids under trial was found better than Langra. Mango hybrid Mallika can prefer for long time storage and it would be also helpful in the long transportation.

## REFERENCES

- [1] Cochran, W.G. and Cox, G.M. 1957. Experimental designs, 2nd Edition, John Willy and Sons.
- [2] Inc New York, Cubin M.
- [3] Emerald, M.E.F. and Sreenarayanan, V.V. 1999. Prolonging storage life of banana fruits by sub
- [4] atmospheric pressure. Indian Food Packer, 53(3): 22-25.
- [5] Joshi, G.D. and Roy, S. K. 1985. Effect of integrated post-harvest handling on bio-chemical
- [6] changes in Alphonso mango fruits. Progressive Horticulture, 17: 56-63.
- [7] Lu, P., Muller, W. and Chacko, E.K. 2000. Spatial variations in xylem sap flux density in the trunk of
- orchard-grown, mature mango trees under changing soil water conditions. Tree Physiology 20: 683–
- 692.
- [8] Morton, J.F. 1987. Mango. In: Fruits of warm climates. Morton, J.F. and Miami, F.L. (eds). Creative
- Resources Systems, Inc. pp. 221-237.
- [9] Ranjan, S. 1992. Screening of mango cultivars for processing. Thesis submitted for M. Sc. (Ag.) degree
- R.A.U., Pusa, Bihar.
- [10] Siddiqui, M.W. 2008. Studies on some aspects of mango ripening. M.Sc. Thesis. Bidhan Chan Krishi
- Vishwavidyalaya, Mohanpur, Nadia, West Bengal, India.
- [11] Siddiqui, M. W., Dutta, P., Dhua, R. S. and Dey, A. 2014a. Changes in biochemical composition
- [12] Of mango in response to pre-harvest gibberellic acid spray. Agriculturae Conspectus Scientificus
- (ACS), 78(4): 331-335
- [13] Singh, D. 2004. Current mango varieties situation and future trends in India. In: Mangoes in
- Pakistan. (Ed.): S. Ahmad. The Horticultural Foundation of Pakistan. 101-105
- [14] Tirmazi, S.I.H. and Wills, R.B.H. 1981. Retardation of ripening of mangoes by post-harvest application
- of calcium. Crop Agriculture, 58: 137-139.

## Mechanical Behaviour and Microstructural Characterization of Carbon Steel Samples from Three Selected Steel Rolling Plants

P. O. Atanda<sup>1</sup>, A. A. Abioye<sup>1,2\*</sup>, A. O. Iyiola<sup>1</sup>

<sup>1</sup> Department of Materials Science and Engineering, Obafemi Awolowo University, Nigeria.

<sup>2</sup> Department of Engineering (Modelling and Simulation), PASAD Research Innovations Nigeria, Lagos, Nigeria.

**Abstract :** The research investigated the mechanical behavior of samples of steel rods obtained from three selected Steel Rolling Companies in South Western part of Nigeria. This was done by carrying out some mechanical tests such as tensile, impact and hardness as well as microstructural examination. Four sets of 16 mm steel rod samples were collected from Tiger steel industries, Phoenix steel and Oxil steel Industries, all located in South West Nigeria. The chemical composition was carried out using a Spectrometer (EDX3600B). Afterwards, different samples were prepared, cut and machined according to ASTM standards dimensions of tensile and impact tests as well as hardness test from which their Ultimate tensile Strength, Yield strength, Percentage elongation, Impact strength and Brinell hardness number were obtained and compared to three standards (ASTM A706, BS 4449 and Nst 65-Mn). Their microstructures were also examined and analyzed. The results showed that the Ultimate tensile strength for the samples from Oxil steel, Phoenix Steel and Tiger steel were  $661 \text{ N/(mm)}^2$ ,  $653 \text{ N/(mm)}^2$  and  $631 \text{ N/(mm)}^2$  respectively while their hardness values were 150 BHN, 178 BHN, 214 BHN respectively. The sample from Tiger steel and Oxil Steel had the finest and most coarse microstructure respectively. In conclusion, it was observed that the results of the sample analysis from the three selected Steel Rolling Companies conformed to most of the standards except the sample from Tiger steel which had a high hardness value compared to the standard.

**Key words:** Microstructures, Tiger steel, Phoenix steel, Oxil steel, steel rolling, characterization

### I. Introduction

According to Smallman and Bishop (1999), determination of the structural character of a material, whether massive in form or particulate, crystalline or glassy, is a central activity of materials science. Through the last few decades a category of steels known as high strength steels have undergone constant research (Bello, 2007 and Sinha, 1989). Nowadays, need of steels has soared up due to newly introduced massive construction projects in civil, mechanical, naval, aeronautical engineering and in other engineering fields. Particularly in developing countries, such as in Ethiopia, India, and China, steel materials are used extensively to develop infrastructure such as road, power, water, and telecommunication (Dawit and Kidan, 2013).

Plain carbon steels are widely used for many industrial applications and manufacturing on account of their low cost and easy fabrication (Smith and Hashemi, 2006). According to Rajan *et al.* (1988), steels with carbon content varying from 0.25% and 0.65% are classified as medium carbon, while those with carbon up to 0.25% C, are termed low carbon. High carbon steels usually have carbon content ranges between 0.65% - 1.5%.

Steel had been produced in bloomery furnaces for thousands of years, steel's use expanded extensively after more efficient production methods were devised in the 17<sup>th</sup> century for blister steel and then crucible steel. With the invention of the Bessemer process in the mid-19<sup>th</sup> century, a new era of mass-produced steel began. This was followed by Siemens-Martin process and then Gilchrist-Thomas process that refined the quality of steel. With their introductions, mild steel replaced wrought iron. Further refinements in the process, such as basic oxygen steelmaking (BOS) in which carbon-rich molten pig iron is made into steel and the Bessemer process, largely replaced earlier methods by further lowering the cost of production and increasing the quality of the metal (Kelle, 1968). Steel with low carbon content has the same properties as iron, soft but easily formed (Smith and Hashemi, 2006). As a result, it can be rolled thin into products like car body panels. It is also extensively used in building and construction works to reinforce concrete. Low carbon steel is the most common form of steel due to the fact that its material properties are acceptable for many applications (Al-Qawabah *et al.* 2012). They are extensively used in making beams and structural shapes for bridges and buildings. In such applications, accurate and precise conformance to standard is highly important as consequences of deviations from these standards and specifications often result in failure while in service. Instances of collapse of buildings in the country which often result in fatal

loss of lives and properties are notable examples of this. Hence, the need to carry out this research on the mechanical behaviour and material characterization of various low carbon steels produced in certain companies within the country becomes imperative. This research covered the study of some mechanical behaviour of the carbon steel samples produced from three selected companies, case studies of Oxil and Phoenix steel, Lagos state, Nigeria and Tiger steel Industries and comparison of the test results with standards.

## II. Methodology

The materials that were used for the project research were samples of carbon steel produced by three selected steel rolling plants which includes: Phoenix Steel Mills Limited in Ikorodu, Lagos, Tiger Steel Industries and Oxil Steel Company in Lagos. The samples were subjected to some mechanical tests which include tensile test, hardness, impact test and fatigue test as well as metallographic analysis. Furthermore, the characterization of the microstructure of the carbon steel samples was also carried out. The chemical analysis of the samples was carried out. Afterwards, the samples from the three steel rolling plants were machined according to the requirements of tensile and impact test. Two samples produced from each of the three steel rolling plants were prepared for each of tensile, impact, and hardness test as well as for the microstructural analysis through metallography. The chemical analysis revealed the chemical composition of the samples i.e. the percentage composition of each element present in the samples is as shown in Table 1.

The tensile test specimens were prepared according to the dimension specifications of the Instron tensile testing machine by machining them using a CNC lathe (CK6132). The standard tensile test samples were subjected to tensile test using the Instron tensile testing machine (Series 3369, Load Cell Capacity 50KN) and a stress-strain curve was plotted from which the percentage elongation (ductility), yield strength and ultimate tensile strength was determined.

The hardness test was carried out using a manually operated Brinell hardness tester. A small cylindrical part of the samples from each of the three steel rolling plants were cut and grinded to get a flat surface after which they were indented by a 10 mm hardened steel ball under a load of 750 kgf for a period of about 15 seconds. The samples were then removed from the Brinell hardness tester after which the diameter of the indentation was read using the Brinell microscope. The hardness value was determined by corresponding the diameter of the indentation with the corresponding hardness value from the Standard table of Brinell hardness number. In order to confirm this hardness values, they were also calculated using the equation 1 below.

$$BHN = \frac{2F}{\pi D[D - \sqrt{D^2 - d^2}]} \quad (1)$$

Where

F is the imposed load (in kg).

D is the diameter of the spherical indenter (in mm).

d is the diameter of the impression of the indenter (in mm).

For this project research, the Izod impact test was employed to determine the impact property. The microstructural characterization of the samples was carried out by cutting the samples using sectioning machine. The samples were mounted in Bakelite using mounting machine, the grinding of the samples were done using grinding machine with emery paper 400, 800, 1000 and 1200µm to obtain mirror like surface. The surfaces were then polished using polishing paste on emery cloth to remove the scratches. Etching of the samples were carried out using nital after which the microstructures were examined using a metallurgical microscope.

## III. Results and Discussion

The result of chemical analysis carried out revealing the percentage composition of elements in the sample is shown in Table 1.

**Table 1:** Table showing the result of chemical composition of the steel samples

Chemical Composition	%C	%Fe	%Mn	%S	%P	%Si	%Cu
OXIL STEEL	0.327	98.171	0.574	0.056	0.077	0.230	0.246
PHOENIX STEEL	0.391	97.975	0.542	0.059	0.086	0.225	0.284
TIGER STEEL	0.488	98.025	0.569	0.045	0.068	0.159	0.235

After the samples underwent the impact test using the Housefield balanced impact testing machine, the amount of energy absorbed by each of the samples from the three steel rolling plants were shown in Table 2.



**Table 2:** Table showing the result of impact test

	<b>IMPACT STRENGTH</b> <b>(1 ft-lb = 1.3558179483314J)</b>	
	<b>In Foots-pound(ft-lb)</b>	<b>In Joules(J)</b>
<b>OXIL STEEL</b>	43.50	58.98
<b>PHOENIX STEEL</b>	41.90	56.81
<b>TIGER STEEL</b>	36.95	50.10

Using the Brinell hardness tester to carry out the hardness test using a 10mm steel ball indenter with a 750 kg load, indentation was made on each sample from the three steel rolling plants. The diameter of indentation was determined using a brinell microscope. The Brinell hardness numbers were as calculated using equation 1 and results tabulated as shown in Table 3:

**Sample from Oxil Steel**

Diameter of indentation, d =2.5mm

$$BHN = \frac{2(10)}{\pi(10)[10 - \sqrt{(10^2 - 2.5^2)}]}$$

$$BHN = 150.36$$

**Sample from Phoenix Steel**

Diameter of indentation, d = 2.3mm

$$BHN = \frac{2(10)}{\pi(10)[10 - \sqrt{(10^2 - 2.3^2)}]}$$

$$BHN = 178.10$$

**Sample from Tiger Steel**

Diameter of indentation, d =2.1mm

$$BHN = \frac{2(10)}{\pi(10)[10 - \sqrt{(10^2 - 2.1^2)}]}$$

$$BHN = 214.1$$

**Table 3:** Table showing the result of the hardness test

	<b>Diameter of Indentation(mm)</b>	<b>Brinell Hardness Number(BHN)</b>
<b>OXIL STEEL</b>	2.50	150.36
<b>PHOENIX STEEL</b>	2.30	178.10
<b>TIGER STEEL</b>	2.10	214.12

The tensile test samples were subjected to tensile test using the Instron tensile testing machine after which stress-strain graph were generated for the three steel rolling plants (Oxil, Phoenix and Tiger steel Industries) samples as shown in Figures 1-3. From the corresponding data generated, the Ultimate tensile strength (UTS), yield strength and percentage elongation were as determined below;

Original gauge length is 30 mm

Diameter of the tensile samples is 4 mm

$$\text{Area, } A = \pi r^2$$

$$r = \frac{d}{2}$$

Where r is the radius of the tensile sample

d is the diameter of the tensile sample.

$$\text{Therefore, } A = \pi \left(\frac{4}{2}\right)^2$$

$$\text{Area of the tensile samples is } 12.57\text{mm}^2$$

**Sample from Oxil Steel**

$$\text{Ultimate tensile strength, UTS} = \frac{\text{Maximum load}}{A}$$

Maximum load (Oxil Steel) is 8301.50 N

$$\text{UTS} = \frac{8301.50}{12.57} \\ = 660.61 \text{N}/(\text{mm})^2$$

Ultimate tensile Strength (Oxil Steel) is approximately **661 N/(mm)<sup>2</sup>**

$$\text{Yield Strength} = \frac{\text{Load at yield}}{A}$$

Load at yield (Oxil Steel) is 5833.09N

$$\text{Yield Strength} = \frac{5833.09}{12.57} \\ = 464.18 \text{N}/(\text{mm})^2$$

Yield Strength (Oxil Steel) is approximately **464 N/(mm)<sup>2</sup>**

$$\text{Percentage Elongation} = \frac{\text{finalgaugelength} - \text{Originalgaugelength}}{\text{originalgaugelength}} \times 100$$

$$= \frac{9.64}{30} \times 100$$

$$= 28.79\%$$

Percentage elongation (Oxil Steel) is approximately **29%**

#### Sample from Phoenix Steel

$$\text{Ultimate tensile strength, UTS} = \frac{\text{Maximum load}}{A}$$

Maximum load (Phoenix Steel) is 8209.86 N

$$\text{UTS} = \frac{8209.86}{12.57} \\ = 653.32 \text{N}/(\text{mm})^2$$

Ultimate tensile Strength (Phoenix Steel) is approximately **653 N/(mm)<sup>2</sup>**

$$\text{Yield Strength} = \frac{\text{Load at yield}}{A}$$

Load at yield (Phoenix Steel) is 5668.31N

$$\text{Yield Strength} = \frac{5668.31}{12.57} \\ = 451.07 \text{N}/(\text{mm})^2$$

Yield Strength (Phoenix Steel) is approximately **451 N/(mm)<sup>2</sup>**

$$\text{Percentage Elongation} = \frac{\text{finalgaugelength} - \text{Originalgaugelength}}{\text{originalgaugelength}} \times 100$$

$$= \frac{8.26}{30} \times 100$$

$$= 27.54\%$$

Percentage elongation (Phoenix Steel) is approximately **28%**

#### Sample from Tiger Steel

$$\text{Ultimate tensile strength, UTS} = \frac{\text{Maximum load}}{A}$$

Maximum load (Tiger Steel) is 7935.53 N

$$\text{UTS} = \frac{7935.53}{12.57} \\ = 631.49 \text{N}/(\text{mm})^2$$

Ultimate tensile Strength (Tiger Steel) is approximately **631 N/(mm)<sup>2</sup>**

$$\text{Yield Strength} = \frac{\text{Load at yield}}{A}$$

Load at yield (Tiger Steel) is 5605.24N

$$\text{Yield Strength} = \frac{5605.24}{12.57} \\ = 446.05 \text{N}/(\text{mm})^2$$

Yield Strength (Tiger Steel) is approximately **446 N/(mm)<sup>2</sup>**

$$\text{Percentage Elongation} = \frac{\text{finalgaugelength} - \text{Originalgaugelength}}{\text{originalgaugelength}} \times 100$$

$$= \frac{8.35}{30} \times 100$$

$$= 27.83\%$$

Percentage elongation (Tiger Steel) is approximately **28%**

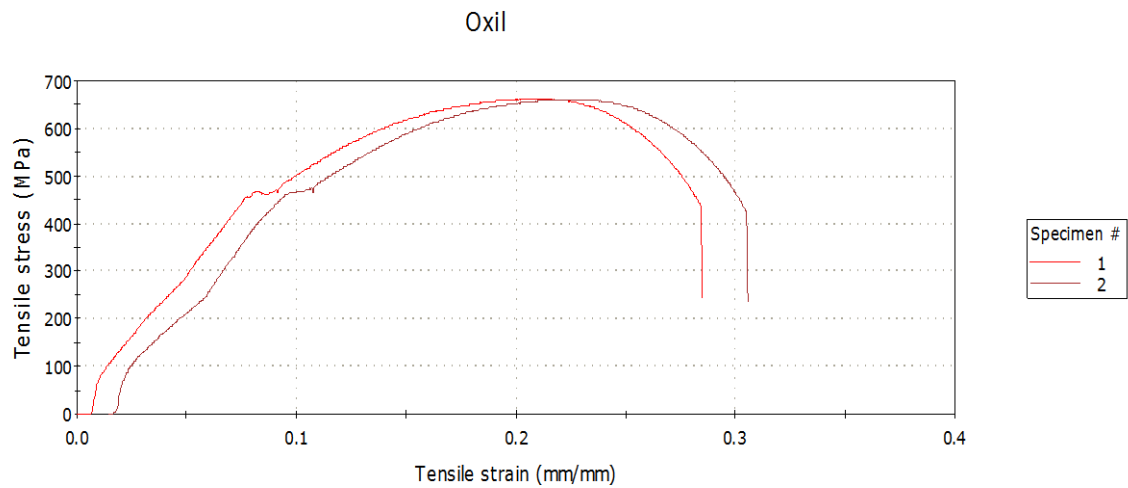


**Figure 1:** Stress Strain curve for samples from Oxil Steel Lagos

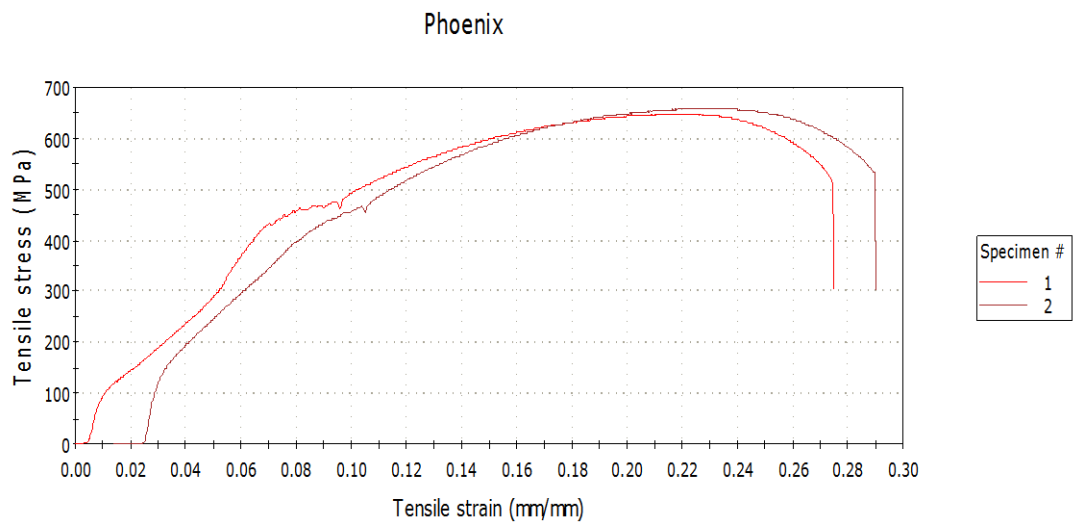


**Figure 2:** Stress Strain curve for samples from Phoenix steel Lagos

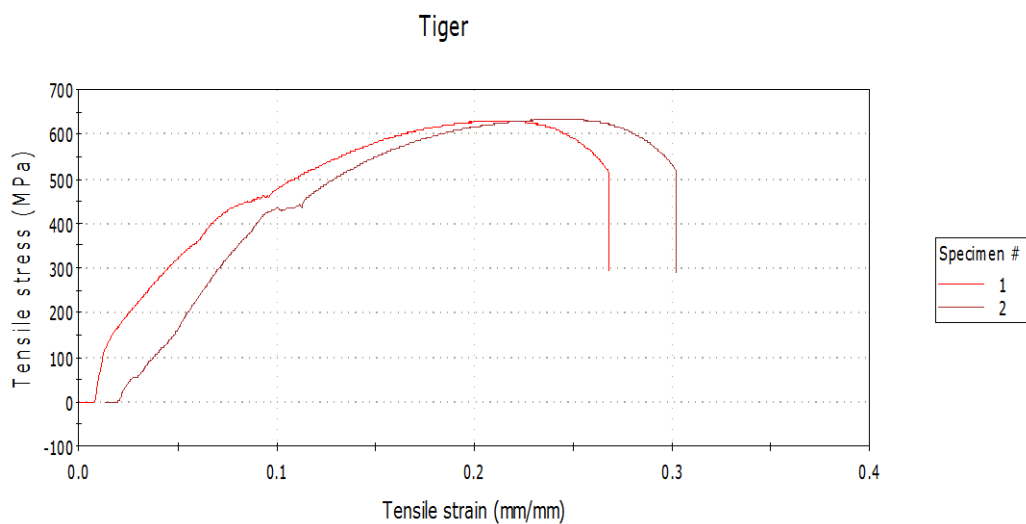
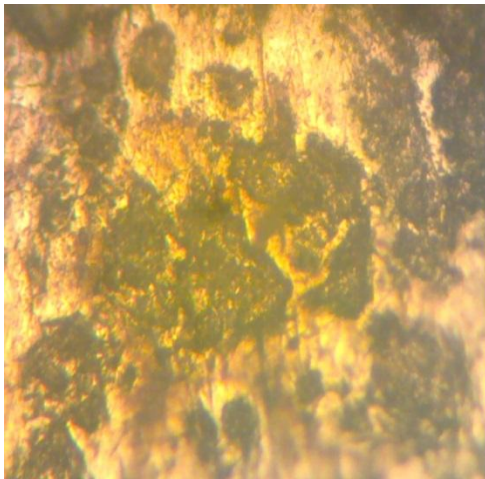


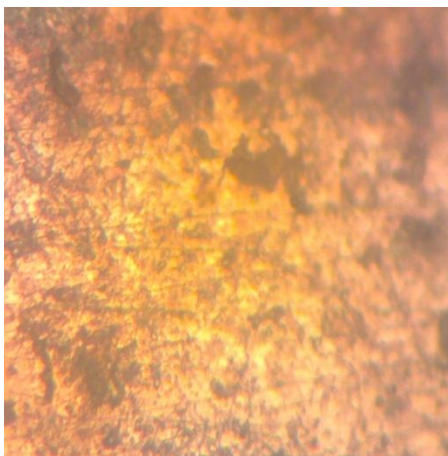
**Figure 3:** Stress Strain curve for samples from Tiger steel industry

The samples from the three steel rolling plants were subjected to observation under the metallurgical microscope in the laboratory after they were grinded and polished. The results were shown in Figures 4 – 6.



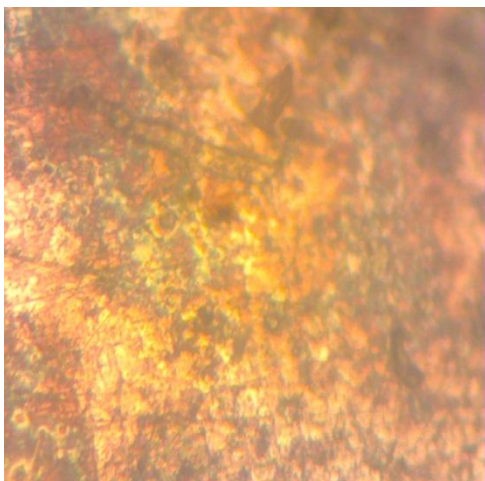
Dark patches-Pearlite Grains, Light areas- Ferrite Matrix

**Figure 4:** Microstructure of Oxil steel sample (X600)



Dark patches-Pearlite Grains, Light areas- Ferrite Matrix

**Figure 5:** Microstructure of Phoenix steel sample (X600)



Dark patches-Pearlite Grains, Light areas- Ferrite Matrix

**Figure 6:** Microstructure of Tiger steel sample (X600)

The elemental make-up of the samples from oxil steel company, Phoenix steel limited and Tiger steels as observed from the result of the chemical analysis carried out revealed a variation in the percentage of elements in the three samples. The percentage carbon content in the sample from Oxil steel was the least (0.327%). Slightly higher was the sample from Phoenix steel (0.391%) while the highest was Tiger steel sample (0.488%).

Comparison these values with the standards used (ASTM A706, Nst 65-Mn and BS 4449 of 1997 standards) as shown in Table 4 and Figure 7 it was seen that the three samples have higher values than all the three standards except Oxil steel which conforms within ASTM A706 and Nst 65-Mn. Phoenix Steel has the highest variation from the standards as its percentage carbon was far higher than any of the standards.

Considering the Sulphur and Phosphorus content, only the sample from Tiger steel fell within any of the three standards as the samples from Oxil steel and Phoenix steel did not conform to any of the standards. Observing the silicon content, all the samples conform to the standard except Tiger steel with the least silicon content (0.159%).

Based on the percentage carbon content of the three samples from the three steel rolling plants, they were all classified as medium carbon steels (between 0.3-0.6%).

**Table 4:** Table showing comparison of the chemical composition of samples with standards

%C	%Fe	%Mn	%S	%P	%Si	%Cu
BS 4449, 1997 0.25	Not Available	Not Available	0.05	0.05	Not Available	Not Available
ASTMA706 0.3	Not Available	1.5	0.045	0.035	0.5	Not Available
Nst 65-Mn 0.35	Not Available	1.6	0.04	0.04	0.3	0.025
<b>OXIL STEEL 0.327</b>	<b>98.171</b>	<b>0.574</b>	<b>0.056</b>	<b>0.077</b>	<b>0.230</b>	<b>0.246</b>
<b>PHOENIX STEEL 0.391</b>	<b>97.975</b>	<b>0.542</b>	<b>0.059</b>	<b>0.086</b>	<b>0.225</b>	<b>0.284</b>
<b>TIGER STEEL 0.488</b>	<b>98.025</b>	<b>0.569</b>	<b>0.045</b>	<b>0.068</b>	<b>0.159</b>	<b>0.235</b>

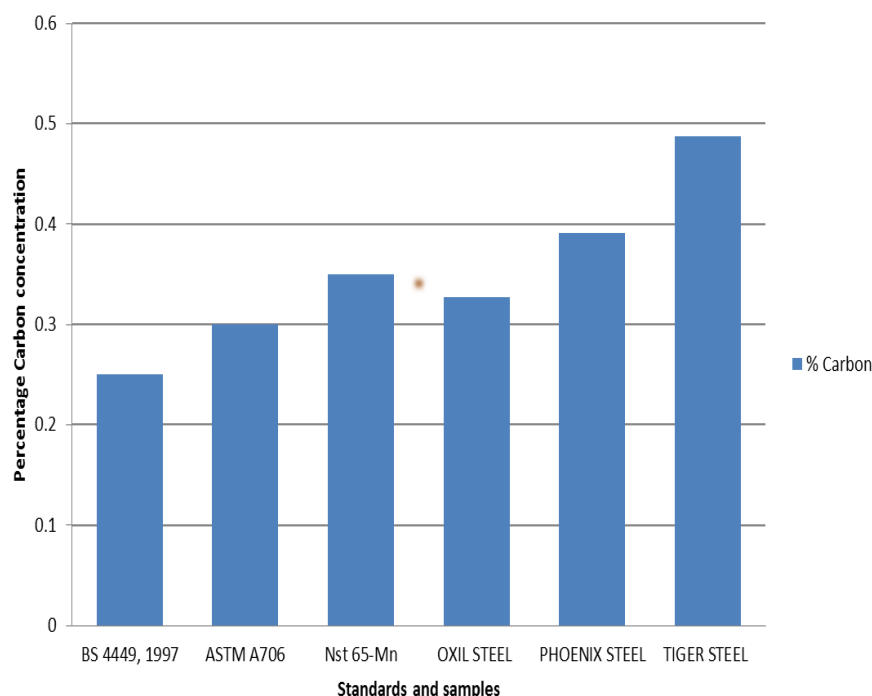


**Figure 7:** Chart showing the percentage carbon content of standards and samples from oxil steel, Phoenix steel and Tiger steel industries

From the results of the impact test, it was seen that the sample from Oxil steel has impact strength of 58.98J; sample from Phoenix steel has impact strength of 56.81J while the sample from Tiger steel has impact strength of 50.10J. Based on these results, the sample from Tiger steel has the least impact energy followed by the sample from Phoenix steel while the sample with the highest impact energy was the sample from Oxil steel. This meant that the sample from Oxil steel would absorb energy during fracture (could withstand more shock load) compared to the other two samples.

The result of the hardness test reveals that the sample from Oxil steel has 150 BHN, sample from Phoenix steel has 178 BHN while the sample from Tiger steel has 214 BHN. Therefore, the sample from Tiger steel has the highest hardness value while the sample from Oxil steel has the least hardness value. These results were buttressed by the percentage carbon content of the samples; the higher the carbon content the harder the material. Comparing the results to the standards (as shown in Figure 8), the sample from Oxil steel and Phoenix steel conformed to two of the standards (ASTM A706 and Nst 65-Mn) but the sample from Phoenix steel did not conform to any of the standards as its hardness value was far higher than the standard values.

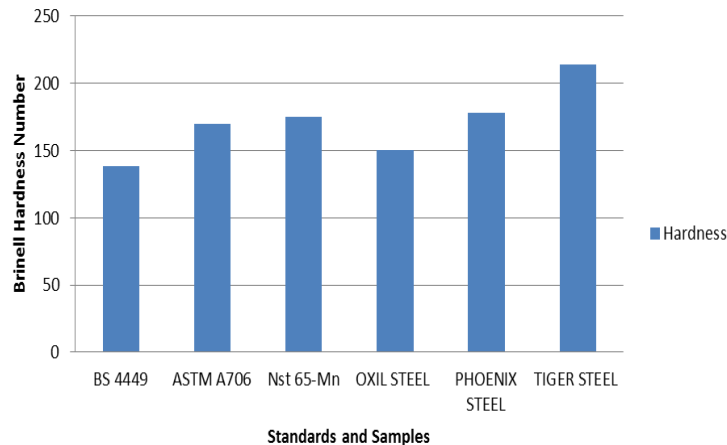


**Figure 8:** Chart showing the Brinell Hardness Number of the samples from Oxil Steel, Phoenix Steel and Tiger steel industries compared with Standards

From the microstructures of the samples shown in Figures 4 - 6, it was observed that the microstructure of the sample from Oxil steel has coarse pearlite grains in the ferrite matrix, the microstructure of the sample from Phoenix steel has a fine (small) pearlite grains while the microstructure of the sample from Tiger steel revealed finer (smaller) pearlite grains embedded in the ferrite matrix. The coarse pearlite grains found in the microstructure of the sample from Oxil steel was confirmed by the fact that it has the least percentage carbon content thus making it the least hard of the three steel samples. The coarse grains were formed due to slow cooling which allows for considerably much time for growth of grains into large sizes. In the contrary, the fine pearlite grains in the microstructure of the sample from Tiger steel was confirmed by the fact that it has the highest percentage carbon content thus making it the hardest of the three steel samples. The fine particles are formed due to more rapid cooling which allowed for less time for the growth of grains into larger sizes.

From the results generated from the tensile test of the samples from Oxil steel, Phoenix steel and Tiger steel, the Ultimate tensile strength (UTS), Yield strength and the percentage elongation were obtained. The UTS for the sample from Oxil steel was  $661 \text{ N/(mm)}^2$ , the UTS for the sample from Phoenix steel was  $653 \text{ N/(mm)}^2$  while the UTS for the sample from Tiger steel was  $631 \text{ N/(mm)}^2$ . Comparing the UTS of the samples with the standards as shown in Figure 9, it could be deduced that the samples all fall within the standards, none of the samples fall below the standards. Considering the yield strength of the samples, the results showed that the yield strength of sample from Oxil steel was  $464 \text{ N/(mm)}^2$ , the yield strength of the sample from Phoenix steel was  $451 \text{ N/(mm)}^2$  while the yield strength of the sample from Tiger steel was  $446 \text{ N/(mm)}^2$ . Comparing these values with the standards, all the sample fall within the standards except the BS 4449, 1997 standards of which all the samples fall below its standards value. From the results, it could be deduced that all the sample have high values of ultimate tensile strength (UTS) and yield strength thus implying high ductility and strength.

Considering the percentage elongation of the samples the results showed that the percentage elongation of sample from Oxil steel was 29%, the percentage elongation of the sample from Phoenix steel was 28% while the percentage elongation of the sample from Tiger steel was 28%. Comparing these values to the standards as shown in Figure 10, it was seen that the percentage elongation of the samples were far higher than the standards. The high values of the percentage elongation of the samples showed that there was a high extent to which the steel samples could be elongated before they eventually fracture thus, they were ductile. This was confirmed by their high values of Ultimate tensile strength and yield strength. Table 5 compared the mechanical test results of the samples.



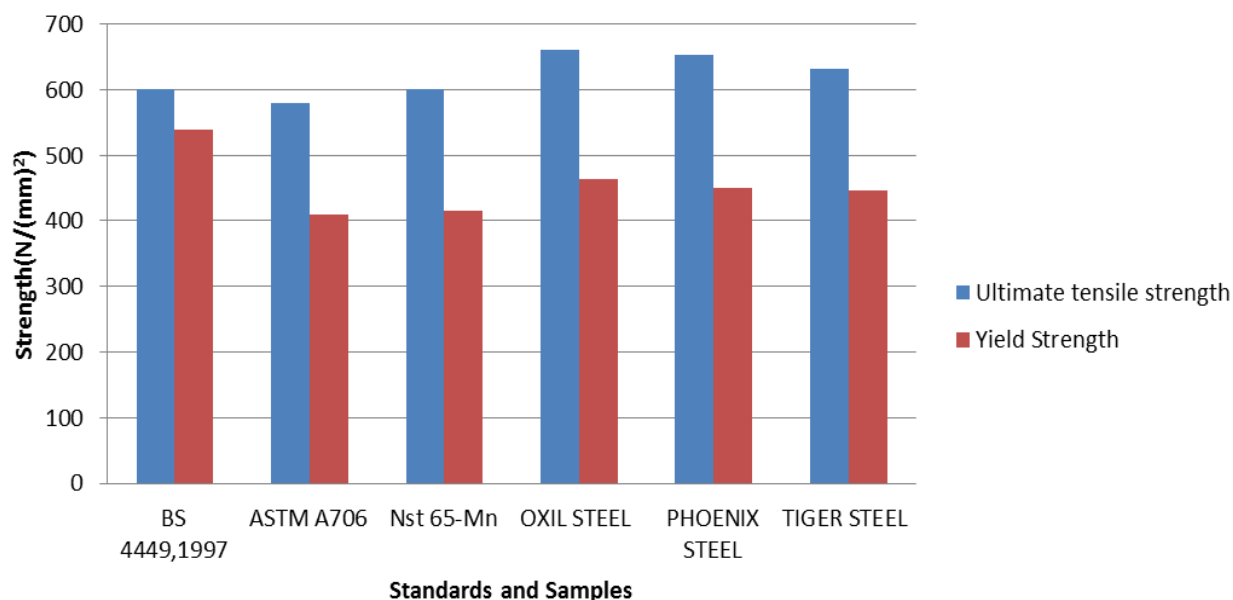


**Figure 9:** Chart showing the Ultimate tensile strength and Yield strength of the Standards and samples from Oxil steel, Phoenix steel and Tiger steel industries

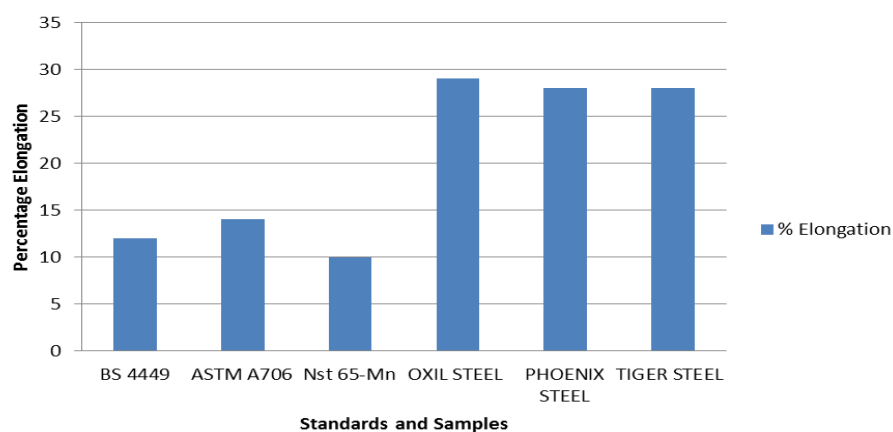


**Figure 4.10:** Chart showing the percentage elongation of samples of Oxil steel, Phoenix steel and Tiger steel industries compared with Standards

**Table 5:** Comparison of the Mechanical test results

	Ultimate Tensile Stress (UTS) (N/(mm) <sup>2</sup> )	Yield Strength (N/(mm) <sup>2</sup> )	Percentage Elongation	Hardness (BHN)	Impact Strength
ASTM A706	580	410	14	170	Not Available
BS 4449, 1997	600	540	12	138	Not Available
Nst 65-Mn	600	415	10	175	Not Available
<b>OXIL STEEL</b>	<b>661</b>	<b>464</b>	<b>29</b>	<b>150</b>	<b>58.98</b>
<b>PHOENIX STEEL</b>	<b>653</b>	<b>451</b>	<b>28</b>	<b>178</b>	<b>56.81</b>
<b>TIGER STEEL</b>	<b>631</b>	<b>446</b>	<b>28</b>	<b>214</b>	<b>50.10</b>

#### IV. Conclusion

From the results of the mechanical tests carried out it could be deduced that all of the samples from the steel industries considered conform to most of the standards except the sample from Tiger steel industry which due to its high percentage carbon content (0.488%) has a very high hardness value compared to the standards. Considering the Ultimate tensile strength, Yield strength and Percentage elongation which are very essential properties in engineering application, all the samples are suitable and meet up with the standards.

The properties of the steel produced from these industries could be maximized depending on the type of application. For an application which requires a high hardness value, Tiger steel will be the most suitable while Oxil steel will be the most suitable for an application that requires high ductility and load bearing ability such as in beams and columns in buildings.

#### REFERENCES

- [1] Al-Qawabah, S.M.A., Nabeel, A., & Al-Qawabehe, U.F. (2012), "Effect of Annealing Temperature on the Microstructure, Microhardness, Mechanical Behavior and Impact Toughness of Low Carbon Steel, Grade 45", *International Journal of Engineering Research and Applications* 2 (3), 1550-1553.
- [2] ASTM international, Tensile Testing, Second Edition (#05106G), p. 3. Copyright © 2004 by ASM International, Materials Park, Ohio, USA)
- [3] Dawit.Bogale and Ermias G. Kidan (2013). 'Low Carbon Steel Characterization under Quasi- Static Strain Rate for Bumper Beam Application'. *International Journal of Research in Mechanical Engineering*, Volume 1, Issue 2, pp. 91-99.
- [4] Kelley, M. Augustus., (1968). 'Basic Oxygen Steel making simulation'. In *Iron and steel in the Industrial Revolution*: T.S. Ashton, New York., version 1.36 User guide, steeluniversity.org, accessed 2014-05-24
- [5] Bello, K.A., Hassan, S.B. and Abdulwahab, M., "Effects of tempering on the microstructure and mechanical properties steel", *Journal of Applied sciences research*, 3 (12) , 2007, pp. 1719-1723
- [6] Rajan, T. V., Sharma C. P. and A. Sharma, "Heat Treatment-Principles and Techniques," Prentice-Hall of India Private Limited, New Delhi, 1988, p. 451.
- [7] Sinha, A. K. ferrous physical metallurgy butter worth, London, 1989, pp: 56
- [8] Smallman, R.E. and Bishop, R.J. (1999). 'Modern Physical Metallurgy and materials Engineering science, process, applications'. 6<sup>th</sup> Edition. Butterworth- Heinemann, Linacre House, Jordan Hill, Oxford OX2 8DP, A division of Reed Educational and Professional Publishing Ltd
- [9] Smith, W.F. & Hashemi, J. (2006). 'Foundations of Materials Science and Engineering,' 4th ed., McGraw-Hill, New York, 2006.

## Measurement of the viscosities of He, Ne and Ar for the determination of their gas – kinetic diameters.

P.N. Ekemezie<sup>1</sup>, E.E. Enekwechi<sup>2</sup> and Odinma S.C<sup>3</sup>

<sup>1</sup>Pure & Industrial Chemistry, NnamdiAzikiwe University, AwkaNigeria)

<sup>2</sup>(Natural Sciences, Federal Polytechnic, Oke Nigeria)

<sup>3</sup>Industrial Chemistry, Caritas University Amoji-Nike Enugu Nigeria)

**Abstract:** The viscosities of He, Ne and Ar gases were measured using pressure transducer to obtain the pressure, time data. Using the viscosity of dry air at the measured 32°C ambient temperature, the evacuation data (pressure, time) were converted to viscosity values thus: He ( $1.03 \times 10^{-4}$  poise), Ne ( $1.72 \times 10^{-4}$  poise), and Ar ( $1.96 \times 10^{-4}$  poise). Finally, the collision diameter of the gases were calculated using appropriate equations to obtain He (0.19nm), Ne (0.22nm), and Ar (0.33nm). The values obtained were compared with those of literature (He = 0.21nm, Ne = 0.24nm, Ar = 0.36nm). Since the values of collision diameter obtained in this experiment are in conformity with those obtained from literature, we can safely conclude that measurement of collision diameter can be used as a quality assay for gases.

### I. INTRODUCTION

In studying gas phase reaction dynamics, it is important to know the effective sizes, e.g., collision diameters, of the molecules involved in the elementary steps of the reaction. One of the ways that this fundamental information is obtained is through measurements of gas viscosity. From the application of gas kinetic theory to "hard sphere" molecules, the square of the collision diameter,  $\sigma$ , may be expressed as follows:

$$\sigma^2 = \frac{5(MRT/\pi)^{1/2}}{16N_A\eta} \quad (\text{cm}^2), \quad (1)$$

in which  $M$  is the molecular weight,  $\eta$  is the viscosity,  $N_A$  is Avogadro's number, and the other symbols have the usual meanings. This equation is derived from the relationship between the viscosity of a (hard sphere) gas and its density,  $D$ , mean speed,  $\langle c \rangle$ , and mean free path,  $\lambda$ : (1)

$$\eta = \frac{5\pi}{32} D\langle c \rangle\lambda \quad (\text{cm}). \quad (2)$$

Equation (1): which can be directly obtained from (2) may be rear-ranged to express the gas viscosity. Thus,

$$\eta = \frac{5(MRT/\pi)^{1/2}}{16N_A\sigma^2} \quad (\text{g s}^{-1} \text{ cm}^{-1}). \quad (3)$$

The cgs units of  $\eta$  are called the *poise*, P. The interesting point about equation (3) is that it predicts that  $\eta$  should be independent of gas pressure [this is because the pressure dependence of the gas density in equation (2) cancels that of the mean free path], and that  $\eta$  should vary with temperature as  $T^{1/2}$  (from the temperature dependence of  $\langle c \rangle$ ). The first prediction seems counterintuitive, but it has been verified over a relatively wide range of pressures. The reasons that  $\eta$  becomes pressure-dependent at low and high pressures stem from departures from laminar flows. The  $T^{1/2}$  dependence has been confirmed experimentally and is unusual because gases demonstrate the opposite type of temperature dependence from liquids; that is, liquid viscosities decrease with increasing temperature.

We will now develop the physical and mathematical basis on which the viscosity of a gas is experimentally determined. The mass transport of a fluid (in this case, a gas) arising from a pressure gradient is represented by the general equation

$$J_x = -C \frac{dP}{dx} \quad (\text{g s}^{-1} \text{ cm}^{-2}), \quad (4)$$

Where  $J_x$  is the flux (mass transported per unit cross section per unit time) of gas in the  $x$  direction as a result of the pressure gradient,  $dP/dx$ ;  $C$  is a positive constant that is inversely proportional to the viscosity. Equation (4) is known as Poiseuille's law (1840) (or in other applications as Fick's first law). The minus sign reflects the fact that the flow direction opposes the pressure gradient (2,3).

The flux can be expressed as  $J_x = (1/A)(dm/dt)$ , where  $A$  is the unit cross section (normal to the flow direction) and  $dm$  is the (infinitesimal) mass transported in a time  $dt$ . To apply equation (4) to the case of a fluid flowing through a straight cylinder of radius  $r$ , we must consider Newton's law of viscosity. It states that the shear force,  $F_x$ , required to move an infinitesimally thin sheet of fluid having unit cross section,  $A$ , in a flow direction parallel to the plane of the sheet is proportional to the velocity gradient of the sheet taken in a direction normal to the flow ( $dv_x/dy$ ). The mathematical statement is

$$\frac{1}{A} F_x = -\eta \frac{dv_x}{dy} \quad (\text{g s}^{-2} \text{ cm}^{-1}). \quad (5)$$

The proportionality constant in equation (5) is the fluid viscosity. Another way of stating equation (5) is that the drag force exerted on a unit plate of flowing fluid is proportional to the change in velocity of adjacent plates. According to equation (5), a fluid flowing through a straight cylinder has the largest flow rate at the center of the cylinder (at the cylinder axis) and is zero at the walls. This particular fluid dynamic condition is known as laminar (or Newtonian) flow and is approached by many gases and (small molecule) liquids (called Newtonian fluids) as long as the flow rate (thus the pressure gradient) is not excessive. At very low pressures, gases deviate from Newtonian (or bulk) flow as the mean free path becomes comparable with the cylinder radius. In this situation, the gas flow is said to be in the molecular, or Knudsen flow regime, and viscosity, which is a bulk property, fails to have significance (4).

The application of Newton's law of viscosity to the flow of a fluid through a straight cylindrical tube of radius  $r$  leads to another statement of Poiseuille's law:

$$\frac{dV}{dt} = -\frac{\pi r^4}{8\eta} \frac{dP}{dx} \quad (\text{cm}^3 \text{ s}^{-1}). \quad (6)$$

In this equation, which is used in viscosity measurements of liquids,  $dV$  is the volume of gas transported through the tube in time  $dt$ , and  $dP/dx$  is the pressure gradient in the tube along the direction of flow.

The infinitesimals  $dV$  and  $dm$  are related through the density,  $D$ , as  $D = dm/dV$ ; thus equation (6) becomes

$$\frac{dm}{dt} = -\frac{\pi r^4 D}{8\eta} \frac{dP}{dx}. \quad (7)$$

Because we are dealing with a gas at relatively low pressures ( $<1\text{atm}$ ), the density can be expressed in terms of its pressure,  $P$ , temperature,  $T$ , and molecular weight,  $M$ , through the ideal gas law, i.e.,  $D = PM/RT$ . Applying this result to equation (7), and recalling that  $n = m/M$ , we can write

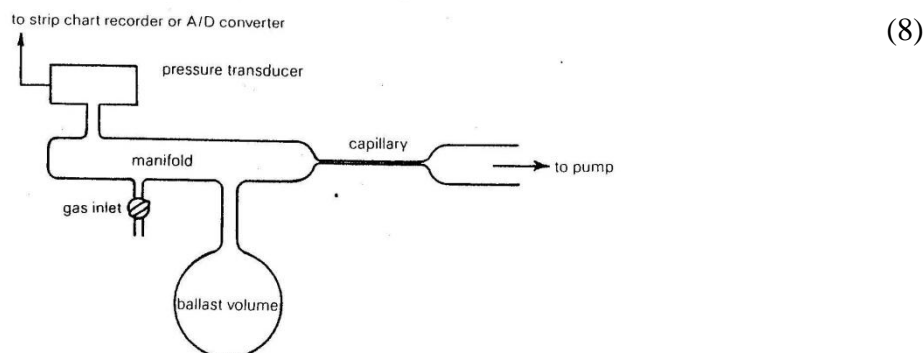


**Figure 1:** Schematic diagram of the evacuation apparatus.

Assuming the flow rate,  $dn/dt$ , to be independent of position ( $x$ ) within the tube, the right-hand side of (8) containing the  $x$  dependence of  $P$  and the left-hand side of (8) can each be set equal to a constant. If we do this [or the right-hand side of (8) and then integrate [between  $P_1(x_1)$  and  $P_2(x_2)$ ], the following result is obtained:

(9)

$$\frac{dn}{dt} = \frac{\pi r^4 (P_1^2 - P_2^2)}{16\eta RT(x_2 - x_1)}$$

$P_1$  and  $P_2$  are pressures at the beginning ( $x_1$ ) and end ( $x_2$ ) of the tube. Note that  $P_1 > P_2$ .

To clarify the rest of this development, a description of the experimental approach is presented. Refer to Figure 1. The gas is introduced to a manifold to which a large ballast volume (about 1 L), a pressure transducer (a device that converts the pressure to a voltage), and a capillary tube are connected. As the gas is evacuated through the capillary tube by a high-speed vacuum pump, the pressure of the system is continuously monitored by the transducer, whose output is displayed on a strip chart recorder. Alternatively, the transducer output is fed into the input port of a laboratory computer for direct data acquisition.

Because this experiment is carried out in such a way that  $P_2 < P_1$ , equation (9) simplifies to

$$\frac{dn}{dt} = \frac{\pi r^4 [P_1(t)]^2}{16\eta RTL}, \quad (10)$$

in which the time dependence of the pressure at the beginning of the tube,  $P_1$ , (the manifold pressure) is explicitly indicated.  $L$  is the total length of the capillary tube (2,5).

By expressing the number of moles transported through the tube,  $dn$ , in terms of the manifold pressure,  $P_1$ , the ideal gas law furnishes this relationship:  $dn = (V/RT)dP$ . After rearrangement, equation (10) becomes

$$\frac{dP}{P^2} = \frac{\pi r^4 dt}{16\eta VL}. \quad (11)$$

$V$  is the total volume of the manifold, ballast volume, etc. The integration of equation (11) with the boundary condition  $t = 0$ ;  $P = P_0$  furnishes

$$\frac{1}{P} = \frac{1}{P_0} + Kt, \quad (12)$$

in which the constant  $K$  is  $\pi r^4 / (16\eta VL)$ . Thus, Poiseuille's law predicts that a plot of the reciprocal pressure of the system being evacuation vs. time should be linear. The slope can, in principle, provide an absolute value of the gas viscosity since  $r$ ,  $V$ , and  $L$  can be determined. Note that the  $r^4$  factor in  $K$  makes  $r$  a very sensitive characteristic. In practice, it is more satisfactory to obtain an empirical value of the constant  $K$  by calibrating the system using a gas of known viscosity, e.g., dry air. In this regard, the approach is similar to that followed in using the Ostwald viscometer in measuring liquid viscosities (6).

### 1.1 Corrections to Poiseuille's Law

Because equation (12) is based on the assumption of laminar, or streamline, flow, it is important to consider the conditions under which this condition is expected to apply. This understanding is vital to proper experimental design. As mentioned above, laminar flow fails to occur at high pressure (where turbulence sets in) and low pressure (when molecular flow and other complications arise). The goal is to identify the pressure regimes in which these two departures from Newtonian flow (hence Poiseuille's law) take place.

### 1.2 High Pressure:

Osborne Reynolds showed (1883) that if the average linear velocity of a fluid flowing through a straight tube exceeds a critical value, turbulent flow sets in; hence, Poiseuille's law becomes invalid. The linear velocity is the speed with which an infinitesimal cross section of the fluid moves through the tube. The value of the linear velocity that approximately marks the transition between streamline and turbulent flow,  $v^1$ , is given by:

$$v^1 = \frac{1000 \eta}{rD}, \quad (13)$$

where  $r$  is the tube radius and  $D$  and  $\eta$  are the density and viscosity of the fluid. Thus quantitative applications of Poiseuille's law should be made for fluids having flow velocities below  $v^1$ . The quotient,  $2rDv/\eta$ , which is dimensionless, is called the Reynolds number. When the Reynolds number exceeds 2000, fluid flow may not be laminar.

In the case where the fluid is an ideal gas of molecular weight  $M$ , equation (13) becomes.

$$v' = \frac{1000 \eta RT}{rMP} \quad (14)$$

The linear velocity of a gas flowing through a tube can be obtained from equation by substituting  $-P/L$  for  $dP/dx$  and  $A \, dx/dt$  (where  $A = \pi r^2$ ) for  $dV/dt$ . The linear velocity,  $v$ , is  $(dx/dt)$ :

$$v = \frac{Pr^2}{8\eta L} \quad (15)$$

$$\frac{v}{v'} = \frac{Mr^3P^2}{8000 RTL\eta^2} < 1. \quad (16)$$

Although equation (16) cannot be used to determine whether laminar flow occurs without knowing the gas viscosity (the object of the experiment),  $\eta$  can be estimated for this purpose. Gas viscosities are generally  $1$  to  $2 \times 10^{-4} \text{ g cm}^{-1} \text{ s}^{-1}$ . In summary, the inequality in equation (16) places an upper limit on  $P$  for the application of Poiseuille's law (3,6).

### 1.3 Low Pressure:

If the pressure at which a gas being forced through a very narrow tube is decreased beyond a certain point, the flow rate of the fluid becomes *larger* than that predicted by Newtonian fluid mechanics. This is called the "slip condition," and it arises because the molecules adjacent to the tube walls do not move with zero velocity (as assumed in Newtonian flow); hence, the bulk gas "slips" through the tube. Poiseuille's law (6) can be written to include a slip correction ( $dP/dx$  is again replaced by  $-P/L$ ):

$$\frac{dV}{dt} = \frac{\pi r^4 P}{8\eta L} \left( 1 + \frac{4S}{r} \right), \quad (17)$$

$S$  is known as the *slip coefficient* and has dimensions of length. Slip becomes important when the quantity  $4S/r$  approaches unity. It can be seen that this deviation becomes more important in tubes of narrow bore. It turns out that the slip coefficient depends on the pressure (as stated above). In one approximation [due to Maxwell (1879)],  $S \sim 2\lambda$ , where  $\lambda$  is the mean free path of the flowing gas. From gas kinetic theory,

$$\lambda = \frac{RT}{\sqrt{2} \pi N_A \sigma^2 P}, \quad (18)$$

where  $\sigma$  is the collision diameter. The inverse pressure dependence of  $S$  can be seen in (18). Actually,  $\sigma$  is often determined from gas viscosity measurements.  $\lambda$  can be alternatively expressed as

$$\lambda = \frac{1.25 \eta (RT/M)^{1/2}}{P}. \quad (19)$$

Thus to avoid slip conditions, which become significant when  $4S/r \sim 1$  [see equation (17)] the pressure must be *larger* than a value that can be obtained from equation (19) (using  $S = 2\lambda$ ), i.e.:

$$P > \frac{10 \eta (RT/M)^{1/2}}{r}. \quad (20)$$

Equations (16) and (20) place upper and lower limits, respectively, on the pressure in the evacuation experiment such that equation (12) is valid (1,2,5).

### 1.4 Collision Diameters:

Once the gas viscosity is determined, its collision diameter can be obtained through equation (1). It is logical to compare  $\sigma$  obtained from gas viscosity with another experimental manifestation of molecular size, namely, the van der Waals  $b$  constant.  $b$ , having units of volume/mole, can be related to the gas collision diameter as follows. Figure 2 shows two identical spherical molecules in close contact during a collision. The center of molecule  $B$  cannot approach the center of molecule  $A$  by an amount less than the distance equal to  $\sigma$ . Therefore, molecule  $A$  effectively removes from the total container volume,  $V$ , an excluded volume,  $V_{\text{excl}}$ . This excluded volume is just  $(4/3)\pi\sigma^3$ , and the net available volume to molecule  $B$  is

$$V_{\text{avail}} = V - (4/3)\pi\sigma^3. \quad (21)$$



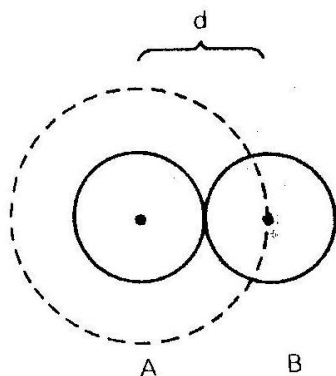


**Fig 2:** Two hard spheres in collisional contact. One

Particle contributes an excluded volume of  $4\pi\sigma^3/3$ , where  $\sigma$  is the collision diameter.

Now if successive molecules are added to the container, the net available volume accessible to the added molecule is

$$V_{\text{avail}} = V - \sum (i - 1)V_{\text{excl}}, \quad (22)$$

and the average volume available to a total of  $N$  added molecules is

$$\langle V_{\text{avail}} \rangle = V - \frac{1}{N} \sum_{i=1}^N (i - 1)V_{\text{excl}}. \quad (23)$$

Because  $V_{\text{excl}}$  is a constant, the summation is simply

$$\frac{1}{N} V_{\text{excl}} \sum_{i=1}^N (i - 1).$$

The summation is equal to  $N^2/2 - N/2$ , and because  $N$  is large (on the order of  $N_A$ ), this expression becomes  $N^2/2$ . Therefore, the average available volume is

$$\langle V_{\text{avail}} \rangle = V - \frac{N}{2} V_{\text{excl}}. \quad (24)$$

But  $\langle V_{\text{avail}} \rangle$  is just the “net volume” term in the van der Waals equation,  $(V - nb)$ , where  $n$  is the number moles of gas. We now have

$$V - nb = V - \frac{N}{2} V_{\text{excl}}. \quad (25)$$

Dividing by  $n$ , we get

$$V_m - b = V_m - 1/2 V_{\text{excl}} \quad (26)$$

where  $V_m$  is the molar volume and  $V_{\text{excl}}$  is the excluded volume of the gas. Finally, the desired result is presented as

$$b = 1/2 V_{\text{excl}} = 2/3 N_A \pi \sigma^3 \quad (27)$$

This equation allows a comparison to be made between  $\sigma$ , the collision diameter, and  $b$ . Moreover, collision diameters can be estimated from van der Waals  $b$  constants (4,5).

## II. MATERIALS AND METHOD

The output of the pressure transducer which produces 10V per 1000torr is connected to the strip chart recorder. The transducer power supply is turned on and the range switch, which indicates the maximum pressure for full-scale pen deflection, is in the proper position. Also, the zero position is set. The stopcock is used following the “two-hand rule” i.e. using one hand to counter-balance the torque exerted on the stopcock by the other. First, the system is calibrated using dry air by first pumping out the manifold, including the capillary tube and ballast bulb. As the pressure falls to a low value (below 1 torr), the recorder pen approaches the zero position and the ambient temperature is recorded.

The gas inlet line is evacuated and the system isolated by shutting off the main manifold stopcock. Gently the dry air valve is cracked open until the manifold pressure rises to an appropriate level. The chart pen should respond by indicating pressure, and it should be stable. The gas inlet line is isolated from the manifold. The recorder chart drive (about 5in/min) is started, and as the pen crosses a vertical line on the chart paper, the capillary stopcock is opened. The pressure falls immediately and after the pressure has dropped to about 5 to 10 percent of the initial value, the entire system is evacuated by opening the main stopcock. The gas inlet line is pumped out and the system filled with another gas. The above procedure is followed until all the gases to be studied are measured.

### III. RESULTS AND DISCUSSION

For each of the evacuation, pressure, time data was obtained thus:

**Table 1: He evacuation**

P/(atm)	1.35	1.05	0.789	0.526	0.132
t/(s)	0	60	120	180	240

**Table 2: Ne evacuation**

P/(atm)	1.58	1.06	0.925	0.702	0.428
t/(s)	0	60	120	180	240

**Table 3: Ar evacuation**

P/(atm)	2.11	1.70	1.18	0.950	0.622
t/(s)	0	60	120	180	240

Using the viscosity of dry air at the measured ambient temperature of 32°C (305K), the evacuation data are converted to viscosity values for each of the three gases after making the respective  $T^{1/2}$  correction. This is done by the application of equations (14) and (16) with the following values obtained: He ( $1.03 \times 10^{-4}$  poise), Ne ( $1.72 \times 10^{-4}$  poise) and Ar ( $1.96 \times 10^{-4}$  poise).

Finally, the collision diameters of the gases are calculated from their viscosities using equation (1) thus: He (0.19nm), Ne (0.22nm), Ar (0.33nm). The values obtained were then compared with those determined from van der Waals b constants.

It is obvious from the evacuation tables 1 – 3 that the pressure increases from HeNe → → Ar. This is expected since the molecular mass increases in that order. The values of viscosity obtained in this experiment are in conformity with those obtained from van der Waals b constant i.e. from literature. Again the values of collision diameter of the gases studied agree with those of literature, and we can therefore safely conclude that determination of gas collision diameter from its viscosity measurement can be used as quality control assay in analytical laboratories.

### REFERENCES

- [1] A.W. Adamson (1986): A textbook of Physical Chemistry, 3<sup>rd</sup> ed. Academic Press (Orlando, Fla), pp.17-18, 55 – 62.
- [2] P.W. Atkins (2010): Physical Chemistry, 9<sup>th</sup> ed. W.H. Freeman (New York), pp.65 – 660.
- [3] G.W. Castellan (2003): Physical Chemistry, 6<sup>th</sup> ed., Addison – Wesley (Reading, Mass), pp.671 – 672, 745 – 755.
- [4] I.N. Levine (2000): Physical Chemistry, 8<sup>th</sup> ed., McGraw-Hill (New York), pp.456 – 462.
- [5] J.H. Noggle (1985): Physical Chemistry, Little, Brown (Boston), pp.5-7, 445 – 451.
- [6] J.R. Partington (2006): An Advanced Treatise on Physical Chemistry, Vol. 10, Longmans (London), pp.5 – 7, 445 – 451.

## Development and Application of Geneva Mechanism for Bottle Washing.

Ujam, A. J<sup>a\*</sup>, Ejeogo, G<sup>b</sup> and Onyeneho, K. C.<sup>c</sup>

a. Department of Mechanical Engineering, Nnamdi Azikiwe University, Awka, Anambra State, Nigeria.

b. Department of Mechanical Engineering, Institute of Management and Technology, Enugu, Nigeria.

c. Department of Mechanical Engineering, Akanu Ibiam Federal Polytechnic, Unwana, Ebonyi State, Nigeria.

**Abstract :** Manual washing of beverage bottles does not give the desired productivity requirement of industrial setting and in the effort to reduce the environmental impact of waste from industrial production, there is an increasing deeply felt need to recover empty glass and plastic containers. This paper therefore aims at developing a Rig (Geneva Mechanism) for bottle washing in a typical brewery or beverage industry. A test rig was designed, fabricated and employed for a performance evaluation. The rig operates on the intermittent rotary motion from a four slot external Geneva Mechanism and requires manual loading and unloading of bottles. The bottles are loaded on subsequent indexing part of the rotating table and are washed one after another. The analysis of design gave the following results: Centrifugal force on the driven pulley ( $F_R$ ) = 0.158N; Bearing reaction at an end, B,  $R_B$  = 403.42N; Bearing reaction at an end, C,  $R_C$  = -152.42N; Radial load due to inertia of driver,  $F_R$  = 20.90N; Axial load due to weight of Pulley,  $W_a$  = 61.70N; Equivalent dynamic load on the bearing,  $W_e$  = 349.31N; Bearing load capacity,  $W_C$  = 2306.80N. These forces were related to generate shear force and bending moment diagrams. This work presents a practical application of Geneva mechanism for worktable indexing and bottle washing.

**Keywords:** Geneva Mechanism, Rotary Motion, Bottle Washing, Productivity, Indexing Time.

### I. Introduction

Geneva mechanism is a simple and widely used timing mechanism that provides intermittent motion from a continuously rotating input. It consists of a rotating drive wheel (Driver) with a pin that reaches into a slot of the driven wheel (Geneva wheel) advancing it by one step.

They are cheaper than cams, have good motion curve characteristics compared to ratchets and maintain good control of its load at all times. In addition, if properly sized to the load, the mechanism generally exhibits very long life. It is used in machine tools to index spindle carriers weighing several tonnes, in transfer machines for indexing work piece from one work station to another, as a turret indexing mechanism in automatic lathe, in counting instruments, peristaltic pump drives in integrated circuit manufacturing, intermittent advance of films in motion-picture projectors and discrete motion drives with high load capacity in robotic manipulators.

One of the most important processes in beverage production is bottle washing. The high quality of the product depends largely on how thoroughly the bottles are cleaned immediately before filling.

Manual washing of bottles does not give the desired productivity requirement of industrial setting. On this note, a mechanized system of washing and detoxification is very imperative in order to achieve the desired productivity for industries.

The need to address this problem has led to the design of a mechanized bottle washing and detoxification system using a rotary table propelled by a Geneva mechanism <sup>[1]</sup>

Krishnakumar et al <sup>[2]</sup>, designed and developed a Geneva mechanism for Film Frame. In their design, a 4-slot mechanism was used in which a driver, (A), rotates at uniform angular velocity and for every revolution of the driver, the Geneva wheel makes a fraction part of the revolution which is a function of the number of slots (fig.1).

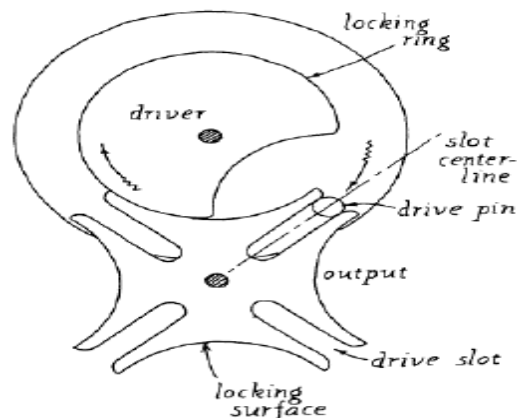


**Fig. 1 4-slot Geneva Mechanism**

Indexing motion mechanisms find several applications in instruments, watches, projectors, machine tools, printing and pressing machinery, packaging and automatic machinery, transfer lines [3]. A wide variety of applications are derived from the Geneva mechanism such as indexing in automatic machinery, peristaltic pump drives in integrated circuit manufacturing, intermittent advance of films in motion-picture projectors and discrete motion drives with high load capacity in robotic manipulators [4-7]. Geneva mechanism is also used in rotary indexing machine to provide synchronous motion and index a worktable to present parts to workstations for processing [8].

The main disadvantage of Geneva mechanism is the discontinuity in the acceleration at the start and the end of the intermittent motion. At these points, the normal acceleration of the rotating crankpin is transmitted to the wheel with an impact, leading to large jerks and undesirable vibrations in the mechanism [9]. Two undesirable characteristics inherent in this mechanism are (1) high contact stress between the drive pin and the wheel slot and (2) vibratory motion of the driven inertia load. Both of these factors adversely affect performance and life of the mechanism [10].

Several methods have been proposed to decrease the wheel acceleration in order to reduce the inertia force and the consequent wear. Johnson [10] designed Geneva mechanism to minimize drive-pin contact stress and gave a procedure for reducing the undesirable vibratory motion. He proposed that there must be an optimum Geneva wheel diameter that minimizes the pin-slot contact stress. Many authors have considered minimizing the inertial forces on the Geneva wheel using a four bar linkage with the drive pin located at a coupler [11-13]. For an internal Geneva wheel, the jerk and undesirable vibrations can be removed by using a four-bar linkage as a driving mechanism instead of a simple crank [14]. He used compound mechanism to eliminate the non-zero accelerations at the initial and ending stage. Fenton [15] also used Geneva mechanism in series such that the output motion starts and ends with zero acceleration. The acceleration increases gradually at the beginning and ends smoothly at the end of the motion cycle. The undesirable shock loadings typical of the simple Geneva mechanisms were completely eliminated. Another proposed method was to employ certain damping elements in the mechanism to reduce the shock [16-17]. Another method was to change the geometry for the wheel slot. Changing the slot shape from a straight radial line to a curved line results in the elimination of shock loading at the beginning and end of the motion cycles and reduces the wheel peak velocity and peak acceleration values, making the mechanism well suited for high speed applications. Curved slots with designed motion law were applied as in the standard cam mechanism. In this approach, the Geneva mechanism with curved slots was basically thought of as an inverse cam mechanism [18-19]. However, basic equations for the surface geometry of the slots were not discussed in their work resulting in unknown conditions for manufacturing, such as undercutting and double point in the curve. Figliolini and Angeles [20] studied the force transmission of the Geneva mechanism with curved slots. Lee and Huang [21] derived the equation for the geometry of curved slots. Lee and Jan [22] designed the profile of the curves for Geneva mechanism with curved slots, derived the mathematical expression in parametric form for the curves and equations for non-undercutting and developed the criteria for undercutting and double points in the design.

## II. Design and Development

The test rig is a 4-slot external Geneva Mechanism for bottle washing consisting of the following features:

1. A water pump connected to pipes and pipe fitting for the channeling of water through the nozzle.
2. A solenoid valve connected to a limit- switch for the regulation of water flow during bottle washing operations.

3. A Geneva mechanism mounted on a Geneva wheel shaft for intermittent positioning of bottles at the washing station
4. A control panel housing the electrical circuit components of the test rig.
5. Bottle holders that grip the bottles at the neck.
6. An electric motor that provides the rotational motion transmitted to the shafts.

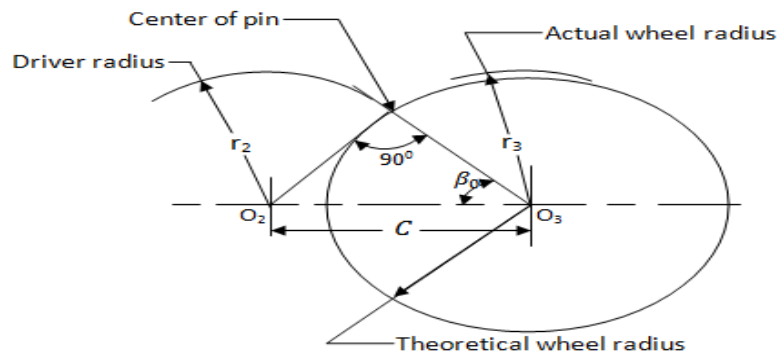
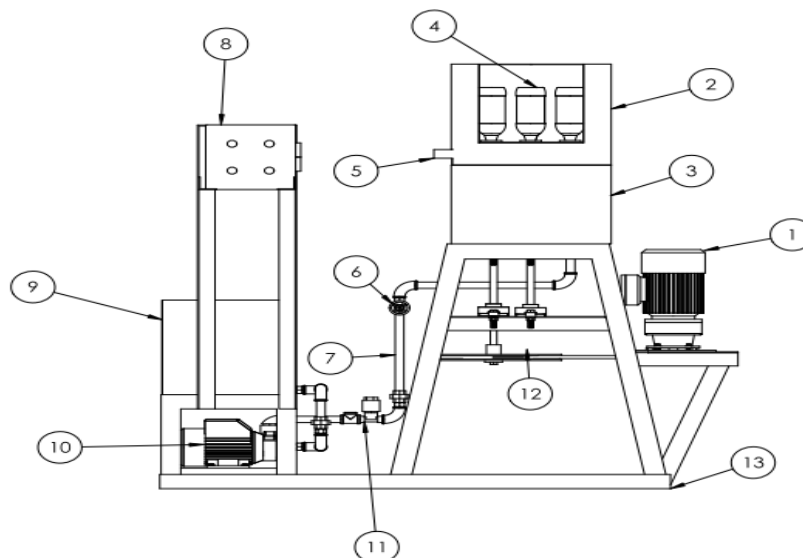


Fig. 2 Design of Geneva Mechanism



S/N	COMPONENT NAME
1	Electric Motor
2	Upper Chamber
3	Lower chamber
4	Bottle
5	Limit Switch
6	Gate Valve
7	Water Pipe
8	Control Panel
9	Water Tank
10	Electric Pump
11	Solenoid Valve
12	Pulley
13	Machine Frame

Fig. 3 Test Rig Assembly

The design is initiated by specifying the Crank (driver) radius, the roller diameter and the number of slots (fig.2), as follows:

The Crank (Driver) radius,  $r_2 = 60\text{mm}$

The roller (pin) diameter = 12mm

The number of slots,  $n = 4$  slots

The angle  $\beta$  is half the angle subtended by adjacent slots, that is;

$$\beta_0 = \frac{360^\circ}{2n} \quad (1)$$

$$\beta_0 = \frac{360^\circ}{2 \times 4} = 45^\circ$$

Where  $n$  is the number of slots in the Geneva wheel.

$$\sin \beta_0 = \frac{r_2}{C} \quad (2)$$

$$C = \frac{r_2}{\sin \beta_0}$$

$$C = \frac{60}{\sin 45^\circ}$$

Where  $C$  is the center distance between the driver shaft and Geneva wheel shaft.

Using Pythagoras theorem,  $C^2 = r_2^2 + r_3^2$

Where  $r_3$  is the radius of Geneva wheel

$$r_3 = \sqrt{C^2 - r_2^2}$$

$$r_3 = \sqrt{84.85^2 - 60^2}$$

$$r_3 = 59.996\text{mm}$$

$$r_3 \sim 60\text{mm}$$

## 2.1 Forces Acting on the Driver Shaft

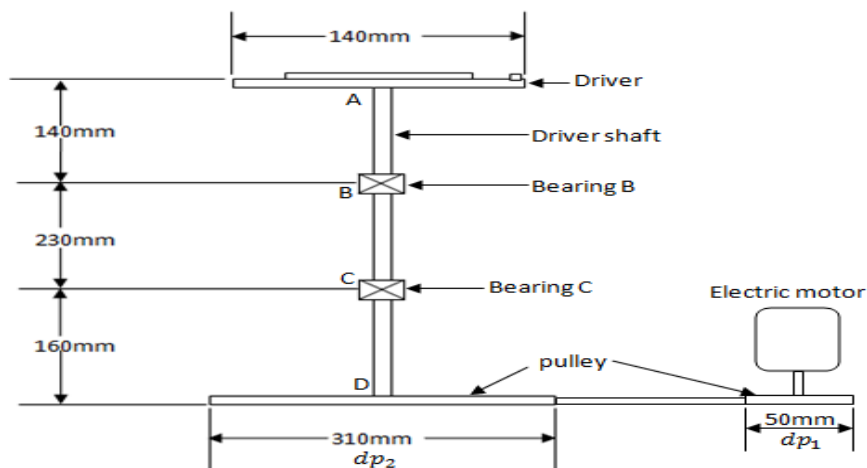


Fig.4 Schematic Diagram showing the drive mechanism of the machine

The shaft is

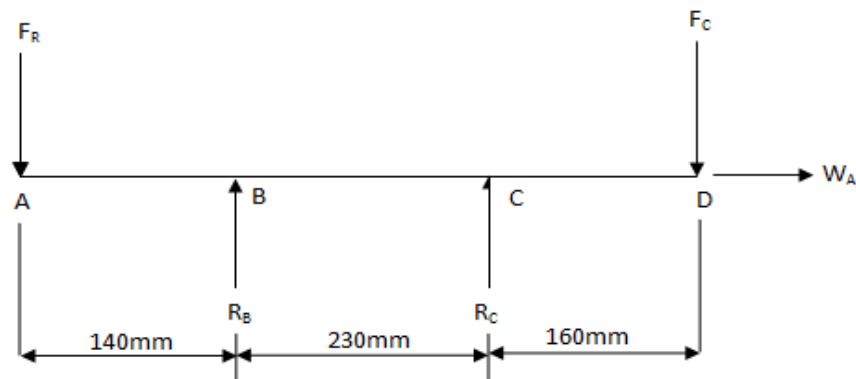


Fig. 5: Force diagram of the driver shaft

Figures 4 and 5 show the drive mechanism and the forces acting on the driver shaft. The forces include the following:



- Centrifugal force  $F_c$  of drive belt on driven pulley
- Bearing reaction  $R_B$  at point B.
- Bearing reaction  $R_C$  at point C
- Radial load  $F_R$  at shaft end A due to inertia load of Driver
- Axial Load  $W_A$  due to weight of pulley, shaft and Driver.

Computation of these forces enables the presentation of a graphic representation of shaft loading from which shear force and bending moment diagrams were obtained. Reaction forces  $R_A$ ,  $R_B$  and axial load  $W_A$  are needed for the specification of bearings while the maximum bending moment on the shaft is an important requirement for shaft diameter computation. Linear dimensions of the shaft in fig.4 and 5 were estimated based on the anticipated length of immersion of the shaft in the chamber lower cover and space requirement for the bearings and driven pulley.

## 2.2 Length of belt connecting the motor pulley and driven pulley

Length of the belt,  $L_b$  is obtained using:<sup>[23]</sup>

$$L_b = \frac{\pi}{2} (dp_1 + dp_2) + \frac{(dp_1 - dp_2)^2}{4C} + 2C \quad (3)$$

Diameter of motor pulley,  $dp_2 = 50\text{mm}$

Diameter of driven pulley,  $dp_1 = 117.5\text{mm}$

Center distance between motor and driven pulley,  $C = 435\text{mm}$

Substituting  $dp_1$ ,  $dp_2$  and  $C$  into the above equation, we have

$$L_b = \frac{\pi}{2} (0.1175 + 0.05) + \frac{(0.1175 - 0.05)^2}{4 \times 0.435} + 2(0.435)$$

$$L_b = 1.1357\text{m}$$

## 2.3 Centrifugal force on the Driven pulley

Centrifugal force  $F_c$  acting on the driven pulley attached to the driver shaft is given by:<sup>[24]</sup>

$$F_c = \frac{M_b v^2}{r}$$

But linear velocity,  $V = \omega r$

$$F_c = \frac{M_b \omega^2 r^2}{r}$$

$$F_c = M_b \omega^2 r$$

Where  $M_b$  = mass of the belt,

$\omega$  = angular velocity of driven pulley,

$r$  = radius of driven pulley

Since Density =  $\frac{\text{mass}}{\text{volume}}$ , mass of the belt  $M_b$  can be computed using the equation:

$$M_b = \rho_b V_b = \rho_b A_b L_b$$

Where  $\rho_b$  = Density of belt material,

$V_b$  = Volume of belt material,

$A_b$  = Cross- sectional area of the belt,

$L_b$  = length of the belt

Mass of the belt,  $M_b = \rho_b A_b L_b$

$$M_b = 1000 \times 9 \times 10^{-5} \times 1.1357$$

$$M_b = 0.1022 \text{ kg}$$

For a selected Driver speed,  $N_2 = 120 \text{ rpm}$

$$\omega_2 = \frac{2\pi N_2}{60}$$

$$\omega_2 = \frac{2\pi \times 120}{60}$$

$$\omega_2 = 12.566 \text{ rad/s.}$$

Electric motor speed,  $N_1 = 47 \text{ rpm}$

$$D_2 = \frac{N_1 D_1}{N_2}$$

$$D_2 = \frac{47 \times 50}{120}$$

$$D_2 \sim 19.58 \text{ m}$$

The Centrifugal force,  $F_c$  becomes

$$F_c = M_b \omega^2 r$$

$$F_c = 0.1022 \times (12.566)^2 \times 0.0098$$

$$F_c = 0.158 \text{ N}$$

## 2.4 Radial load $F_R$ at upper shaft end

The Radial load  $F_R$  at the shaft end due to the Driver and Geneva wheel can be expressed as:

$$F_R = M_D \omega^2 r_D + M_G \omega^2 r_G \quad (4)$$

Where  $M_D$  = mass of driver,  $M_G$  = mass of Geneva wheel,

$r_D$  = radius of driven Driver,  $r_G$  = radius of Geneva wheel,

$\omega$  = angular velocity of driver shaft,

Mass of Driver and locking ring (cam),  $M_D = 1502\text{g}$ , mass of Geneva wheel,  $M_G = 454\text{g}$  (measured with Tripple Beam balance, capacity: 2610g)

$$F_R = M_D \omega^2 r_D + M_G \omega^2 r_G$$

$$F_R = [1.502 \times (12.566)^2 \times 0.07] + [0.454 \times (12.566)^2 \times 0.06]$$

$$F_R = 20.903\text{N}$$

Using a factor of safety of 12. This is the designated value for steel under shock load which is similar to the shock load of the Geneva mechanism.

$$F_R = 12 \times 20.903$$

$$F_R = 250.84\text{N}$$

## 2.5 Reaction loads $R_B$ and $R_C$

Considering the force diagram, for equilibrium of forces,

$$R_B + R_C = F_R + F_c$$

$$R_B + R_C = 250.84 + 0.158$$

$$R_B + R_C = 250.998$$

Taking moment about B,

$$F_R(0.14) + R_C(0.23) = F_c(0.16 + 0.23)$$

$$(250.84 \times 0.14) + R_C(0.23) = 0.158(0.16 + 0.23)$$

$$R_C(0.23) = -35.056$$

$$R_C = -152.4174\text{N}$$

$$R_B + R_C = 250.998$$

$$R_B = 250.998 - R_C$$

$$R_B = 250.998 + 152.417$$

$$R_B = 403.415\text{N}$$

$$\text{Thus, } R_B = 403.415\text{N}, R_C = -152.4174\text{N}$$

## 2.6 Maximum bending moment ( $BM_{\max}$ )

Referring to fig.5, Bending moments are:

$$\text{At A, } BM_1 = 0$$

$$\text{At B, } BM_2 = 250.84(0.14) = 35.1176\text{Nm}$$

$$\text{At C, } BM_3 = 250.84(0.14 + 0.23) - 403.415(0.23) = 0.02535\text{Nm}$$

At D,  $BM_4 = 250.84(0.53) - 403.415(0.39) + 152.4174(0.16) = 0$

The maximum bending moment,  $BM_{max}$  is 35.1176Nm and will be used for computation of shaft diameter.

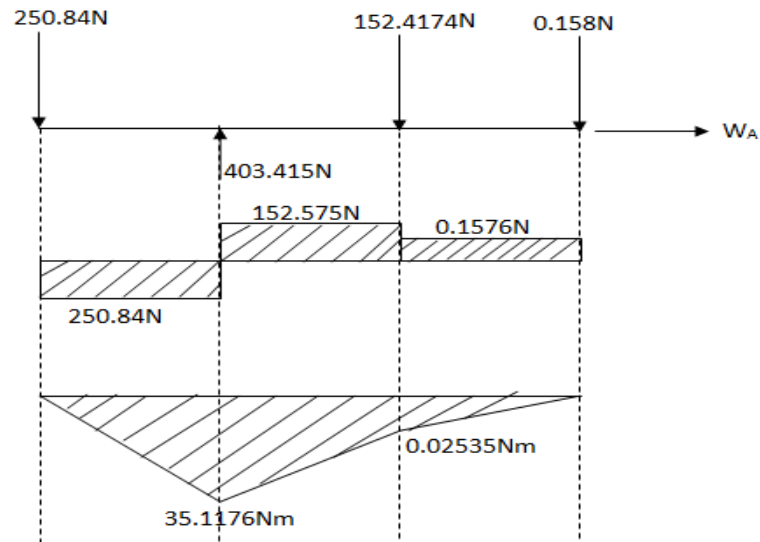


Fig. 6 Shear force and bending Moment diagrams

## 2.6 Driver Shaft Diameter

The shaft diameter  $d_s$  is computed in accordance with ASME code equation for shafting <sup>[11]</sup>

$$d_s^3 = \frac{16}{\pi \sigma_s} \sqrt{(k_b BM_{max})^2 + (k_t T_m)^2} \quad (5)$$

Where  $k_b$  = combined shock and fatigue factor applied to bending moment

$k_t$  = combined shock and fatigue factor applied to torsional moment

For a rotating shaft,  $k_b = 1.5$  and  $k_t = 1.0$

ASME code states for commercial steel shafting with keyway,

$$\sigma_s(\text{allowable}) = 40 \text{ MN/m}^2$$

$$BM_{max} = 35.1176 \text{ Nm}$$

$T_m$  is the torsional moment of the shaft and is given by,

$$T_m = F_c \times rp_2$$

Where  $rp_2$  is the radius of the driven pulley ( $rp_2 = \frac{D_2}{2}$ )

$$T_m = 0.158 \times 0.00979$$

$$T_m = 1.547 \times 10^{-3} \text{ Nm}$$

Substituting, we have

$$d_s^3 = \frac{16}{\pi \times 40 \times 10^6} \sqrt{(1.5 \times 35.1176)^2 + (1 \times 1.547 \times 10^{-3})^2}$$

$$d_s^3 = 1.27 \times 10^{-7} \sqrt{2774.803 + 2.3932 \times 10^{-6}}$$

$$d_s = 0.0188m$$

$$d_s = 18.84mm$$

Applying a factor of safety of 1.7, the shaft diameter becomes

$$d_s = 18.84 \times 1.7 = 32.028mm$$

For this work, a shaft of diameter 32mm is selected being the available stock in the local market.

## 2.7 Axial load $W_a$ on the Driver shaft

The axial load  $W_a$  (fig. 5) on the Driver shaft is very useful data for the calculation of the equivalent load on bearings and for bearing selection.

The axial load on the Driver shaft can be expressed by:

$$W_a = \text{Weight of Driver } W_{t_D} + \text{Weight of Driver shaft } W_{t_{sh}} + \text{Weight of driven pulley } W_{t_p}.$$

$$\text{i.e } W_a = W_{t_D} + W_{t_{sh}} + W_{t_p}.$$

$W_{t_D}$  was obtained using Tripple beam balance, capacity 2610g as 1.5kg.

$W_{t_{sh}}$  and  $W_{t_p}$  were obtained using a Diamond top loading balance, capacity 10Kg as:

$$W_{t_{sh}} = 2.52Kg$$

$$W_{t_p} = 2.15Kg$$

Substituting  $W_{t_D}$ ,  $W_{t_{sh}}$  and  $W_{t_p}$  into the equation for  $W_a$  and using acceleration due to gravity g, as  $10 \text{ m/s}^2$ , yields:

$$W_a = [1.5 + 2.52 + 2.15]10$$

$$W_a = 61.7N$$

## 2.8 Equivalent dynamic load $W_e$ on bearing

Radial bearings are often subjected to simultaneously acting radial and axial loads. If the resultant load is constant as in the case of the Driver shaft, then the equivalent dynamic load  $W_e$  can be expressed by the equation:

$$W_e = X \times V \times W_R + Y \times W_a \quad (6)$$

Where V= rotation factor,

X and Y are the radial and axial load factors respectively.

For deep groove ball bearings,  $V = 1$ ,  $X = 0.56$  and  $Y = 2$  [24]

$W_R$  is the radial load ( $R_B = 403.415N$ ,  $R_C = 152.4174N$ ). The higher of the two values that is  $R_B = 403.415N$  is taken for the purpose of bearing safety and uniformity. Thus taking  $W_R = 403.415N$  and substituting the values of  $X$  and  $Y$  in the above equation results in:

$$W_e = 0.56 \times 1 \times 403.415 + 2 \times 61.7$$

$$W_e = 225.9124 + 123.4$$

$$W_e = 349.3124N$$

## 2.9 Bearing load capacity $W_c$

The relationship between the rating life  $L$ , the equivalent dynamic load  $W_e$  and the bearing load capacity  $W_c$  is represented by: [24]

$$W_c = W_e \left( \frac{L}{10^6} \right)^{1/k} \quad (7)$$

$K$  is a constant with value equal to 3 for ball bearings, and

$W_e = 349.3124N$ ,  $L = 60 \times N \times L_H$  (revolutions),  $N = 20rpm$ ,  $L_H = 40000hours$ .

$$L = 60 \times 120 \times 40000$$

$$L = 288 \times 10^6 rev$$

The bearing load capacity is thus calculated as:

$$W_c = 349.3124 \left( \frac{288 \times 10^6}{10^6} \right)^{1/3}$$

$$W_c = 2306.8N$$

## III. Conclusions

The test rig uses Geneva mechanism to index a table intermittently for bottle washing. The test rig was designed, constructed, assembled and used to run the experimental study. As the drive speed of the Geneva mechanism increases, the cycle time, washing time and indexing time decreases while the maximum pin-slot contact force and washing efficiency increases. The washing efficiency of the test rig from 5rpm to 19 rpm increased from 81.57% to 96.89%. It is concluded that at 19rpm, the designed bottle washing machine had washing time of 2.434 seconds and maximum efficiency of 96.89%.

## References

- [1] Ejeogo Gerald (2014) "Development and Analysis of Geneva Mechanism for Bottle Washing" M.Eng Thesis, department of mechanical & Production Engineering, Enugu State University of Science & Technology, Enugu, Nigeria.
- [2] Krishnakumar M., Prabakaran A., Sudhakar K., Senthilkumar R., (2011) "Design and Fabrication of Film frame by Geneva Mechanism", Thanthai Periyar Government Institute of Technology, Vellore
- [3] Figliolini G., Rea P., Angeles J., (2007) "Synthesis of Geneva Mechanism and their equivalent Pure-Rolling Cams", 12th IFTOMM World Congress, Besancon France
- [4] Beltz R. K and Hurst J. C., (1975) "Peristaltic pump metering and dispensing system". Technical Digest – Western Electric Company, USA, No. 37 3-4.
- [5] Egorov O.D. Nadezhdin IV, (1988) "Use of Geneva Mechanisms in Industrial Robots", Soviet Engineering Research, vol.8, no.11, USA 134-137.
- [6] Meyer G., (1988) "A tested method for precise Intermittent Motion", Machine Design vol. 60, no.1, 140-143.
- [7] Pazouki M.E., Jones J.R., (1982) "The kinematic synthesis of a linkage driven Geneva Mechanism", Mechanism and Machine theory, 17(3), 221-228.
- [8] Groover P. Mikell, (2009) "Automation, Production Systems and Computer integrated Manufacturing", Third Edition, Pearson Education 467-471.



- [9] Sujan V. A. and Meggiolaro M. A., (2000) “**Dynamic Optimization of Geneva Mechanism**”, International Conference on Gearing, Transmissions and Mechanical Systems, Daizhong Su, Professional Engineering Publishing, London 687-696
- [10] Johnson R. C., (1956) “**How to Design Geneva Mechanisms to Minimize Contact Stresses and Torsional Vibrations**”, Machine Design 28, NO.6, 107-111.
- [11] Hall Allens JR., Holowenko Alfred M. S. and Laughlin Herman G., (2009). “**Schaum’s Outline Series of Theory and Problems of Machine Design**”, Tata McGraw- Hill Edition.
- [12] Shigley J.E. and Uicker J.J, JR., (1995) “**Theory of Machines and Mechanisms**”, Second Edition, Singapore: McGraw-Hill, Inc. 372-376.
- [13] Tao, D.C., Krisnamoorthy S. (1978) “**Mechanism and Machine Theory**”, 13, 585-591.
- [14] Dijkstra E.A., (1966) , “**Jerk-free Geneva wheel driving**”, Journal of Mechanisms 1 235-283.
- [15] Fenton E.A., (1975) “**Geneva Mechanisms connected in series**”, ASME Journal of Engineering for Industry 97, 603-608.
- [16] 16. Sadek, E. A, Lloyd J. L, Smith M.R., (1990) “**A new design of Geneva drive to reduce shock loading**”, Mechanism and Machine Theory 25, 589-595.
- [17] Cheng C.Y., Lin Y., (1995) “**Improving dynamic performance of the Geneva mechanism using non-linear spring elements**”, Mechanism and Machine Theory 30, 119-129.
- [18] Fenton R.G., Zhang Y., Xu J., (1991) “**Development of a new Geneva mechanism with improved kinematic characteristics**”, ASME Journal of Mechanical Design 113, 40-45.
- [19] Lee H.P., (1998) “**Design of a Geneva mechanism with curved slots using parametric polynomials**”, Mechanism and Machine Theory 33 (3), 321-329.
- [20] Figliolini G., Rea P., Angeles J., (2007) “**Synthesis of Geneva Mechanism and their equivalent Pure-Rolling Cams**”, 12th IFTOMM World Congress, Besancon France.
- [21] Lee H.P., (1998) “**Design of a Geneva mechanism with curved slots using parametric polynomials**”, Mechanism and Machine Theory 33 (3), 321-329.
- [22] Lee Jyh-Jone, Jan Bin-Heng, (2008). “**Design of Geneva mechanism with curved slots for non-undercutting manufacturing**”, Mechanism and Machine Theory.
- [23] Khurmi R. S. and Gupta J. K., (2004) “**A textbook of Machine Design**”, S. Chand and Company Ltd, New Delhi,
- [24] Khurmi R. S. and Gupta J. K., (2005) “**Theory of Machines**”, S. Chand and Company Ltd, New Delhi,.

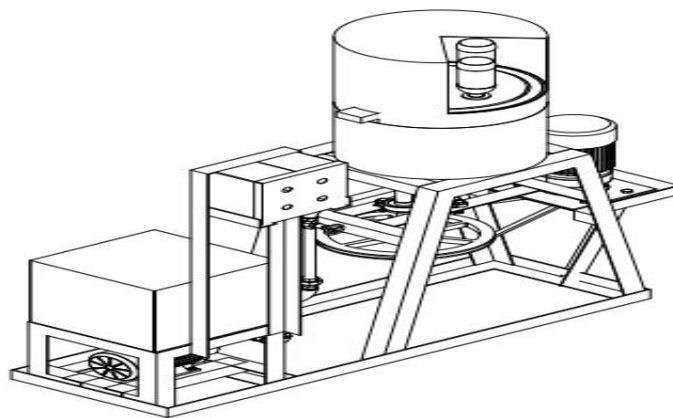
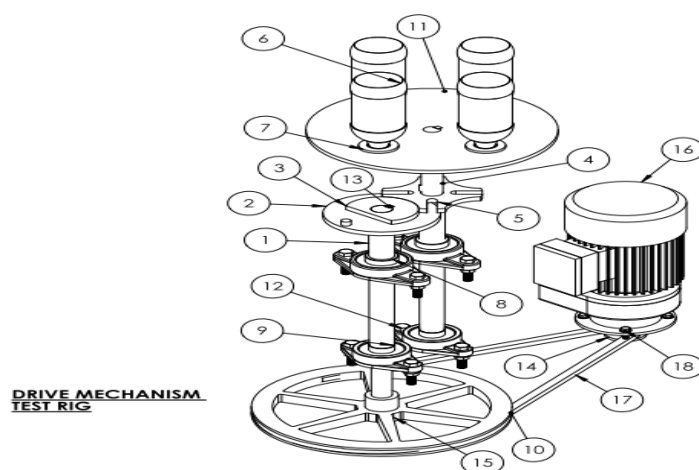


Fig.7 Rig Assembly



ITEM NO.	PART NUMBER	DESCRIPTION	QTY.
1	Driver Shaft	Mild steel Rod	1
2	Driver plate	Mild steel Plate	1
3	Cam	Mild Steel Plate	1
4	Geneva Shaft	Mild steel Rod	1
5	Geneva Wheel	Mild Steel Plate	1
6	Amstel Bottle	Stock	4
7	Bottle holder	Teflon	4
8	bearing 30mm	Stock	2
9	bearing 25mm	Stock	2
10	Driven Pulley	Aluminium Blank	1
11	Table	Stainless Steel Plate	1
12	M10 x 1.5 x 50	Stock	9
13	Key	Mild Steel Rod	3
14	Driver Pulley	Aluminium Blank	1
15	Pulley support	Mild Steel Plate	1
16	Geared electric motor	Stock	1
17	Belt	Stock	1
18	M6 x 1.0 x 20	Stock	4
25	M10 x 1.5 nut	Stock	8

Fig.8 Drive Mechanism

## Transport and Mechanical Characteristics of Corrosion-Inhibited High-Strength Self-Compacting Concrete

Marva Blankson<sup>1,\*</sup>, Savaş Erdem<sup>2</sup> and Ezgi Gürbüz<sup>2</sup>

<sup>1</sup>Department of Civil Engineering, The University of Technology Jamaica, Kingston-Jamaica

<sup>2</sup>Department of Civil Engineering, University of Istanbul, Avcılar Campus, Istanbul-Turkey

**Abstract:** This paper is on the study of traditional silica fume (SG) self-compacting concrete (SCC) samples that was made as control and then incorporated with carboxylic inhibitor (SM) to study the transport, rheological and mechanical responses of the inhibited samples. Comparison with the respective SG control, showed that the carboxylic inhibitor resulted in the reduction of the homogeneity of the SM samples and there was the development of flaws that could have contributed to the reduction in strength of the SM samples. When the concentration of the inhibitor was increased from the basic content to 100% higher, there was a noticeable increase in the chloride migration resistance of the SM samples. The study also showed that the transit time of the ultrasonic pulse that was transmitted was slower in the carboxylic inhibited-samples.

**Keywords :** Chloride Migration; Mechanic Properties; Rheology; Self-compacting Concrete.

### I. INTRODUCTION

Chloride-induced corrosion is one of the major deteriorating agents leading to the degradation of reinforced concrete structures. The chloride from marine environments, de-icing agents, admixtures and even concrete constituents, can attack the steel in reinforced concrete and contributes not only to early deterioration but also to increased maintenance activities. At this point it should be pointed out that the protection strategy of many corrosion-inhibiting compounds seems satisfactory as far as staving off the initiation of corrosion in the first fifty years of reinforced concrete members. However, there is a plethora of important buildings that are established as monumental edifices (such as the Burj Al Arab, Dubai) and others that may form part of essential services (such as the Øresund Bridge, Sweden and the Sydney Harbour Bridge, Australia) that will require longevity. For over 50 years corrosion inhibitor has been used in traditional reinforced concrete to protect the steel from corrosion. Moreover, with the present international emphasis on sustainability and low carbon emission, more consideration is given to reinforced concrete design that will not just span decades but centuries. However, there are other issues that are pertinent to the use of corrosion-inhibited SCC. With rising sea levels and the greater incidence of storm surges leading to inundation of the built environment, the issue of the reduction/depletion of the inhibiting capacity of the concrete and the matter of self-healing of corroded reinforced concrete will be of greater concern.

In more recent years SCC was developed and it is reported as having the potential to produce a durable material [1] mainly by nature of the refinement [2] and relatively low level of porosity in the interfacial zone in its microstructure [3]. Currently, researches are advancing the design of SCC admixed with corrosion inhibitor with a view to combine the attributes of the individual materials in one product.

This paper will focus on the study of traditional silica fume (SG) self-compacting concrete (SCC) samples that was made as control and then incorporated with carboxylic inhibitor to study the transport, rheological and mechanical responses of the inhibited samples.

### II. EXPERIMENTAL PROGRAMME

#### 2.1 Materials

Self-compacting concrete samples were made with ordinary Portland cement CEM1 52.5R and with silica fume admixture. The gradings of the cement and silica fume powders are depicted in Fig. 1. The cement was donated by Castle Cement Ltd, UK. The silica fume was provided by Elkem, Norway. A carboxylic type corrosion inhibitor was used in the experiment. The carboxylic inhibitor is an organic migrating compound that is formulated with a high range water-reducing admixture and viscosity modifying agent. A polycarboxylic high range water-reducing admixture was used in SCC mixtures that were not admixed with the multi-phase corrosion inhibitor.

The concrete mixtures were proportioned with and without corrosion inhibitors as shown in Table 1. The silica fume SCC without inhibitor (SG) was made as the control for the carboxylic silica fume SCC (SM). The combined grading of the used aggregates is shown in Fig. 1. The basic corrosion-inhibited SCCs used the concentration of inhibitor that is exhibited in Table 1 but some samples were also made with 2x the basic concentration. After the mixing of the concrete, the fresh material was used for the slump flow tests and for the casting of cubes, prisms, cylinders. The samples were cast without vibration. After de-moulding, all concrete samples were cured until 28 days.

## 2.2 Tests

Compressive strength tests were carried out on 100 x 100 x 100 mm samples and three concrete cubes were used for the determination of compressive strength for each SCC sample. A Zwick universal testing machine was used to determine the flexural tensile strength of the concrete specimens. Four 100 x 100 x 500 mm prisms were used for the four point flexural tensile test. A PUNDIT (portable ultrasonic non-destructive digital tester) was used to determine the dynamic modulus of elasticity and other parameters of each of the SCC samples. The non-steady state chloride migration test was done on 100 mm diameter x 50 mm thick specimens in accordance to NT Build 492 [4] test method. The reference [5] and real test set-up used in this study is shown in Fig. 2. The fractures surfaces of the samples were also characterized using the digital image analysis technique.

## III. RESULTS AND DISCUSSION

### 3.1 Rheology and Mechanical Properties

Table 3 shows the slump flow and flow rate values of the inhibited SCC and the silica fume control as measured from the Abrams cone. All the slump flow measurements were greater than 550 mm – the minimum slump flow requirement for SCC (EFNARC, [6]).

The 28-day compressive strengths of the SCC samples are shown in Table 4. The compressive strength of the respective carboxylic SM samples were 37% less than the corresponding SG control samples. However, further comparison with the respective SG controls showed that the carboxylic inhibitor increased the 28-day tensile strength of the SM sample. The tensile strength of SM samples were approximately 42% higher than the respective SG samples. Therefore it is evident that there are other mechanistic-related variables that are affecting the strength of the inhibited SCC samples.

The other result that is shown in Table 4 is that of the PUNDIT test. When comparison is made with the respective control, the transit time of the ultrasonic pulse that was transmitted was slower in the carboxylic inhibited-samples (SM) and this contributed to close to 100 m/ $\mu$ s reduction in the velocity of the SM samples. The PUNDIT dynamic moduli of the samples are also provided in Table 4.

### 3.2 Transport Property

The coefficients of non-steady state migration of chloride  $D_{nssm}$  of 28-day SCC samples are shown in Table 5. The average measurement from three specimens was used for the  $D_{nssm}$  reading of each sample. The SM SCC had a  $D_{nssm}$  coefficient that was approximately 12% higher than that of the SG control. It was further shown that the  $D_{nssm}$  values of the SM samples increased by 84% above that of the respective SG samples as the concentration of inhibitor increased by 100%.

In the SM SCC samples, the  $D_{nssm}$  coefficients showed that the addition of the carboxylic inhibitor increased the transport of chloride ions in the concrete. The PUNDIT velocities also showed that the homogeneity of the SM samples was reduced and this facilitated a higher chloride migration. However, the difference in the  $D_{nssm}$  coefficients of the SM and the SG samples is very low.

### 3.1 Failure Pattern

Cracking of the SM sample showed a more meandering pattern than the pattern in the control SG sample, and there were a couple of cracks branching from the main cracks. The manner of cracking in the SM sample is attributed to the more heterogeneous structure (Table 3) that resulted from the use of the carboxylic inhibitor in the silica fume SCC. As cracks preferentially travel through the path of least resistance, the ITZ properties become of major importance for the behaviour of this concrete under compressive loading. The stronger ITZ in the SM SCC concrete would efficiently participate in transferring stress through the composite, resulting in a greater compression force.

When the fracture extended to the surfaces of the SG samples, the cracks appeared less gradually and the cracks were larger, which showed a fracture that is typical of brittle materials. There were also manifestations of transverse cracking in the silica fume samples. The typical fractured surfaces and calculated fractal dimensions of the samples are shown in Fig.3 and Fig.4, respectively. A higher fractal dimension for the SM SCC sample indicates that more energy was dissipated under compression loading compared to the SG SCC sample.

## IV. FIGURES AND TABLES

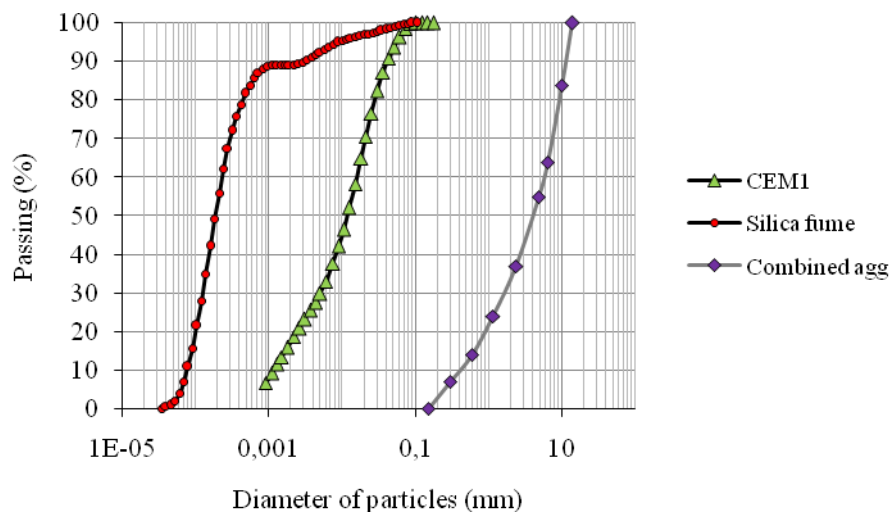


**Figure 1.** Particle size distribution of cement, silica fume and aggregate

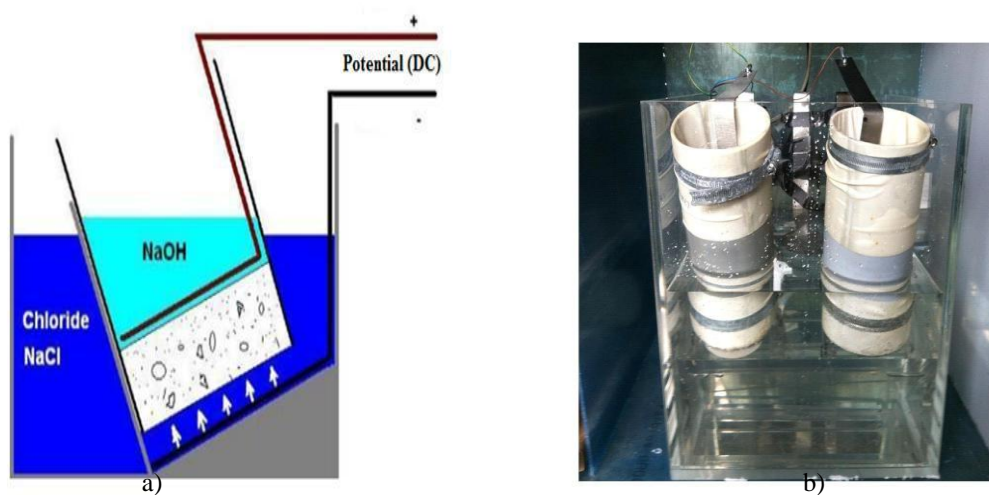


**Figure 2.** The reference (a) and real (b) test set-up used in this study for chloride migration measurement

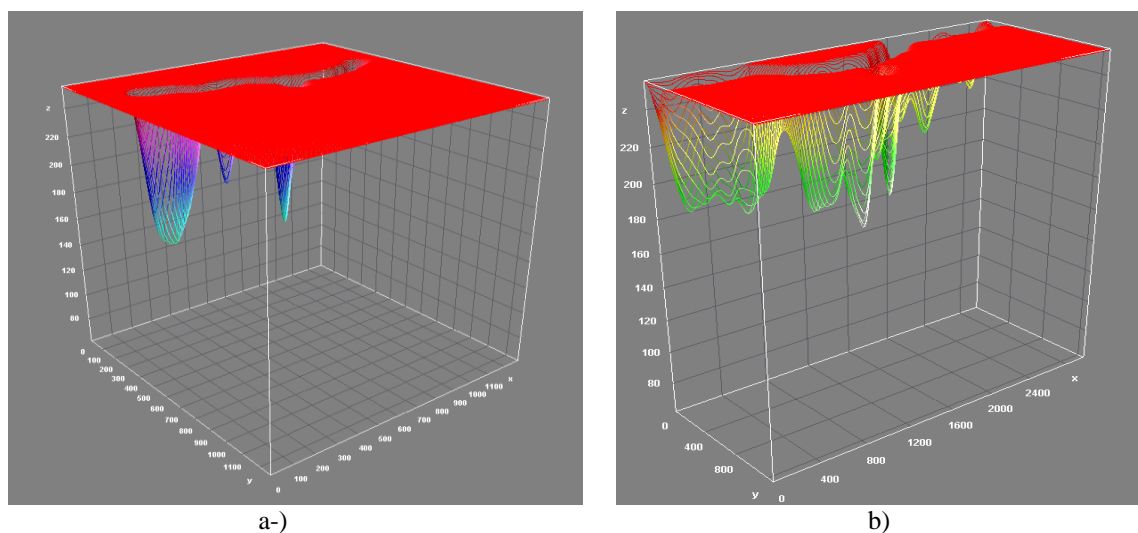


**Figure 3.** Typical fractured surfaces of the samples a-) SG sample and b-) SM sample

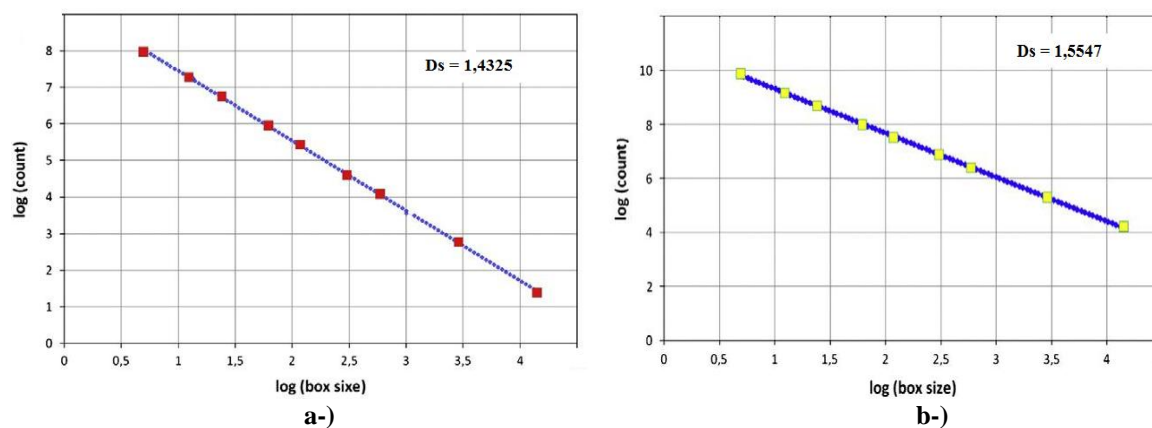


**Figure 4.** Calculated fractal dimensions of the samples a-) SG sample and b-) SM sample

Table 1 Basic proportions of SCC mixtures

Materials	SG	SM
Cement - kg/m <sup>3</sup>	542	542
Silica fume - kg/m <sup>3</sup>	28	28
Coarse aggregate - kg/m <sup>3</sup>	868	868
Sand - kg/m <sup>3</sup>	778	778
Water - kg/m <sup>3</sup>	180	180
W/P ratio (wt.)	0.32	0.32
Corrosion inhibitor* - %		0.300 approx. (carboxylic)
HRWRA# - %	1 (carboxylate)	

\* Minimum recommended percentages based on mass of dry ingredients

# Minimum recommended based on total mass of ingredients

Table 2 Properties of Fresh Concrete

	SM	SG
Slump flow (mm)	780	610
Flow rate (s)	6	7

Table 3 Mechanical Properties of SCC

	SM	SG
Relative density	2.28	2.41
Compressive strength (MPa)	68	93
Flexural tensile strength (MPa)	12.2	8.6
Pundit velocity (m/μs)	4668	4766
Dynamic moduli of elasticity (GPa)	45.11	49.1

Table 4 Non-steady state chloride migration coefficients

SCC samples	SM	SG	SM(2x)
$D_{nssm} \times 10^{-12} \text{ (m}^2/\text{s)}$	$1.9 \pm 0.4$	$1.7 \pm 0.5$	3.5

## V. CONCLUSION

The study of the inhibited SCC samples revealed that the homogeneity of the SM samples was reduced and this facilitated a higher chloride migration. This will, in turn, probably increase the propensity of the SM samples to corrosion. However, the difference in the  $D_{nssm}$  coefficients of the SM and the SG samples is very low and hence the protection strategy of the carboxylic compound was able to reduce the corrosion. The 28-day compressive strengths of the SM samples became less than the strength of the respective SG controls at the same age.

## REFERENCES

- [1] Zhu, W. and Bartos, P. J. M. (2003) Permeation properties of self-compacting concrete. *Cement and Concrete Research*, 33 (6), 921 – 926.
- [2] Kanellopoulos, A., Petrou, M. F. and Loannou, L. (2012) Durability performance of self-compacting concrete. *Construction and Building Materials* 37, 320 - 325.
- [3] Leemann, A., Münich, B., Gasser, P. and Holzer, L. (2006) Influence of compaction on the interfacial transition zone and the permeability of concrete. *Cement and Concrete Research* 36 (8), 1425 – 1433.
- [4] NT Build 492 Chloride migration coefficient for non-steady state migration experiments Concrete, Mortar and Cement-based Repairs Materials. Nordic council of ministers.
- [5] Luo, L.; De Schutter, G. Influence of corrosion inhibitors on concrete transport properties. *Materials and Structures* 2008, 41, 1571-1579.
- [6] EFNARC (2005) The European guidelines for self-compacting concrete – Specification, production and use. (Online) Available at: [http://www.europeanconcrete.eu/index.php?option=com\\_docman&task=doc\\_details&gid=1&Itemid=5](http://www.europeanconcrete.eu/index.php?option=com_docman&task=doc_details&gid=1&Itemid=5) (Accessed March 3, 2013).



## Design and Simulation of a Banking Network System

Abdul Hannan<sup>1</sup>, M.A.Jobayer Bin Bakkre<sup>2</sup>, Rajib Chandra Ray<sup>3</sup>,  
Md.Selim Hossain<sup>4</sup>.

<sup>1,2,3</sup>Dept. of Computer Science & Engineering, Jahangirnagar University, Dhaka, Bangladesh.

<sup>4</sup>Dept. of Computer Science & Engineering, Shahjalal University of Science and Technology, Sylhet, Bangladesh.

**ABSTRACT:** The general aim of this project is to simulate a banking system which is secure and easy to use. Previously the system was manual, not secure, also working slowly. This proposed system overcomes the lacking of the existing manual system. All branches of the Bank situated at District level provide the Banking services to customers and had to send report to the central branch manually, which sometimes creates problem to get, up-to-date information rapidly. But now through this system whenever any transaction will be taking place it will store in the central database and authorized person can get necessary information or report when they get into the system from any branches through Wide Area Network (WAN). To implement our project we have used OSI model. This system is using Packet Tracer 5.3 for network simulation, Wamp Server, PHP Mysql, for Banking Web application Security. After implementation of all functions, the system is tested in different stages and it was successful for its purpose.

**KEYWORD-** Relevant literature, Methodology, Analysis design & development, Limitation & Future work.

### I. INTRODUCTION

An ideal Bank Networking system will be fully network base and easy with friendly user interface staff task management system where any banking system manage their networking system somehow Head office , Branch Office, and other office are maintain LAN, MAN, WAN, VLAN, VLSM, VPN and some branch are maintain by manageable switch. LAN is used by Local Area Networking system for example one office and a one building. And MAN are using by the Metro Politian area Network for Example small town, and WAN are use by the WIDE AREA NETWORK. In this networking system are used by all banking users can use by shared their data very easily. So that every user use to take about Network Structure & Security of Banking System instantly this way anywhere.

#### 1.1 Objectives

1. To design and simulate a banking network system which is secure.
2. To simulate a banking network system that will easily manage any banking task.
3. To manage the banking network by a central system

#### 1.3 Justification of study

The trend of growth of Online Banking brings many security issues and increasing cost of implementing higher security system for both Online Banking users and the banks. Classers said security is all about risks and associated cost in his paper .The most critical issue of Online Banking security is to protect valuable information that is susceptible to unauthorized access by attackers. Hence, the banks must constantly increase security. At the same time, the banks must manage costs to make a profit. In contrast, increasing security is increasing the cost for attackers to break into the system, and increasing the punishment that the attackers may suffer. Hence the Internet criminals/attackers/crackers may lose motivation for hacking a high security online banking system.

#### 1.4 Scopes of study

The scope of the Network Structure & Security of Banking System includes.

1. Online based day to day transmission.
2. Save time and cost because of day to day transmission.
3. Established relation between one branch to another
4. Connect all branches to head branch in same network.
5. Online based update and maintain everyday work.

## II. LITERATURE REVIEW

### 2.1 Review of relevant literature

Networks can also be characterized in terms of spatial distance as local area networks (LANs), metropolitan area networks (MANs), and wide networks (WANs). A given network can also be characterized by the type of data transmission technology in use on it (for example, a TCP/IP or Systems Networks Architecture network); by whether it carries voice, data, or both kinds of signals; by who can use the network (public or private); by the usual nature of its connections (dial-up or swathed, dedicated or no switched, or virtual connections); and by the types of physical links (for example, optical fiber, coaxial cable, and Unshielded twisted Pair).

The flowing methods to be traditional (old) way of recurrent

- Data transfer / transition send branch office to head office by manually.
- Need extra cost for transmission because of manually transmission.
- Time based transmission.
- Low security system .Data carries or transfers by human.
- User unfriendly because of slow process.
- Very complex to maintain.

### 2.2 Computer Networking

A computer network is a system for combination among two or more computers. These networks are fixed (cabled, permanent) or temporary (as via modems). A computer network of computer networks that use the TCP/IP network protocols to facilitate data transmission and exchange intranet a restricted computer network; a private network created using World Wide Web software.

### 2.3 IP address

An IP address consists of 32 bits of information. The 32 bit IP address is a structured or hierarchical address. 32 bits are divided 4 sections. And every section is 8 bit address the 32 bits addresses are divided two parts one is Host section, and another is m section. 32 bits addresses have also 5 classes, which is,

	bits	8bits	8bits	8bits
<b>Class A:</b>	Network	Host	Host	Host
<b>Class B:</b>	Network	Network	Host	Host
<b>Class C:</b>	Network	Network	Network	Host
<b>Class D:</b>	Multicast			
<b>Class E:</b>	Research			

Network address of Class A: 1 to 126

Network address of Class B: 128 to 191

Network address of Class C: 192 to 223

Network address of Class D and E: The address between 224 and 255 are reserved for class D and E networks. Class D is used for multicast address, Class E is used for scientific purpose.

### 2.4 VLSM

Network administrators must anticipate and manage the physical growth of networks. This may require them to buy or lease another floor of a building for new network equipment such as racks, patch panels, switches, and routers. Network designers must choose address schemes that allow for growth. Variable-length subnet mask (VLSM) is used to create efficient and scalable address schemes. IPv4 offered an address strategy that was scalable for a time before it resulted in an inefficient allocation of addresses. IPv4 may soon be replaced with IP version 6 (IPv6) as the dominant protocol of the internet. IPv6 has virtually unlimited address space and implementation has begun in some networks. Over the past two decades, engineers have successfully modified IPv4 so that it can survive the exponential growth of the Internet. VLSM is one of the modifications that has helped to bridge the gap between IPv4 and IPv6.

#### 2.4.1 Why is it used?

As IP subnets have grown, administrators have for ways to use their address space more efficiently. This page introduces a technique called VLSM. With VLSM, a network administration can use a long mask on networks with few hosts, and a short mask on subnets with many hosts.

#### VLSM is used for following reasons

- The ultimate solution is IPv6 with 128-bit address space.
- It allows for 340, 283, 366, 920, 938, 463, 374, 607, 431, 768, 211, 456 address.

### 2.4.2 Importance of VLSM

Efficient use of organizations assigned IP address space. Route aggregation VLSM. Efficient use of the organization's assigned IP address space Assume that a network administrator has decided to configure the 130.5.0.0/16 network with a /22 extended-network prefix. This design allows for 64 subnets with 1,022 hosts each. Fine if the organization plans to deploy a number of large subnets. What about the occasional small subnet containing only 20 or 30 hosts? About 1,000 IP host addresses wasted for every small occasional subnet.

### 2.5 Networking devices

A computer network is comprised of different devices to share, transmit, and boost the signal, voice and data. Network devices or components are the physical parts connected to a network. The basic network devices, Individual computers, Hub, Switch, Bridges, Routers. The following is the Devices.

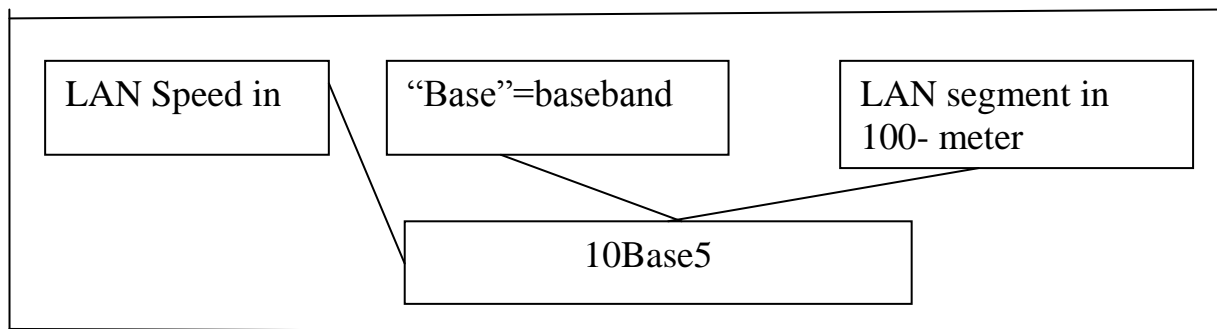
Switch, Router

### 2.6 ETHERNET

Ethernet was originally developed by digital, Intel and Xerox (DIX) in the early 1970's and has been designed as a 'broadcast' system, i.e. stations on the network can send messages whenever and wherever it wants. All stations may receive the messages, however only the specific station to which the message is directed will respond. The original format for Ethernet was developed in Xerox Palo Alto Research Center (PARC) California in 1972 Using Carrier Sense Multiple Access with Collision Detection (CSMA/CD) it had a transmission rate of 2.94Mbps and could support 256 devices over cable stretching for 1km. the two inventors were Robert Metcalf and David Boggs. The 'Ether' part of Ethernet denotes that the system is not meant to be restricted for use on only one medium type, copper cables, fiber cables and even radio waves can be used .

#### 2.6.1 PHYSICAL CONNECTIONS

IEEE 802.3 specifies several different physical layers, where Ethernet defines only one. Each IEEE 802.3 physical layer protocol has a name that summarizes its characteristics.



#### 2.6.2 ETHERNET FRAME FORMATS

Field length,  
In bytes

7	1	6	6	2	46-1500	4
Preamble	S O	Destination address	Source address	Type	Data	FCS

Field length:-  
In bytes:

7	1	6	6	2	46-1500	4
Preamble	S O F	Destination address	Source address	Type	Data	FCS

SOF = Start of frame delimiter

**Figure: Ethernet and IEEE 802.3 Frame Formats**

FCS = Frame check sequence

SOF = Start of frame delimiter

FCS = Frame check sequence

Both Ethernet and IEEE 802.3 Frames begin with alternating pattern of ones and zeros called a preamble. The preamble tells receiving stations that a frame is coming. The byte before the destination address in both an Ethernet and an IEEE 802.3 frame is a state of frame delimiter. This byte ends with two consecutive one bits, which serve to synchronize the frame reception portions of all stations on the LAN. Immediately following the preamble in both Ethernet and IEEE 802.3 LANs are the destination and source address fields. Both Ethernet and IEEE 802.3 addresses are 6 bytes long.

### III. METHODOLOGY

#### 3.1 METHODOLOGY

In this project “Design and Simulation of a Banking System” discuss the total banking network structure & some security features. We are survey in the different bank and collect some data or information. The OSI layer was introduced by the International Organization for Standardization (ISO) in 1984 in order to provide a reference model to make sure products of different vendors would interoperate in networks. OSI is short for Open Systems Interconnection. Data transmitted between software programs passes all 7 layers. The Application, Presentation and Session layers are also known as the Upper Layers. The Data Link and Physical layers are often implemented together to define LAN and WAN specifications.

#### 3.2 When to use the OSI model

One of the first things we learn when we started working in the field of computer networking is the OSI model. The OSI model is used to describe how data should pass across a network. It is broken up into 7 layers, starting with layer 1 as the lowest layer and moving up to layer 7. The 7 layers are labeled, starting with layer 1 at the bottom, 1-Physical, 2-Data Link, 3-Network, 4-Transport, 5-Session, 6-Presentation, and 7-Application. There are many things that live at each layer. Layer 1, the Physical Layer, has to do with all things that are used to provide physical connectivity. Some of them are Ethernet cables, Fiber cables, and wall jacks. The most common networking device at Layer 1 is a hub. It provides device connectivity and that is about it. Hubs have no brain, and cannot be managed at all. With hubs, the broadcast domain (which is the segment of the network where all nodes can reach each other by broadcast) and the collision domain (which is the segment of a network where data packets can collide with one another) are the same, and include every port on every hub connected together on a physical segment

#### 3.2.1 BENEFITS OF OSI MODEL

The separating sales communications and multi-level marketing into smaller logical sections, the OSI model simplifies how networking protocols are created. The OSI model was designed to ensure different types of equipment (like adapters, routers, hubs and network adaptors) are compatible.

1. Provide a wide variety of choice. Customers have a wide variety of choice since software/ hardware from different manufactures work together in harmony. In addition, the OSI model can fit to any compatible software/hardware from different users in other parts of the world.
2. It does not rely on a specific operating system. OSI is convenient since errors are dealt with at each level, as different levels operate automatically independent of each other. This makes it easier to troubleshoot problems that may arise at each stage, by separating the networks into small manageable pieces.
3. The user can understand the common terms used in networking. OSI model also help the user to understand different networking terms and functional relationship applied on multiple networks. In addition, the user also understand how new technologies are developed in the existing networks.
4. Interprets product functionality at each stage. The OSI model simply uses different stages of functionality. For instance, each stage has specific functions to ensure all networks operate without technical hitches. Also, each layer has its own interface specifications and a well-defined connector.
5. Encrypt data for security purposes. Decryption and encryption services are also available for security purposes. Expansion and compression of messages is simplified to ensure it travels from one system to another efficiently.

6. It is easier to add multiple network models. The OSI model is designed in such a way that user further extend new protocols within the process. This means you can use additional layered architecture other than the existing one. Due to its complexity, poor performance can be obtained in day to day applications, thereby it requires great technical know-how.

### 3.3 TCP/IP Network Model

Although the OSI model is widely used and often cited as the standard, TCP/IP protocol has been used by most UNIX workstation vendors. TCP/IP is designed around a simple four-layer scheme. It does omit some features found under the OSI model. Also it combines the features of some adjacent OSI layers and splits other layers apart. The four network layers defined by TCP/IP model are as follows.

## IV. ANALYSIS DESIGN AND DEVELOPMENT

### 4.1 Requirement Gathering Technique

#### Functional Requirements

Banking system in Bangladesh all banks has an IT department. IT department solution all type of IT problem and serve the core network. IT creates a core network diagram. This diagram involves all type of useable network mechanism (Switch, Router, Firewall, Server) etc. Simulation is the most important of any system.

An accurate system design, accurate performance and accurate Simulation give best performance of a system.

#### 4.1.1 Analysis of Requirement

The description of the services and constraints are the requirements for the system and the process of finding out, analyzing, documenting and checking these services and constraints is called requirements engineering. The hardware and software requirement which we need in our project is given below.

#### 4.2 Hardware Requirement

IBM compatible , Intel Pentium 4, Intel core-i3 based PC with a monitor ,keyboard and mouse, system must have 1 GB Ram, Hard disk 80 GB or of available memo.

#### 4.3 Software Requirement

This following software we have used to implement our project-

- Windows XP or.
- Windows 7 or.
- Windows 8 platform.
- Packet Tracer 5.3.3
- Switch.
- Router.
- Firewall.
- Server.

#### 4.3.1 Packet Tracer 5.3

LAN, MAN, VLAN, ACL, VPN, & Banking Network Combine diagram, Protocol, and different branch transmission simulation.

#### 4.4 Data Flow diagram

Data Flow diagram is a way of expressing system requirements in graphical form. It defines the flow of data, the process and the area where they are store.

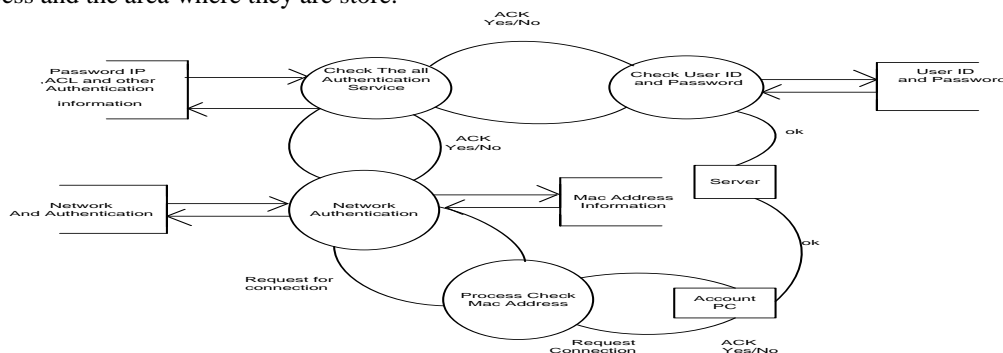


Fig: Data Flow diagram

#### 4.4.1 Symbol of DFD

- A square define the data source.
- Arrow defines the data flow.
- A circle represents a process that transforms incoming into outgoing data flow.
- An open rectangle is a data store – data at rest or a temporary repository of data.

#### 4.5 ROUTER

A router is a special type of computer. It has the same basic components as a standard desktop PC. It has a CPU, memory, a system bus, and various input/output interfaces. However, routers are designed to perform some very specific functions that are not typically performed by desktop computers. For example, routers connect and allow communication between two networks and determine the best path for data to travel through the connected networks. Just as computers need operating systems to run software applications, routers need the Internet work Operating System (IOS) software to run configuration files? These configuration files contain the instructions and parameters that control the flow of traffic in and out of the routers. Routers use routing protocols to determine the best path for packets. The configuration file specifies all the information for the correct setup and use of the selected or enabled, routing and routed protocols on a router.

##### 4.5.1 ROUTER CONFIGURATION

Here discussed about the routing configuration

##### Setting Hostname

A router should be given a unique name as one of the first configuration tasks. This task is accomplished in global configuration mode with the following command.

Now router configuration start

Router (config) #hostname JU

WUB (config) #

##### Now setting Router Password:

##### Console password:

Router(config)#line console 0

Router(config-line)#login

Router(config-line)#password<password>

##### Virtual Privileged EXEC Mode:

Router(config)#line console 0 4

Router(config-line)#login

Router(config-line)#password<password>

##### Secure Privileged EXEC Mode

The enable password and enable secret commands are used to restrict access to the privileged EXEC mode. The enable password is only used if the enable secret has not been set. The enable secret command should be used because the enable secret command is encrypted. The enable passwords command is not encrypted.

Router (config) #enable password <password> Router(config)#enable secret <password>

##### Password

##### Encryption

The service password-encryption command applies a weak encryption to all unencrypted passwords. The enable secret <password> command uses a strong MD5 algorithm for encryption.

Router (config) #service password-encryption

##### Backup Configuration File :

A current copy of the configuration can be stored on a TFTP server. The copy running-configuration TFTP command can be used to store the current configuration on a network. TFTP server.

Router# copy running-config tftp

##### Interface Configuration:

Serial Interface

Each connected serial interface must have an IP address and subnet mask to router IP packet. Configuration the IP address with the following commands:

Router:r(config)#interface serial 0/0/0

Router(config)#ip address<ip address> <subnetmask>

##### Setting Clock Rate & No Shutdown:

By default, Cisco routers are DTE devices but they can be configured as DCE devices.

By default, interfaces are turned off, or disabled. To turn on or enable an interface, the command no shutdown



is entered. If an interface needs to be administratively disabled  
 For maintenance or troubleshooting, the shutdown  
 Command used to turn off the interface.  
 Router (config) #interface serial 0/0/0  
 Router(config-if)#clock rate 400000  
 Router(config-if)#do wr  
 Router(config-if)#exit

#### 4.6 ROUTING PROTOCOL

A routing protocol is used by routers to dynamically find all the networks in the internet work and to ensure that all routers have the routing table. Basically, a routing protocol determines the path of a packet through an internet work. Examples of routing protocols are Static, RIP, EIGRP, and OSPF.

#### 4.7 Administrative Distances

Administrative distance is the feature used by routers to select the best path when there are two or more different routers to the same destination from two different routing protocols. Administrative distance defines the reliability of a routing protocol.

Router source	Default Distance
Connected interface	0
Static router	1
EIGRP summary route	5
External BGP	20
Internal EIGRP	90
IGRP	100
OSPF	110
IS-IS	115
RIP	120
EGP	140
EIGRP external route	170
Internal BGP	200
Unknown	255

**Table: default administrative distances.**

#### 4.8 CLASSIFICATION OF DYNAMIC ROUTING PROTOCOL.

Dynamic routing protocols do not change how routing is done. They just allow for dynamic altering of routing tables. There are two classifications of protocols:

**4.8.1 Interior Gateway Protocols (IGPs)** exchanges routing information within a single autonomous system. Common examples include.

**4.8.2 Exterior Gateway Protocols (EGPs)** route between separate autonomous systems. EGPs include.

- EGP (The original exterior gateway protocol used to connect to the former internet backbone network ~ now obsolete).
- BGP (Border Gateway Protocol: current version, BGPv4m, was adopted around 1995).

#### 4.8.3 RIP Routing Updates

RIP sends routing-update messages at regular intervals and when the network topology changes. When a router receives a routing update that includes changes to an entry, it updates its routing table to reflect the new router. The metric value for the path is increased by 1, and the sender is indicated as the next hop. After updating its routing table, the router immediately begins transmitting routing updates to inform other network routers of the change. These updates are sent independently of the regularly scheduled updates the RIP routers send.

#### 4.8.4 RIP Configuration

The command syntax is as follows:

Router (config) #router rip  
 Router (config-router) #network network-number net-mask

#### 4.9 IGRP Configuration

To configure the IGRP routing process use the router igrp configuration command. The command syntax is as follows. Router A (config) #router igrp as-number

Router A (config) #network network-number net-mask

There as number identifies the IGRP process.

To specify a list of networks for IGRP routing process, se the network router configuration command. To remove an entry, use the no form of the command.

##### 4.9.1 EIGRP Features and Operation

EIGRP is sometimes referred to as a hybrid routing protocol because it has characteristics of both distance-vector and link-state protocols. For example, EIGRP doesn't send link-state packets as OSPF does; instead, it sends traditional distance-vector updates containing information about networks plus the cost of reaching them from the perspective of the advertising router. This makes EIGRP suitable for very large networks. EIGRP has a maximum hop count of 255. There are a number of powerful features that make EIGRP a real standout from IGRP and other protocols. The main ones are listed here.

- Support for IP, IPX, and Apple Talk via protocol-dependent modules
- Considered classless (same as RIPv2 and OSPF)
- Support for VLMS/CIDR
- Support for summaries and discontinuous networks networks
- Efficient neighbor discovery
- Communication via Reliable Transport Protocol (RTP)
- Best path selection via Diffusing Update Algorithm (DUAL)

##### 4.9.2 EIGRP Configuration

EIGRP is an ideal choice for large, multi-protocol networks built primary on Cisco routers.

RouterA(Config)#router eigrp as-number

RouterA(Config)#network network-number net-mask.

#### 4.10 OSPF Features and Operation

OSPF configuration requires that the OSPF routing process be enabled on the router with network addresses and area information specified. Network addresses are configured with a wildcard mask and not a subnet mask. The wildcard mask represents the links or host addresses that can be present in this segment. Area IDs can be written as a whole number or dotted decimal notation.

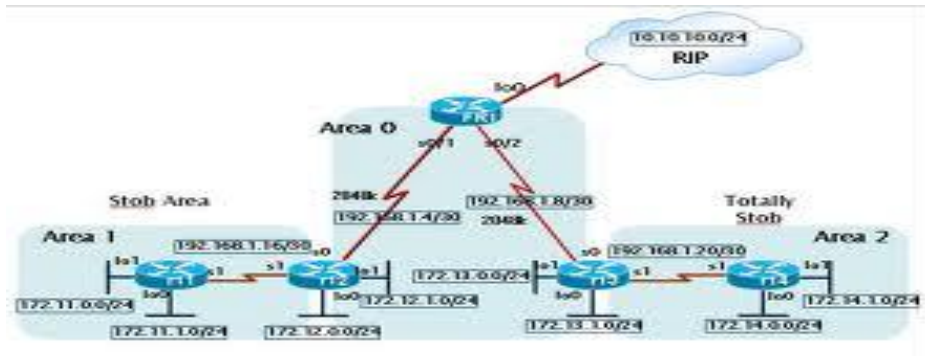


Figure: An OSPF as Consists of Multiple Areas Linked by Routers.

OSPF provides the following features [8];

- Consists of areas and autonomous systems
- Minimizes routing update traffic
- Allows scalability

##### Supports VLSM/CIDR

- Has unlimited hop count
- Allows multi-vendor deployment (open standard)

Is supposed to be designed in a hierarchical fashion, which basically means that you can separate the larger internetwork into smaller internetworks called areas. This is the best design for OSPF.

#### 4.10.1 OSPF Configuration

To enable OSPF routing, use the global configuration command syntax:

Router (configure) #router ospf process-id

Router (configure-router) #network address wildcard-mask area area-id.

#### Now discuss and simulate the RIP Protocol.

Routing Information Protocol (RIP) is a true Distance-Vector routing protocol. It sends the complete routing table out to all active interfaces every 30 seconds. RIP only uses hop count to determine the best way to a remote network, but it has a maximum allowable hop count of 15, meaning that 16 is deemed unreachable.

**Network structure:** Banking system in Bangladesh all banks has an IT department. IT department solution all type of IT problem and serve the core network. IT creates a core network diagram. This diagram involves all type of useable network mechanism (Switch, Router, Firewall, Server) etc. Simulation is the most important of any system. An accurate system design, accurate performance and accurate Simulation give best performance of a system.

#### 4.11 Usable Protocol:

In banking network system data transfer for router configuration using two types of routing protocol.

- RIP (Version 2)
- OSPF

OSPF protocol uses the following bank

- HSBC
- Standard Chartered

RIP (Version 2)

- NCC bank
- BRAC bank

#### 4.12 Project Structure:

Now we discuss and simulate the OSPF protocol.

Open Shortest Path First (OSPF) is a routing protocol developed for Internet Protocol (IP) networks by the interior gateway protocol (IGP) working group of the Internet Engineering Task Force.

#### 4.13 Now discuss and simulate the RIP Protocol.

Routing Information Protocol (RIP) is a true Distance-Vector routing protocol. It sends the complete routing table out to all active interfaces every 30 seconds. RIP only uses hop count to determine the best way to a remote network, but it has a maximum allowable hop count of 15, meaning that 16 is deemed unreachable.

#### 4.14 What is ATM?

ATM is Automated Teller Machine. Now it's making peoples life very easy as they get their money when they need. So, they do not need to carry either big amount of money or the cheque book all the time. To get rid from this burden they need to deposit money in the bank by opening an account and then the bank will be given a Card i.e. an ATM card with a PIN number to them. By using that they can withdraw money from any ATM machine of that bank. When they insert the card in the machine and the PIN number the machine will show few instructions on the screen. By that time verification (PIN Number and Account Number) will be done with the main bank computer as they are connected. If the verification is correct then the user will choose an instruction and the ATM will dispense money to the card holder.

#### 4.15 Internal Structure of ATM

In the following pictures we have the internal structure of two different type of ATM machine.

And also it can be divided into two different parts:- Upper Unit, -Lower Unit

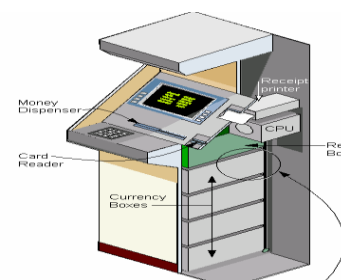
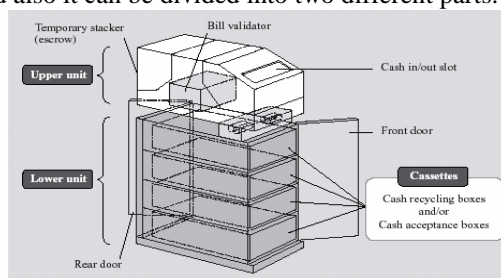


Fig: Shows the Complete Internal Structure.

#### 4.16 Interactive components of ATM

**Card Reader:** Customer inserts their card in it when there is written “Please Insert Your card” on the screen.

**Keypad:** Use for PIN code input, choices, amount of money etc as the input to the ATM machine.

**Display Screen:** This screen shows all the instructions or options for the customers ‘convenience.

**Screen Buttons:** When options are given on the screen one user can choose any of the options accordingly by the use of button on left or right side of the screen. These buttons select the option from the screen.

**Cash Dispenser:** Withdrawal money is given by this slot.

**Deposit Slot:** To deposit money this slot is use.

**Speaker:** Speaker provides the facilities to the customer by giving auditory feedback.

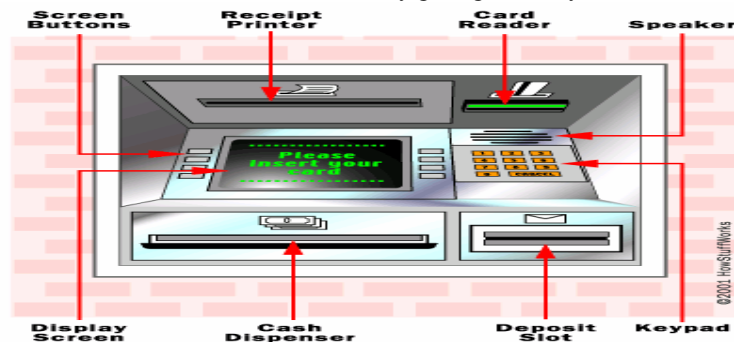


Fig: Interactive Components of ATM

#### 4.17 Possible Type of Data stored in Magnetic Stripe Card

Mainly magnetic strip hold the following information:

- Cardholder Name
- Card Number / Account Number
- Expiration Date and
- Additional Data if needed

#### 4.18 Algorithm use for Card Number Generation

LUHN's algorithm is used for card number generation and encoding. It is also called mod 10 algorithms. Card number must be 13 to 16 digits. And the last digit is the check digit. To calculate check Digit:

1. First drop the last digit from the card number (because that's what we are trying to calculate).
2. Reverse the number.
3. Multiply all the digits in odd positions (The first digit, the third digit, etc) by 2.
4. If anyone is greater than 9 subtract 9 from it.
5. Sum those numbers up.
6. Add the even numbered digits (the second, fourth, etc) to the number you got in the previous step.
7. The check digit is the amount you need to add to that number to make a multiple of 10. So if you got 68 in the previous step the check digit would be 2. You can calculate the digit in code using check digit =  $((\text{sum} / 10 + 1) * 10 - \text{sum}) \% 10$ . For Credit Card Number Validation use 10 mod Algorithm:

- First step: number is reversed and then every second digit is doubled

Example:

378282246310005

Reverse

5 0 0 0 1 3 6 4 2 2 8 2 8 7 3

Second digit

0 0 6 8 4 4 14

- Second step: resulted values will be added to those of which are not multiplied.

$= 5 + (0) + 0 + (0) + 1 + (6) + 6 + (8) + 2 + (4) + 8 + (4)$

$+ 8 + (14-9) + 3 = 60.$

#### 4.19 What is ATM Card?

ATM card is also like magnetic strip card. It is also a data carrier which electronically reads and writes data.

ATM cards mainly a debit card.

#### 4.21 Connection Type of ATM

ATM connections mainly have two types:

- Dial up Connection using Modem
- Leased Line Connection

#### 4.22 ATM Service Providers in Bangladesh

-Standard Chartered, HSBC, BRAC Bank, Bank Asia & NCC etc.

4

#### 30 Survey Report

##### Bank Asia

Bank Asia uses ETN (Electrical Transaction Network) network which is a United International ATM service provider. ETN combined nine banks to give E-Cash services. Network equipments like ATM machine, switches etc are setup by ETN.

#### 4.23 Ways of Transaction

In Bank Asia transactions are divided into three main categories

- My bank to others bank A customer of a bank uses other banks ATM.
- Others bank to my bank other banks customer uses ATM of Bank Asia.
- My bank to my bank a customer uses its own bank ATM machine.

#### 4.24 Connectivity Type

For ATM machines Bank Asia (provided by ETN) uses two types of connections. They use leased line for connection. Bank Asia uses two connection lines because if one line is down immediately other one will be activated within a minute. These connections are:

- DDN (under T&T)
- Metro net

#### 4.25 No. of Digit Uses

Bank Asia uses 18 digit ATM card (provided by ETN). They divide 18 in five sections for the identification of those banks, Account number, branch etc.

1-6 digits	7-9 digits	10-12 digits	13-17 digits	18 digits
International Identification number (IIN)	Regional code	Branch code	Account number	Computer generated

**Fig: Classification of 18 Digit Number**

##### IIN

First six digits are different for those nine banks. So, ATM machine can easily identify among these banks.

##### Regional Code

0These 3 digits are used to distinguish between different districts Branch Code.

##### Branch Code

These 3 digits are used to distinguish between different districts

##### Account Number

These five digits are the account number which differentiate among the user and unique for each user.

#### 4.26 Problems of ATM

Bank Asia has few problems with their ATM machines

- Do not have Bangle Interface
- ATM booths are not available in every locality.

#### 4.27 SECURITY

Security is most important part for online banking system. We use the different method for provide strong online banking security system and use owasp top ten project provide online banking security. Ensuring comprehensive network security visibility is no easy task. Uncover expert tips on how to improve network security visibility with network flow analysis tools, cloud security monitoring solutions, and anomaly-based monitoring technology.

#### 4.28 AUTHENTICATION MECHANISM

Authentication is the process of establishing whether a client is who or what it claims to be in a particular context. A client can be an end user, a machine, or an application. The authentication mechanism is responsible for creating a credential, which is an internal product representation of a successfully authenticated client user. The abilities of the credential are determined by the configured authentication mechanism.

##### 4.28.1. Challenge handshake Authentication Protocol (Chap)

CHAP is an authentication scheme used by point to point servers to validate the identity of remote clients. CHAP periodically verifies the identity of the client by using a three-way handshake. CHAP provides protection against playback attack by the peer through the use of an incrementally changing identifier and of a variable challenge-value. CHAP requires that the client make the secrete available in plaintext form.

**CHAP Packets**

Description	1 byte	1 byte	2 bytes	1 byte	Variable	Variable
Challenge	Code = 1	ID	Length	Challenge length	Challenge value	Name
Response	Code = 2	ID	Length	Response length	Response value	Name
Success	Code = 3	ID	Length		Message	
Failure	Code = 4	ID	Length		Message	

**4.29 ACCESS CONTROL LIST (ACL)**

ACLs are lists of conditions used to test network traffic that tries to travel across a router interface. These lists tell the router what types of packets to accept or deny.

01. ACLs can be created for all routed network protocols such as IP and Internet
02. Packet Exchange (IPX).
03. ACLs can be configured at the router to control access to a network or subnet.
04. To filter network traffic, ACLs determine if routed packets are forwarded or blocked at the router interfaces.

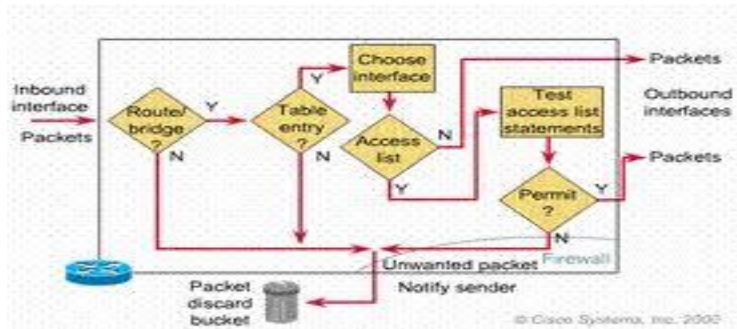


Figure: ACLs working Area

**4.29.1 ACLs can be used to perform the following task**

- Limited network traffic and increase network performance
- Provide traffic follow control
- Provide a basic level of security for network access.
- Decide which types of traffic are forwarded or blocked at the router interfaces.
- Control which areas a client can access on a network.
- Script hosts to permit or deny access to a network.

**4.29.2 How ACLs Work:**

ACL is made up of statements that define whether packets are accepted or rejected at inbound interfaces.

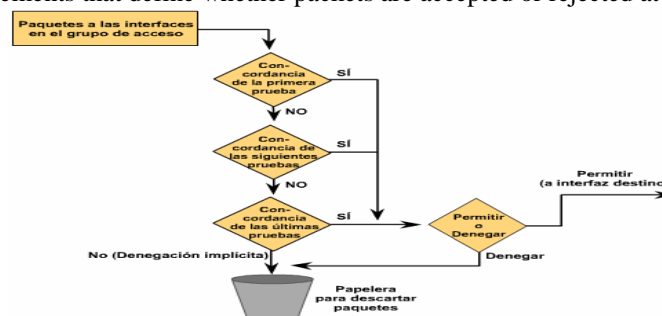


Figure: ACL Working Flowchart.

**4.30 Virtual Local Area Network (VLAN)**

VLAN is another process of secure the network security. In the banking system using the VLAN head office to other branch office for provides the integrated security. VLAN configuration using a manageable Cisco switch. Configure the switch and separate the each department. Each department only access the own department data cannot access the other department data without permission.



#### 4.30.1 Virtual private Network (VPN)

VPN follows a client and server approach. VPN clients authenticate users, encrypt data, and otherwise manage sessions with VPN servers utilizing a technique called **tunneling**.

### V. SUMMARY STEP WORK DESCRIPTION

#### DESCRIPTION

The aim of this system is to overcome the lacking of the manual system. All branches of the Bank situated at District level provide the Banking services to customers and had to send report to the central branch manually, which sometimes create problem to get up-to-date information rapidly. But now through this system whenever any transaction will be taking place it will store in the central database and authorized person can get necessary information or report when they get into the system from any branches through Wide Area Network (WAN). Routers are generally known as intermediate systems, which operates at the network layer of the OSI reference model, routers are devices used to connect two or more networks (IP networks) or a LAN to the Internet. A router acts as a packet filter when it forwards or denies packets according to filtering rules. As a Layer 3 device, a packet-filtering router uses rules to determine whether to permit or deny traffic based on source and destination IP addresses, source port and destination port, and the protocol of the packet. These rules are defined using access control lists or ACLs. Banking system in Bangladesh all banks has an IT department. IT department solution all type of IT problem and serve the core network. IT creates a core network diagram. This diagram involves all type of useable network mechanism (Switch, Router, Firewall, Server) etc. Simulation is the most important of any system. An accurate system design, accurate performance and accurate Simulation give best performance of a system. Now we discuss and simulate the OSPF protocol. Open Shortest Path First (OSPF) is a routing protocol developed for Internet Protocol (IP) networks by the interior gateway protocol (IGP) working group of the Internet Engineering Task Force (IETF)

### VI.CONCLUSION

Now a days, technological development, and automated system development is more essential and crying need for the expansion of banking services because They will need less employers by using automated system. On top of that Security is a major issue regarding banking issues. With this system network will be more easy to handle and it will route the data in a shortest path in a vast distributed system. In future we will try to implement it in real life so that banks can use it and get benefited from this project.

#### 6.1 Future work

- ✓ Add time based transmission.
- ✓ Security system will be upgraded .
- ✓ Make the project more user friendly.
- ✓ Real life implementation.

#### 6.2 Limitations

- ✓ The main Limitation is to implement the project in real world . Because we only simulate it via packet tracer.
- ✓ Due to less time and work pressure we could not add more features which could make the project more useful.

### REFERENCE

- [1] J.Claessens, V. Dem, D. Cock, B. Preneel, J. Vandewalle (2002) "On the Security of Today's On-line Electronic Banking Systems".
- [2] Andrew S. Tanenbaum, (2002)"Computers network".
- [3] CCNA study Guide, Available At: [https://www.google.com.bd/?source=search\\_app&gws\\_rd=cr,ssl&ei=y9bVYniG4KsuQTuvY84#q=Todd+Lammle,+%E2%80%99CCNA+study+Guide%E2%80%99D,BPB+Publications,+Edition:+5<sup>th</sup>](https://www.google.com.bd/?source=search_app&gws_rd=cr,ssl&ei=y9bVYniG4KsuQTuvY84#q=Todd+Lammle,+%E2%80%99CCNA+study+Guide%E2%80%99D,BPB+Publications,+Edition:+5<sup>th</sup>).
- [4] Computer Network Device, Available At: <http://basic-networking.blogspot.com/2007/08/computer-network-devices-and-component.html>
- [5] IPv4- Address Classes Available At: [http://www.tutorialspoint.com/ipv4/ipv4\\_address\\_classes.htm](http://www.tutorialspoint.com/ipv4/ipv4_address_classes.htm)
- [6] Stuttgart Available At: <http://www.ba-stuttgart.de/~schulte/html/55771.html#HDR3>
- [7] [http://cisco.com/univercd/cc/td/doc/cisintwk/ito\\_doc/ethernet.htm#1020850](http://cisco.com/univercd/cc/td/doc/cisintwk/ito_doc/ethernet.htm#1020850)
- [8] Definition Available At : [www.definition.com](http://www.definition.com)
- [9] OSPF Available At: <http://www.answers.com/topic/open-shortest-path-first>
- [10] Understanding of ATM in Bangladesh Available At: [http://www1.searchresults.com/web?l=dis&q=understanding+ATM+in+bangladesh&o=APN10645&apn\\_dtid=^BND406^YY^BD&shad=s\\_0042&apn\\_uid=9734054855124](http://www1.searchresults.com/web?l=dis&q=understanding+ATM+in+bangladesh&o=APN10645&apn_dtid=^BND406^YY^BD&shad=s_0042&apn_uid=9734054855124).
- [11] Access Control List (ACL) Available At: [http://en.wikipedia.org/wiki/access\\_control\\_list](http://en.wikipedia.org/wiki/access_control_list).
- [12] standard-access-control-list Available At: <http://www.answers.com/topic/standard-access-control-list>.
- [13] Computer networking Available At: [http://compnetworking.about.com/od/vpn/g/bldef\\_vpn.htm](http://compnetworking.about.com/od/vpn/g/bldef_vpn.htm).
- [14] OWASP Available At: [https://www.owasp.org/index.php/Category:OWASP\\_Top\\_Ten\\_2013\\_Project](https://www.owasp.org/index.php/Category:OWASP_Top_Ten_2013_Project).

## An Intelligent Line Follower Using Ldr Sensor

Abdul Hannan<sup>1</sup>, M.A. Jobayer Bin Bakkre<sup>2</sup>, Md. Selim Hossain<sup>3</sup>,  
Rajib Chandra Ray<sup>4</sup>

<sup>1,2,4</sup>Dept. of Computer Science & Engineering, Jahangirnagar University, Dhaka, Bangladesh.

<sup>3</sup>Dept. of Computer Science & Engineering, Shahjalal University of Science and Technology, Sylhet, Bangladesh.

**ABSTRACT :** Line follower robot is a robo car that can follow a path. The path can be visible like a black line on the white surface (or vice-verse). It is an integrated design from the knowledge of Mechanical, Electrical and Computer engineering. This paper presents a 700gm weight of a 9W LDR sensor based line follower robot design and fabrication procedure which always directs along the black mark on the white surface.

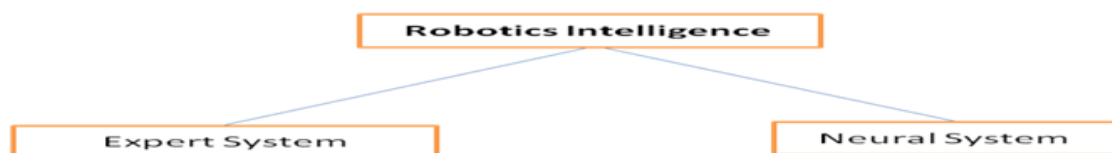
**Keywords-** LFR, System Requirements, System Development, Experimental Result, Future Direction.

### I. INTRODUCTION

#### What is Robot?

Robots are machines which do a task which would otherwise be done by human labor. Robot may or may not possess intelligence.

#### Robotics Intelligence



#### Line Follower Robot (LFR)

#### What is Line Follower?

Line follower is a machine that can follow a path. The path can be visible like black line on a white surface (or vice versa) or it can be invisible like a magnetic field. The follower machine-LFR



Line Follower Robot (LFR)

Line Follower Robot (LFR)

**How it works?**

Sensors read how much light is reflected Microcontroller determines the light value Motors speed up or slow down to keep robot following line

**II. SYTEM REQUIREMENTS****Actuator**

Actuators are the muscles of the manipulators. Common types of actuators are servomotors, stepper motors, pneumatic cylinders etc.

**Sensor**

Sensors are used to collect information about the internal state of the robot or to communicate with the outside environment. Robots are often equipped with external sensory devices such as a vision system, touch and tactile sensors etc which help to communicate with the environment

**Controller**

The controller receives data from the computer, controls the motions of the actuator and coordinates these motions with the sensory feedback information.

- PIC 16F690
- Stepper motors
- While 2Pieces
- Copper Board
- Some Ware
- Sensor (LDR)
- Dc Motor
- Motor Driver IC-L293D
- Ferric Chloride
- Proteus 8
- Eagle Software
- Connector
- Mobile Battery 2 pieces +5v
- PCB Board
- Language Program

**III. SYSTEM DEVELOPMENTS****Materials**

The materials for building the body or framework of the robot must be strong enough for the job, easy to work, durable and low cost. Also it should look good — have a shiny or attractively colored surface. Some kinds of plastic food container have all of these qualities. Project 6.1 illustrates how-to build the robotic mechanisms and circuits into a ready-made box. If there happens to be a spare unused box in the kitchen cupboard, it costs nothing. The main snag is that it may not be exactly the right shape or size. Converting a sandwich box into a robot is a short-cut way of getting into robotics, and the programs it runs can be really high-level, but a purpose-built body is more professional. The following sections describe some of the most popular materials.

**Wood**

Wood is rarely thought of as a robot-building material but, at times, it can be just what we need. It is strong for its weight and easily cut, drilled, painted, carved and glued. Nylon nuts and bolts, from electronic parts suppliers, are necessary if there is a risk of the bolts causing a short circuit. This could happen if a circuit-board is bolted to a metal panel. In such cases use nylon bolts and nuts or plastic stand-offs. The tool is the glue gun, which melts glue sticks and has a nozzle for applying the molten glue to the work piece. A glue gun is a handy tool to have on the workbench for all kinds of gluing jobs. The glue sticks are melted by the electric heating coil in the gun. Press the trigger to extrude molten glue from the nozzle.

**Tools**

The tools you need for constructing robots partly depend on the materials you use. For Foam Board the main tools are a steel ruler, a craft knife and a plastic chopping board (use one discarded from the kitchen) or cutting mat. You need a few other tools for mounting the motor and circuit boards. For building an aluminum framed robot such as the Gantry, a drill press is almost essential and so is a hacksaw. When you have decided what materials are to be used, select your tools from those described below.

**Cutting tools**

A junior hacksaw, with a 150 mm long blade is good enough for most jobs, such as cutting wood or plastic, and for circuit boards. For cutting aluminum or brass stock a regular hacksaw is faster and gives a straighter cut. If you have problems with cutting things square or if you need to cut at a particular angle, a miter saw is a great help. It keeps the saw blade vertical and perpendicular to the length of the work piece. It has gauges to help cut pieces to equal lengths. The frame that carries the blade can be rotated to cut at angles other than 90°, the angle being settable on a graduated scale. A miter saw is almost essential for building the Gantry. A file saw, reamer and junior hacksaw.

### Drills

Although a hand-turned drill is adequate in many ways, an electric drill is a boon when there is much drilling to be done. Robot building seems to require a lot of it. If you already have a small power drill for jobs about the house, it may not be worthwhile to get anything more professional. A drill press is not expensive, is so much easier to use and produces better results. A drill press helps put the holes in the right places and at right angles. Use it for aluminum, brass, wood or plastic, preferably running it at its lowest speed.

### Other tools

Screwdrivers are obviously essential but only small sizes with regular blades up to 4 mm wide. Metric bolts usually need a small-size Positive screwdriver. A set of jeweler's screwdrivers is useful on occasions. An assortment of small files of various shapes is handy for smoothing cut edges and shaping parts of mechanisms. A set of needle files is also worth having. An engineer's steel rule 300 mm long, graduated in millimeters, completes the tool kit.

### Planning a Mobile Robot Body

Things before starting the building process,

#### Chassis

- Ready-made chassis such as a plastic food storage box. Easy and quickly built.
- An existing toy. Generally easy and quick, but there could be snags.
- Chassis made from sheet plastic or foam board. Easy but takes longer. Gives scope for invention.
- Chassis made from sheet aluminum. You need tools and experience to make it.

#### Wheels

- How many? Three is a popular number.
- Drive (traction) wheels at front or rear.
- Steering by tank method (two independent drive wheels, two motors).
- Steering by automobile method, one motor, with differential gear (complicated)

#### Shape

- A robot that is about as long as it is wide turns much more easily in a confined space (such as the average family room).
- A robot that is much taller than it is wide is more likely to fall over on uneven surfaces, if it hits an obstacle, or when it accelerates or decelerates quickly.
- If the robot is to have jaws for picking up a load, it needs to have a broad base for stability.

There are more detailed design points in the next two sections.

### Road wheels

The main points about a road wheel are its diameter and the nature of its tread. A larger diameter is better on a rough or uneven surface because the wheel can more easily ride up over ridges and is less likely to get stuck in grooves. Also it allows there to be a larger clearance between the surface and the underside of the chassis. If the surface is smooth and even, for example the rails of a gantry, small wheels have the advantage of light weight. It is all too easy for a robot design to finish up by being heavier than the motor can drive. Using small wheels helps to avoid this. Types help the robot to run without slipping. The simply programmed robots usually start and stop abruptly. This leads to skidding or slipping. We rely on a robot being able to run in a straight line but slipping makes it run in irregular curves. Unless it is continually taking its bearings from a fixed landmark, it soon gets lost. Wheels slip, even when they have treads, but treads help to avoid serious slipping. **DC motor** Although motors are electrical and therefore might be a topic for the electronics Chapter, they move the mechanical parts so need to be talked about here. The discussion focuses on small low-voltage DC motors. When selecting a motor for a project, one of the main points is its operating voltage, for this partly decides the size and weight of the battery that must be carried. Motors running on 12V need eight AA cells. These are too heavy a load for a small robot such as the Scooter. The Quipster is larger and heavier so needs more powerful

motors to propel it. This robot runs on a pair of 12 V motors, powered by a battery of eight AA cells. If we needed maximum power we would use dry cells, but rechargeable cells are more economical. Eight LiMH cells produce 9.6 V, and will drive the motor with sufficient power. The next point to consider is the gearbox. It is rarely that a robot mechanism can be driven directly from a motor turning at several thousand revolutions per minute. If the motor does not have a built-in gearbox, it is almost certain that you will need to build or buy one. A built-in gearbox is neater, more convenient, and probably cheaper than a separate one.

## Robot Electronics

### Circuit board

The components of an electronic circuit are nearly always assembled on a rectangle of circuit board. This is made from insulating material and has conducting copper tracks on its underside to make the connections between components. In the circuits described in this book, we use components that have wire terminals. The wires are pushed through holes in the board and soldered to the tracks on the other side of the board. Another type of component is the surface mount device (SMD) which has terminal pads that are soldered to tracks on the same side of the board. No holes are required. SMDs are very small and difficult to handle, so we do not use this type in the book. Take care not to ask for the SMD type by mistake when buying components. One of many more elaborate circuit boards intended for integrated circuits (which include PICs)

**Connecting Wire:** Three kinds may be needed:

- Single-stranded insulated connecting wire, 0.71 mm diameter. Used for wiring up circuit boards. Can be bought by the meter, and a meter or two in two or three different colors is worth keeping in stock.
- Multi-stranded flexible insulated connecting wire (sometimes called bell wire), 13 × 0.12 mm (that is, 13 strands, each 0.12 mm diameter). Use for connections to off-board components such as motors, and for connections between boards. Stock a few meters in a few different colors.
- Tinned copper wire, bare, 0.71 mm diameter. We prefer this to insulated wire for wiring up circuit boards. Not having to strip its ends saves time and the risk of short circuits is minimal. The exposed wires provide plenty of contact points for use when testing the circuits.

### Solder

Solder is a mixture of 60% tin and 40% lead. It comes as wire with a central core of resin. For building electronic circuits the narrower gauge, 0.71 mm diameter is preferred. Recently introduced regulations mean that lead solder may no longer be used in certain countries, including those in the European Union. Lead-free solder must be used instead. This usually consists of a mixture of tin and antimony. It is available in wire form, 0.71 mm in diameter.

### Insulation

It is often essential to stop currents from flowing where they should not flow. Use PVC insulating tape to wrap around wires or terminals that are at risk. Use it also to wrap round joints where two wires have been soldered together. A reel of red and a reel of blue will cover most needs. Insulated sieving is PVC tubing a few millimeters in diameter. It is made in a range of colours. It is handy for protecting bare wires or where two wires are soldered together. Most slaving is of the heat shrink variety. It fits loosely over the joint but, when heated by holding a hot soldering iron near it, it shrinks to half its original diameter. This anchors the insulation firmly in place. Heat shrink tubing is sold in packs of assorted diameters and colours. A pack will last for years.

### Designing tools

Circuit designs are developed and tested on a breadboard before soldering them to a circuit board. The board has an array of sockets, connected in groups. Terminal wires are bare-ended wires which are pushed into these sockets to connect them electrically. An assortment of jumper wires of various lengths is used with the breadboard. They are sold as sets, but you can make them yourself by cutting and stripping the ends of a few dozen pieces of single cored (essential) connecting wire. Let them vary in length from about 2 cm to about 10 cm. It is a good idea to prepare a few wires stripped at one end and with a miniature crocodile clip soldered at the other. Another useful item for bread boarding and for circuit testing generally is a set of a dozen or so test leads in a variety of colors. These are made from light-duty flexible wire and have a hooked test clip at each end. Another indispensable item is a test meter, or millimeter. Preferably it should be digital and should measure DC voltages up to, say, 20 V. It may measure currents up to 1 A, but current measurements are not often made in robot circuits. It should measure resistance and capacitance. Continuity checking and diode testing facilities are well worth having. Digital meters are favored because of their low input impedance (they take very little current from the test circuit) and their 4-figure precision (but three figures are enough for most purposes). But a rapidly changing voltage produces an annoying and unreadable scramble of digits on the display. This is when analogue meters come into its own even a cheap old model that you nearly threw away. Its wavering needle tells you almost all you want to know about voltage swings.

### Soldering tools



A soldering iron is an essential item. A soldering station with thermostatic control is nice to have but a simple electrically heated iron will do. The main points are that it should be low power, about 15 W, and the bit should be no more than 2 mm in diameter.

### Other Tools for Electronics

A wire and cable stripper removes the insulation from the end of the connecting wire in a single action. It saves a lot of time. But most wire strippers are designed for use by electricians. They will strip the insulation from hefty mains cable, or TV antenna cables, but not from the thin wires such as we use in electronic hobby projects. Choose with care. Wire cutters of the side cutter type trim the component leads short after they have been soldered to the board or terminal. They give a neat finish to the work and no other tool does the job.

### Components

- Variable resistors: The miniature horizontal preset type is good for bread boarding. Sometimes called trim pots. Handy values are 470  $\Omega$ , 1 k $\Omega$ , 4.7 k $\Omega$ , 10 k $\Omega$ , 100 k $\Omega$ , and 1 M $\Omega$ .
- Capacitors: Their main use in our circuits is for smoothing spikes and pulses out of the supply. Stock a few MKT polyester capacitors, value 100 nF.
- Transistors: Probably the most often needed is the BC548 for use in transistor switches, but other types can be used for this purpose. The table lists types to choose from.

### Power Supplies

The various types of power supply — batteries and PSUs — are discussed on p. 57. Here we work out what voltage the supply should have and go into more detail about how to provide it. The first stage in planning the supply is to list the devices and circuits in the system and what they will need. All systems will include one or more PICs so start with this. The most recent PICs operate at any voltage between 2 V and 5.5 V. This wide range gives a degree of flexibility except that it does not include 6 V, which could be conveniently provided by four alkaline cells. The nearest is four NiMH (or NiCd) at 4.8 V. In practice, though rated at 1.2 V per cell they give 1.3 V when fully charged. The system will almost certainly include one or more motors. Usually the motor is chosen for its dimensions and its running speed (and perhaps its price). Provided its operating voltage is not more than 12 V, we either run it at this voltage or on a lower voltage on which it will run fast enough. Other devices in the system may have special requirements. For example, CMOS logic circuits of the 4000 series require between 3 V and 15 V, which is easily met, but the 74HC series need between 2 V and 6 V. They cannot be run on the same supply as a 12 V motor. Some of the solid state buzzers and bleeper's have a wide range of operating voltages but others have not, so check this point before you buy. If everything can run at the same voltage it makes the circuit design much simpler. This is why it is preferable to use low-voltage (3 V or 6 V) motors that can run on the same supply as the PIC. Sometimes a 12 V motor, solenoid or relay is the only suitable type and we have to set up two supplies. The power supply circuit, single or double, should also include an on-off switch and preferably an indicator LED to light when it is switched on. Some circuits for this are shown overleaf. If the drive motors have their own supply it is a good idea to give them a separate switch. It is then possible to run the PIC and test it without the robot shooting all over the place.

### The Controller Circuits

Because the electronic system of the robots is modular, the controller board has little on it except for the PIC. The drawing shows the essentials. The switch S1 is the power supply switch seen in the drawing opposite. The polyester capacitor C1 is to absorb voltage spikes on the positive supply line. When power is first switched on, channels RA0 to RA2, RA4, RB4, RB5, RC0 to RC3, RC6 and RC7 are all analogue inputs. The rest are digital inputs. The analogue channels can be defined individually as digital and all channels except RA3 can be defined as outputs. Outputs are always digital. When they are configured as inputs, the channels of Ports A and B (except for RA3) can all have weak pull-ups. These can be brought into action individually. The weak pull-up acts like a high-value resistor between the input pin and the supply line. The input is read as logic high, unless it is strongly grounded to the 0 V rail. Channel RA3 is an exception. It can be configured as a digital input with no weak pull-up. The circuit for this is shown in dashed lines. It requires an external resistor. If the channel is configured as MLCR, to reset the controller, it automatically has a weak pull-up and does not need the external resistor.

### Input Circuits

#### Analogue Input

The analogue output from a sensor such as a photodiode (see above) or light dependent resistor circuit can be read by using the PIC's internal analogue-to-digital converter. This has a 10-bit output, so we can read the sensor with high precision. It is not just a matter of high versus low. The PIC van is programmed to do different things at different light levels.

#### Sensors



A robot needs to be aware of what is happening in the world around it. That is why all our robots are equipped with several sensors linked to the controller. This section lists sensors that are often used in robotics. Resistive sensors respond to changes in a quantity such as light or position and their response is a change in their resistance. A change in resistance is easily measured by passing a current through the sensor and generating a changing voltage which is sent to the controller. Usually the sensing circuit is a potential divider with the sensor as one of the resistances.

### **Light sensors**

The most commonly used light sensor in our robots is a light dependent resistor which, as its name implies is a resistive sensor. The resistance of a typical LDR, such as the ORP12, ranges from 1 M $\Omega$  or more in darkness to about 80  $\Omega$  in bright sunlight. Indoors, with indirect daylight or artificial illumination, their resistance is a few kilo ohms. LDRs respond to light of most colors, with a peak response in the yellow. Of all the light sensors, the LDRs are the slowest and their response times are several tens or hundreds of milliseconds. Although this is seems quite fast to humans, the PIC works much faster than this. Programs may need a short delay to allow time for the LDR to catch up with it. The potential divider (see drawing opposite) can have a fixed resistor, a variable resistor, or both. The variable resistor allows for setting the output voltage for any given light level. The total resistance should be in the same range as the average resistance of the LDR under the expected operating conditions. Another popular light sensor is the photodiode. The action of these depends on the fact that the leakage current when the diode is reverse biased varies with light intensity. The circuit is on p. 73. The leakage current is very small. In darkness it is only a few nanoamps and rises to about 1 mA in bright light. The resistor has a resistance of a few hundred thousand ohms, so the current generates a reasonable voltage across it. Often a 330 k $\Omega$  resistor provides suitable output voltage. The output must be connected to a high impedance input so that the voltage is not pulled down. The PIC is a CMOS device so has high-impedance inputs. A photodiode is generally more responsive to light from the red end of the spectrum. Some are especially sensitive to infrared. These are used with infrared LEDs for reading optical encoders (p. 84). They are employed as sensors in line-following robots because they are less subject to interference from external sources of visible light. The response time of a photodiode is fast, generally a few hundred nanoseconds, so there are no problems with this. A phototransistor (overleaf) has properties similar to those of a photodiode, though their response time is longer. They are connected in the same way as an npn transistor in a common-emitter amplifier. Phototransistors often lack a base terminal and, if present, the base is usually left unconnected. The reason that a phototransistor can operate with a base current is that the light falling on the transistor releases a supply of electrons. These electrons act in the same way as a base current. Phototransistors are often packaged with an amplifier circuit or a Darlington transistor output on the same chip for greater sensitivity. There are similar devices based on photodiodes.

### **Digital Output**

The analogue output from a light sensor is usually processed by the PIC's in-built comparators but sometimes there are not enough of these, and in any case it is simpler to handle the triggering level in the hardware. This circuit uses an op amp comparator to convert the analogue output into digital.

The op amp has two inputs and there is no feedback, so the difference between the input voltages is multiplied by the open loop gain of the amplifier. The output swings very sharply from low to high when the voltage at pin 3 exceeds the voltage at pin 2. The voltage at pin 3 is always half the supply. The voltage at pin 2 varies directly with light intensity. It is set by adjusting VR1 to bring it to half supply when the LDR is receiving light of the triggering intensity.

### **Detecting Colors**

A robot may be required to detect the color of an object. For example, it may have the task of sorting building blocks of different colors. A simple way to do this is to illuminate the object with light from two or three different colors, one at a time. A single LDR light sensor measures the amount of light reflected from the object. As a test run of the technique, small (30 mm) squares of colored paper are illuminated by light from red, green and blue high-intensity LEDs. An LDR is exposed to the light reflected from these squares. The LDR is part of a circuit like that on p. 75, and the output voltage is sent to a comparator. With a suitable setting for its reference Voltage, the comparator's output is read for each colored paper and for each colored LED. The output is 0 for low reflection or 1 for high reflection. Here are some typical readings.

### **Output Circuits**

### Direct drive

The maximum current that can be sourced at any single terminal pin is 25 mA. The maximum current that can be sourced by the three ports at any instant is 200 mA. The same figures apply also to sinking current. A current of 25 mA is sufficient to drive a regular LED but not the high brightness or extreme brightness types, which take 30 to 50 mA or more.

### Stepper Motors

As their name suggests, stepper motors turn step by step. The commonest type has a step size of  $7.5^\circ$ , so that it takes 24 steps to make one revolution. This produces a slightly jerky motion but it is satisfactory for most purposes and the programming is simple. This description refers to unipolar stepper motors which have permanent magnets and  $7.5^\circ$  steps. The motor generally has six wires, which are connected to the windings as shown in the drawing opposite. The robot projects in this book are based on the PIC16F690 microcontroller, made by Microchip Technology Inc. But all PICs have a common basic architecture and electrical properties so the circuits described in this book can usually be made to work with several other types of PIC.

### Programming a PIC

The PIC16F690 is especially suitable for hobby robotics because:

- It is one of the newer PICs.
- It uses the latest nano Watt Technology. The standby current is only 1 nA when operating on a 2 V supply. At the other end of the scale, its operating current when running at 4 MHz, on its maximum supply of 5.5 V, is less than 1 mA. Low voltages and currents are ideal for driving mobile robots.
- If we opt to base timing on the built-in internal oscillator, all but two of its 20 pins are available as digital inputs and outputs. The robot can have what it needs – lots of sensors and actuators.
- It has Flash memory, ideal for programming hobby robots.

### Programming a PIC

<pre>void main() {   TRISA = 0x04;   TRISB = 0x00;   TRISC = 0x00;   PORTA = 0x04;   PORTB = 0x00;   PORTC = 0x00;   CM1CON0 = 0x00;   CM2CON0 = 0x00;   ANSEL = 0;   ANSELH = 0;   PORTC = 0x00; // Enable initial value of LED   while(1)   {     // condition for car going on forward     if(RC0_bit == 0 &amp;&amp; RC1_bit == 0) // Two sensor     ON when car on forward     {       PORTC = 0b01010000; // RC4 And RC6 pin will be       high and car will on forward     }     // condition for car going on left</pre>	<pre>else if(RC0_bit == 0 &amp;&amp; RC1_bit == 1) {   PORTC = 0b01000000; // RC5 and RC6 high now   car will go on LEFT } // Condition for car going on right else if(RC0_bit == 1 &amp;&amp; RC1_bit == 0) {   PORTC = 0b00010000; // RC4 and RC7 high now   car will go on right }  // Condition for car going on Break else {   PORTC = 0x00; } }</pre>
--	---

As you can see if you look at the programming examples of the projects, there are program routines that we use over and over again. Some may differ in detail but essentially they are repeats. It makes more sense to save these as separate text files, so that you can load them and put them into your current project. They may need a little editing here and there but this is nothing compared with the effort needed to type them in from scratch every time you need them. Not only does it save typing effort, but it reduces the risk of typing errors too. The program segments listed in this Part are a selection of the most often needed routines. The listing opposite begins with a title frame. It is not strictly necessary, but in a few months' time you may have forgotten what the program is supposed to do. Every line of the title frame must begin with a semi-colon so that it is ignored by the assembler. The first active line of the listing tells the assembler which PIC you are using. Then comes the configuration directive which sets up the key features of the way the PIC is to operate.

### The PIC16F690 Block Diagram

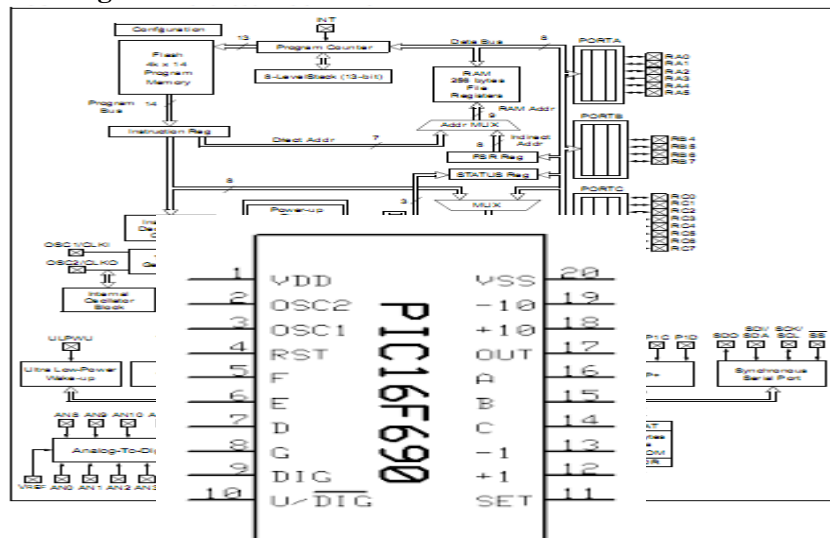


Fig: The PIC16F690 Block diagram.

### Light Dependent Resistor (LDR) Diagram

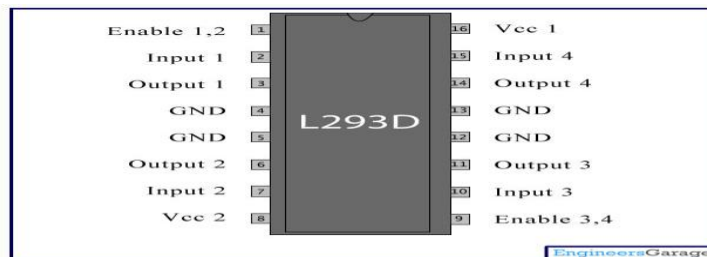
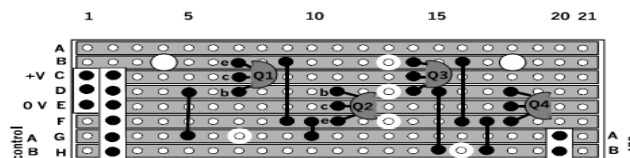


Fig: Light Dependent Resistor (LDR) diagram

### Motor Control Board

This has an H-bridge for controlling the direction of the motor. It is mounted on the lid, beside the motor/gearbox unit (photo p. 180).



The motor control board has two connecting sockets for the supply lines. This allows it to be daisy-chained to other boards and units in the system.

Fig Moto Driver IC-L293D diagram.

Connections are made to this board in the same way as to the controller board, by pushing the stripped ends of the wires into sockets. Alternatively, solder the wires directly to terminal pins or to individual sockets that push terminal pins.

### Circuit Diagram

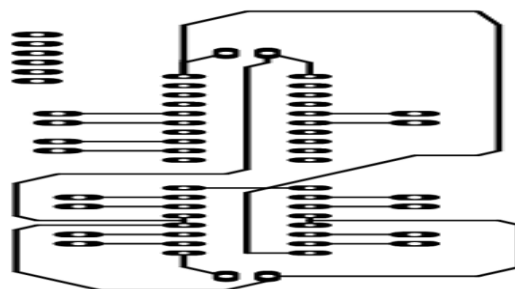


Fig: Circuit Diagram

## Activities of Mobile Robots

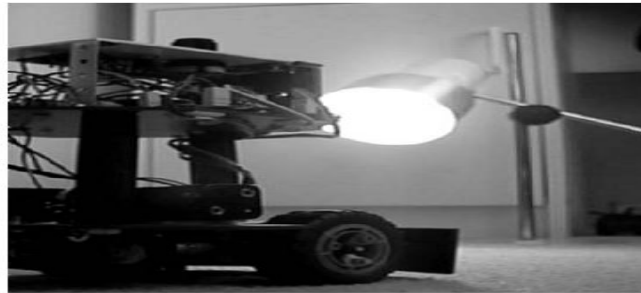
### Moving around

By definition, all mobile robots move from place to place. They need to be able to move forward, to reverse, and to turn to the left or right. Robots are often operated in confined spaces so it useful to be able to spin on one spot. Variable speed is less important and often unnecessary.

The chassis of the programming C has two motors, one for the rear drive wheels and the other for steering

### Detecting and Responding to Light

Sight is probably the most important of all human senses. The same applies to mobile robots. Some can detect a lamp which is several meters distant, and aim themselves towards it. Or maybe they will go in the opposite direction, to end up in the safety of dark corner.



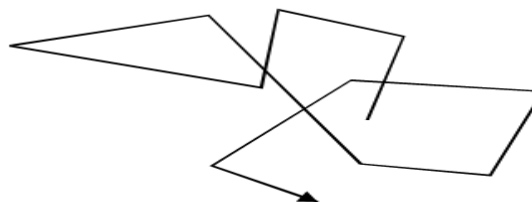
The Quester robot homes on a source of light.

## Activities of Gantry Robots

A gantry robot operates over a clearly defined rectangular area. It picks up objects from any point in the area and sets them down at another point in the area. The tool (often a gripper) is suspended from a small trolley-like frame, and can be lowered and raised. The frame has wheels and runs on a pair of rails so that it can travel from one side of the area to the opposite side. This set of rails is on a larger frame at right angles to the first set, so the smaller can be moved to any point within the area. Thus the location of the tool is defined by two coordinates, its x-position and its y-position. It is easy to design sensors that can read the x and y coordinates and a gantry robot is therefore much easier to program for applications that require precise navigation. Gantry robots are used in industry when very heavy loads are to be handled. The hobby versions are suited for less strenuous tasks. They are excellent for playing board games such as chess, draughts and checkers. Like mobile robots, gantries can be programmed to solve mazes. But mobile robots are apt to lose their bearings. Because the travelling frames can be precisely positioned beekeeping track of their x and y coordinates, a gantry robot can never lose its bearings.

## Random Activity

Randomness may sound an unlikely topic for a robotics book but it has its applications. A robot that is reliably built and programmed performs its tasks in an orderly and inflexible manner. Humans are not normally like this. Indeed, if people are too rigid in their behavior we may complain that they are 'acting like a robot' or that the person is 'an automaton'. If a robot is programmed to run for a short, randomly-chosen distance, then turn through a random angle, and continue indefinitely in the same routine its path is totally random. We say that it is literally performing a Monte Carlo Walk. We say 'literally' because the same term can be applied to other random sequences that are not actually walks.



A Monte Carlo Walk usually results in staying in more-or-less the same place.

Usually we do not aim for total randomness. For example, a robot detects an obstacle in its path, backs up, turns slightly to avoid the obstacle and then continues forward. The stopping, backing and turning are fixed responses. Whether it turns left or right on given occasion is determined as random. We cannot predict which way it will turn next. This introduces randomness into its behavior, but not too much. Random behavior is produced in the

software, using a random number generation routine. Actually its output is not genuinely random, but a predictable series of values that repeat after such a long interval that it appears to be random. This is actually pseudo-random. Randomness has other and more serious applications. A robot that is solving a maze maybe programmed to make a random choice whenever it has to go either left or right at adjunction. If it is also programmed to remember which choices it made at each junction and which choices took it successfully to its goal, it can eventually learn to run the maze correctly. This is the basis of learning by trial and error. The same type of learning technique can be applied to other learning tasks.

#### IV. EXPERIMENTAL RESULT

The line following robot project challenged the group to cooperate, communicate, and expand understanding of electronics, mechanical systems, and their integration with programming. The successful completion of every task demonstrated the potential of mechatronic systems and a positive group dynamic. Overall, the line following robot was a tremendous success and an incredible learning opportunity for everyone involved.

##### Cost Estimation for the project

1) PIC16F690	1.8 \$
2) Soldering Iron	5.55 \$
3) Mini hand PCB driller for student version	24.63 \$
4) LDR sensor (7.89X2)	0.20 \$
5) Glue gun	3.08 \$
6) Glue stick	0.25 \$
7) 40 pin premium male to female connecting wires	2.41 \$
8) DC gear motor box and wheel pair(260X2)	6.42\$
9) L293D IC	1.06\$
10) Project board	3.15\$
11) Printed circuit board (PCB) 40"X24"	11.00\$
12) Diode 1A10 (5X2)	0.15\$
13) Ball caster	0.62\$
14) White LED (1.20X2)	0.15\$
15) Ferric chloride for PCB design 500gm	4.35\$
16) Transistor BC517 (31X2)	0.78\$
17) Mobile battery +5V (350X2)	7.42\$
18) Miscellaneous	13.00\$

<b>Total</b>	<b>86.02\$</b>
--------------	----------------

##### Application

- Industrial automated equipment carries.
- Automated Guided Vehicles (AGV).
- Second wave robotic reconnaissance operation.
- Tour guides in museums and other similar application
- Restaurant services.

#### V. CONCLUSION & FUTURE DIRECTION

##### Conclusion and Future Direction

Light Dependant Resistor (LDR) can be used to differentiate different color lines with different sensitivity levels.

Our future target is to enhance performance of the existing Line Following Robot with integrating,

- Software control of the line type (Dark or light) to make automatic detection.
- Obstacle detecting sensors to avoid physical obstacles and continue on the line.
- Distance sensing and position logging and transmission.
- Weight carry move to 24 hours any manufacture company.
- Choice of line is made in the hardware abstraction and can not be changed by software.

- Calibration is difficult and it is not easy to set a per fact value.
- The steering mechanism is not easy.
- Few curves are not made efficiently and must be avoided.

### REFERENCES

- [1] Chris and Dawn Schur's Robotics and Artificial Life Forms, <http://www.schurstrophotography.com>
- [2]. Ameeta Agarwal and Aijun An. Unsupervised Emotion Detection from Text using Semantic and Syntactic Relations.
- [3]. Carlo Strapparava and Rada Mihalcea. Learning to Identify Emotion in Text.
- [4]. Artificial Intelligence: A Modern Approach *Third Edition*, by Stuart J. Russell and Peter Norvig.
- [5]. Assembly Language Programming of Organization of the IBM by Ytha Yu & Charles Marut.
- [6]. Fundamental of Electric Circuits Fourth Edition by Charles K. Alexander & Matthew N.O. Sadiku. and Introductory Circuit Analysis "Robert L. Boylested" Eleventh Edition.
- [7]. Abdul Hannan "Emotion Detection from Text" International Journal of Engineering Research and Development *e-ISSN: 2278-067X, p-ISSN: 2278-800X, www.ijerd.com Volume 11, Issue 07 (July 2015), PP.23-34.*
- [8]. A. Balahur, J.M. Hermida, and A. Montoyo. Detecting implicit expressions of sentiment in text based on commonsense knowledge. In Proceedings of the 2nd Workshop on Computational Approaches to Subjectivity and Sentiment Analysis, WASSA '11, pages 53-60, Stroudsburg, PA, USA, 2011. Association for Computational Linguistics.



## Cultivating Technological Innovation in the Mind

<sup>1</sup>PROF ANYATA BENEDICT U.(Ph.D), <sup>2</sup>AKPAN PAUL P. (M.Sc)

<sup>2</sup>UNEKE LOUIS A. (M.Eng),

<sup>1</sup>Department of Civil Engineering, University of Benin, Benin City, Nigeria, West Africa.

<sup>2</sup>Department of Civil Engineering, Rivers State Polytechnic, Bori, Nigeria, West Africa.

**ABSTRACT:** *Cultivating innovation in the mind is imperative to successfully move technology to the next level. Technology is growing rapidly in developed countries and has almost reached its peak. Developing countries and continents like Africa on the other hand are now seen as a breeding ground to explore in technological innovation. Researchers and entrepreneurs are shifting base to Africa where they can achieve maximum profit resulting from under development of the continent. Reefs, city and web are used to explain the best way to cultivate innovation. The city and web are such engines of new innovation because both environments are powerfully suited for the creation, diffusion and adoption of good ideas. The seven keys of cultivating innovation include tropical humidity, illiteracy, poor power surge of electronic use for research, good concept of the liquid networks, slow hunches, serendipity, acceptance of error in cultivating innovation, Exaptation, coffee breaks, application of programming interface and the use of quadrant as a tool. These keys are recommended to be put to use by every individual who has the mindset of driving technological innovation to the next level.*

**Keywords:** *Innovation, Technology, Hunches, Serendipity, Creation, Coral Reefs, Exaptation, Quadrant, Networking, Programming Interface, Squelch, City and Web*

### I. INTRODUCTION

One of the age-old great questions of life is where do good things come from? This is a pivotal question that demands accurate and intelligent answer. The necessity that is embedded in the answer to this very important question resulted to this distinctive school of thought. [1] proposed a framework for answering these questions. The goal of this research in view of proffering solution to this question is to elucidation on how to cultivate technological innovation. Good things come from innovation and our ability to cultivate it is a panacea to the question. There are suggested ways to live, interact and work that can promote innovation. A walk during leisure time, developing hunches, writing down dreams and aspiration as soon as they are conceded, effective documentation and management, making serendipity a habit, manage generative mistakes, embracing multiple hobbies, attending to innovative brain storming in coffee houses and frequenting other liquid networks, following links, developing good ideas, borrowing, recycle and re-inventing ideas are possible ways to effectively cultivate innovation. Also, in the light of this fact, we shall consider the fundamental drivers of innovation. Where good things come from: the natural history of innovation is divided into seven sections with each addressing the fundamental factor that facilitates innovation.

Again, the research is about the space of innovation. The African institutions and some other environments squelch new ideas while other environments seem to breed them effortlessly. Greater percent of the environment in the universe do not welcome new ideas. They are generally opposed to change. They are entangled with fear to develop new idea and prefer to religiously work based on people's ideas. This attitude is traditionally induced in them because of the method of education. From primary to tertiary school they are groomed on studying peoples thought and opinion and they stick to it. They do not have the drive to develop new idea because they believe that they are not ripe, fit or have the ability to do so. They criticize, discourage and possibly kill fresh ideas. Most tertiary institution in developed countries like the US, United Kingdom, China, Japan, and other environment has undying drive to develop fresh idea. They have the will power to develop the creative ingenuity in them. They believe in the intent to create, which vibrates like an electron in its energized and excited state ready to move from the present energy level to the next energy level. This can be seen as little as in those primary schools where children are encouraged to come up with creative works as craft for continuous assessment.

## II. LETERATURE REVIEW

The argument of this study is that a series of shared properties and patterns reoccur again and again in unusually fertile environment. This is so because they are innovatively unproductive. They can not or do not know how to cultivate innovation in their productive environments. They are left with no option than to repeat ideas. They invent same thing year in and out because there is no fresh idea. A typical example is found in most final year thesis in tertiary institutions in Africa, same business ideas in a competitive business environment and use of same curriculum for a program for years without any modification or yearly review. This condition does not occur in an environment where fresh ideas are their watch ward. In innovative environments new properties and patterns are galvanized in their product. A good example can be drawn from good product developed in some Asian countries like Japan, China, and other countries like the United States of America and the United Kingdom [2].

However, the more we embrace these patterns of breeding new innovative ideas effortlessly in our private work habits and hobbies, in our office environment, in the design of new software tools the better we will be at tapping our extraordinary capacity for innovative thinking. The creative ingenuity in an individual can not be discovered if no attempt in developing innovative habit and hobbies is made. We should allow it flow naturally in us and make it a culture. [3] discussed how to cultivate innovation in real time. If we allow innovative thinking to be induced in us then the ability to discover and produce new good product continuously will become a culture. We should be innovative in our office environment. Think of simpler method of executing tedious jobs; develop machines and equipment that will enable us carry out our duties ergonomically, and economically. Occupational health and Safety should be introduced in our work places. It is said that health is wealth. New software tool should be developed to ease the work we are doing since we are in computer jet age. For instance Computer aided design (Cad) software for civil engineering structural analysis, design, drafting and detailing can be used to execute job to reduce job duration from one year to less than a month. Software programs ease and reduce the duration of executing jobs effectively and efficiently [4].

Reefs, city and web may be used to explain further the best way to cultivate innovation. [5] ideas show that the coral reefs create an environment where biological innovation can flourish. [6] dwelled so much on biological innovation. He explored the anatomy of living organism where He pictured that the existence of animals begins from plants. He invented good ideas that open the minds of medical practitioners. Today his coral reefs have created a fertile environment for biological innovation to flourish. Scientific reasoning is sharpened by his ideas. His ideas were pivotal to the successes recorded by great philosopher and scientists in the medical profession.

The world is now a global village through advent of the computer. The internet is an interface that links the City and web. The city and web have been great tools of innovation because both environments are powerfully suited for the creation, diffusion and adoption of good ideas. The problems generated by activities of people, economic and financial challenges, growing population, poor technology, and unhealthy environment can be solved through innovative ideas. These ideas can be savaged by exploring the web where you can rub minds and integrate thought and opinions of great people that have ever lived. It is not a bad idea to compare several thought and opinion of great minds. It will spur the individual to be innovative and prepare a platform that can result into refined and better ideas. The problems associated with developing the city can be solved by extracting good ideas from the web. This is why [7] inferred that the city and the web have been such engines of innovation because both environments are powerfully suited for progressive creation, diffusion and adoption of good ideas. This is exactly where good things come from [8].

Consequently, [9] law proposed that as a city gets bigger, they generate ideas at a faster clip. This is because the growth of a city is a factor of the growing population, possible land mass, increased financial challenge, economic problem, health challenge, waste management system issues, transportation problem, information and communication lacuna, education challenge, and many more. All these challenges put together can be solved by generating good ideas. As the city gets bigger, the need and want of the people get bigger leaving us with the opportunity to hastily solve them with good ideas. For instance, if one power generating set can serve a business organization as it grows and expand its business activities the need to improve the power system becomes necessary. The organization may deem it fit to buy another one to support the initial one to save the life of the power generating set. Another good example is the family. As newly wedded couple a one room apartment bungalow can accommodate them but with the passage of time when they start producing children they will be forced to acquire a larger flat. If they keep multiplying like a typical African to twelve children or more then their current accommodation will not serve them. They may need even larger flat. Also, as the children grow up to maturity, they will be forced to go and build their own home. Thus good ideas must be introduced to increase the health, solve health problem that must creep in from time to time, cloth, feed, educate them and so on. The larger the family, the more the need to generate good ideas to satisfy their unlimited wants. [2] discussed the seven all-time greatest ideation techniques.

Hence, something about the environment of a big city makes its residents significantly more innovative than residents of smaller towns. Bigger cities are faced with more challenge than smaller ones. The unlimited needs and want of the people become more insatiable demanding. The solution of their problems lies solely on good ideas. More innovations are needed to contain the problem. Bigger city with improved innovation grows faster in wealth than smaller ones. This is the reason great nations like china take solace on innovations. They have one of the largest populations in the world with less natural resource yet one of the best economies in the world because of improved innovative ideas. They believe that if you have good thinking, it will result to good ideas and the result will be good product. "Good thinking, good product". Smaller cities are faced with less challenge in their environment that leaves greater percent of such city less innovative except those that want to develop there economy. Unlocking talent is a key to organizational agility and Innovation [2].

### **III. METHOD**

In this research seven keys of cultivating innovation shall be considered. The seven keys shall be used to exhaustively explain how to cultivate innovation in the mind. The methods in development of the mind to come out with useful innovations are tropical humidity, illiteracy and poor power surge, concept of liquid networks, slow hunch, serendipity, error in cultivating innovation, coffee breaks, and application programming interface platform. Each of the methods will be discussed.

### **IV. ANALYSIS**

Firstly, tropical humidity, illiteracy, poor power surge are inhibitors to cultivating innovation and illustrate the adjacent possible. Ninety five percent of medical technology exported to developing countries breakdown easily with the first five years of use. This is as a result of power surges, tropical humidity, and hospital staff inability to read the repair manual. The power ratings of most electrical appliance are not the same. They vary from one hundred and ten to four hundred and above. Some do not have good power surge control system that protects them during fluctuation. Users may be required to buy protective devices due to their fragile nature to power fluctuations. Because most hospital staff is not trained in the use of such equipment, the equipment gets easily malfunctioned and packs up. Most machine malfunctions in developing countries are caused by power surge. The malfunctioning of these machines inhibits research and development which don't provide good breeding ground to cultivate innovation.

The weather is another factor that discourages the advancement of innovations. The tropical humidity of most developing countries is not compactable to most of those by the foremost inventors. Most medical machines are supposedly manufactured for use in cold environment. The use of such machine in a very hot climate results in over heat that affects their mother boards, power packs and fragile integrated circuits. They generate much heat and ought to be used in cold environment to reduce the heat. In hot environment the temperature increases beyond the maximum temperature to which they are configured to operate hence the consequent of blow up the machine or alternatively of the results obtained from them. This is the reason most of the machines that work do not give accurate results.

Unfortunately, illiteracy plaques the proper use of some of the hospital machines. Most hospital staff can not read the English repair manual. This is why some machine that can be put to use are not used at their maximum capacity. The repair manual that should guide them on how to refurbish and put them to effective usage are thrown away or stocked in shelves and drawers as a result of illiteracy.

Consequently, as an example of good ideas, MIT professor Timothy Presero and Boston Doctor Jonathan Rosen created an incubator built out of automobile part because steady supply of spare part or trained repair technicians in the developing world can not be guaranteed. The incubator is called the NeoNuture device. The external part of the device looks like an incubator while the interior is made up of automobile parts. The interior has an automobile headlight that supplies the warmth, dash board fan that provides air circulation and door chimes that Arthur provides sound alarms. The reason why the automobile parts are used as component of the machine is because the part can be easily found and replaced when it goes bad. The machine produced is an example of good ideas and technological innovation.

The second key used to cultivate innovation explains the concept of the liquid networks. A good idea is a network. [10] in one of his book titled the act of creation stipulates that the act of creation is something that happens exclusively in the mind. Creation is conceived in the mind in the form of idea; built up gradually by furnishing several considerations that will enable it yield success. It will remain pregnant in the mind until it is delivered. At the delivery stage the consideration will be dramatized in action. The action is the production stage where the product can be manufactured in large quantities and patented.

More over, on a base level, it is true that ideas happen inside of the mind but those minds are invariably connected to external network that shape the flow of information and inspiration. The external networks are good ideas from people that will help to encourage and support the safe landing of such idea. Good ideas survive easily in the mist of experienced people that are ready to join hands and work to ensure that innovative dreams come through [11]. Sometimes it might not be through personal interactions and intense brain storming, it can be through the web, twitter, and other social media. Therefore, it is not the network itself that is smart but it is the individuals that get smarter because they are connected to the network. The network itself catalyzes the individual to work harder, brainstorm until dream comes through. The individual in cause of intensive research on the work acquire adequate insight on the subject area that makes him more knowledgeable and smatter. This is because they stay connected to the network. The network is the source of information. Information is the key to the success of good ideas. Just as a tree with the longest tap root will look greener than others because they feed better so also will any individual with innovative acumen and closer to the network achieve greater success. Also a tree planted by the river side will be greener and bear much fruit in season and out of season because it is close to the source of water and other nutrient. A good inventor must stay close to the network.

The third key exposes us to the concept of the slow hunch. A new idea is a new perspective on a problem or a recognition hat has gone unexplored to date. A new idea demand new approach, laws, theory, principle, methods and system of resolving a problem. Isaac Newton introduced the laws of motion and called it Newton's law of motion. As at that time it was a new Idea. Thomas Edison discovered the incandescent bulb. It was a new idea. Breakthroughs are called slow hunches because they usually take time to develop. Good ideas like pregnancy develop gradually from one stage to the other until it matures. The development processes takes a very long time and are vigorous and rigorous to achieve. Hence, when the ideas metamorphose into innovation it is called breakthrough. A successful breakthrough is regarded as a hunch.

The long incubation period of hunches is also their strength, because true insight requires you to think out something that no one has thought out before in quit the same way. Breakthrough takes long time to actualize because it demands thinking and brainstorming in view of the fact that new innovation is meant to be established. It is stressful because sometimes new ideas can be established from an existing one. This is the reason why in mathematics a problem can be solved in different ways. Different formula can be use to solve one problem. This long incubation period is the strength of the hunch. The longer period used to achieve a breakthrough exposes the individual to much details on the idea he is developing. This will give him the opportunity to make several errors and correct them, polish his work beautifully. Bharat, a principal scientist at Google, created a software tool that organizes and clusters news items. Google new story went from a hunch in Bharat's mind to a shipping product in one year [12].

The fourth key to cultivating innovation is serendipity. It is the occurrence and development of events by chance in a happy or beneficial way. It is the faculty or phenomenon of finding valuable or agreeable things not sought for. Serendipity is the luck that takes the form of finding valuable or pleasant things that are not looked for. A hunch is a simple network of cells firing in side the brain in an organized pattern. For that hunch to blossom into something more substantial, it has to connect with other ideas. The hunch requires an environment where surprising new connections can forge. Good inspiration is best conceived when the mind and the brain connect well without friction or interference. This is why it is very important that the environment be such that it can welcome more inspiration. Calm and reserve environment are places where resources and information can be easily reached. Environment where connecting the network of great ideas will not be an issue. Ultimately, the neurons and synapses of the brain itself are large cultural environment that the brain occupies. Specifically, serendipity is built out of happy accidents, to be sure, but what makes them happy is the fact that the discovery you have made is meaningful to you. There is great immeasurable joy that exist the moment a hunch is achieved. The individual becomes extra ordinary happy for the fact that the discovery materialized to a meaningful idea. It was this joy that made a famous scientist Archimedes to run out naked from his house shouting "eureka" meaning I have found it. This occurred during one of his discovery which he used to propound the Archimedes principle. Hence, serendipity completes a hunch, or opens up a door in the adjacent possible that you have overlooked. Good ideas occurred to people while they are out on a stroll. For instance when going for a walk or taking a long shower. Inspiration most often comes during our leisure time. The brain allows good ideas to flow when it is relaxed. If you have such inspiration at such time it is necessary to vent immediately [13].

Accordingly, the secret to organizational inspiration is to build information networks that allow hunches to persist, disperse and recombine. For instance, Google has a company e-mail list where employees can suggest new product. Information networks tap both individual and collective intelligence. These systems create architecture for organizational serendipity [14].



Furthermore, the fifth key to cultivate innovation effectively explains the importance of error in cultivating innovation. Good ideas are more likely to emerge in environments that contain a certain amount of noise and error. The noise enables the individual to increase concentration and focus on the goal at hand while the error expands one's knowledge in it. It is important that we are not discouraged by the number of errors encountered in the cause of developing good ideas. Each error encountered should be seen as discovering a way of not doing it. Thomas Edison the inventor of the incandescent bulb conducted the experiment nine hundred and ninety-nine times. He did not allow the failure to kill the dream rather each time he failed, he said he has found one way of not doing it. He finally succeeded in the one thousandth attempt.

Hence, mistakes are an inevitable step on the part to true innovation. It is said that to err is human. This is true because a mistake is a natural and inevitable step that leads us to serendipity. The history of spectacularly right has a much longer history of being spectacularly wrong, again and again. Experience shows that any knowledge acquired at a stretch does not last in the memory but the one that goes through much vigor and rigor looms large in the screen of our memory and lasts longer. Our mistakes make us perfect. Benjamin Franklin said that the history of error of mankind is more valuable and interesting than that of their discoveries. The truth is that it is easy to remember a solution that is refined from much error. The errors are regarded more valuable and interesting because they emphasize the number of ways of not getting at the solution.

Notwithstanding, it is important to emphasize on exaptation. Exaptation is a kind of borrowing. [15] once used this to explain the concept of exaptation. He said an organization develops a trait optimized for a specific use, but then the trait gets hijacked for a completely different function. If a good idea is developed for a particular purpose and later it is hijacked for another purpose then that is exaptation. The story of the World Wide Web is a story of continuous exaptation. Tim Berners-Lee created a platform adapted for scholarship that was exapted for shopping, and sharing photos, and watching video along with a thousand other uses that would have astounded Berners-Lee when he created his first HTML-based directories in the early nineties.

Importantly, the sixth key to effectively cultivate innovation is the coffee breaks. The coffee breaks are a pivotal concept that aids effective cultivation of innovation. This is the reason why APPLE is consistently ranked as the most innovative company in the world. Apple development circle looks more like a coffee house than an assembly line. All the groups ranging from design, manufacturing, engineering, sales, and other departments meet continuously through the product-development circle, brainstorming trading ideas and solutions, strategizing over the most pressing issues, and generally keeping the conversation open to diverse groups of perspectives. Many of history's great innovators managed to build a cross-disciplinary coffeehouse environment within their own private work routines.

Tool seven explains much more on the platforms to cultivate innovation. An open platform in software is often called an API, which stands for application programming interface. An API is a kind of lingua franca that software applications can use reliably to communicate with each other. A set of standardized rules and definitions that allow programmers to build new tools on top of another platform or to weave together information from multiple platforms. When WEB users make geographical mashups using Google Maps, they write programs that communicate with Google geographic data using their mapping API. Again, in this section twitter is considered a good factor that bates cultivation of innovation. In the online world, the most celebrated case study in innovative power of stacked platforms has been the rapid evolution of the social networking service twitter. You write a tweet about what you had for lunch and within minutes that information is being harnessed to assist a number of different tasks. The information is not only flowing in the system, it is being recycled and put to new uses.

Let us consider the tool that this paper classified as the fourth quadrant. The quadrant is classified into four sections. The first section of the quadrant is called the market/ individual. This is a small, coordinated team, single inventor who planned to capitalize directly from the sale or licensing of their invention. A good example is a printing press. The second quadrant is called the marketing/ network. It is a large number of groups working on the same program. Multiple private firms interact and plan to capitalize directly from the sale or licensing of their invention. Example is an airplane. The third quadrant is called the non-marketing / individual. It is the amateur scientist or hobbyist who shares his or her ideas freely. Example of this quadrant is X-rays. The fourth quadrant is called the non-marketing/network. It is an open source or academic environment where ideas can be built upon in a large, collaborative network. An example is the Microscope.

Hence, since innovation is subject to historical changes, the fourth quadrant distinguishes shapes at different historical periods. The fourth quadrant should be a reminder that more than one formula exists for innovation. The wonders of modern life did not emerge exclusively from the proprietary clash between private firms. They also emerged from open networks.

## V. CONCLUSION

You may not be able to turn your government into a coral reef, but you can create comparable environments on the scale of everyday life. They can be done in the workplace if you exhibit the attitude of developing new ideas, work tirelessly to actualize your dream by using the seven keys of cultivating innovation. In these ways you consume media to get desired information and augment your memory with new ideas that can be cultivated to innovation. You can create leisure time. Go for a walk, cultivate hunches, write everything down, but gather and store your data well. Embrace serendipity, manage generative mistakes, take on multiple hobbies, frequent coffee houses and liquid network, follow the links, let other built on your ideas, borrow, recycle and re-invent.

## RECOMMENDATION

We strongly recommend that institutions should include this concept in their curriculum. The method of teaching should be practically and innovatively driven. Student should be trained to believe that they can develop new ideas and not to always use borrowed ideas without contributing to knowledge. They should be exposed to the seven keys of cultivation of ideas so that it will become a habit to develop new ideas.

## BIBLIOGRAPHY

- [1] Johnson, S. (2011) *Where Good Ideas Come From: The Natural History of Innovation*, River head trade.
- [2] Chuck Frey (2013) *Cultivating Innovation Champions*, inabling factors, innovationsmanagement.se publishing  
<http://www.innovationsmanagement.se/2013/01/30/cultivating>.
- [3] Liz Pearce(2013) *How to Cultivate Innovation in Real Time*, Business daily new.  
<http://www.businessnewsdaily.com/4196-innovation-shifts-odds-success.html#sthash.8LrPabDk.dpuf>
- [4] Jeff Foust (2013) *The Space Review: Technology's role in space innovation*. Bookmark and Share in 180 Google+ circles.  
Retrieved from <http://www.thespacereview.com/article/2348/1>
- [5] Charles Darwin (2013) *Coral Reef Adventures*. MacGillivray Freeman. Retrieved from  
<http://www.coralfilm.com/about.html>
- [6] Anna F. and Kathleen A. (2009) *Discovering Darwin at NOAA Central Library: Resources on Charles Darwin, Evolution, and the Galapagos Islands*, U.S. Department of Commerce National Oceanic and Atmospheric Administration . Retrieved from  
<http://www.lib.noaa.gov/researchtools/subjectguides/darwinbib.pdf>
- [7] Stephen Johnson (2012) *Everything Bad is Good for You : Reef, City, Web*. Retrieved from  
<http://www.everythingbadisgoodforyou11.blogspot.com/2012/12/reef-city-web.html>
- [8] Stephen Johnson (2007) *Everthing Bad is Good For You*. AEU Summit, keynote presentation. Washington DC. Retrieved from  
<http://www.360Kid.com>
- [9] Brian K. (2011) *Shift to the Future: Ideas and Innovation*. - in 570 Google+ circles. Retrieved from  
<http://www.shift2future.com/2011/11/ideas-and-innovation.html>
- [10] Arthur Koestler (2014). *The Act of Creation*, mirror, pdf.yt,  
<https://pdf.yt/d/rDIHDXbS3uvtgXcr>
- [11] Roger von Oech (2012) *The Best of All Creativity Books* .Palo Alto, California
- [12] Mousumi S. (2012) *Krishna Bharat, the Creator of Google News - Success Stories*  
<http://www.successtories.co.in/krishna-bharat-the-creator-of-google-news/>
- [13] Gabriel K. and Stephanie C.(2008) *Intentional Innovation: How Getting More Systematic about Innovation Could Improve Philanthropy and Increase Social Impact* . Kellogg Foundation .
- [14] John D. (2011) *The Power Of Pull': Maximising Serendipity Through Quality Social Networks (For Innovation)* CLPS -Edge Hill University, and Lorraine Johnston, Newcastle University
- [15] Gould, S. J.; Vrba, E. S. (1982). "Exaptation - a missing term in the science of form". *Paleobiology* 8 (1): 4–15. JSTOR 2400563



## Comparative Study of Path Loss Models for Wireless Communication in Urban and Sub-urban Environment for Port Harcourt, Nigeria.

Akujobi Ekeocha<sup>1</sup>, Nosiri Onyebuchi<sup>2</sup> and Achumba Ifenyinwa<sup>2</sup>

<sup>1</sup>. Department of Computer Science, University of Port Harcourt, Nigeria

<sup>2</sup>. Department of Electrical and Electronic Engineering Futo, Owerri, Nigeria

**ABSTRACT:** The study was based on the comparative analysis of radio propagation models for Global System for Mobile Communications at 900MHz. Drive test analyses were carried out from two selected terrains in Rivers State namely GRA Phase II and Aggrey Road classified as urban and suburban areas respectively, to evaluate the best propagation model for the study area. The data obtained were used to compare the various prediction models namely; Cost 231, Okumura-Hata and ECC-33. Mean path loss values of 115.16dB for Okumura-Hata and 117.79dB for COST 231 and 280.88dB for ECC-33 respectively were predicted in the urban environment. Mean path loss values of 115.16dB, 114.76dB and 314.84dB were predicted by Okumura-Hata, Cost 231 and ECC-33 models respectively in the suburban environment. ECC-33 over estimated path loss and gave the highest prediction in both environments. Okumura-Hata model showed better performance in urban while COST 231 performed better in the suburban environment. Okumura-hata and COST 231 models are recommended for deployment in urban and suburban environments respectively.

**Keywords** -Path Loss, Propagation Model, Received Signal Strength, Empirical models, wireless communication

### I. INTRODUCTION

Planning has been identified as a key factor before the implementation of designs, and also setting up of wireless communication systems. One basic requirement for an effective and reliable signal transmission is the knowledge of the received signal strength and its variability at different distances within the surrounding base station [1]. The propagation of wireless signals is subject to various propagation mechanisms and heavily influenced by the environment which results to a reduction in the signal strength. Path loss is described as a reduction in the transmitted power of an electromagnetic wave as it propagates through space. It is a major component in the analysis and design of link budget of a communication system. It depends on frequency, antenna height, receive terminal location relative to obstacles and reflectors, and link distance, among many other factors [2]. Propagation path loss model prediction plays an important role in the design of cellular systems to specify key system parameters such as transmission power, frequency and antenna heights [2].

A number of propagation prediction models for mobile radio communication systems have been developed. However, the selection of the most suitable model for any given geographical region is not a simple task, but depends on descriptions of terrain and effect of vegetation which vary widely from one place to another [3]. Propagation models are divided into three groups; the empirical models, semi-deterministic models and deterministic models [4]. Empirical models which are based on measurement data, statistical properties and few parameters. Examples of this model category are Okumura model and Hata model. Semi-deterministic models are based on empirical models and deterministic aspects, examples are the Cost-231 and Walfish-Ikegami. Deterministic models, these are site-specific, they require enormous number of geometry information about the city, computational report and more accurate model [4].

This study was aimed at carrying out field measurements to evaluate the received signal strength and path loss, compare the measured path loss with predicted models for GRA Phase II and Aggrey Road in Port Harcourt, River State, Nigeria.

## II. LITERATURE REVIEW

Over the years, different propagation path loss models have been developed for performance assessment of wireless communication systems. To achieve high quality of service delivery, various researchers have undergone research studies on the behaviour of radio wave within different environments under diverse environmental and geographical conditions. The models derived are specific for the respective environment.

In [5], a study conducted in India, they opined that path loss propagation models may give different results if used in different environments other than one which they were designed. Different path loss models were compared with measured field data. The field measurement data were obtained in urban, suburban and rural environments at 900 MHz and 1800 MHz frequency bands with the help of spectrum analyser. The analysis showed that ECC-33 and SUI models results performed better in urban areas. In suburban areas, ECC-33, Standard University Interim (SUI) and COST 231-Hata models showed good performance. Okumura – Hata and Log – distance models showed better performance in rural areas.

According to [1], they compared empirical models for cellular transmission in River State. In their study, downlink data was collected at various distances on live Globacom WCDMA network at 2100 MHz frequency. Result of predictions from three path loss models and the measured path loss were compared and simulated using MATLAB software. The COST 231 Hata showed better result from the comparison and thus recommended that an adjustment be made to the Cost 231 Hata model for cellular communication in the area.

According to [6], they developed a statistical path loss model that could be applied in the South South region of Nigeria. In their work, data was collected from 10 existing microcells operating at 876 MHz in Port Harcourt. The environment was categorized into urban (Category A) and suburban (Category B). The results showed that the Path loss increases by 35.5dB and 25.7 dB per decade in the urban (Category A) and suburban (Category B) areas respectively. Variations in path loss between the measured and predicted values from the Okumura-Hata model were calculated by finding the Mean Square Errors (MSE) to be 10.7dB and 13.4dB for urban and suburban terrains respectively. They opined that the comparison between the modified Hata models and measured values for the two categories showed a better result and thus was effective for use in the study area.

## III. PROPAGATION MODELS

### 3.1 Free Space Path Loss Model

Path loss in free space defines how much strength of signal is lost during propagation from transmitter to receiver. This model is applied in an environment that is characterized by less or no obstructions to wireless signal. Free space path loss depends on frequency and distance.

The following equation represents the free space path loss as in [3]:

$$P_L = 32.45 + 20 \log_{10}(d) + 20 \log_{10}(f) \quad (1)$$

Where,

f: Frequency (MHz)

d: T-R separation (m)

### 3.2 Okumura-Hata Model

Hata model is expressed as a mathematical formulation to mitigate the best fit of the graphical data provided by the classical Okumura model. Hata model is used for the frequency range of 150 MHz to 1500 MHz to predict the median path loss for the distance d from transmitter to receiver antenna in 20 km range and height of transmitting antenna is considered 30 m to 200 m and receiver antenna height is 1 m to 10 m. The model is represented in equation 2 as given by [4]:

$$P_L = A + B \log_{10} d - C \quad (2)$$

Where,

$$A = 69.55 + 26.16 \log_{10}(f_c) - 13.82 \log_{10}(h_b) - a(h_m)$$

$$B = [44.9 - 6.55 \log_{10}(h_b)] \log_{10}(d)$$

$$C = 5.4 + 2 \left[ \log_{10} \left( \frac{f_c}{28} \right) \right]^2$$

$$a(h_m) = 3.2 (\log_{10}(11.75 h_m))^2 - 4.79, f > 400 \text{ MHz}$$

$f_c$  = carrier frequency

$h_m$  = transmitter antenna height in meter

$h_b$  = receiver height in meter

$d$  = transmitter-receiver distance in km

$a(h_m)$  = mobile station antenna height correction factor

### 3.3 COST 231 Hata Model

The COST 231 Hata model was developed as an extension to Hata-Okumura model. This model operates in the frequency range from 500MHz to 2GHz, applied in the prediction of path loss for three different environments like urban, suburban and rural. It consists of a correction factor for these three environments. The path loss equation for this model can be expressed as [6]:

$$P_L = 46.3 + 33.9 \log_{10} h_t - a(h_r) + [44.9 - 6.55 \log_{10} h_t] \log_{10} d + C \quad (3)$$

$C = 0$  or 3dB, for suburban areas and metropolitan cities

$h_t$  = Transmitting Antenna height in meter

$$a(h_r) = (1.11 \log_{10} f_c - 0.7)h_r - (1.5 \log_{10} f_c - 0.8),$$

for suburban environment

$a(h_r)$  = mobile station antenna height correction factor

$f_c$  = Carrier frequency in MHz

$d$  = Transmitter-receiver separation distance in km

$h_r$  = Receiver antenna height in meter

### 3.4 ECC-33 Model

The ECC-33 model formulation is based on original measurements from Okumura model. The model is most widely used in large and medium size cities, areas having crowded and tall buildings. The operation range of this model is up to 3000MHz and distance range from 1 to 100 km. The model is expressed as [9]:

$$P_L = A_{fs} + A_{bm} - G_b - G_r \quad (4)$$

Where,

$A_{fs}$  [dB] = free space attenuation

$A_{bm}$  [dB] = basic median path loss

$G_b$  = Transmitter antenna height gain factor

$G_r$  = Receiver antenna height gain factor

Further expressed as,

$$A_{fs} = 92.4 + 20 \log_{10}(d) + 20 \log_{10}(f_c)$$

$$A_{bm} = 20.41 + 9.83 \log_{10}(d) + 7.894 \log_{10}(f_c) + 9.56 [\log_{10}(f_c)]^2$$

$$G_b = \log_{10} \left( \frac{h_b}{200} \right) \{13.958 + 5.8 [\log_{10}(d)]^2\}$$

$$G_r = [42.57 + 13.7 \log_{10}(f_c)] [\log_{10}(d_r) - 0.585]$$

## IV. MATERIALS AND METHOD

### 4.1 Description of the Propagation Terrain

The study area is located in the River State, with coordinates (04°48'54" N, 06°59' .52"E) and (04° 45 .06"N, 07° 02 .24 E). The area under study was categorized as suburban and urban environment with narrow streets, trees and moderately high buildings.

### 4.2 Data Collection Process

A drive test was conducted within the study area; GRA phase II and Aggrey road, Nigeria with a vehicle driven along predefined routes. The drive test survey routes follow the design from a cell reference. The cell reference is a telecommunication road map which shows drive test routes to cover antenna sectors. Transmission Evaluation and Monitoring System (TEMS) Investigation software was used on a laptop with a Global Positioning System (BU353) and a TEMS Mobile Station (Sony Ericsson w995) connected through Universal Serial Board (USB) ports. The personal computer serves as the communication hub for all equipment in the system. The Global Positioning Satellites (GPS) provides the location tracking for the system during data collection. This enables the system to determine the position of the Mobile Station (MS) on a global map which is already installed on the laptop. The MS was used to initiate calls during data collection process. While driving was going on, the handset was configured to automatically make calls to a fixed destination number. Each call lasted for 1minute hold time and the call was dropped. The phone remained idle for some period of time then

another call was made. The collected data was saved in Log file format for further processing, Actix Analyser was used for the post processing.

#### 4.3 Drive Test Survey Route

The drive test survey route was carefully planned with the aid of a cell reference (cell ref) such that the measurement collection process involved base stations sited within an area marked for investigation. The survey route was also indicated on the map to aid accessibility of the drive test vehicle to the active sector of the base station in consideration. The distance covered was ensured to be long enough to allow the noise level of the receiver to be reached. The routes covered in this study were GRA phase II and Aggrey road. These routes were chosen based on their uniqueness in order to represent the features of these cities. Fig 1.0 Showed the TEMS view of the drive test routes.

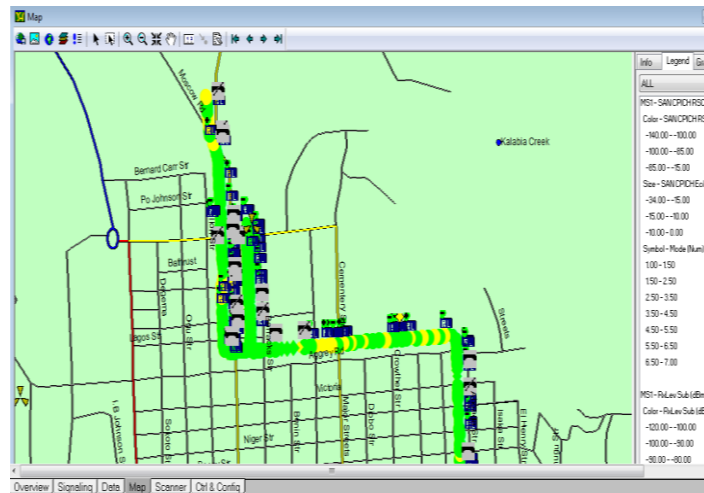


Figure 1: View of drive test routes

### V. RESULTS AND DISCUSSION

The path loss values from the three existing models are presented using equation (2), (3), (4) and were compared with the field measured values and their results displayed in figs 2 and 3.

Table 1: Network Parameters for Urban and Sub-urban

Parameters	Values
Frequency	900MHz
Transmitting Antenna Height	40m
Receiving Antenna Height	1.5m

Table 2: Empirical and Measured Path loss values for Urban Environment

Distance (km)	ECC-33(dB)	COST-231 (dB)	OKUMURA-HATA (dB)	MEASURED (dB)
0.1	262.65	93.00	90.27	100
0.2	269.55	103.30	100.63	106
0.3	273.93	109.30	106.67	104
0.4	277.19	113.61	110.97	120
0.5	279.81	116.90	114.31	158
0.6	282.00	119.67	117.03	158
0.7	283.90	121.97	119.34	158
0.8	285.57	123.96	121.33	113
0.9	287.07	125.72	123.09	112
1.0	288.42	127.30	124.67	128
1.1	289.66	128.72	126.08	135
1.2	290.81	130.02	127.39	136

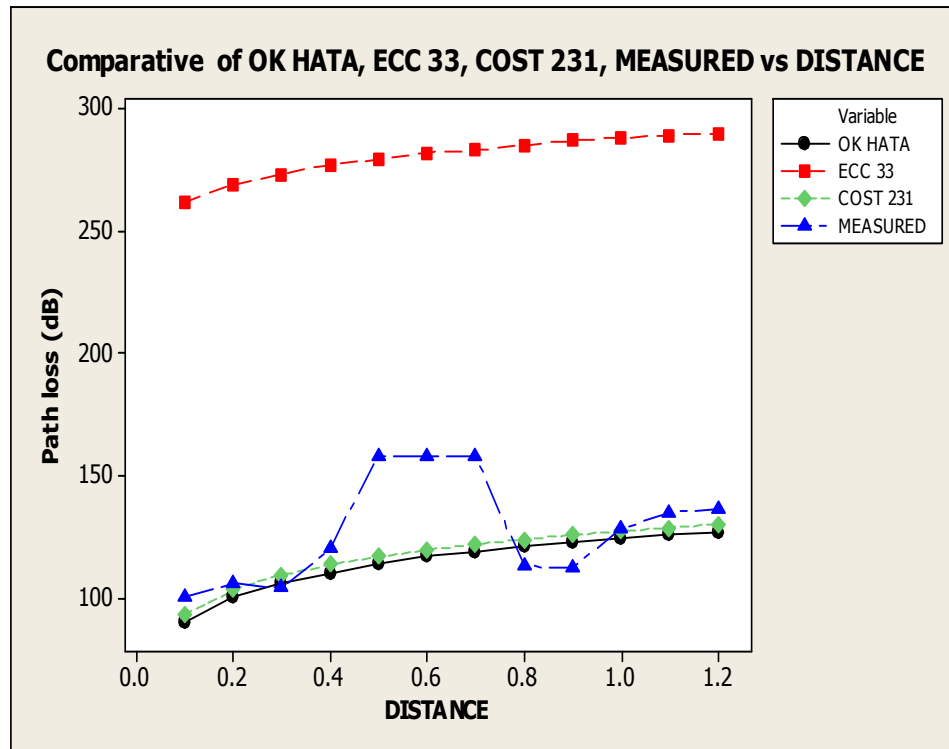


Figure 2: Comparison between predicted and measured Path loss in an urban environment

The prediction results of empirical propagation models employed in this study are represented graphically. The values of the predicted Path loss and the field measured data were plotted against the distance of separation between the Base Station (BS) antenna and the Mobile Station (MS) antenna. Fig 2.0 showed the result of Path loss prediction from Okumura-Hata, COST 231, ECC-33 and the measured Path loss from the urban propagation environment. The result of the drive test carried out within the coverage area of the cell reported a mean RSS of -83dBm. Mean measured Path loss values of 115.16dB, 117.79dB and 280.88dB were predicted by Okumura-Hata, COST 231-Hata and ECC-33 Models respectively. COST 231 and Okumura-Hata models showed some level of similarity with slight difference. The ECC-33 model predictions were high compared to Okumura-Hata and Cost 231. The high Path loss prediction recorded from ECC-33 clearly showed that the environment of study needs to be considered in the siting of GSM base stations. The measured Path loss showed some level of fluctuations resulting from obstructions of physical structures within the environment or topology. The COST 231 Hata model was chosen for the optimization of this environment.

Table 3: Empirical and Measured Path loss values for Suburban Environment

Distance (km)	ECC 33(dB)	COST 231 (dB)	OKUMURA HATA (dB)	MEASURED (dB)
0.1	296.60	89.88	90.27	111
0.2	303.51	100.25	100.63	113
0.3	307.89	106.31	106.69	114
0.4	311.15	110.61	110.99	131
0.5	313.77	113.95	114.32	116
0.6	315.96	116.67	117.04	158
0.7	317.86	118.97	119.35	140
0.8	319.53	120.97	121.34	158
0.9	321.02	122.73	123.10	152
1.0	322.38	124.30	124.68	128
1.1	323.62	125.71	126.10	141
1.2	324.77	127.03	127.40	124

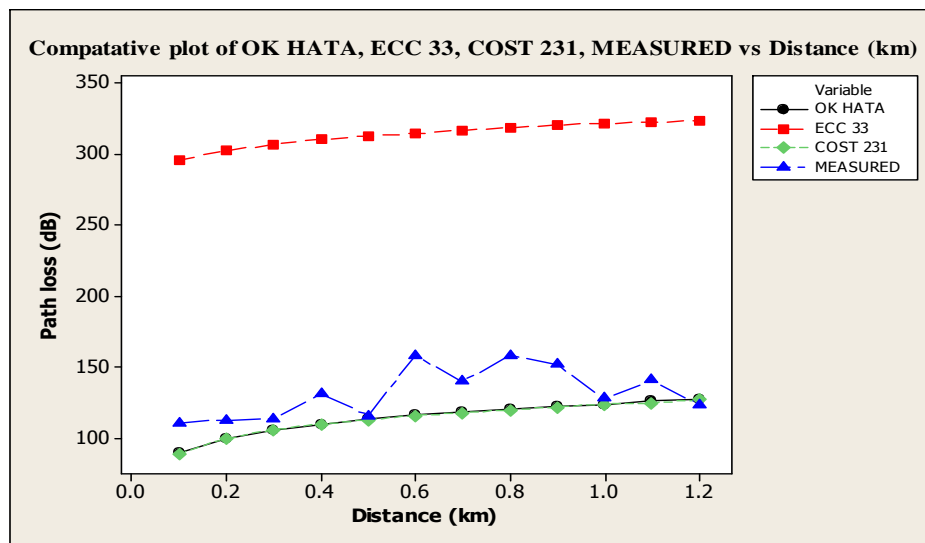


Figure 3.0: Comparison of Predicted and Measured Path loss in suburban environment

Fig 3.0 showed a plot of the predicted propagation models and measured radio propagation characteristics of the transmitted signal within the suburban environment. Okumura-Hata, COST 231, and ECC-33 Models predicted mean Path loss values of 115.16dB, 114.76dB and 314.84dB respectively. The ECC-33 model over predicted path loss compared to Okumura-Hata and COST 231. The deviations between Okumura-Hata model and COST 231 models can be considered as negligible. The mean Received Signal Strength (RSS) obtained from the propagation environment within the radio coverage of the cell was -79.39 dBm.

Table 4: Measured Received Signal Strength for Urban Environment

S/N	Measured RSS (Urban)	Measured RSS(Suburban)
1	-67	-65
2	-73	-66
3	-71	-64
4	-83	-67
5	-77	-67
6	-91	-66
7	-81	-66
8	-80	-69
9	-79	-74
10	-95	-76
11	-102	-77
12	-103	-78



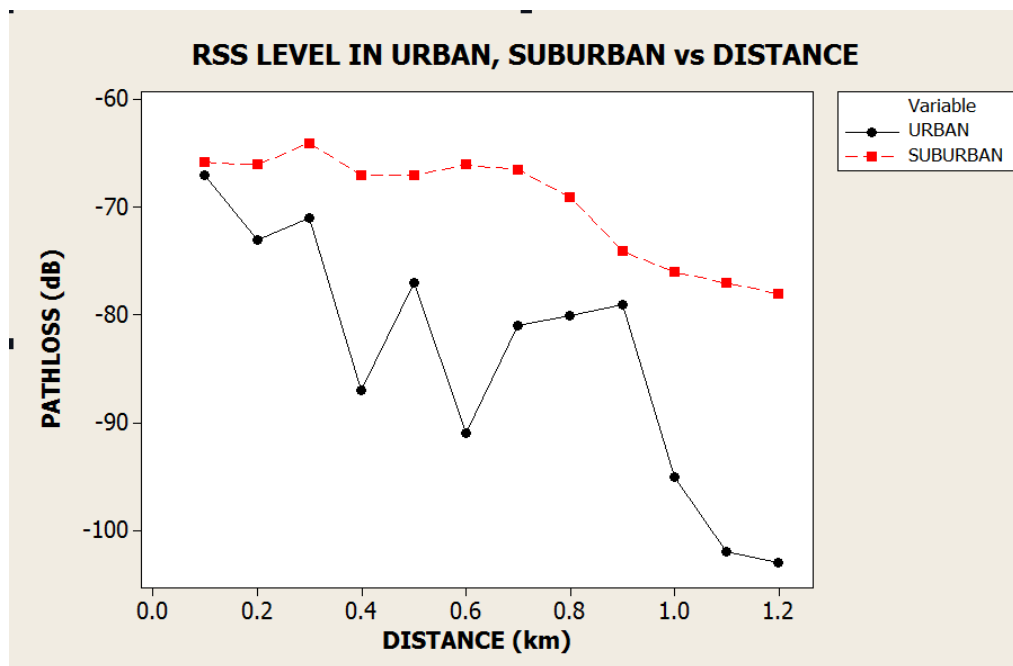


Figure 4.0: RSS plots in urban and suburban environment

Fig 4.0 represented a plot of the (RSS) in the suburban environment. There is a gradual degradation of the signal strength as compared to the urban environment. In the urban plot, the existence of signal fluctuations indicates obstructions encountered along the signal path. These obstructions are high rise buildings in close proximity, as well as trees sandwiched between houses within the environment. These obstructions account for call drops, cross talk, and loss of signal experienced in the study area.

## VI. CONCLUSION

In this research, the received signal strength and path loss of a mobile communication system was measured in an urban and suburban environment respectively. The predicted Path loss was compared with measured data using a graphical representation, the performance of all models were analysed and it was shown that Cost 231 and Okumura-Hata models showed considerable performance and could be adjusted for better performance. It can be said that the performance of radio propagation models are environment dependent. Thus, the influence of environmental factors must be emphasised and properly accounted for when considering base station sites. Therefore, one of the best possible ways of obtaining a better radio channel characteristics is to optimize the existing path loss models based on measured data collected from a specific area.

## REFERENCES

- [1] Akinwale B.O.H, and Biebuma J.J, "Comparative Analysis of Empirical Path Loss Model for Cellular Transmission in Rivers State", *American Journal of Engineering Research (AJER)*, ISSN 2320-0936, Volume 02, Issue- 08, PP 24 – 31, 2013.
- [2] Nwalozie Gerald .C, Ufoaroh S.U, Ezeagwu C.O, Ejiofor A.C, "Path Loss Prediction for Gsm Mobile Networks for Urban Region of Aba, South-East Nigeria".*International Journal of Computer Science and Mobile Computing*, Vol.3 Issue.2, PP. 267-281, 2014.
- [3] PranjaliRaturi, Vishal Gupta, SamreenEram , "Proposed Propagation Model for Dehradun Region" *International Journal of Soft Computing and Engineering (IJSCE)*, ISSN: 2231-2307 Volume 3, Issue 6, 2014.
- [4] Mardeni, R and Kwan K.F, "Optimization of Hata Propagation model of Sub-Urban Area in Malaysia", *Progress in Electromagnetic Research C*, Vol 13, 91 – 106, 2010.
- [5] SharmaP.K and R.K. Singh, "Comparative Analysis of Propagation Path Loss Models with Field Measured Data".*International Journal of Engineering Science and Technology*, Vol. 2(6), 2014.
- [6] Ubom, E.A, Idigo V.E, Azubogu A.C, Ohaneme C.O. and Alumona T.L (2011). "Path loss Characterization of Wireless Propagation for South - South Region ofNigeria". *International Journal of Computer Theory and Engineering*, Vol.3, No3. PP 360-364.
- [7] Ujjawalbahuguna, Bhagirathi Pradhan (2014), "A Review on Path Loss Models for Suburban Regions Using Fuzzy Logic" *International Journal of Computer Engineering & Science(IJCES)*.ISSN: 2231-6590, 2014
- [8] Ogbulezie J.C, M.U. Onuu, J.O. Ushie, B.E. Usibe, "Propagation Models for GSM 900 and GSM 1800MHz for Port Harcourt and Enugu, Nigeria", *Network and Communication Technologies*; vol. 2, No. 2, 2013.PP 1-10.
- [9] KumariManju, YadavTilotma and PoojaYadav, "Comparative Study of Path loss Models in different Environments". *International Journal of Engineering Science and Technology (IJEST)*, Vol. 3 No. 4 April 2011.

## Hybridised Single-Phase Cascaded Multilevel Inverter Topology Using Reduced Number of Power Switches

<sup>1</sup>G. C. Diyoke, <sup>1</sup>O. A. Nwaorgu, <sup>1</sup>I. K. Onwuka

<sup>1</sup>Department of Electrical and Electronic Engineering, Michael Okpara University of Agriculture, Umudike Abia State Nigeria.

**Abstract:** This paper presents a hybridized single-phase cascaded multilevel inverter topology using reduced number of power switches. The multicarrier, phase disposition pulse width modulation technique is used to generate the switching signals for the power switches. The circuit configuration, mode of operations and the switching functions are given. At a modulation index of 0.8, the desired multilevel inverter's output voltage is obtained. The inverter topologies are subjected to the same values of an R-L load. Logic circuit configuration of the proposed cascaded multilevel inverter is displayed, which generates the firing pulses. The first quarter of the quarter symmetry output voltage waveform is analysed with different displacement angles calculated. Fast Fourier transform analyses of the output voltages of cascaded diode clamped and proposed are displaced under 0.8 modulation index and their respective THD obtained. THD values of 14.38%, 10.32% and 10.43% for cascaded capacitor clamped, diode clamped and proposed are obtained respectively. The proposed configuration with less number of power switches is validated with cascaded diode clamped configuration using simulation approach. Similar results are obtained.

**Index Terms** - Inverter, multicarrier, multilevel, Fast Fourier transform, total harmonic distortion.

### I. INTRODUCTION

Nowadays, Fossil fuel is the major energy supplier of the world economy. This type of energy source has a great advance effect such as global warming which causes serious depletion of ozone layer and air pollution. Therefore, with regard to the worldwide trend of green energy, solar power technology has become one of the most promising energy sources [1]. According to the law of conversion of energy, Sun energy is converted into electrical energy with uncontrolled low d. c. voltage output. Furthermore, an inverter is used to convert direct current into single or poly-phase alternating current. Due to high harmonic content of this conventional inverter a new inverter topology was developed which helps to improve on the problem associated with the conventional type. The staircase waveforms produced from several levels approach the sinusoidal waveform with low harmonic distortion; thus reducing filter requirements [2]. Multilevel inverter configuration is one of the most vital discoveries in power electronics in the recent years. The unique structure of multi-level voltage source inverters allow them to reach high voltages with low harmonics without the use of transformer or series connected synchronized switching devices. As the number of voltage levels increases, the harmonic content of output voltage waveform decreases significantly [3]. Applying this concept, the power conversion is performed with enhanced power quality [4].

Among various multilevel topologies, the most important ones are [5]. Diode Clamped Multilevel Inverter (DCMI) and Flying Capacitor Multilevel Inverter (FCMI) and Cascaded Multilevel Inverter (CMI). The main drawbacks of DCMI topology, with level number higher than three, is the necessity of a capacitor voltage balancing control circuit and the high voltage drop across the clamped diodes. FCMI uses flying capacitors as clamping devices. These configurations have several attractive properties in comparison with DCMI, including the advantages of the transformerless operation and redundant phase leg states that allow the switching stresses to be equally distributed between semiconductor switches [3, 4]. The first, simplest and the most modular topology is CMI [1]. CMI can avoid more clamping diodes or voltage balancing capacitors in the power circuit configuration. It involves series of single phase conventional inverter or hybridised multilevel inverter topologies. Henceforth, the major fault associated with CMI configuration is the need for separated DC sources which are not readily available without the use of transformers. In some specific applications such as photovoltaic systems, electric vehicle motor drive, separate dc sources exists and can be used in the CMI configuration.

For the modulation of multilevel inverters, carrier-based modulation schemes are normally used, largely divided into two categories: phase-shifted carrier pulse width modulation and level-shifted width modulation [6]. Fig. 1 shows the multilevel converter modulation methods. The modulation control schemes for the multilevel can be divided into two categories, fundamental switching frequency and high switching frequency PWM such as carrier-based PWM, selective harmonic elimination and multilevel space vector PWM. Multilevel SPWM needs multiple carriers [7]. One of the simplest modulation strategies for CMI is phase shifted carrier modulation technique where the  $n$  carriers of the full bridge cascaded inverters are phase shifted by  $180/n$  degrees [1]. This modulation technique is utilized due to its simplicity. It is observed that this method of modulation is not suitable for all resistive-induction loads and it is also associated with high harmonic contents. Due to shortcomings of this modulation technique, in this paper, sinusoidal pulse width modulation (PWM) technique is implemented.

In this paper, a hybridised single-phase cascaded multilevel inverter topology using reduced number of power switches is proposed. The power circuit configuration of (Diode clamped Multilevel cascaded inverter) DCMCI and proposed hybridized cascaded MI are presented in Section II. The Pulse width modulation (PWM) control method is introduced in Section III. The simulation results for validating the improvements of the proposed inverter topology are in Section IV. In Section V conclusion is presented.

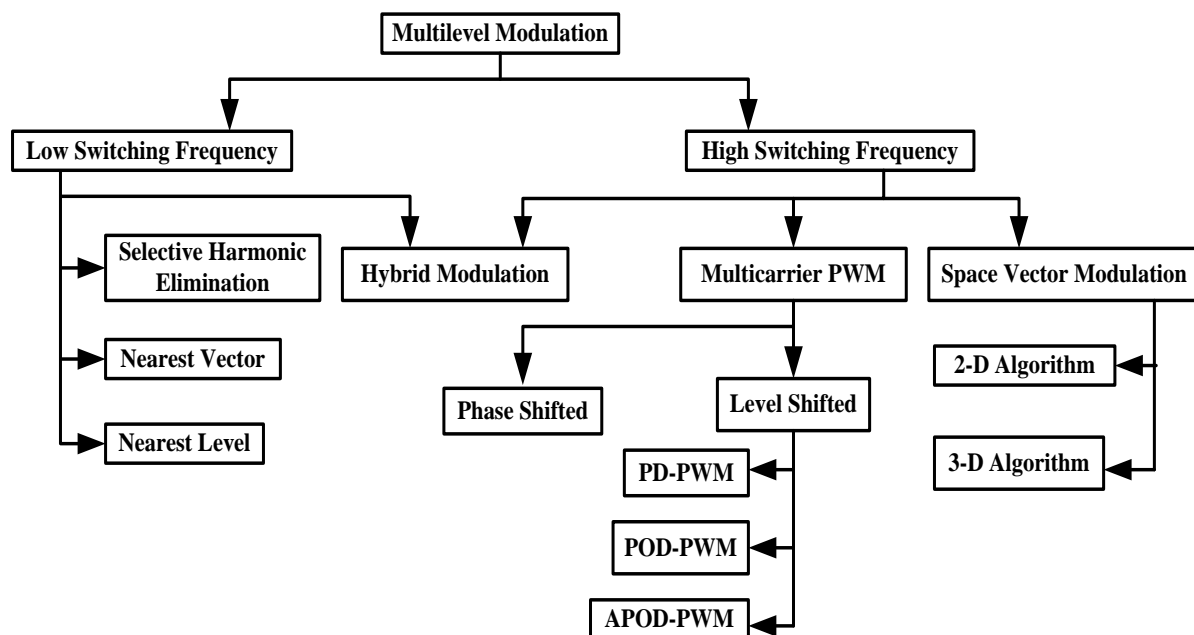


Fig. 1 Multilevel converter modulation methods

## II. POWER CIRCUIT CONFIGURATION OF THREE-LEVEL INVERTER TOPOLOGIES.

The Fig. 2 below shows, a power circuit configuration of a Diode clamped multilevel cascaded inverter topology. Each of the cells comprises of a single-phase three-level diode clamped inverter with one dc source and two voltage divided capacitors. Also, each of the cells comprises of eight power switches with anti-parallel diodes and four clamping diodes. Furthermore, each of the cells contains four upper switches and four lower switches. Thus, the power switches can be arranged in the form of four power switches per leg voltage.

The proposed hybridized single-phase cascaded multilevel inverter topology is shown in Fig. 3. The inverter is comprised of two cells of single-phase conventional H-bridge, one bidirectional power switch, two capacitors which serve as dc voltage divider. The bidirectional circuit is connected to the centre tap of the capacitor voltage divider. In Figs. 1 and 2, the proper switching of the inverter can generate the following output-voltage levels:  $2V_{dc}$ ,  $3V_{dc}/2$ ,  $V_{dc}/2$ ,  $0$ ,  $-V_{dc}/2$ ,  $-3V_{dc}/2$ ,  $-2V_{dc}$ . The addition of switches  $S_A$  and  $S_B$  must be properly switched considering the direction of the flow of the load current [4]. The switching pattern adopted by DCMCI and proposed inverter topologies are shown in Figs. 6 and 7 respectively. Thus, Table 1 shows the switching combinations that generated the output voltage level aforementioned above.

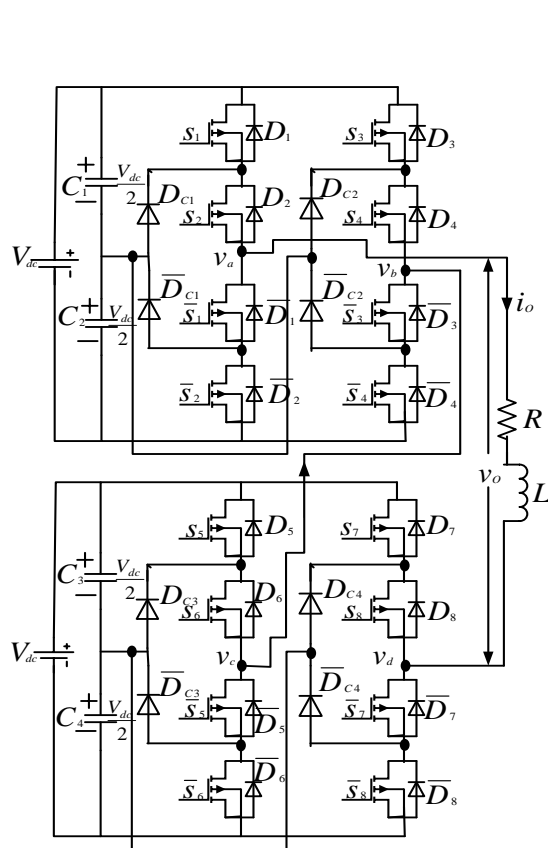


Fig. 2 Configuration of the ideal diode clamped single-phase cascaded multilevel Inverter.

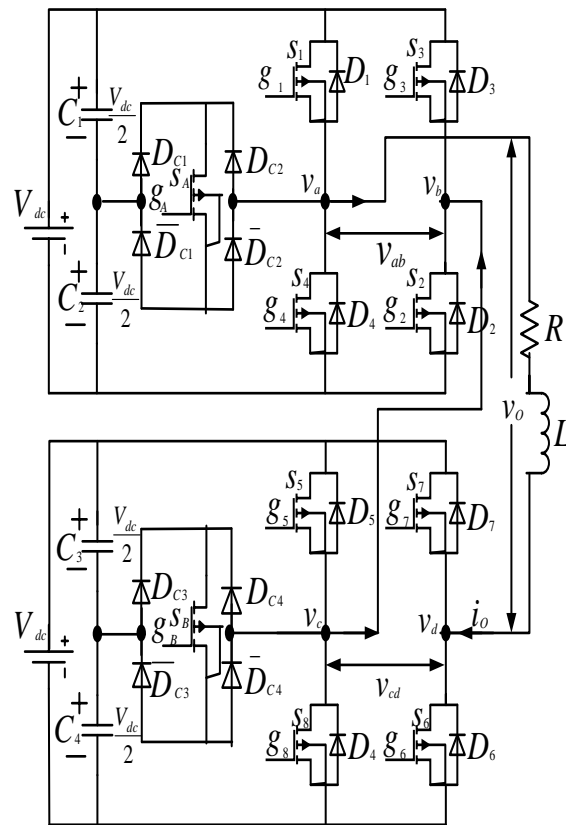


Fig. 3 Configuration of the proposed single-phase cascaded multilevel inverter.

Table 1 Output voltage according to the switches on/off (1/0) conditions

S/N	$s_1$	$s_2$	$s_3$	$s_4$	$s_5$	$s_6$	$s_7$	$s_8$	$s_A$	$s_B$	$v_a$	$v_b$	$v_c$	$v_d$	$v_{ab}$	$v_{cd}$	$v_o$
1	0	1	0	0	0	1	0	1	1	0	$\frac{V_{dc}}{2}$	0	0	0	$\frac{V_{dc}}{2}$	0	$\frac{V_{dc}}{2}$
2	1	1	0	0	0	1	0	1	0	0	$V_{dc}$	0	0	0	$V_{dc}$	0	$V_{dc}$
3	1	1	0	0	0	1	0	0	0	1	$V_{dc}$	0	$\frac{V_{dc}}{2}$	0	$V_{dc}$	$\frac{V_{dc}}{2}$	$\frac{3V_{dc}}{2}$
4	1	1	0	0	1	1	0	0	0	0	$V_{dc}$	0	$V_{dc}$	0	$V_{dc}$	$V_{dc}$	$2V_{dc}$
5	0	1	0	1	0	1	0	1	0	0	0	0	0	0	0	0	0
6	1	0	1	0	1	0	1	0	0	0	$V_{dc}$	$V_{dc}$	$V_{dc}$	$V_{dc}$	0	0	0
7	0	0	1	0	1	0	1	0	1	0	$\frac{V_{dc}}{2}$	$V_{dc}$	$V_{dc}$	$V_{dc}$	$-\frac{V_{dc}}{2}$	0	$-\frac{V_{dc}}{2}$
8	0	0	1	1	1	0	1	0	0	0	0	$V_{dc}$	$V_{dc}$	$V_{dc}$	$-V_{dc}$	0	$-V_{dc}$
9	0	0	1	1	0	0	1	0	0	1	0	$V_{dc}$	$\frac{V_{dc}}{2}$	$V_{dc}$	$-V_{dc}$	$-\frac{V_{dc}}{2}$	$-\frac{3V_{dc}}{2}$
10	0	0	1	1	0	0	1	1	0	0	0	$V_{dc}$	0	$V_{dc}$	$-V_{dc}$	$-V_{dc}$	$-2V_{dc}$

### III. PWM MODULATION

Multilevel inverters using pulse-width modulation are being increasingly preferred for high-power applications. The advantages of multilevel inverters are their ability to generate voltage waveforms with lower harmonics, without resorting to high-frequency PWM switching [8]. Multicarrier phase disposition PWM control scheme is employed in the generation of the gating signals. Basic principle of the proposed switching strategy is to generate gate signals by comparing the rectified sinusoidal modulating/reference signal, at fundamental frequency, with four triangular carrier waves having higher switching frequency and in-phase, but different offset voltages [4].

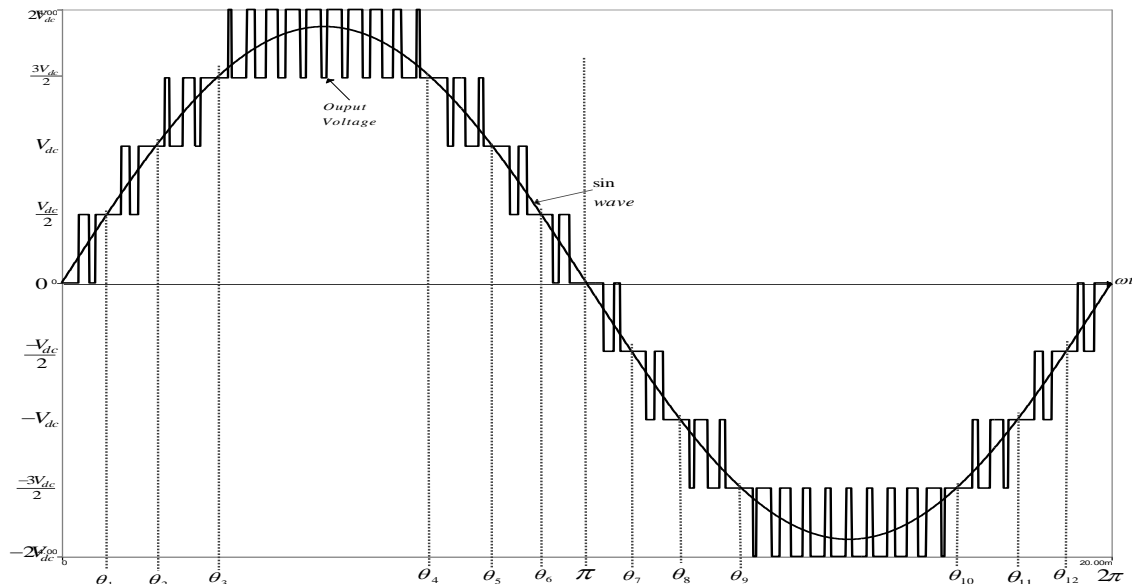


Fig. 4 Inverter Output Voltage and switching angles.

For one period of the expected output voltage and reference voltage is given in Fig. 4. This voltage plot profile shows how much our expected output voltage waveform differs from the reference waveform. The two inverter topologies operate through eight modes. Therefore (1) is generated from Fig. 4 and also showcases the eight modes operation.

$$f(\omega t) = \left\{ \begin{array}{l} 0 \text{ and } \frac{V_{dc}}{2}, 0 < \omega t < \theta_1, \text{ mode 1} \\ \frac{V_{dc}}{2} \text{ and } V_{dc}, \theta_1 < \omega t \leq \theta_2, \text{ mode 2} \\ V_{dc} \text{ and } \frac{3V_{dc}}{2}, \theta_2 < \omega t < \theta_3, \text{ mode 3} \\ \frac{3V_{dc}}{2} \text{ and } 2V_{dc}, \theta_3 < \omega t < \theta_4, \text{ mode 4} \\ \frac{3V_{dc}}{2} \text{ and } V_{dc}, \theta_4 < \omega t < \theta_5, \text{ mode 3} \\ V_{dc} \text{ and } \frac{V_{dc}}{2}, \theta_5 < \omega t < \theta_6, \text{ mode 2} \\ \frac{V_{dc}}{2} \text{ and } 0, \theta_6 < \omega t < \pi, \text{ mode 1} \\ 0 \text{ and } -\frac{V_{dc}}{2}, \pi < \omega t < \theta_7, \text{ mode 5} \\ -\frac{V_{dc}}{2} \text{ and } -V_{dc}, \theta_7 < \omega t \leq \theta_8, \text{ mode 6} \\ -V_{dc} \text{ and } -\frac{3V_{dc}}{2}, \theta_8 < \omega t < \theta_9, \text{ mode 7} \\ -\frac{3V_{dc}}{2} \text{ and } -2V_{dc}, \theta_9 < \omega t < \theta_{10}, \text{ mode 8} \\ -\frac{3V_{dc}}{2} \text{ and } -V_{dc}, \theta_{10} < \omega t < \theta_{11}, \text{ mode 7} \\ -V_{dc} \text{ and } -\frac{V_{dc}}{2}, \theta_{11} < \omega t < \theta_{12}, \text{ mode 6} \\ -\frac{V_{dc}}{2} \text{ and } 0, \theta_{12} < \omega t < 2\pi, \text{ mode 5} \end{array} \right\} \quad (1)$$

The phase angle depends on modulation index  $M_a$ . Theoretically, for a single reference signal reference signal carrier signal, the modulation index is defined to be

$$M_a = \frac{A_m}{A_c} \quad (2)$$

While for a single-reference signal and dual carrier signal, the modulation index is defined to be [9]

$$M_a = \frac{A_m}{2A_c} \quad (3)$$

Generally, the expression of modulation index is given as [2]

$$M_a = \frac{A_m}{A_c(k-1)} \quad (4)$$

Where  $A_c$  is the peak-to-peak value of the triangular carrier signals,  $A_m$  is the apex value of the rectified sinusoidal reference and  $k$  is the number of output voltage level synthesized per half-cycle; in this case,  $k=5$ .

When modulation index is less than 0.25, the phase angle displacement is

$$\theta_1 = \theta_2 = \theta_3 = \theta_4 = \theta_5 = \theta_6 = \frac{\pi}{2} \quad (5)$$

$$\theta_7 = \theta_8 = \theta_9 = \theta_{10} = \theta_{11} = \theta_{12} = \frac{3\pi}{2} \quad (6)$$

Furthermore, when the modulation index is more than 0.25 and less than or equal to 0.50, the phase angle displacement is determined by

$$\theta_1 = \sin^{-1}\left(\frac{A_c}{A_m}\right) \quad (7)$$

$$\theta_2 = \theta_3 = \theta_4 = \theta_5 = \frac{\pi}{2} \quad (8)$$

$$\theta_6 = \pi - \theta_1 \quad (9)$$

$$\theta_7 = \pi + \theta_1 \quad (10)$$

$$\theta_8 = \theta_9 = \theta_{10} = \theta_{11} = \frac{3\pi}{2} \quad (11)$$

$$\theta_{12} = 2\pi - \theta_1 \quad (12)$$

Moreover, when the modulation index is more than 0.50 and less than or equal to 0.75, the phase angle displacement is determined by

$$\theta_1 = \sin^{-1}\left(\frac{A_c}{A_m}\right) \quad (13)$$

$$\theta_2 = \sin^{-1}\left(\frac{2A_c}{A_m}\right) \quad (14)$$

$$\theta_3 = \theta_4 = \frac{\pi}{2} \quad (15)$$

$$\theta_5 = \pi - \theta_2 \quad (16)$$

$$\theta_6 = \theta_7 = \pi - \theta_1 \quad (17)$$

$$\theta_8 = \pi + \theta_2 \quad (18)$$

$$\theta_9 = \theta_{10} = \frac{3\pi}{2} \quad (19)$$

$$\theta_{11} = 2\pi - \theta_2 \quad (20)$$

$$\theta_{12} = 2\pi - \theta_1 \quad (21)$$

Finally, when the modulation index is greater than 0.750, the phase angle displacement is determined by

$$\theta_1 = \sin^{-1}\left(\frac{A_c}{A_m}\right) \quad (22)$$

$$\theta_2 = \sin^{-1}\left(\frac{2A_c}{A_m}\right) \quad (23)$$

$$\theta_3 = \sin^{-1}\left(\frac{3A_c}{A_m}\right) \quad (24)$$

$$\theta_4 = \pi - \theta_3 \quad (25)$$

$$\theta_5 = \pi - \theta_2 \quad (26)$$

$$\theta_6 = \pi - \theta_1 \quad (27)$$

$$\theta_7 = \pi + \theta_1 \quad (28)$$

$$\theta_8 = \pi + \theta_2 \quad (29)$$

$$\theta_9 = \pi + \theta_3 \quad (30)$$

$$\theta_{10} = 2\pi - \theta_3 \quad (31)$$

$$\theta_{11} = 2\pi - \theta_2 \quad (32)$$

$$\theta_{12} = 2\pi - \theta_1 \quad (33)$$

The frequency modulation index [10] is given as

$$M_f = \frac{f_c}{f_m} \quad (34)$$

Where,  $f_c$  is the frequency of the carrier wave and  $f_m$  is the frequency of the sinusoidal wave.

For  $M_a$  equal to or less than, 0.25, only the lower triangular carrier wave (Tri) is compared with the rectified reference wave (Sin). The inverter's behaviour is similar to a conventional full-bridge. If  $M_a$  is greater than 0.25 and less than 0.50, two triangular carrier signals, Tri and Tri1, are compared with the rectified reference wave. The inverter's output voltage behavior is similar to a fundamental multilevel inverter. Furthermore, when  $M_a$  is



greater than 0.50 and less than 0.75, three triangular carrier signals, Tri, Tri1 and Tri2, are compared with the rectified reference wave (Sin). Four levels of output voltage are synthesized on positive half cycle. Finally, when  $M_a$  is set to be greater than 0.75 for nine levels of output voltage to be produced in this work. In this case, all the four triangular carrier signals, Tri-Tri3 have to be compared with the reference to generate switching signals for the power switches [4].

In Fig. 5, it can be seen that eight switching signals:  $g_1, \bar{g}_1, g_2, \bar{g}_2, g_5, \bar{g}_5, g_6$ , and  $\bar{g}_6$  are operating at the rate of carrier signals' frequency; whereas eight other switching signals:  $g_3, \bar{g}_3, g_4, \bar{g}_4, g_7, \bar{g}_7, g_8$ , and  $\bar{g}_8$  are operating at the fundamental frequency. In Fig. 6, it can be seen that six switching signals:  $g_1, g_4, g_5, g_8, g_A$  and  $g_B$ , are operating at the rate of carrier signals' frequency ( $f_c$ ); whereas four other switching signals:  $g_2, g_3, g_6$  and  $g_7$ , are operating at the fundamental frequency ( $f_m$ ). In Fig. 7 shows how the overall firing circuit signals of the proposed hybridised single-phase cascaded multilevel inverter are generated.

Fig. 7(A) depicts how rectified reference wave (Sin) is been generated from the fundamental reference sine wave (50Hz) by passing the signal through rectifier circuit. Signals  $g_2$  and  $g_6$  are generated by comparing the reference sine wave with zero potential. Consequently, inverting  $g_2$  and  $g_6$  yield  $g_3$  and  $g_7$ . Signal  $g_1$  is generated by combination of Op-Amp comparators, AND and OR gates. Also, the carrier signals Tri1, Tri2 and Tri3 are generated from fundamental carrier triangular wave operating at 2KHz with the aid of level-shifter circuits.

In Fig. 7(B), the switching signals of  $g_4, g_5$  and  $g_8$  are generated with the help of signal generated in Fig. 7(A). In the same way, switching signals of  $g_A$  and  $g_B$  are generated with the help of Figs. 7(C) and 7(D) respectively. For easy troubleshooting and to avoid complexity in the circuit configurations in Fig. 7, it is embedded in a subsystem using Matlab-Simulink with two inputs and eight outputs as the case maybe.

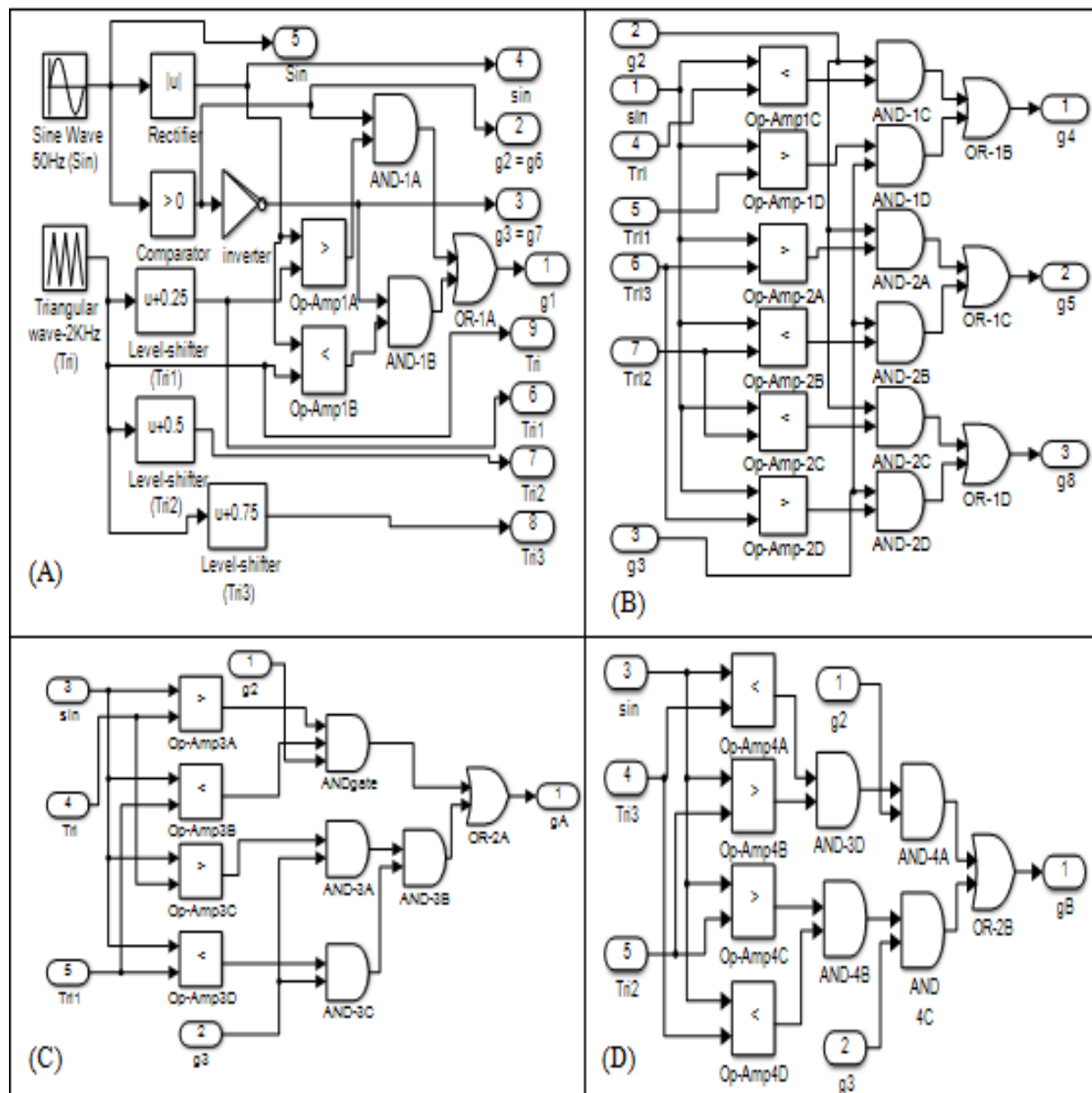


Fig. 7 Logic control circuit for the proposed multilevel inverter topology.

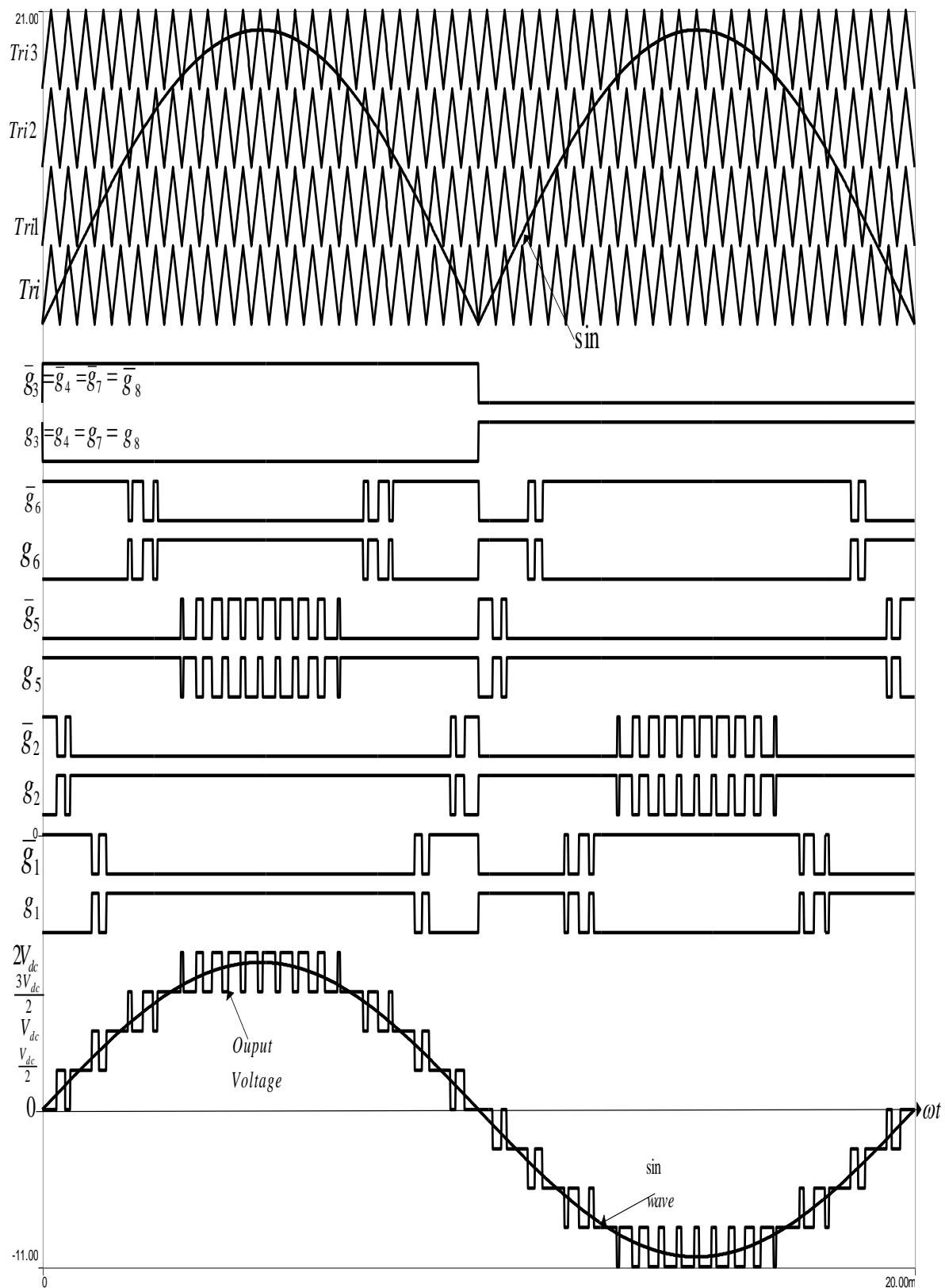


Fig. 5 Switching patterns of the diode clamped single-phase, five-level cascaded multilevel inverter.

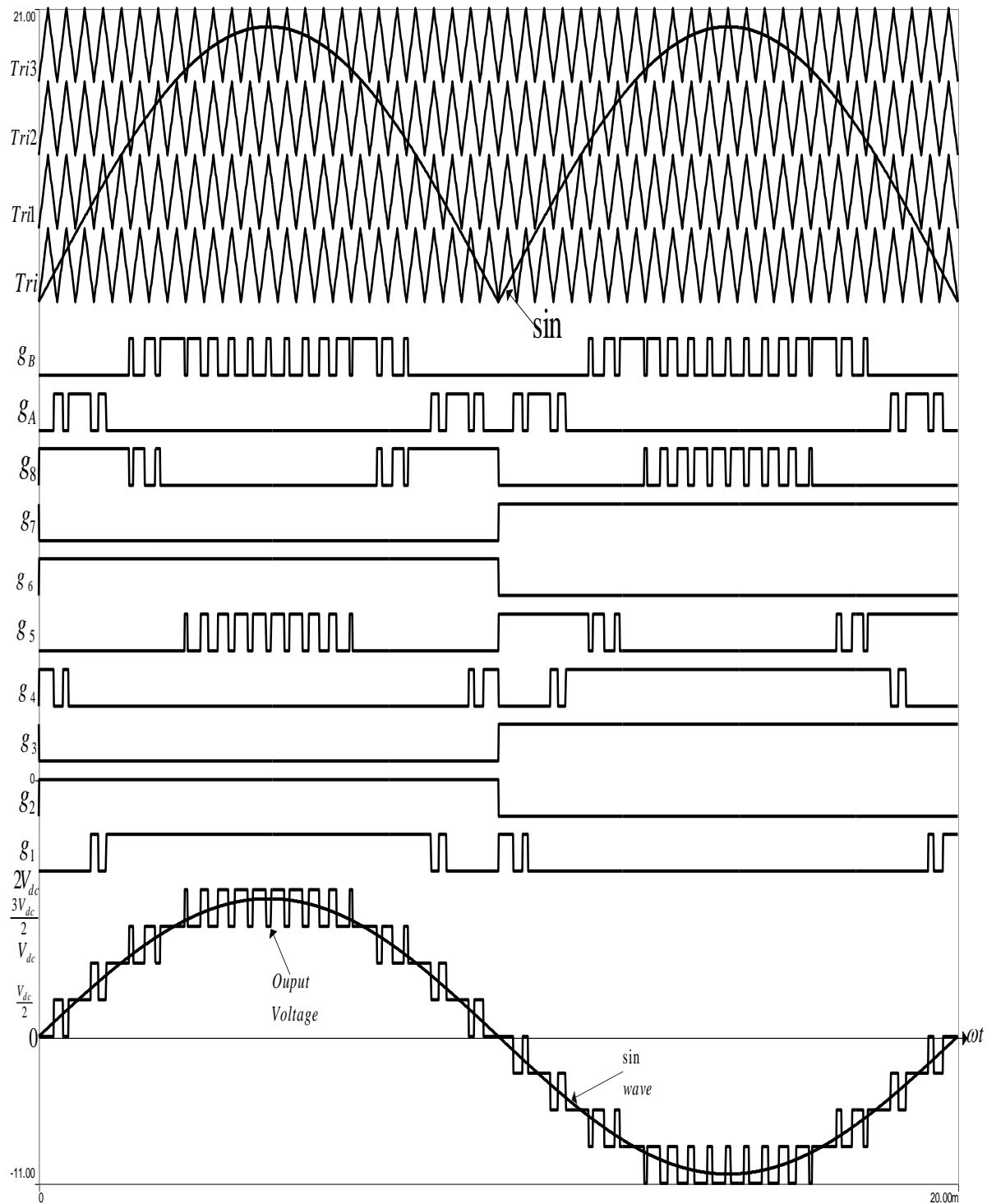


Fig. 6 Switching patterns of the proposed single-phase, five-level hybridised cascaded multilevel inverter.

The output voltage control of inverters requires varying both the number of pulses per half-cycle and the pulse widths generated by modulating techniques. Fig. 8 shows the first quarter of the quarter-wave symmetric waveform with twenty one phase displacement angles. The output voltage contains odd harmonics over a frequency spectrum. Assuming  $a_0 = a_n = 0$ , therefore (35) can be rewritten as (40).

The Fourier series of the periodic function of the output voltage can be expressed as

$$V_o(\omega t) = a_0 + \sum_{n=1}^{\infty} (a_n \cos n\omega t + b_n \sin n\omega t) \quad (35)$$

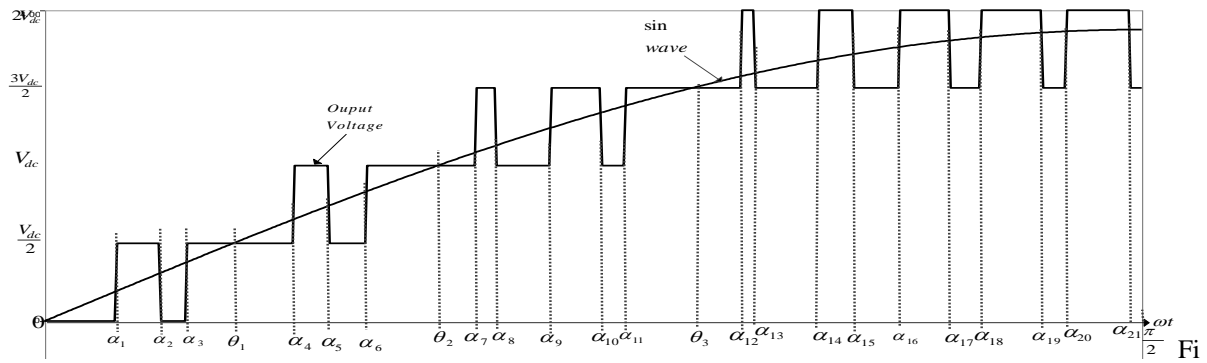


Fig. 8 The first quarter of the quarter-wave symmetric waveform.

At the interval of 0 and  $\theta_1$ , we have

$$f_1(\omega t) = \begin{cases} \frac{V_{dc}}{2}, & \alpha_1 < \omega t < \alpha_2 \\ \frac{3V_{dc}}{2}, & \alpha_3 < \omega t < \theta_1 \end{cases} \quad (36)$$

At the interval of  $\theta_1$  and  $\theta_2$ , we have

$$f_2(\omega t) = \begin{cases} \frac{V_{dc}}{2}, & \theta_1 < \omega t < \alpha_4 \\ V_{dc}, & \alpha_4 < \omega t < \alpha_5 \\ \frac{V_{dc}}{2}, & \alpha_5 < \omega t < \alpha_6 \\ V_{dc}, & \alpha_6 < \omega t < \theta_2 \end{cases} \quad (37)$$

At the interval of  $\theta_2$  and  $\theta_3$ , we have

$$f_3(\omega t) = \begin{cases} V_{dc}, & \theta_2 < \omega t < \alpha_7 \\ \frac{3V_{dc}}{2}, & \alpha_7 < \omega t < \alpha_8 \\ V_{dc}, & \alpha_8 < \omega t < \alpha_9 \\ \frac{3V_{dc}}{2}, & \alpha_9 < \omega t < \alpha_{10} \\ V_{dc}, & \alpha_{10} < \omega t < \alpha_{11} \\ \frac{3V_{dc}}{2}, & \alpha_{11} < \omega t < \theta_3 \end{cases} \quad (38)$$

At the interval of  $\theta_3$  and  $\frac{\pi}{2}$ , we have

$$f_4(\omega t) = \begin{cases} \frac{3V_{dc}}{2}, & \theta_3 < \omega t < \alpha_{12} \\ 2V_{dc}, & \alpha_{12} < \omega t < \alpha_{13} \\ \frac{3V_{dc}}{2}, & \alpha_{13} < \omega t < \alpha_{14} \\ 2V_{dc}, & \alpha_{14} < \omega t < \alpha_{15} \\ \frac{3V_{dc}}{2}, & \alpha_{15} < \omega t < \alpha_{16} \\ 2V_{dc}, & \alpha_{16} < \omega t < \alpha_{17} \\ \frac{3V_{dc}}{2}, & \alpha_{17} < \omega t < \alpha_{18} \\ 2V_{dc}, & \alpha_{18} < \omega t < \alpha_{19} \\ \frac{3V_{dc}}{2}, & \alpha_{19} < \omega t < \alpha_{20} \\ 2V_{dc}, & \alpha_{20} < \omega t < \alpha_{21} \\ \frac{3V_{dc}}{2}, & \alpha_{21} < \omega t < \frac{\pi}{2} \end{cases} \quad (39)$$

$$V_o(\omega t) = \sum_{n=1,3,5}^{\infty} b_n \sin n\omega t \quad (40)$$

Where,

$$b_n = \frac{4V_{dc}}{n\pi} \left[ \int_0^{\theta_1} f_1(\omega t) \sin(n\omega t) d(\omega t) + \int_{\theta_1}^{\theta_2} f_2(\omega t) \sin(n\omega t) d(\omega t) + \int_{\theta_2}^{\theta_3} f_3(\omega t) \sin(n\omega t) d(\omega t) + \int_{\theta_3}^{\pi} f_4(\omega t) \sin(n\omega t) d(\omega t) \right] \quad (41)$$

$$\text{Where } \alpha_1 < \alpha_2 < \alpha_3 < \alpha_4 < \alpha_5 < \alpha_6 < \alpha_7 < \alpha_8 < \alpha_9 < \alpha_{10} < \alpha_{11} < \alpha_{12} < \alpha_{13} < \alpha_{14} < \alpha_{15} < \alpha_{16} < \alpha_{17} < \alpha_{18} < \alpha_{19} < \alpha_{20} < \alpha_{21} < \frac{\pi}{2}$$

Therefore, the coefficient  $b_n$  is given by

$$b_n = \frac{2V_{dc}}{n\pi} \left[ \cos(n\alpha_1) - \cos(n\alpha_2) + \cos(n\alpha_3) + \cos(n\alpha_4) - \cos(n\alpha_5) + \cos(n\alpha_6) + \cos(n\alpha_7) - \cos(n\alpha_8) + \cos(n\alpha_9) - \cos(n\alpha_{10}) + \cos(n\alpha_{11}) + \cos(n\alpha_{12}) - \cos(n\alpha_{13}) + \cos(n\alpha_{14}) - \cos(n\alpha_{15}) + \cos(n\alpha_{16}) - \cos(n\alpha_{17}) + \cos(n\alpha_{18}) - \cos(n\alpha_{19}) + \cos(n\alpha_{20}) - \cos(n\alpha_{21}) - \frac{3}{2} \cos\left(\frac{n\pi}{2}\right) \right] \quad (42)$$

The Higher harmonic contents would be eliminated if

$$b_3 = b_5 = b_7 = b_9 = b_{11} = b_{13} = b_{15} = b_{17} = b_{19} = b_{21} = b_{23} = b_{25} = b_{27} = b_{29} = b_{31} = b_{33} = b_{35} = b_{37} = b_{39} = b_{41} = b_{43} = 0. \quad (43)$$

Solving these equations in equation (43) by iterations using Matlab program, we get  $\alpha_1 = 5.3606^\circ$ ,  $\alpha_2 = 8.0233^\circ$ ,  $\alpha_3 = 10.6585^\circ$ ,  $\alpha_4 = 21.4047^\circ$ ,  $\alpha_5 = 24.0745^\circ$ ,  $\alpha_6 = 26.6632^\circ$ ,  $\alpha_7 = 37.9141^\circ$ ,  $\alpha_8 = 40.1660^\circ$ ,  $\alpha_9 = 43.8252^\circ$ ,  $\alpha_{10} = 48.3582^\circ$ ,  $\alpha_{11} = 50.3648^\circ$ ,  $\alpha_{12} = 50.5074^\circ$ ,  $\alpha_{13} = 50.8514^\circ$ ,  $\alpha_{14} = 62.6155^\circ$ ,  $\alpha_{15} = 64.2135^\circ$ ,  $\alpha_{16} = 69.4697^\circ$ ,  $\alpha_{17} = 72.2154^\circ$ ,  $\alpha_{18} = 76.6397^\circ$ ,  $\alpha_{19} = 80.2819^\circ$ ,  $\alpha_{20} = 84.0820^\circ$ , and  $\alpha_{21} = 88.1564^\circ$ .

#### IV. SIMULATION RESULTS

In order to see the performance of the conventional 5-level cascaded diode clamped and proposed inverter topologies, a MATLAB-SIMULINK software simulation was used. The PWM switching patterns generated aforementioned are used to drive the power switches ( $s_1 - s_8, s_A$  and  $s_B$ ). Dc-source voltage in each cell is 100V, and dividing capacitor value of 3900μF by 50V. An R-L load is connected at the output terminals of the inverter; whose values are 50Ω and 0.05mH, respectively. Figs. 9[a] and 9[b] show the cascaded diode clamped output  $V_{ab}$  and  $V_{cd}$  respectively for two cycles. Thus, Figs. 9[c] and 9[d] depict the inverter output voltage and current respectively. For a modulation index of 0.8, a THD 10.32% is obtained as shown in Fig.10.



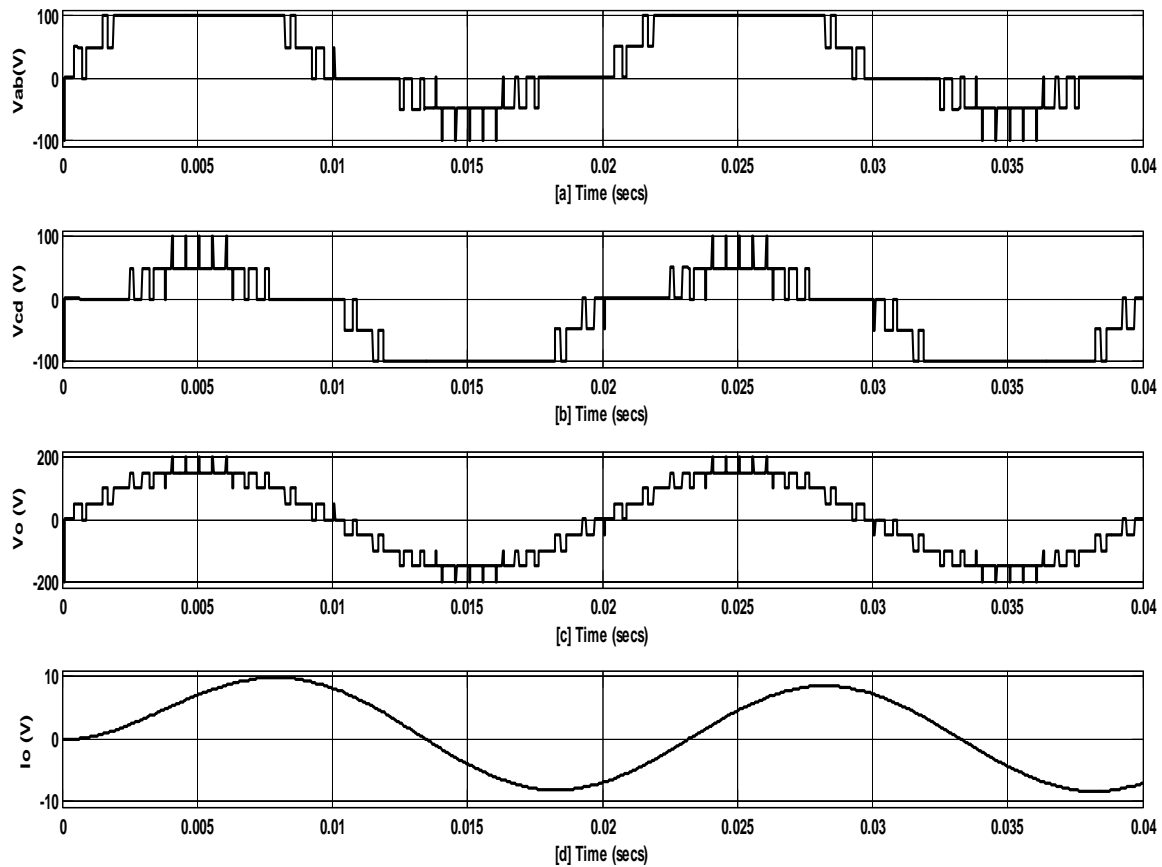


Fig. 9 Simulation result of voltage and current of cascaded diode clamped multilevel inverter.

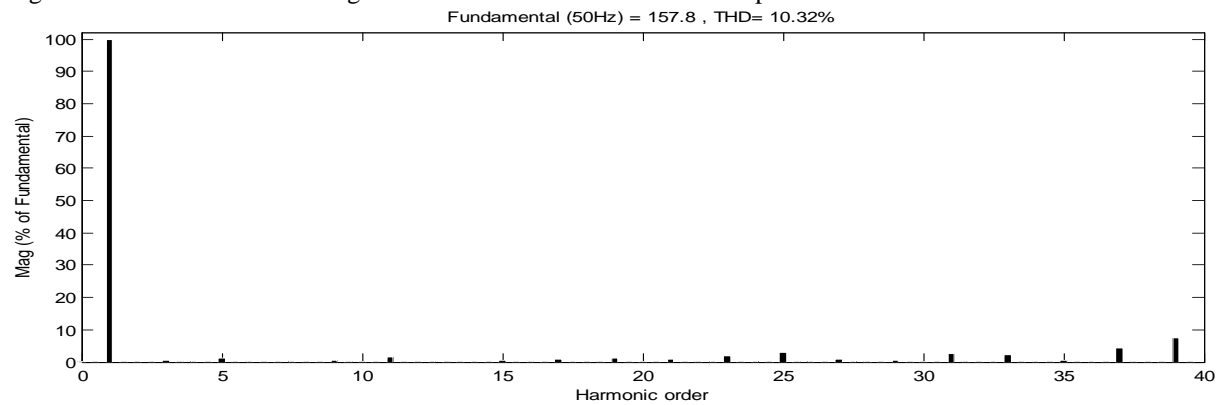


Fig. 10 Harmonic profile of the inverter output voltage for cascaded diode clamped inverter.

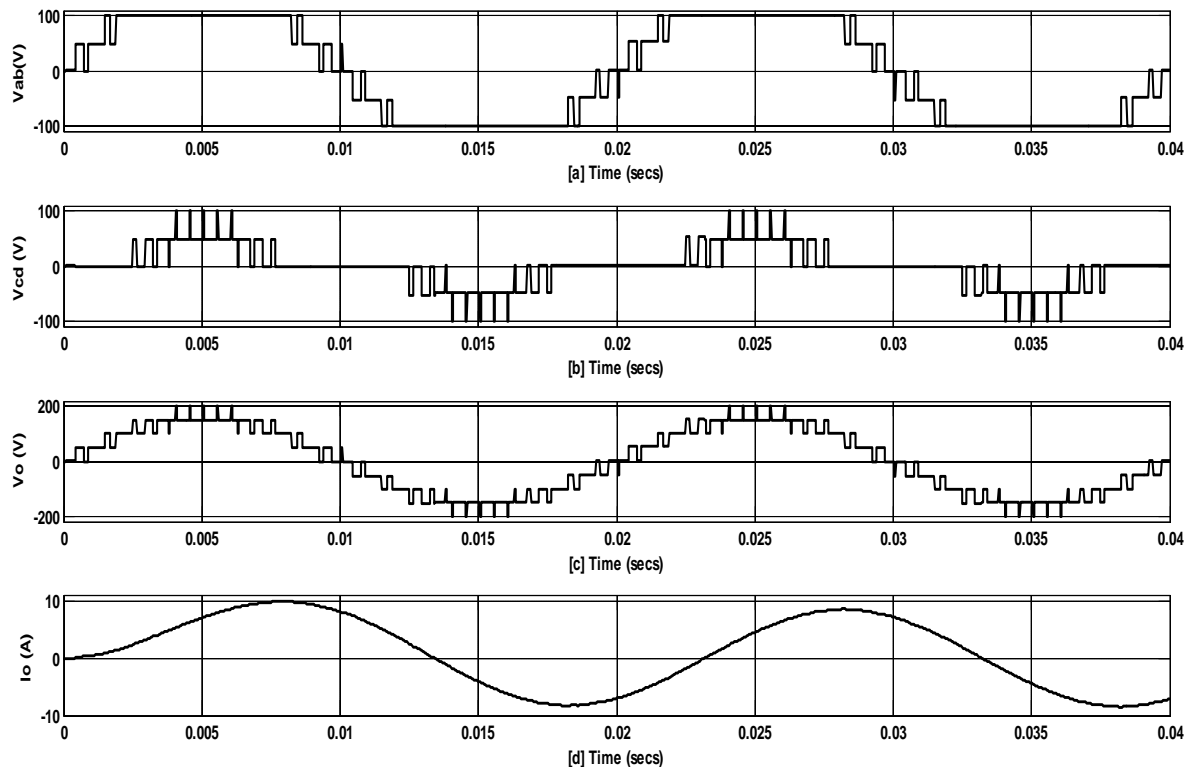


Fig. 11 Simulation result of voltages and current of cascaded proposed multilevel inverter.

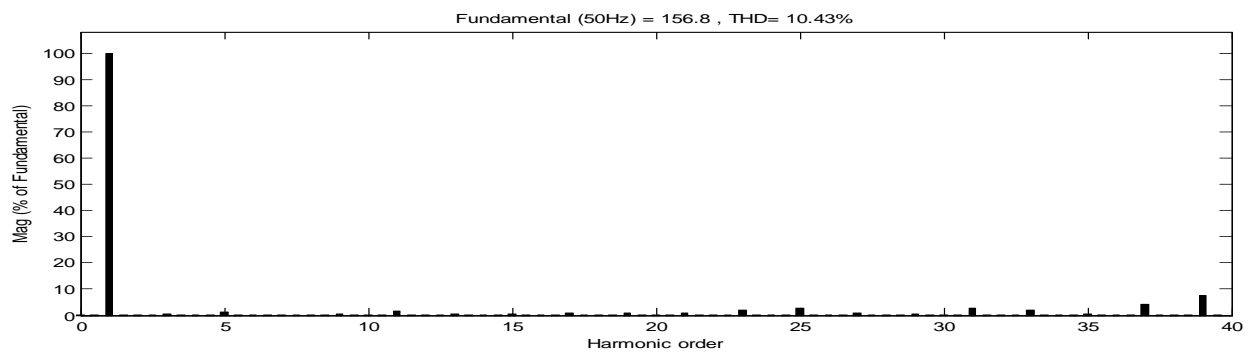


Fig. 12 Harmonic profile of the inverter output voltage for cascaded proposed inverter.

In Figs. 11[a] and 11[b] show the cascaded diode clamped output  $V_{ab}$  and  $V_{cd}$  respectively for two cycles. Thus, Figs. 11[c] and 11[d] depict the inverter output voltage and current respectively. For a modulation index of 0.8, a THD 10.43% is obtained as shown in Fig.12. Table 2 depicts total harmonic distortion comparison between the different cascaded H-bridge and proposed power circuit configurations.

Table 2 Comparison of THD

Cascaded H-bridge Power Circuit Topology	Line-Line Voltage THD (%)
5-Level FLC	14.38
5-Level NPC	10.32
5-Level Proposed	10.43

## V. CONCLUSION

This paper has proposed a hybridised single-phase cascaded multilevel inverter topology using reduced number of power switches. The operational principles, modulation technique and switching functions has been analysed in detail. The desired output voltage form has been obtained at modulation index of 0.8 and frequency index of 40. Also, the per cell output voltage has been obtained through simulation. The proposed topology has a

THD of 10.43% in the output voltage waveform. The modulation approach and the proposed power circuit configuration adopted in this work will contribute immensely in reducing the power inverter cost and weight.

### REFERENCES

- [1] S. Ali Khajehoddin, Praveen Jain, and Alireza Bakhshai, "Cascaded multilevel Converters and Their Applications in Photovoltaic Systems" 2<sup>nd</sup> Canadian Solar Buildings Conference Calgary, June 10-14, 2007. Pp 1-6.
- [2] C. I. Odeh and D. N. Nnadi "Hybrid PWM Scheme for Cascaded Capacitor-Clamped Multilevel Inverter" A paper presented at the International Conference on Electric Power Engineering, held at final year Electrical class, University of Nigeria, Nsukka. (ICEPENG 2015) Oct 14<sup>th</sup>-Oct 16<sup>th</sup> 2015, Pp 119-125.
- [3] R.S. Kanchan, P. N. Tekwani, M. R. Baiju, K. Gopakumar and A. Pittet, "Three-Level Inverter Configuration with Common-Mode Voltage Elimination for Induction Motor Drive".
- [4] R. Senthilkumar and Jovitha Jerome "A Novel Cascaded Multilevel Inverter for High Power UPS Application", European Journal of Scientific Research, ISSN: 1450-216X vol. 60 No. 2 (2011), pp. 207-223.
- [5] J. I. Jithin and A. B. Sathish Raj "A New Topology for A Single Phase 21 Level Multi Level Inverter Using Reduced Number of Switches" International Journal of Engineering Research & Technology (IJERT) ISSN: 2278-0181 vol. 2 Issue 2, February-2013.
- [6] Charles I Odeh, Damian B. N. Nnadi "Single-Phase 9-Level Hybridised Cascaded Multilevel Inverter", The Institution of Engineering and Technology Power Electron., 2013, pp 1-10.
- [7] Y. Xue, L. Chang, S. B. Kjaer, J. Bordonam and T. Shimiza, "Topologies of Single-Phase inverters for small distributed power generators: an overview," IEEE Transactions on power electronics, vol. 19, no 5, pp. 1305-1314, sept. 2004.
- [8] T. Prathiba, and P. Renuga "A comparative study of Total Harmonic Distortion in Multilevel Inverter Topologies", Journal of information engineering and Applications, ISSN 2224-5782(print) vol 2, No.3, 2012.
- [9] Nasrudin A. Rahim, Krishnamadana Chaniago and Jeyraj Selvaraj "Single-Phase Seven Grid-Connected Inverter for Photovoltaic System", IEEE Transactions on Industrial Electronics, vol. 58, No. 6, June 2011, pp. 2435-2443.
- [10] S. Mekhilef and A. Masaoud, "Xilinx FPGA Based Multilevel PWM Single Phase Inverter", Online at <http://ejum.fsktm.um.edu.my>, vol. 1, No. 2, December 2006 pp 40-45, 2006 Engineering e-Transaction, University of Malaya.

## Minimizing Corona on Power Distribution Lines Using Optimization by Graphical Method

Osita Oputa

Department of Electrical/Electronic Engineering , Michael Okpara University of Agriculture.

**Abstract** – Each time Corona phenomenon occur in a transmission or distribution line, it result a high power loss, hence reducing transmission efficiency and profitability in electricity business. It may be practically impossible to eradicate these corona losses, however, efforts must be made towards minimizing its occurrences. Research has proven that increasing the spacing of the three phase in power transmission lines reduce the effect of corona. However, increasing the phase spacing increases the line inductance and hence the reactive power loss along the line which may cause low voltage (or voltage instability) at load centers. This paper will find the exact spacing between conductors of the three phases at which the corona losses will be minimal and at the same time the reactive power lost due to the inductance caused by the spacing will not exceed recognized standard. A cable/conductor sizes of  $150\text{mm}^2$  will be analyzed will be used in the analysis; on using a  $150\text{mm}^2$  size of cable for transmitting 7.5MVA, a conductor spacing of 87cm was found to be the best with corona loss of 2.80kVA/km and a corresponding reactive power loss of 5.28kVA/km. Further increase in conductor spacing will although reduce corona lost, the corresponding reactive power lost will be beyond the acceptable limit.

**Key Words:** minimizing corona power lines.

### NOMENCLATURE

$L_c$	Corona Power Loss (kW/km/Phase)
$Q_c$	Corona Power Loss (kVA/km/Phase)
$Q_{CT}$	Total Corona Power Loss in all 3- $\phi$ (kVA/km)
$Q_L$	Line Reactive Power Loss (kVA/km/Phase)
$f$	Supply Frequency (50Hz)
$r$	Radius of conductor (cm)
$d$	Mean Geometrical Distance Between Conductors of Different phases (cm)
$I_L$	Line Current (A)
$X_L$	Total Line Reactant ( $\Omega$ )
$R_L$	Total Line Resistance ( $\Omega$ )
$V_{ph}$	r.m.s Value of the Phases Voltage (kV)
$V_{cc}$	Corona Critical Voltage.
$L_R$	Red Phase Inductance (H/km)
$L_Y$	Yellow Phase Inductance (H/km)
$L_B$	Blue Phase Inductance (H/km)
$L$	Total Length of Line
$\delta$	Relative air density

### I. INTRODUCTION

Whenever there is a potential difference (PD) between conductors of different phases spaced apart by a distance far greater than the conductor's diameter, it causes the air surrounding the conductors to be under electrostatic stress. If the PD is increased continually, at a certain voltage, a visible faint luminous glow of violet color is observed along with a hissing noise, this phenomenon is known as corona [1], [2]; this is accompanied by the

production of ozone gas. This phenomenon is as a result of the insulation breakdown of the air surrounding the conductors. This corona effect or phenomenon is affected by factors that range from working voltage, whether conditions, conductor sizes and the spacing between the conductors of the different phases. Evidence has shown that corona is associated with the following

1. Electric power losses (which depend on the weather condition)
2. Formation of ozone gas which can react with bar conductors causing corrosion.
3. An irregular waveform voltage drop which may cause some interference with nearby communication lines [3].

As a result of these effects associated with this corona phenomenon, efforts must be made to reduce their rate of occurrence and the magnitude of the corona whenever it occurs. Different methods that can be employed to do this include

1. Increasing the spacing between the conductors of the different phases.
2. Using conductors with large diameters.
3. Using bundled conductors.

This paper shall concentrate on the first method of reducing corona. However, the spacing between the conductor must be done with caution; this is because a high the conductor spacing results high inductance of the phases. This high inductance can result high power losses along the line. Hence, a best spacing between the conductors shall be obtain; this spacing shall be at the point or distance where corona is minimum and at the same time the line power loss will also be minimal.

## II. MODEL FORMULATION

Corona shall be minimized by minimizing the corona power loss (objective function) subject to certain constraint.

### 2.1 OBJECTIVE FUNCTION

Of all the effects of corona, the power loss experience after the occurrence of corona can be easily quantify; hence, we can try to minimize the power loss with its occurrence subject to certain constrains. The power loss due to corona during a fair weather is given by

$$L_c = \frac{241}{\delta} (f + 25) \left[ \sqrt{\frac{r}{d}} \right] [V_{ph} - V_{cc}]^2 \times 10^{-5} \quad (1)$$

Where

$$V_{cc} = 21.26 r \log_{\frac{d}{r}} \times m_1 m_2 \quad (2)$$

$$\delta \approx 1, \quad m_1 \times m_2 = 1. \quad (\text{Source [3]})$$

Thus, the reactive power part of the corona loss is

$$Q_c = \frac{241}{\delta} \times \tan(\cos^{-1} p.f) (f + 25) \left[ \sqrt{\frac{r}{d}} \right] [V_{ph} - V_{cc}]^2 \times 10^{-5} \quad (3)$$

Assuming the same phase conduction for all phases, the total reactive power loss for the three phase is

$$Q_{cT} = \frac{3 \times 241}{\delta} \times \tan(\cos^{-1} p.f) (f + 25) \left[ \sqrt{\frac{r}{d}} \right] [V_{ph} - V_{cc}]^2 \times 10^{-5} \quad (4)$$

We can minimize corona from eqn (4) by finding an optimal value of 'd', and 'r' for which corona will be minimal. This paper shall concentrate on finding the optimal 'd' while treating 'r' as a constant as only  $150 \text{ mm}^2$  cable is use for transmission lines.

### 2.2 CONSTRAINT FUNCTION

IEE and other standard gave a maximum allowable voltage drop of 5% - 7% of working voltage along the line; but this research shall use 5%. Hence, the maximum allowable power loss is  $[5\%] I_L V_{ph}$  per phase. But voltage drop along the line is  $I_L (R_L + jX_L)$ . Therefore,

$$Q_L = I_L^2 (R_L + jX_L) \quad (5)$$

The line to neutral inductance for the red, yellow and blue phases of a 3 phase line are respectively

$$L_R = 2 \times 10^{-4} \left[ \ln \frac{1}{r} + 0.3466 - j0.6 \right] \quad (6)$$

$$L_Y = 2 \times 10^{-4} \ln \frac{d}{r} \quad (7)$$

and

$$L_B = 2 \times 10^{-4} \left[ \ln \frac{d}{r} + \frac{1}{2} \ln 2 + j 0.866 \ln 2 \right] \quad (8)$$

Considering the yellow phase alone for simplicity,  $X_L = 2\pi fL$ ,

$$Q_L = I_L^2 X_L \quad (9)$$

Assuming the current that flow in the 3 lines are the same, total line reactive power loss incurred in the 3-Ø is

$$Q_{LT} = 2\pi f \times I_L^2 [L_R + L_Y + L_B] \quad (10)$$

Minimizing corona can therefore be done by minimizing Eqn (4) subject to Eqn (10).

### III. SYSTEM ANALYSIS

For this research, our analysis will consider a short line of about 24km, 33kV distribution line that feeds 7.5MVA substation at a power factor of 0.9 with an approximate current of 132A flow in each line; (a sub-circuit of Umuahia distribution circuit in Abia State, Nigeria). Information got Enugu Electricity Distribution Company (EEDC) is that the size of conductor used for that circuit is 150mm<sup>2</sup> ( $r = 0.70\text{cm}$ ) but we shall also extend our analysis to using 100mm<sup>2</sup> ( $r = 0.56\text{mm}$ ) cable size.

For simplicity, we take the yellow phase into consideration alone.

$$V_{ph} = \frac{33\text{kV}}{\sqrt{3}} = 19.052\text{kV}$$

For a 150mm<sup>2</sup> cable

Eqn (3) can becomes

$$Q_c = 0.0735[d]^{-1/2} [19.052 - 1.1872 \times 10^{-4} \ln d]^2 \quad (11)$$

The plot of  $Q_c$  against  $d$  from 50cm to 150cm is given in fig 1.

Also, from Eqn (9), the reactive power loss in the yellow phase is

$$Q_L = 132^2 \times [6.28 \times 10^{-5} \ln d + 2.2419 \times 10^{-5}] \quad (12)$$

The plot of  $Q_L$  against  $d$  also from 50cm to 150cm is given in fig 2 below.

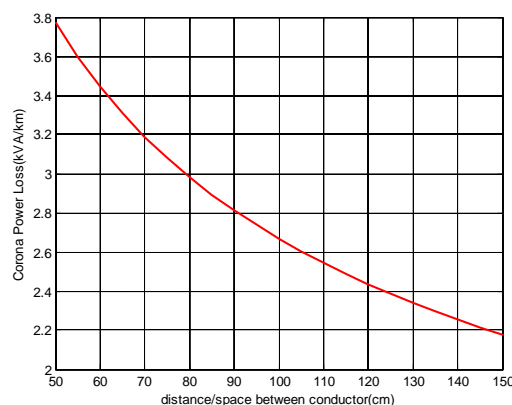


Fig 1.



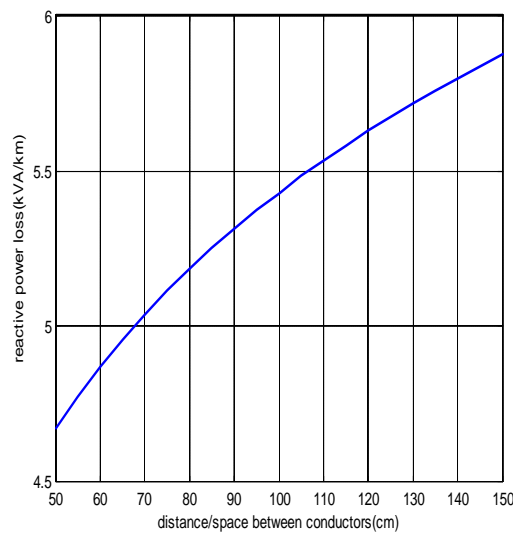


Fig 2

IEEE standard says a maximum of 5% voltage drop can be tolerated. Hence, a voltage drop of 0.21% can be tolerated for the line under analysis.

Form IEEE standard, in each phase the receiving end voltage must not drop below  $[V_{ph} - IX_{LR} \leq 0.21\% V_{ph}]$ ; multiplying both sides of the inequality by the line current  $I_L$ , it means that the reactive power loss must not exceed  $0.21\% V_{ph} \times I_L = 0.21\% \times \frac{33}{\sqrt{3}} \times 132$  this will represent extreme condition.

Combing the two plots on one plane and taking into account the extreme condition. The plot is given below.

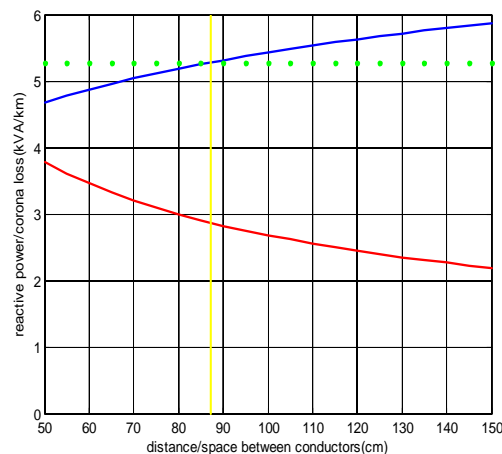


Fig 3.

#### KEY ON PLOTS

- RED: Corona Reactive Power Loss  
 BLUE: Reactive Power Loss Due to  $I_L^2 \times X_{LN}$   
 GREEN: Boundary or Extreme Point

For a 100mm<sup>2</sup> cable

The objective function is

$$Q_c = 0.0657[d]^{-1/2}[19.0519 - 9.4976 \times 10^{-5} \ln d]^2 \quad (13)$$

The constraint is given below

$$Q_L = I^2[6.28 \times 10^{-5} \ln d + 3.6424 \times 10^{-5}] \quad (14)$$

The plot of corona loss ' $Q_c$ ' and reactive power loss due to  $I_L^2 \times X_L$  against ' $d$ ' for  $d$  between 50cm to 150cm are shown in figures 4 and 5 respectively.

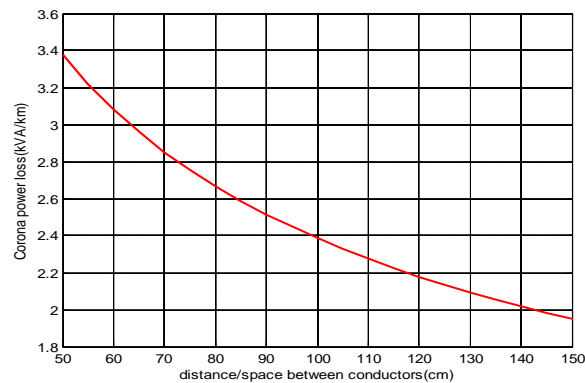


Fig 4

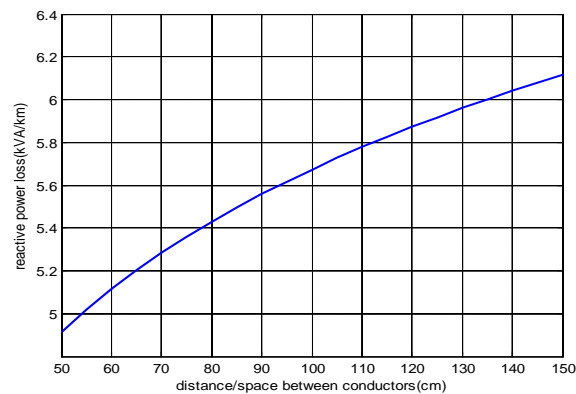


Fig 5

Again, combining the 2 graphs on the same plane and taking into account the extreme condition. The plot is given below

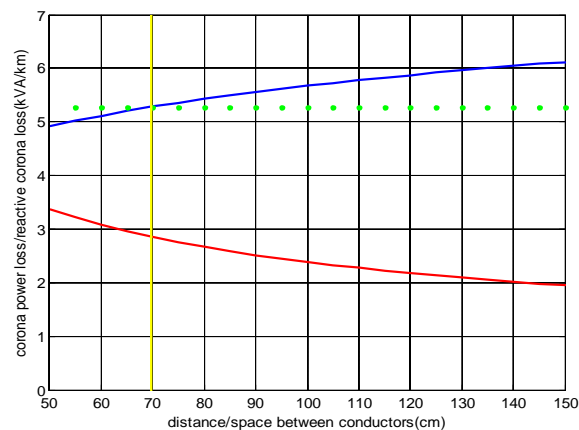


Fig 6

The tabulation of the results got from the graphs of different sizes of conductors is shown on table 1.

TABLE 1

Conductor sizes ( $\text{mm}^2$ )	Optimal Distance between conductors (cm)	Corona Loss $Q_c$ (kVA/km)	IEEE maximum allowable reactive power loss ( $\text{kVA/km}$ )= $0.21\%V_{ph}I$
150	87.20	2.80	5.28
100	69.90	2.78	5.28

#### IV. DISCUSSION OF RESULT

When using  $150\text{mm}^2$  cable, as seen from figure 3, a reactive power of  $4.7\text{kVA/km}$  will be lost in the line when a spacing of 50.0cm between the conductor (phases) is used. This reactive power loss increases as the spacing between conductors is increased as seen from the graph (the blue curve). However, with that 50cm spacing between the conductors,  $3.75\text{kVA/km}$  will be lost due to corona and this decreases as the spacing is increased (the red curve). This means that the minimal corona loss can be obtain by using a spacing of 150cm. But note that a spacing of 150cm will give raise to a reactive power lost of  $5.8 \times \text{kVA/km}$  in the line. Here corona power loss is less but with a higher reactive power loss compared to using a smaller value of spacing of conductor. Using the recommended allowable voltage drop per kilo meter and considering the line current flowing, the maximum reactive power that can be lost in the line is  $5.28\text{kVA/km}$  (this is shown in the green dotted line). This means that the spacing used should not give rise to more than the recommended reactive power lost per kilometer in the line (from the recommended voltage drop per kilo meter). This is shown on the graph at  $d = 87.20\text{cm}$ .

When using  $100\text{mm}^2$  cable, figure 6 shows that a reactive power of  $4.9\text{kVA/km}$  will be lost in the line when a spacing of 50.0cm between the conductor (phases) is used. However, with that 50cm spacing between the conductors,  $2.80\text{kVA/km}$  will be lost due to corona and this decreases as the spacing is increased (the red curve). This means that the minimal corona loss can be obtained by using a spacing of 150cm. But note that a spacing of 150cm will give raise to a reactive power lost of  $6.15\text{kVA/km}$  in the line. Here corona power loss is less but with a higher reactive power loss compared to using a smaller value of spacing of conductor. Using the recommended allowable voltage drop per kilometer and considering the line current flowing, the maximum reactive power that can be lost in the line is  $5.28\text{kVA/km}$  (this is shown in the green dotted line). This means that the spacing used should not give rise to more than the recommended reactive power loss per kilometer in the line (from the recommended voltage drop per kilometer). This is shown on the graph at  $d = 69.90\text{cm}$ .

#### V. CONCLUSION

It has been observed that the spacing between conductors of a three phase transmission or distribution line can be used to control the corona loss of the line. This research has shown that the higher the spacing of the conductors, the reduced corona loss in the power line, but the higher the line inductance and consequently, the higher the reactive power lost. To find the best spacing between the conductors of the phases means finding a balance between the corona lost and reactive power lost. This reactive power lost also depends on the line current which is a function of the power being transmitted or distributed. Using the guide (IEEE Regulation) that the lost in voltage along the line should not exceed 0.21% of phase voltage per kilometer for a short line, and with a certain line current  $I_L$  flowing, this means that the lost in power for a short line should not exceed  $0.21\%V_{ph} \times I_L$  (VA). It is on this basis that we find the best distance between conductor phases for any system. The size of conductor or cable used in the power line also affects the best spacing of the phases of the conductor.

#### VI. RECOMMEDATION

On designing any transmission or distribution line, the method used in the analysis of this research should be adopted to minimize corona losses that may result.

#### REFERENCES

- [1] D.V Razevig and M.P. Chourasia. "High voltage Engineering" Khana Publishers, Delhi – 110006. (2007). pp 115-149.
- [2] Rakosh Das Begamudre. "Extra High Voltage AC Transmission Engineering". New Age International Publishers, Delhi. (2008). pp 113 – 137.
- [3] J. B. Gupta. "A Course in Power Systems" S. K. Kataria and Sons, Delhi -110006. (2007). pp 100 – 112.
- [4] Lo K.L. and Gers J.M. "Feeder Reconfiguration for Losses Reduction in Distribution Systems". Journal of Academic Research, Colombia. (2006). pp 241 – 252.

- [5] Abdullah N.R.H., Ismail M. and Mohammad M.O. "Transmission Loss Minimization and Power Installation Cost using Evolutionary Computation for Improvement of Voltage Stability". Proceedings of the 14th International Middle East Power Systems Conference, Cairo, Egypt. (2010). pp 825 - 830.
- [6] James A. M. (2005): Electric Power System Applications of Optimization. McGraw-Hill Company Ltd., New York. (2005). pp 86 – 102.
- [7] Moghadam M. F. and Berahmandpour H. A. "A New Method for Calculating Transmission Power Losses Based on Exact Modeling of Ohmic Loss". 25th International Power Conference, Iran, 10-E-PTL-2297. (2010). pp 1 - 6.
- [8] Marwan M. M. and Imad H.I. "Power Losses Reduction in Low Voltage Distribution Networks by Improving the Power Factor in Residential Sector" Pakistan Journal of Applied Sciences, 2(7), (2002). pp 727 - 732.
- [9] Numphetch S., Uthen L., Umaporn K., Dusit U. and Thanatchai K. "Loss Minimization Using Optimal Power Flow based on Swarm Intelligences". ECTI Transactions on Electrical, Electronic and Communication Engineering, 9(1). (2011). pp 212 - 222.
- [10] K. A. Stroud. "Advance Engineering Mathematics". Palgrave Macmillan, New York, U.S.A. (2011). pp 1014 – 1021.
- [12] Kreyszig Erwin. "Advanced Engineering Mathematics". Wiley John and Sons (Asia) Pte Ltd. (2011). pp 948 – 970.
- [13] B. R. Gupta "Power system analysis and design" S. Chand, New Delhi, (2007). pp 134 – 143.
- [14] Lee K.Y., Ortiz J.L., Park Y.M. and Pond L.G. "An Optimization Technique for Power Operation". IEEE Transaction on Power Systems, 1(2), (1986). pp 153-159.
- [15] International conference on Large High Voltage Electric System (CIGRE), "Interference Produced by Corona Effect on Electric Systems, Paris, 1974.
- [16] Ramesh L., Chowdhury S.P., Chowdhury S., Natarajan A.A. and Gaunt C.T. "Minimization of Power Loss in Distribution Networks by different Techniques". International Journal of Electrical Power and Energy Systems Engineering, 2(1), (2009). pp 1 - 6.
- [17] Thabendra, T., Yaw, N., Sanjeev, K.S., Bhuvana, R., & David, A.C. "Multi-Objective Optimization Methods for Power Loss Minimization and Voltage Stability", Journal of Advanced Power Systems, 9(2), (2009). pp 1 - 10.
- [18] Onohaebi O.S. and Odiase O.F. "Empirical Modelling of Power Losses as a Function of Line Loadings and Lengths in the Nigeria 330KV Transmission Lines". International Journal of Academic Research, 2(3), (2010). pp 47 - 53.

## Sequential Extraction Analysis of Cu, Pb, Ni and Zn in Cereals and Soils

Mohammed, S.S., Abdullahi, M.A. and Imam, M. M.

*Department of Applied Science College of Science and Technology*

*Kaduna Polytechnic, Kaduna – Nigeria*

*Mohammed, S.S., Department of Applied Science, College of Science and Technology Kaduna Polytechnic, Kaduna – Nigeria.*

**Abstract:** The estimation of Cu, Pb, Ni and Zn in guinea corn, maize and soil sample from Kaduna metropolis, Nigeria was carried out. The objective of the study was to determine the bioavailable Cu, Pb, Ni and Zn in guinea corn, maize and soil samples by flame Atomic absorption spectrometry (FAAS) using sequent extraction techniques. The concentrations of the metals in the cereals and soils vary from one sampling site to another. The t-test  $p = 0.000 < 0.05$  for Ni, Cu, Zn and Pb respectively indicated a significant difference between the concentrations of metals in maize and guinea corn for all the four types of metals. It showed that maize contains more Ni than guinea corn contained more Zn than in guinea corn with a mean of 166.99mg/kg against 5.42mg/kg. Maize contained more than guinea corn with a mean of 37.62mg/kg against 3.17mg/kg. On the other hand, it showed that guinea corn contained more Cu than maize with a mean of 46.2mg/kg against 21.88mg/kg. Similarly, it showed that maize soil contained about ten times more Ni than guinea corn soil with a mean of 38.23mg/kg against 3.91mg/kg. It also showed that maize soil contained more Zn than guinea corn soil contained more Pb than guinea corn soil with a mean of 28.57mg/kg against 3.32mg/kg. The test also indicated that the guinea corn contained more Ni than Cu with a mean of 28.45mg/kg against 3.68mg/kg.

**Keywords:** Sequential extraction, bioavailability, AAS, guinea corn, maize.

### I. INTRODUCTION

Heavy metals occur in soils of the world and are essential to plants and animals. We ingest them through food, water and air. Their concentrations are usually low and hazardous with little or no environmental disturbance<sup>[1]</sup>. Most heavy metals remain in the soil nearly indefinitely as soils have long memories and do not degrade them. Runoffs as well as dust falls can result in accumulation in the roadside dusts/soils at levels that are toxic to organisms in the surrounding environments. These heavy metals remain bound to organic matter unless they are remobilized as windblown dust<sup>[2]</sup>. Living organisms require trace amounts of some metals like, cobalts, copper and zinc but their excess levels can be detrimental<sup>[3]</sup>. Other heavy metals such as mercury, lead and cadmium have no known or beneficial effects on organisms and their accumulation overtime in the bodies of mammals can cause illness<sup>[3]</sup>.

The tetra alkyl lead accounts for 20% of lead used by mankind and accounts for the main environmental lead pollution problem. Street dusts and roadside soils on busy streets may contain Pb in the range of 1000 to 4000mgKg<sup>-1</sup><sup>[4]</sup>. Other sources of Pb would be attributed to mining and smelting of the ores, effluent from storage battery industries, emissions from automobiles exhausts<sup>[1]</sup> lead, affects every organ system in the body. It is absorbed into the body and distributed to the blood, soft tissue and bones<sup>[5]</sup>.

Municipal refuse, automobiles and agricultural use of pesticide and fungicides containing ZnSO<sub>4</sub> are sources of Zn environmental pollution<sup>[6]</sup>. Zinc influences growth rate and bone development, the integrity of the skin, the development and function of the reproductive organs. It also helps in wound healing capacity<sup>[1]</sup>.

The sources of nickel pollution are the air borne effluent from industrial units, emission of nickel into the atmosphere by the burning of fossil fuels and other anthropogenic practices<sup>[7]</sup>. Initial symptoms of toxicity due to nickel are nausea, dizziness, headache, chest pain, etc<sup>[7]</sup>.

Iron and steel industries, fertilizer industry, burning of wood, disposal of municipal and industrial wastes are some of the sources of copper pollution<sup>[8]</sup>. Defects in pigmentation, bone formation, reproduction, myelin of the spinal cord, cardiac function and connective tissue formation are manifestations of copper deficiency<sup>[8]</sup>.

In this research, Cu, Pb, Ni and Zn concentrations in guinea corn and maize samples were analyzed. The concentrations of these metals in the corresponding soil samples in the cereals were extracted using the chemical reagents such as the mixture of  $\text{HNO}_3/\text{H}_2\text{O}_2$ ;  $1.0\text{mol L}^{-1}$  oxalic acid,  $0.05\text{mol L}^{-1}$  EDTA and  $1.0\text{mol L}^{-1}$  acetic acid. The relation between the concentrations of these metals in the cereals and soil samples was also investigated.

## II. MATERIALS AND METHODS

A flame atomic absorption spectrophotometer model 8010 Young Lin was used for Cu, Pb, Ni and Zn determinations. In the extraction procedures,  $1.0\text{mol L}^{-1}$  oxalic acid,  $0.05\text{mol L}^{-1}$  EDTA and  $1.0\text{mol L}^{-1}$  acetic acid were used.

### Preparation of Samples:

The research covered seven agricultural sites in Kaduna, Nigeria. The sites are: Nasarawa (NS), Sabon Tasha (ST), Unguwar Mu azu(UM), Tudun Wada (TW), Kakuri (KK), Mando (MD), Kabala West (KB) and Kachia (KC). The samples were collected during the harvest season ( Oct- Nov., 2008, 2009 and 2010). The soil samples were collected from the different areas enumerated at a depth of about 10cm below the surface<sup>[9]</sup>. The guinea corn and maize samples were collected at each of the locations. Guinea corn and maize samples were chosen for the purpose of this research work as they are the staple food being produced and consumed in these areas, Kachia. A town situated about 130km away from Kaduna was taken as a control, (Fig. 1). The cereals were thoroughly washed with water and allowed to drain on a filter paper. Both the cereal and soil samples were dried at  $85^\circ\text{C}$ . All the analysis were carried out in the Analytical Laboratory of Department of Applied Science, College of Science and Technology, Kaduna Polytechnic, Kaduna-Nigeria.

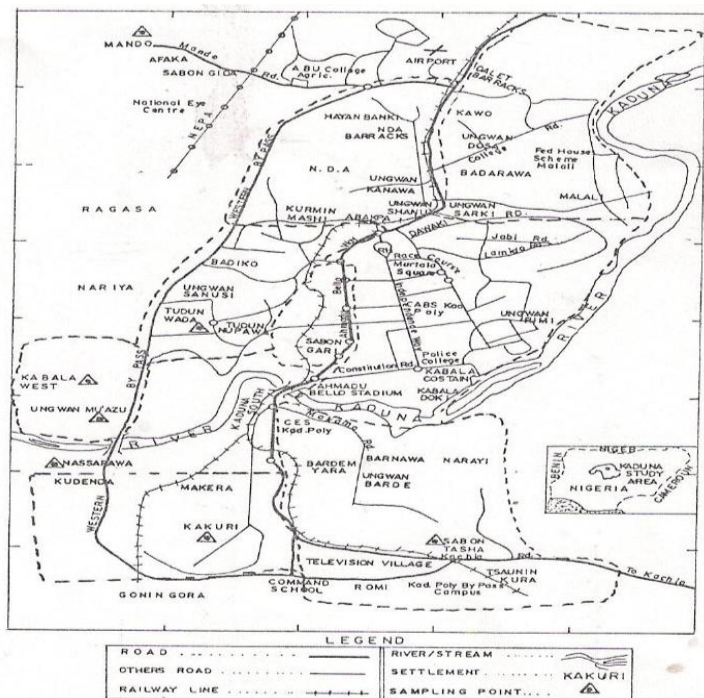


Fig. 1: Map of Kaduna Metropolis showing the sampling locations

### Wet ashing of Cereals:

Five(5)g each of oven dried guinea corn and maize samples were accurately weighed into an evaporating dish and a steel at  $480^\circ\text{C}$  in an ashing furnace for 4h. Ten  $\text{cm}^3$  of a mixture of nitric acid- hydrogen peroxide (2+1) was added to the ashed sample and dried with occasional shaking on a hot plate and cooled,  $4\text{cm}^3$  of  $1.5\text{mol L}^{-1}$  nitric acid was then added and centrifuged sixty  $\text{cm}^3$  water was added to the clear digest and was filtered. This was analysed for Cu, Pb, Ni and Zn, using FAAS model 8010 Young Lin. A blank digest was carried out in the same way.



**Digestion and extraction:**

A modified sequential extraction method <sup>[10]</sup> developed by Yaman was used <sup>[9]</sup>. Ten cm<sup>3</sup> of a mixture of nitric acid-hydrogen peroxide (2+1) was added to 5g of soil sample and dried with occasional shaking on a hot plate and cooled. Four cm<sup>3</sup> of 1.5mol L<sup>-1</sup> nitric acid was added to the remainder, centrifuged and diluted to 60cm<sup>3</sup> with water and filtered. The clear digest was analysed for Cu, Pb, Ni and Zn. Using FAAS model 8010 Young Lin. A blank digest was carried out in the same way. Soil extracts were obtained by shaking separately, 5g of soil samples with 10cm<sup>3</sup> of 0.05mol L<sup>-1</sup> EDTA (for carbonate and organically bound phase), 1.0mol L<sup>-1</sup> oxalic acid (for oxide phases) and 1.0mol L<sup>-1</sup> acetic acid (for carbonate phases). The mixture was evaporated with occasional shaking on a hot plate. Four cm<sup>3</sup> of 1.5mol L<sup>-1</sup> nitric acid was added to the remainder and centrifuged. The digest was diluted to 60cm<sup>3</sup> with water and filtered and then analyzed for Cu, Pb, Ni and Zn using FAAS model 8010 Young Lin. A blank digest was carried out in the same way.

**III. RESULTS AND DISCUSSION****Metal content in cereals and soils**

The metal content in cereals and soils vary from one sampling site to another. Some sampling sites had higher concentration of the metal in cereals than the corresponding soils, while in others, the concentration of the metals was higher in the soils than the corresponding cereals. The copper and nickel contents of the soils from some of the sampling locations were above the tolerable limit. The higher concentrations of these metals in the areas could pose a problem to plant nutrition and food chain. Thus, constituting a direct health hazard <sup>[11]</sup>.

The t-test  $p = 0.000 < 0.05$ , for Nickel, Copper, Zinc and Lead respectively indicated a significant difference between the concentration of metals in maize and guinea corn for all the four types of metals. It showed that maize contains more Nickel than guinea corn with a mean of 43.24 mg/kg against 2.87 mg/kg. Similarly, maize contained more Zinc than in guinea corn with a mean of 166.99 mg/kg against 5.42 mg/kg. Maize contained more Lead than guinea corn with a mean of 37.62 mg/kg against 3.17 mg/kg. On the other hand, it showed that guinea corn contained more Copper than maize with a mean of 46.21 mg/kg against 21.88 mg/kg (Figs. 2 and 3).

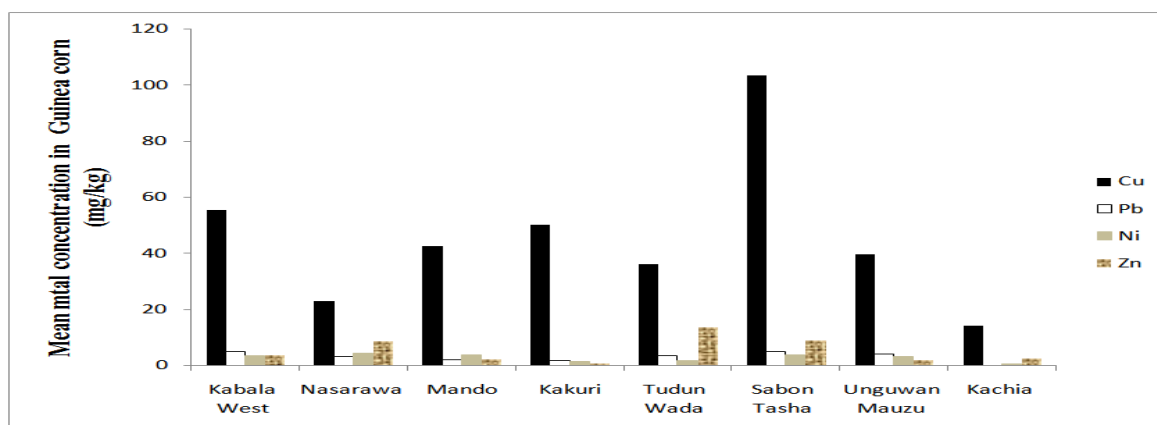


Fig. 2: Plot for mean Cu, Pb, Ni, Zn in guinea corn.

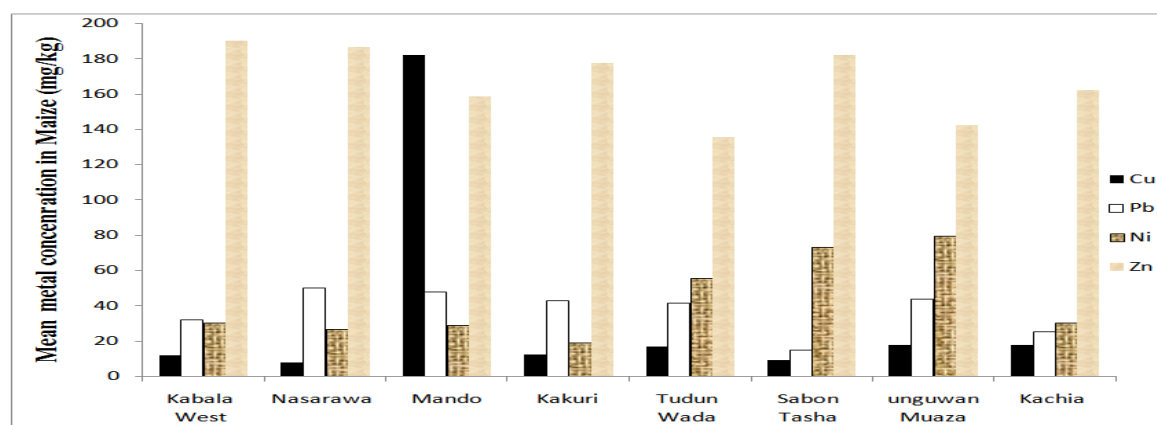


Fig. 3: Plot for mean Cu, Pb, Ni, Zn in maize.

### Metal Speciation

The distribution of copper, lead, nickel and zinc in the soils vary from one sampling location to another. The metals generally exist in the forms; residual, oxide, carbonate/organic and Fe-Mn oxide.

The values of these elements recorded from the various sites revealed that they are either residual, oxide, carbonate/organic or Fe-Mn oxide species. The metal species associated with Fe-Mn oxide fraction is tightly held and bound and thus not readily bioavailable. Its release into the soil solution depends on strong depletion of minerals content of the soil solution<sup>[12]</sup>.

The t-test  $p = 0.000 < 0.05$  for Nickel, Copper, Zinc and Lead respectively indicated a significant difference between the concentrations of the metals in maize soil and guinea corn soil for all the four types of metals. It showed that maize soil contained about ten times more Nickel than guinea corn soil with a mean of 38.23 mg/kg against 3.91 mg/Kg. Similarly, it showed that maize soil contained more Zinc than guinea corn soil with a mean of 28.45 mg/Kg against 3.88 mg/Kg. Again, maize soil contained more Lead than guinea corn soil with a mean of 28.57 mg/Kg against 3.32 mg/Kg. On the other hand, it showed that guinea corn contains more Nickel than Copper with a mean of 28.45 mg/Kg against 3.68 mg/Kg (Figs. 4 and 5).

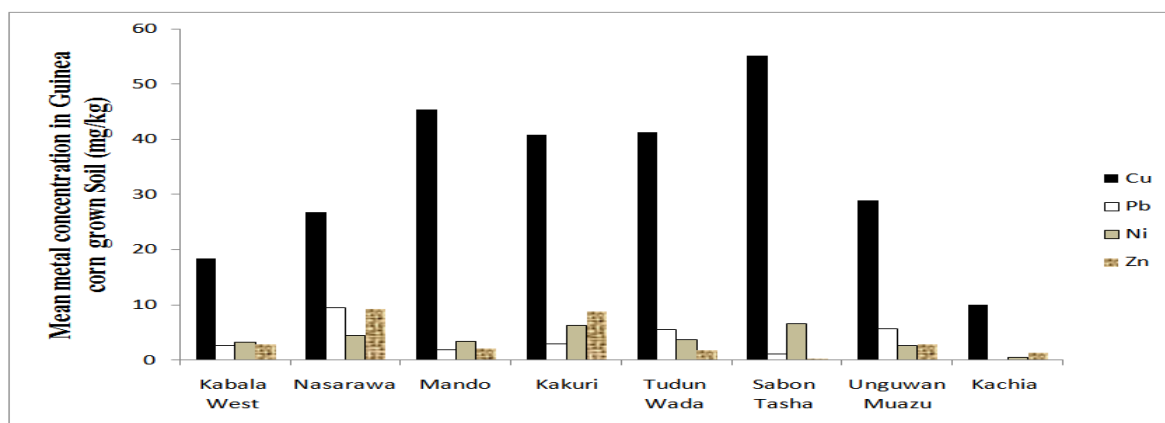


Fig.4: Plot for mean Cu, Pb, Ni, Zn in Guinea corn grown soils.

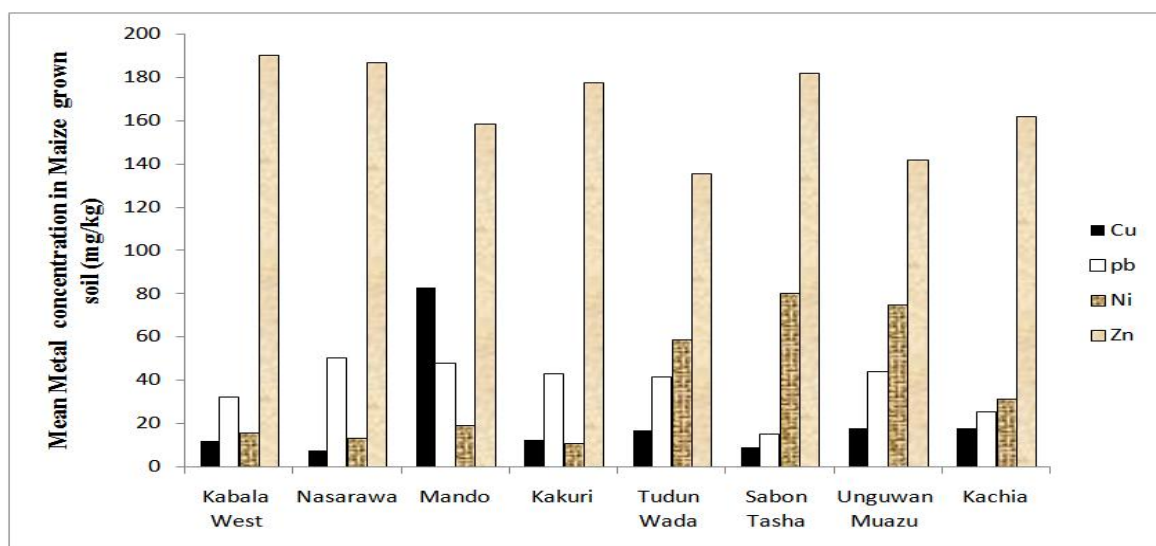


Fig.5: Plot for mean Cu, Pb, Ni, Zn in maize grown soils.

### IV. CONCLUSION

Measurement of the metals concentration in soils is useful for determining the extent of contamination and for measuring any net change in soil metal concentration overtime. The method doesn't however give an indication as to the chemical form of the metal in the soil system<sup>[13]</sup>. A more commonly used procedure is the hot nitric acid-hydrogen peroxide procedure<sup>[9]</sup>. Which is a partial digestion of the soil solid phase.

## REFERENCES

- [1] Hodel, D.R. and Chang, A.C. (2004). Trace Elements and Urban Gardens, University of California Cooperative Extension UCCE Newsletter 3:14 – 19.
- [2] Turer, D., Maynard, J.B. and Sonsalore, J. J. (2001). Heavy metal contamination in soils of urban highways: comparison between run off and soil concentrations at Cincinnati; Ohio. *Water and Soil pollution*. 132: 293-314.
- [3] Kuhn, I., Brandl, R. and Klotz, S. (2004). The Flora of German Cities is naturally species rich. *Evolutionary Ecology Research*, 6:149- 764.
- [4] Berthelson, B.O., Steinnes, E., Solberg, W. and Jingsen, L. (1995). Heavy metal concentrations in plants in relation to atmospheric heavy metal deposition. *Journal of Environmental Quality*, 24(5): 1018-1026.
- [5] Yaman, M., Dilgin, Y. and Gucer, S. (2000). Speciation of lead in soil and relation with its concentration in fruits. *Analytical Chimica Acta*. 410: 119-125.
- [6] Stoeppler, M. (1991). Cadmium, In: Merian E. (ed). *Metals and their compounds in the environment* VCH. Verlag Segsellschaft mbH, Weinheim New York 803-851.
- [7] Hawkes, S.J. (1997). What is a heavy metal? *Journal of Chem. Edu. (JCE)* 74 (11): 1374.
- [8] Jones, K.C. (1991). Contamination trends in soils and crops. *Environmental Pollution*, 69(4): 311-326.
- [9] Yaman, M. Okumus, N., Bakirdere, S. and Akdeniz, I. (2005). Zinc speciation in soils and relation with its concentration in fruits. *Asian Journal of Chemistry*. 17(1): 66-72.
- [10] Tessier, A., Campbell, P.G.C and Bisson , M.(1979). Sequential extraction procedure for the speciation of particular TRACE METALS. *Anal. Chem.* 51:844-850.
- [11] Seward, M.R.D. and Richardson, D.H.S (1990). In *Heavy Metal Tolerance in Plants: Evoluntary aspects* ; Show, A.J., Ed., CRC Press: Boca Raton, FL. 7-19.
- [12] Xian, X. (1989). Effect of Chemical Forms of Cadmium, Zinc and Lead in polluted soils on their uptake by cabbage plants. *Plant soil*. 113: 257-264.
- [13] Miller, W.P., Martens, D.C and Zelazny, L .W (1986). Effect of sequence in extraction of trace Metals from soils. *Sci. Soc. AM. J.* 50:598-601.

## Assessment of Ni and Cd Bioavailability in soils around selected Automobile Workshops of Kaduna, Nigeria.

Mohammed, S.S., Abdulmalik, I. A, Yusuf, H.

Department of Applied Science, College of Science and Technology, Kaduna Polytechnic P.M.B 2021 Kaduna – Nigeria.

**Abstract:** The identification of the chemical forms or phases of Ni and Cd in soil is necessary for estimating their biological availability, physico-chemical reactivity and transport in the environment and into the food chain. In the study, the Ni and Pb concentrations of soil samples obtained from selected automobile workshops were determined using Flame Atomic Absorption Spectrometry (FAAS). A modified Tessier extraction procedure was employed for the digestion and extraction of the soil samples using different digestion and extraction media. The results showed that the concentrations of Ni and Cd in the samples varied from one workshop to another. The Ni concentration bound to the residual phase was found out to be highest followed by that bound to exchangeable phase. The Ni distribution in the various media followed the pattern:  $\text{HNO}_3$ :  $\text{H}_2\text{O}_2$  >  $\text{MgCl}_2$  >  $\text{EDTA}$  > Oxalic acid. Similarly, Cd concentration bound to carbonate/ organic phase was found to be highest followed by that bound to oxide phase. The pattern of distribution is  $\text{EDTA}$  > Oxalic acid >  $\text{HNO}_3$ :  $\text{H}_2\text{O}_2$  >  $\text{MgCl}_2$ .

**Keywords:** Bioavailability, metal content, soil, Automobile workshop.

### I. INTRODUCTION

Nickel is a nutritionally trace metal for at least several animal species, micro- organisms and plants, and therefore either deficiency or toxicity symptoms can occur when respectively, too little or too much Nickel is taken<sup>[1]</sup>. Although Nickel is vital for the function of many organisms, concentrations in some areas from both anthropogenic release and naturally varying levels maybe toxic to living organisms<sup>[2]</sup>. Nickel is generally distributed uniformly through the soil profile but typically accumulates at the surface from deposition by industrial and agricultural activities. Nickel can exist in soils in several forms such as inorganic crystalline minerals or precipitate, complexes and absorbed on organic cations surface or on inorganic cations exchange surfaces, water soluble, and free-ion or chelated metal complexes in soil solution<sup>[3]</sup>. Cadmium is emitted into the atmosphere from natural sources mainly volcanic activities and from anthropogenic sources. Metal production (drying of Zinc concentrate and roasting, smelting and refining of ores) is the longest sources of anthropogenic atmosphere cadmium emissions, followed by waste incineration. Other sources, include the production of nickel-cadmium batteries, fossil fuel combustion and generation of dust by industrial processes such cement manufacturing<sup>[4]</sup>. The largest sources of cadmium in Landfills are smelters, iron, steel plants, electroplating wastes and battery production<sup>[5]</sup>. Cadmium is used as anticorrosive coating in electroplating, as a pigment and as a component of nickel-cadmium batteries<sup>[4]</sup>. Health effects have been demonstrated in industrial workers heavily exposed to cadmium oxide fumes and dust<sup>[5]</sup>. Bronchitis, emphysema, anaemia and renal stones have been reported<sup>[4]</sup>. Much researches have been conducted on heavy metals contamination in soils from various anthropogenic sources such as industrial wastes<sup>[6,7,8]</sup>, automobile emission<sup>[9,10]</sup>, mining activity. In this research, Ni and Cd concentrations in soil samples were determined by Flame Atomic Absorption Spectrometry (FAAS). The soil samples were extracted using chemical reagents such as the mixture of  $\text{HNO}_3/\text{H}_2\text{O}_2$ ,  $\text{MgCl}_2$ , oxalic acid and EDTA.

### II. MATERIALS AND METHODS

A flame atomic absorption spectrophotometer model 8010 Young Lin was used for the Ni and Cd determination. In the extraction procedures,  $\text{HNO}_3/\text{H}_2\text{O}_2$  (2+1), 1.0M  $\text{MgCl}_2$ , 1.0M Oxalic acid and 0.05M EDTA were used.

### Preparation of Samples

The research covered four different automobile workshops in Kaduna Metropolis, Nigeria. The sites are Poly Road, (PR), Tudun Wada Cinema Road (TWC), Oriapala Mechanic Village (OMV) and Hamdala Swimming Pool Road (HSP). The samples were collected in November, 2012. Triplicate samples were collected from each automobile workshop randomly at a distance of 100meter depth of 10cm from soil surface <sup>[11]</sup>.

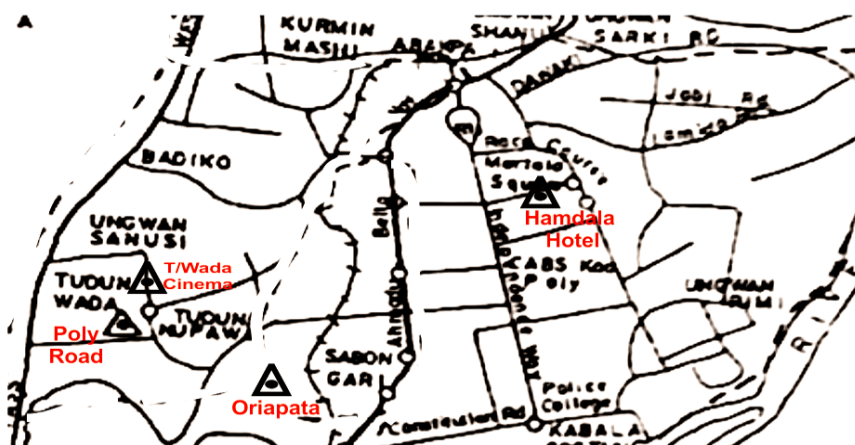


Fig. 1: Map of Kaduna Metropolis showing sampling sites

### Digestion and Extraction of Soil

Soil extracts from automobile workshops were obtained by shaking separately 5g of soil sample with 10ml of  $\text{HNO}_3/\text{H}_2\text{O}_2$  (2:1), 0.05M (for residual phase). 0.05M  $\text{Na}_2\text{EDTA}$  (for carbonate and organically bound phase), 1.0M Oxalic acid (for oxide phase) and 1.0M Magnesium Chloride (for exchangeable phase). The mixture was evaporated with occasional shaking on a hot plate. Four  $\text{cm}^3$  of 1.5M nitric acid was added to the remainder and centrifuged. The digest was diluted to  $60\text{cm}^3$  with distilled water and filtered. The resultant solution was analysed for Ni and Cd using FAAS model 8010 Young Lin. A blank digest was prepared in the same way.

### III. RESULTS AND DISCUSSIONS

The nickel content in the soil samples obtained from the selected automobile workshops varied from one sampling location to another, which maybe due to the fact that the activities vary from one workshop to another and that some of the workshops are closer to main road as compared to other workshops. The distribution of the metal in the soil samples showed that it exists in carbonate/organic, oxide, exchangeable and residual functions. The concentration of Nickel bound to residual phase with 60% in the samples obtained from the automobile workshops as shown in Fig. 2.

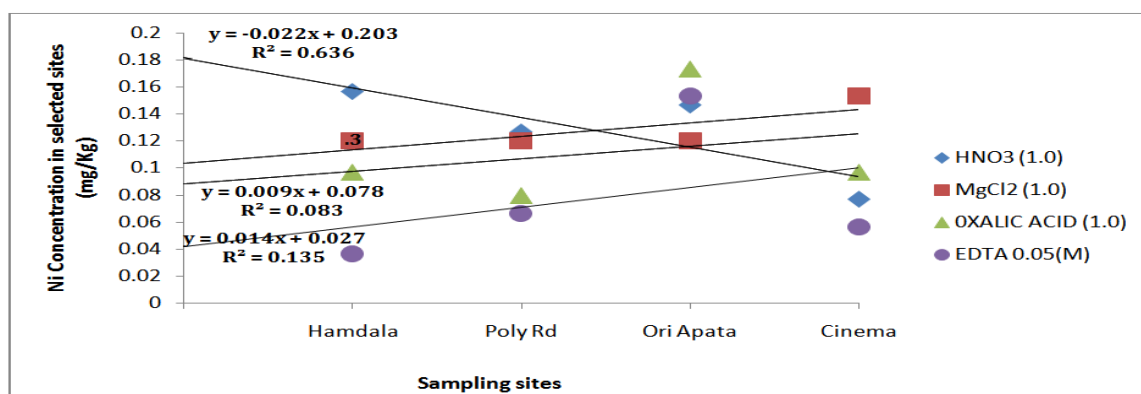


Fig. 2: Concentration of Ni against sample sites

This could be attributed to the nearness of their workshops to major roads and other anthropogenic activities such as the use of alloy steels and rechargeable batteries in these areas <sup>[12,13]</sup>. From the correlation study, Ni has the highest concentration as compared to the other metals in Hamdala and Poly road auto-mechanic workshops with correlation coefficients of 0.9827 and 0.9610 respectively. This maybe attributed to busy nature of the

roads around these workshops and the serious use of motor oil and finished tyres in the workshops<sup>[14]</sup>. The cadmium distribution in the selected automobile workshops varied from one location to another which maybe attributed to charging of automobile batteries and other anthropogenic activities which vary from one workshop to another<sup>[15]</sup>. The metal existed in carbonate/organic, oxide, residual and exchangeable fractions. The concentration of cadmium was found to be highest in carbonate/ organic fraction as shown in Fig. 3.

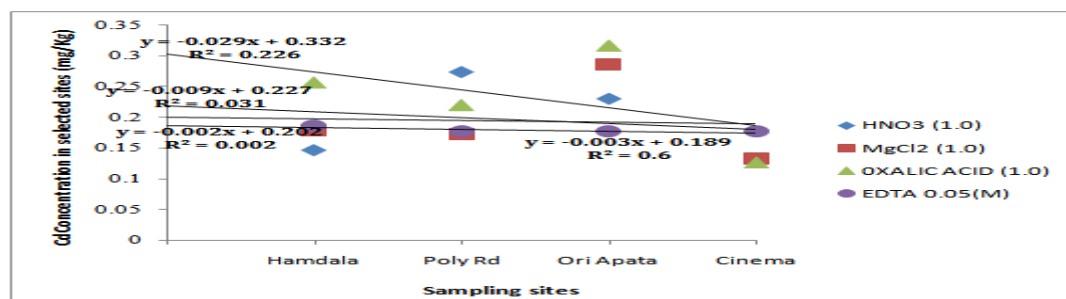


Fig. 3:Concentration of Cd against sample sites

Which shows that the metal is bioavailable and mobile in this fraction.<sup>[16]</sup> Correlation study showed that Cadmium concentration was found to be highest in Tudun Wada Cinema workshop with a correlation coefficient of 0.7327 as compared to the other metals. This could be attributed to the specialized nature of the workshop where only diesel powered heavy dirty vehicles are repaired availability of used lubricating oils and discarded lead-cadmium batteries<sup>[17, 18, 19]</sup>.

#### IV. CONCLUSION

The metals were distributed between residual, oxide, exchangeable and carbonate fractions. An increase of the metal concentrations in some of the sampling locations suggest higher anthropogenic activities in such areas which indicated possible soil pollution as a result of the activities carried out in such locations.

#### REFERENCES

- [1] Bencko, V., (1983). Nickel: A review of its occupational and environmental toxicology. *J. Hyg. Epidem. Micro Immun.*, 27:237.
- [2] Diagomanolin, V., M.Farhong, M. Ghazi-Khan-Sazi and N.Jafar Zadeh, (2004). Heavy metals (Ni, Cr, Cu) in the Karoon waterway river, Iran. *Toxicol Letts.*, 151(1):63.
- [3] Bennett, B.G., (1982). Exposure of man to environment nickel- an exposure commitment assessment. *Sci.Total.Environ.*, 22(3): 203
- [4] Hodel, D.R and Chang, A.C (2004), Trace Elements and Urban Gardens. University of California Cooperative Extension UCCE Newsletter 3:14-19.
- [5] Stoeppler, M. (1991). Cadmium, In: Merian E. (ed) metals and their compounds in the environment VCH. Verlag Segsellschaft mbH, Weinheim- New York 803-851.
- [6] Yusuf, K.A., (2006). Evaluation of the three stage BCR (European Community Bureau of Reference) sequential extraction procedure to assess the potential mobility and toxicity of heavy metals in roadside soils. *Pak. J. Sci. Ind. Res.*, 49:181-188.
- [7] Adeniyi, A.A and O.O Okediye, (2004). Assessing the speciation pattern of lead and zinc in surface water collected from Abege Creek, Ijora, Lagos, *Pak.J. Sci. Ind. Res.*, 47: 430-434.
- [8] Kakula, S.E and O. Osibanjo, (1988). Trace heavy metal pollution studies in sediments of the Niger Delta area of Nigeria. *J. Chem. Soc. Nigeria*, 11:315-322.
- [9] Arowolo, T.A, O. Bamgbose and O.O Odukoya, (2000). The chemical forms of lead in roadside dusts of metropolitan Lagos, Nigeria. *Global J. Pure, Appl. Sci.*, 6:483-487.
- [10] Ma, L.Q and G.N. Rao, (1997). Chemical fraction of cadmium, copper, nickel and zinc in contaminated soils. *J. Environ. Qual.*, 26:259-264.
- [11] Yaman, M., Okumus, N., Bakirdere, S. and Akdeniz, I. (2005). Zinc speciation in soils and relation with concentration in fruits. *Asian Journal of Chem.* 17(1): 66-72.
- [12] Kashem, M.A and Singh. B.R., (1998). Heavy metal contamination of soil and vegetation in the vicinity of industries in Bangladesh. *Water, Air, Soil Pollut.*, 115:347-361.
- [13] Ayodele, J.T. and Mohammed, S.S.,(2011). *Speciation of Nickel in soils and cereal.res. J. Appl. Sci. Engineering Tecnol.*, 3(3):202-209.
- [14] Hashim, D.R. Siddiqni, I. and Shaieh, G.H. (2006). Accumulation of heavy metals in tarry Deposit on leave at various location at Karachi. *Jour. Chem. Sci. Par* 28(2):125-129.
- [15] Ikeda, M., Zhang, ZW., Shimbo, S., Watanabe, T., Nakatsuka, H., Moon,CS., Matsuda- Inoguchi, N. and Higashikawa, K. (2000). Urban population exposure to lead and cadmium in east and south-east Asia. *Science of the Total Environment*. 249: 373-384.
- [16] Yaman, M., Dilgin, Y. and Gucer, S. (2000). Speciation of lead in soil and relation with its concentration in fruits. *Analytical Chimica Acta* 410:119-125.
- [17] Adu, A.A., Aderiola, O.J., Kusemiju, V. (2012). An assessment of soil Heavy Metal Pollution by various allied artisans in automobile, welding workshops and petrol station in Lagos State, Nigeria. *Sjeer* 2012. 290 -298. Doi:10.7237/sjeer/2905.
- [18] Scott-Fordsmand, J.J, (1997). Toxicity of nickel of nickel to soil organisms in Denmark Rev. Environ. Contam. Toxicol., 148: 1.
- [19] Kabala, C. and B.R Singh, (2001). Fractionation and mobility and copper, lead and zinc in soil profiles In the vicinity of a copper smelter. *J. Environ. Qual.*, 30: 485- 492.



## Secure SMS Mobile Transaction with Peer to Peer Authentication Design for Mobile Government

Mohammad Khalaf Rahim Al-juaifari

*Mohammad.aljuaifari@uokufa.edu.iq*

*University Of Kufa-Iraq*

**Abstract:** Currently, many researches in Mobile government secure transmission of plaintext with universal availability in all GSM networks had been proposed. The most important characteristic of this research is a new system that contains all the capabilities and plugging security holes in the algorithms and methods used in previous systems design. The main reason of the intensification of efforts for the purpose of security in a mobile government is the real threat that accompanies the movement of transaction from the sender to the recipient. Moreover, mobile government used in improving convenience is one the clearest manifestations of the development of society and solving various problems using other method related to availability, speed, financial, in addition to the administrative issues related to the fight against corruption side a side with E-government. In this paper, illustrating how a mobile phone can provide citizens and Non-government organizations with mobile government services relevant to the design and implementation of security mechanisms coinciding with the birth of the third generation technology in Iraq so as to ensure the highest level of security transaction provided by UMTS security is also built upon GSM network.

**Keywords:** SMS (Short Message Service), Mobile Government (M-government), Electronic Government (e-Government), Global System for Mobile (GSM), third-generation (3G), Universal Mobile Telecommunications System (UMTS), 3GPP (Third Generation Partnership Project), OTP (One Time Password), GSM (Global System for Mobile Communications), SHA (Secure Hashing Algorithm), Elliptic Curve Digital Signature Algorithm (ECDSA), message digest (MD).

### I- INTRODUCTION

The entry of mobile phones in the online world, the opportunity that mobile phones offer has pulled more people into the wireless world, and citizen-mobile related services such as voice communication, but is also used in governance, Mobile Democracy and many more. M-Government combines both terms 'mobility' and 'e-Government' and Offers a lot of potential like: availability (more people is on), speed, better administration, saving cost & time ...etc. Generally, text, voice, sound or image message sent over a public communications network is called (SMS), which can be stored in the network or in the recipient's terminal equipment until it is collected by the recipient. There is no such scheme that support complete SMSs security, Lack of security still the main issue in mobile government although a lot of numbers of SMS-based mobile protocols have been proposed. For instance, SMS based transactional services available in UK, Europe, and many cities across North America after the telecom industry de-regulation and adoption of UMTS is a so-called "third-generation (3G)," broadband, packet -based transmission of text, digitized voice, video, and multimedia at data rates up to and possibly higher than 2 megabits.

In [1] describes the wide using of SMS day by day as in figure 1 shows the increasing use of SMS from 2006 to 2016. 2014, 2015 and 2016 is forecasted.

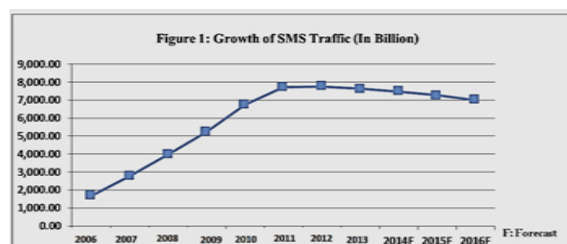


Fig. 1: Growth of SMS Traffic

Increasing may happened because more organizations used communication with their client and others, Mobile phones now have 5G,4G, LAN and WLAN connectivity not only 3G, use 3G in proposed system that including simulates the reality of the current communication technology in Iraq.

Biometric protection considered as costly way in case they are used in the security system of government mobile and other internet applications, especially when designing an authentication for customers, so in the system OTP algorithm using which allows executing password once by preventing trying to predicate password using irreversible and random sequence.

The main objective of this paper is to show how mobile phone can serve citizens and firms in mobile government. Hence, it provides different services to citizens. It is developed as a new technique to deliver service and the government transfer make citizens easy to access public services. The changes in the Internet and World Wide Web technologies and services lead to new developments in the way e-government efforts provide services to citizens and businesses, and in the way governments handles their internal operations. Frontline SMS project1 aims to Frontline SMS allows data exchange between remote entities (PCs, Laptop, etc.) based on SMS messages. Another example one of the revolutionary developments comes from adoption of wireless mobile technologies in government related activities: m-government to present technological drivers of m-government and present cases where these technologies are being used. Finally, concludes with discussions of mainly security challenges for m-government implementations currently and in the future.

## **II- RELATED WORKS:**

By default SMS does not guarantee confidentiality and integrity to the message content. Therefore SMS is not totally secure and reliable [2]. In [3] Mobile Government: 2010 and Beyond has been finalized with the contribution and effort of several supporters of m-government.

Although modern smart phones provide users a variety of different communication capabilities, SMS technology is still favored all over the world (MBAONLINE, 2011). The popularity of SMS technology has led to a plethora of SMS based services. Also the public sector tries to make use of SMS technology's popularity. SMS based m-Government services can already be found in various countries around the world. Comprehensive overviews of existing SMS based projects and initiatives are given in (Mobile Solutions Ltd, 2010) and (Zefferer, 2011). SMS has played an essential role in developing countries for many years. Especially in rural areas, reliable fixed-line communication networks are often not available. Contrary, mobile communication networks are often well evolved even in underdeveloped regions. Yet, they are limited to GSM technology most of the time. The consequent restriction to telephony and text messaging improve communication capabilities in regions with underdeveloped infrastructures. For instance, an SMS based service is Kenya's Blood Bank-SMS project2. Due to missing reliable fixed-line communication networks, statuses of blood banks are exchanged via an SMS based service between different hospitals. A lot of trying to develop new system easier to manage, independent of SMS gateway, and less expensive such as in [4].

There are various other SMS based services from the health sector available in developing countries. In South Africa, citizens can request location information on HIV testing centers via SMS. Text to Change3 is a health education initiative that aims to inform people in developing countries about diseases such as malaria or AIDS using text messaging technologies. In developed countries, reliable fixed-line communication networks are usually well evolved. Mobile communication networks are thus just one out of multiple communication and information alternatives and mainly used to satisfy demands of the typical western always-on society. Hence, SMS based services in developed regions differ from those of developing countries in various aspects. In fact, most existing SMS based services aim to improve convenience. For instance, in various European cities parking fees can be paid via text messages4. In Norway, also tax declarations can be done with the help of SMS messages5, which has significantly eased the entire tax declaration process for citizens. Various countries in both developing and developed regions make use of SMS to broadcast relevant information to their citizens. For instance, in Venice, Italy, citizens are supplied with flood warnings per SMS6. In London, UK, the Metropolitan police forward bomb alerts and similar security warnings to registered citizens via SMS7.

Nowadays, the (3GPP) is responsible for the development and has led to the development of various useful SMS based services. In [5] SMS is a popular medium for many Services such as mobile banking, news alerts etc...

In such scenarios, SMS based transactional services can be useful, The approach introduced in this paper implements transactional services on SMS basis and incorporates electronic signatures to meet security requirements of such services. In addition, it is also possible to use a SIM card to perform certain cryptographic

operations, while executing the remaining part of the application through the ME, like in the mobile payment scheme presented by Hassinen et al. [6].

With Internet rapidly developing, SMS with e-commerce plays an important role in business transactions and is conducting business communications and solutions over the networks and through computers and mobiles [7] to give limitations of SMS technology, most SMS based services are rather informational than transactional. This is reasonable since transactional services can have higher security requirements that are difficult to meet with SMS based approaches. Therefore, transactional services are traditionally provided through web based approaches, which allow an easier integration of cryptographic methods such as electronic signatures. Unfortunately, there are scenarios in which web access is not available and web based services cannot be accessed. The term SMS refers Short Message Service SMS stands for Short Message Service. It is a technology that enables the sending and receiving of messages between mobile phones. SMS first appeared in Europe in 1992. Later it was ported to wireless technologies like CDMA and TDMA. GSM and SMS standards were originally developed by ETSI. ETSI is the abbreviation for European Telecommunications Standards Institute. maintenance of the GSM and SMS standards has been done by [7]. (GSM) is the most popular standard for mobile telephony systems in the world [8].

There is a need to provide an additional encryption on the transmitted messages and Global Service for Mobile communications with the greatest worldwide number of users. As suggested by the name SMS, data that can be held by an SMS message is very limited. One SMS message can contain at most 140 bytes (1120 bits) of data, so it can contain up to [9].

### III- Proposed Solution:

The system implied OTP with digital signature for user authentication, OTP support to work with Applet running on a mobile phone or PDA. OTP via SMS text message, OTP is generated at a center and sent as a text message to the server side by using RADIUS protocol for validating the OTP values validating Active Directory, Lightweight Directory Access Protocol and internal database. The OTP value is passed as a standard RADIUS request to the vendor-specific OTP authentication server.

A signature generates with user's signing key in case of matching password authentication and the OTP authentication. After applying Ciphering on SMS, electronic signatures applied to meet the requirements for integrity of digital data and non-repudiation of origin then transmitted signed encrypted SMS.

Proposed security mechanism should satisfy secure, easy to implement no storage of secret cryptographic keys,

#### 3.1. The M-GOV Infrastructure:

M-GOV Infrastructure designed to achieve trust and confidence, authentication, integrity, confidentiality and non-repudiation. Storage of documents so as to ensure the security and integrity preservation in addition to the possibility of data retrieval and update ... Fig. 2 describes the M-government conceptual infrastructure, whose components are described in short in the following.

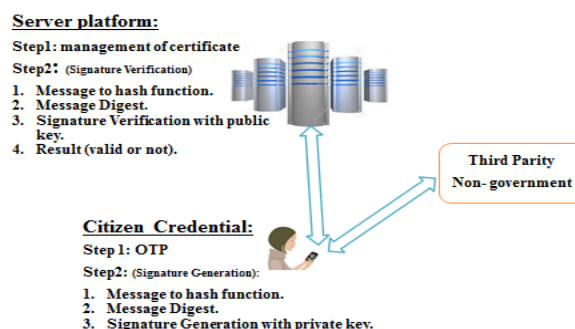


Fig. 2: M-government infrastructure

By providing appropriate credentials, Citizens and M-Government can be securely mutually authenticated and communicate using digital signatures and certificates. Public Key Infrastructure can be considered as public authorities, third party and notarization services entities. Notarization services contain time stamping, digital signing and secure storage to be available for third parity. In [10] supports authentication and confidentiality

implemented through the RSA, DSA and ECDSA signature schemes. Main aspects of proposed system consist of three modules these are achieving entity authentication, and achieve key exchange.

**First is Initialization:** Installing the application software on the user's mobile phone, PDA, tablet etc. registering the user details into the system, generating the user name and password for Citizens. **Second is OTP:** It is a password that is valid for only one login session or transaction.

OTP in [11] security supported by preventing stealing password then hacker should control phone in addition to user name and password. OTP Programs run on mobile device to provide a PIN with token that change with time and implement the confidentiality by encrypting the message using a symmetric secret one-time password. The one-time password is only shared between the citizen and the server. The strength of the confidentiality depends on the security strength of the passwords generation algorithm. It is assumed that only the authorized users will know his passwords.

**Third is Secure Message** is protocol used to implement the integrity of the message digest, the hashed value of the message content calculated server application and the mobile phone application. If the content is altered during transmission, the hashing algorithm will generate a different digest value at the receiver side. If the digests mismatch, the receiver will know that the integrity of the message has been compromised.

### III- Secure Message method:

#### 3.1 Proposed System Design:

A new system shown in figure 3 has been proposed starts from sender side (message handler) and installing the application in mobile phone then register the user by The following points represent the procedures that used to design proposed system:

- UTMS networks media that proposed in the system.
- The security and efficiency of this protocol is analyzed.
- Hashing algorithm applied on the message before transaction operation.
- The MD is then inputted into a Digital Signature Algorithm (DSA) which generates/verifies the signature for the message.

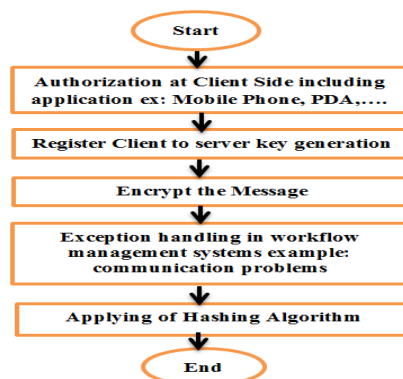


Fig. 3: Proposed Procedure Diagram

Figure 4 shows that SMS is comprised of the header and the payload (which is the content of the message). The header provides four bytes to specify metadata and the size of the payload. The maximum length of the payload is usually 160 characters at 8-bit per character.

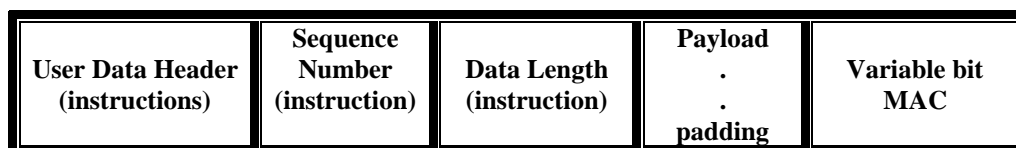


Fig. 4: SMS message structure

**3.2 SHA-1 Algorithm:** used for applying user name and password after that encrypting the message operation.

### 3.2.1 SHA-1 features:

In this part of proposed system is SHA-1 which have the properties of: its outputs a 160 bits digest of any sized file or input, uses a 512 bit block size and has a maximum message size of  $2^{64} - 1$  bits, word size 32 bits, 80 rounds, and internal state | output size is 160 bits without having conditions on the chaining variables.

Other SHA-1 characteristics are:

- Different messages that produce the same MD.
- Any changes made to the messages will result in a different MD.
- Signing the MD makes the message more efficient since the MD is a smaller size then the message.
- The same hash function is needed to verify the message.
- SHA-1 is computationally infeasible to find a message that corresponds to a given MD.

A secure Hash Algorithm (SHA) is necessary to ensure the security of the Digital Signature Algorithm (DSA).

Each round uses a different K and different nonlinear mixing function f in figure below:

### 3.2.2 SHA-1 Algorithm Framework:

Step 1: Append Padding with and 0's Bits makes message length to 64 bits less than an even multiple of 512.

Step 2: 64 bits are append Length to the end of the padded message.

Step 3: Prepare 80 processing functions

Step 4: Prepare 80 processing constant words

Step 5: buffers of words (32 bits)

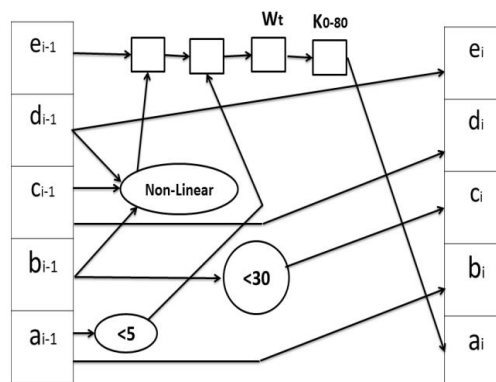


Fig. 5: SHA-1 block diagram

As shown in figure 5 above the description of following are:

$X1 \text{ (output)} = M1 \text{ (512 bits)} + x0 \text{ input (160 bits)}$ ; where m1 expand from 512 to 2560 bits.

Initialization is 4 rounds of (20 iterations each) repeat algorithm on the procedure until compressing whole messages in to single 160 bit vector.

Initialize four rounds of 20 iterations each distributed from k0 to k80.

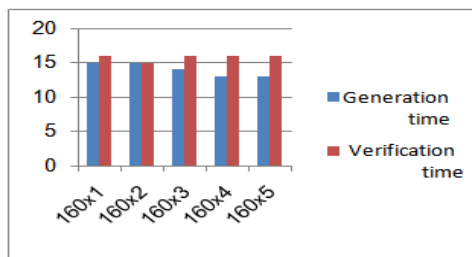


Fig. 6: ECDSA with SHA-1 Digital

#### IV- Implementation:

Programming Platform can be implemented by using Java Micro Edition (J2ME).net framework and others with corresponding data base connectivity.

Fig. 7: Client side Registration to M-Government

http://127.0.0.1:8080/MobileGovServer/Menu.htm

#### Information Index

Citizen	View	Delete
Bills	View	Delete
Phone NO.	Insert	Update
Police Information	Insert	Update
Job Information	Insert	Update
Emergency Information	Insert	Update
Holiday Information	Insert	Update
Missing Persons	Insert	Update
Other Information	Insert	Update

Fig. 8: Citizen Information (Editing Page Server Side)

http://127.0.0.1:8080/M-GovServer/ViewUsers

Citizen Information Records

Citizen ID	Name	Gender	Date of Birth	Address	Mobile	E-mail	Password	OTP
0	Mohammad aljuaifari	Male	11/3/1983	Iraq-Najaf	07801330422	mohammad.aljuaifari@uokufa.edu.iq	moham345	463986
0	Mohammad Khalaf	Male	12/6/1991	Iraq-Baghdad	07814613443	mohammadkhalafrahim@gmail.com	34652906	NULL
0	Ali Hussien	Male	11/8/1992	Iraq-Baghdad	07814613443	ali_hussien1999@gmail.com	ali1234	\$73420
0	Nada Hussien	Female	5/6/1996	Iraq-Baghdad	07814613443	nada_hussien2913@yahoo.com	4539876	\$73445
0	Zainab Hussien	Female	9/6/1984	Iraq-karbala	07814613443	zainab_hussien2913@uokufa.edu.iq	zainab8765	\$77432

Fig. 9: Registered Citizen with M-Government in Server Side

Hash function is needed to verify the message. The MD is then inputted into a Digital Signature Algorithm signature generation and verification

Based on [9] develops digital Signature algorithm based on ECDSA and results shows that signature generation and verification using of ECDSA is better than DES, AES RSA, ElGamal, and Blowfish due to low computational power since it provides high security than the default cryptography in use on the web with smaller key size.



By applying one time password algorithm with message digest in proposed system as shown in figure below:



```

INFO: Starting service Catalina
Jul 12, 2011 1:56:54 PM org.apache.catalina.core.StandardEngine start
INFO: Starting Servlet Engine: Apache Tomcat/6.0.0
Jul 12, 2011 1:56:54 PM org.apache.catalina.core.StandardHost start
INFO: /xml-validation disabled
Jul 12, 2011 1:56:59 PM org.apache.catalina.core.ApplicationContext log
INFO: ContextListener: contextInitialized()
Jul 12, 2011 1:56:59 PM org.apache.catalina.core.ApplicationContext log
INFO: SessionListener: contextInitialized()
Jul 12, 2011 1:57:01 PM org.apache.coyote.http11.Http11Protocol start
INFO: Starting Coyote HTTP/1.1 on http-8009
Jul 12, 2011 1:57:01 PM org.apache.jk.common.ChannelSocket init
INFO: JK: ajp13 listening on /0.0.0.0:8009
Jul 12, 2011 1:57:01 PM org.apache.jk.server.JkMain start
INFO: JK running 1000 times=0/118 config=null
Jul 12, 2011 1:57:01 PM org.apache.catalina.startup.Catalina start
INFO: Server startup in 7959 ms

```

Fig. 10: Message Digest Implementation

MD5 for encrypting and decrypting message: user name and password: The SHA-1 for text mohammadkhalaf is: **2c29979418c4daebd7d31b53350ded2ecff450ea** (DSA) Which generates/verifies the signature for the message. Runs in 80 rounds.

## REFERENCES

- [1] Growth History of SMS Source: PortioResearchLtd. [http://www.portioresearch.com/en/blog/2013/the-15-trillion-\\$-dollar-story-of-sms.aspx](http://www.portioresearch.com/en/blog/2013/the-15-trillion-$-dollar-story-of-sms.aspx)
- [2] "A Security Mechanism for Secure SMS Communication" HULISANI RATSHINANGA, JOHNNY LO AND JUDITH BISHOP.
- [3] Computer Science Department, University of Pretoria, South Africa hratshin, jlo, jbishop @cs.up.ac.za Mobile Government: 2010 and Beyond white paper, 2010.
- [4] Salman Firdaus bin Haji Sidek, "The Development of the Short Messaging Service (SMS) Application for the School Usage", 978-1-4244-6716-7/10/\$26.00, 2010@ IEEE, pp 1382-1386
- [5] C.Narendiran, S.Albert Rabara, N.Rajendran, "Performance Evaluation on End-to-End Security Architecture for Mobile Banking System", 2008@IEEE.
- [6] M. Hassinen, K. Hypponen, and K. Haataja, "An Open, PKI-Based Mobile Payment System," in ETRICS, 2006, pp. 86–100.
- [7] M. Toorani and A. Beheshti Shirazi, "SSMS - A secure SMS messaging protocol for the m-payment systems", in Computers and Communications, IEEE Symposium on, July 2008@IEEE, pp 700–705.
- [8] Nassim Khozooyi, Maryam Tahajod, Peyman Khozooyi, "Security in Mobile Governmental Transactions", 2009 Second International Conference on Computer and Electrical Engineering, 978-0-7695-3925-6/09 \$26.00 © 2009 IEEE, pp 168-172.
- [9] Alfredo De Santis, Aniello Castiglione and Umberto Ferraro Petrillo "An Extensible Framework for Efficient Secure SMS" International Conference on Complex, Intelligent and Software Intensive Systems, 2010@IEEE, pp 843-850.
- [10] Neetesh Saxena and Narendra S. Chaudhari "Secure Encryption with Digital Signature Approach for Short Message Service", 2012 World Congress on Information and Communication Technologies Stefan Certic "The Future Of Mobile Security"
- [11] CS Network Solutions Limited <http://www.cs-networks.net>
- [12] Neetesh Saxena, Narendra S. Chaudhari "Secure Encryption with Digital Signature Approach for Short Message Service", 2012 World Congress on Information and Communication Technologies.

## Use of Coke Oven Gas during shutdown period of Direct Reduced Iron Plant for Steam Generation: Experimentation and Optimization

Harish C. Dalai<sup>1</sup>, Dr. N.C.Nayak<sup>2</sup>

<sup>1</sup>M Tech Scholar, Department of Mechanical Engineering, Indira Gandhi Institute of Technology, Sarang, India-759146,

<sup>2</sup>Reader, Department of Mechanical Engineering, Indira Gandhi Institute of Technology, Sarang, India-759146,

**Abstract:** Development of any country is largely based on its magnitude of industrial growth. Steel industries in India took a leading role in the world after mid-sixties. During the last five decades, the steel industries all over the world made considerable developments in new methods for reducing iron ore directly to metallic iron for use as commercial scrap substitute in the manufacture of steels. BSL has been producing steel and other products over last two decades and the above process is used in BSL for one decade. Direct reduction is a process, which extracts high metallic solid iron by removing oxygen from iron ore or any other iron oxides without passing through molten stage, i.e. solid state reduction. The product, so formed is known as directly reduced iron (DRI) or Sponge Iron. Due to shortage of raw material or any other problem in DRI sections, the DRI section undergoes a temporary short down. During the shutdown period the equipments tend to be idle. To keep the equipment ready for operation as well as to maintain the plants economy an alternate methodology is used in this research. Various operations are: CO gas from Coke Oven, DRI, Steam Generation, and Power Generation.

**Key words:** Coal base, direct reduced iron, alloy, coke oven gas, steam generation

### I. Introduction

Steel is an alloy of iron with varying amounts of carbon and some other elements such as Manganese, Chromium, Nickel, Molybdenum, Zirconium, Vanadium, Tungsten and so on. Currently there are over 3000 catalogued grades of steel available [1]. The global steel production touched 109. Million tons in the year 2007 making an increase of 7.6% compared with 2006. The largest steel producing countries are China, Japan and United States. The largest consumers are Singapore (1,200kg), Taiwan (over 970kg) and Korea (830kg) per capita [2]. India's steel production ranked 7<sup>th</sup> in the world in the year 2012 up from 9<sup>th</sup> in the year 2013. A look at the past production figures over the last century attests a significant shift in the geography of Steel making. In 1990, USA was producing 37% of the world steel as against 14% at present [3]. With post war industrial development Asian production now accounts for almost 40%, Europe (including the former Soviet Union) for 36% and North America for 14.5%. Since the late 1960s there has been a leveling off of the rate of growth in steel production, which is partly attributable to greater efficiency in the use of steel and less wastage [4]. Progress in steel making is also indicated from the uses of Bessemer converter at the turn of the 19<sup>th</sup> century to the introduction of oxygen conversion processes in the 1950s and continuous casting in the 1960s. Steel is one of the most recycled non-expendable industrial materials recycled. Material is used in all steel production [5]. Even after decades of use, steel is salvaged and over 40% of steel production is based on recycled material including scraps.

#### 1.1 Objectives of research

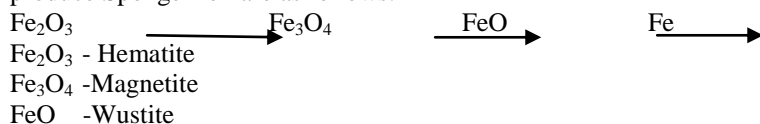
- Efficient use of shut down kiln to avoid it's ideal condition of equipments for further operation.
- Use of by product gas from recovery coke oven plant to generate steam for power generation.
- To generate steam, it requires lesser investment and one time investment. It has less maintenance cost in future.
- To generate steam, no high skilled labour is required. Semi skilled labour can operate easily which is easily available.

- v. To generate steam, this is the most pollution free method using by product gas of recovery coke oven plant.
- vi. To generate steam, this is only one method which can continue during shut down of recovery coke oven plant, by using coke oven gas from gas holder.

## II. Review of literature

Direct Reduced Iron, also called Sponge Iron, is produced by direct reduction of iron ore by a reducing gas produced from coal or natural gas. This gas is mainly Carbon Monoxide gas. The process is known as direct reduction because iron ore is reduced in solid state itself. Iron ore doesn't melt [6]. The conventional route for making steel consists of sintering or pelletization plants, coke ovens, blast furnaces, and basic oxygen furnaces. Such plants require high capital expenses and raw materials of stringent specifications. Coking coal is needed to make a coke strong enough to support the burden in the blast furnace [7]. Integrated steel plants of less than one million tons annual capacity are generally not economically viable. The coke ovens and sintering plants in an integrated steel plant are polluting and expensive units. Direct reduction, an alternative route of iron making, has been developed to overcome some of these difficulties of conventional blast furnaces [8]. DRI is successfully manufactured in various parts of the world through either natural gas or coal-based technology. Iron ore is reduced in solid state at 800 to 1,050 °C (1,472 to 1,922 °F) by coal. The specific investment and operating costs of direct reduction plants are low compared to integrated steel plants and are more suitable for many developing countries where supplies of coking coal are limited [9]. Hence, it is concluded that:-

The direct reduction is a process, which extracts high metallic solid iron by removing oxygen from iron ore or any other iron oxides without going through molten stage. It is a solid state reduction process [10]. The product, so formed is known as Directly Reduced Iron or Sponge Iron. The progressive stages of reduction of iron ore to produce Sponge Iron are as follows:



## III. Theory and Methodology

### 3.1 Bhushan Steel Plant (BSL): An Overview

Bhushan Steel Plant, biggest plant is in Odisha, it has signed an agreement with the Government of Odisha for setting up of a three million tons capacity steel plant at Meramandali in Dhenkanal district, and as part of its total integration of the steel value chain, Bhushan Steel is in the process of setting up a power plant and an advanced hot rolling plant on 3,200 acres (13 km<sup>2</sup>) at Meramandali in Dhenkanal district near Angul, at a cost of 52 billion and its subsequent backward integration and expansion to 4 million tons.

### 3.2 Present financial & management status

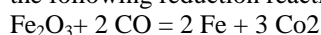
Gross sales of Bhushan Steel grew from Rs.5 billion in 2001 to Rs.40 billion in 2007. It earned net profits of Rs.3.13 billion in 2007 and exported goods worth Rs.12.57 billion. Its exports include steel for both the automotive and white goods industry and the list of countries it is exporting to includes several developed countries.

The Khopoli plant in Maharashtra was commissioned in 2004 and has been producing colour coated sheets, high tensile steel strappings, hardened and (aluminium and zinc coated sheet) for the first time in India, along with CRCA steel to cater the need of Automobile Industry. At its Sahibabad plant in Ghaziabad, Uttar Pradesh, it has a 1700 mm mill, which produces the widest sheets in India for the automotive industry. It has highly automated systems.

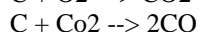
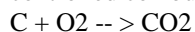
At its Meramandali, Dhenkanal plant in Odisha, Bhushan Steel produces hot rolled coils and has mills for hot rolling. Construction of the first phase and second phase is completed. Bhushan Power and Steel Limited have seven plants at four locations – Chandigarh, Derabassi in Punjab, Bangihatti, near Dankuni in West Bengal, and Thelkolo in Odisha.

## IV. Data collection

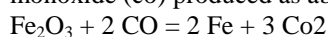
Coal based Direct reduction process is classified based on the reducing agent namely solid. Most solid reduction process use non-coking coal as reducing agent due to abundantly available non-coking coal. The process proposed to be adopted is the rotary kiln proposes using Non-coking coal and iron ore [11]. Iron are undergoes the following reduction reaction in all the processes:



As shown in above reactions, carbon monoxide is reducing gases. These reducing gases can be obtained by controlled combustion of coal, according the boudouard reaction produces carbon monoxide.

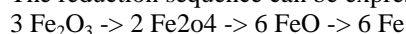


As maintained earlier direct reduction is the conversion of oxide feedstock to the metallic state with such conversion taking place entirely in the solid state (at no time does the material become molten). The carbon monoxide (co) produced as above reduces iron oxide to metallic iron [12].



However, the reduction from oxide to metal does not occur in one step, but by gradual removal of oxygen giving, rise to various intermediary oxides.

The reduction sequence can be expressed as follows:



Hematite, magnetite, wustite iron

## V. Result and discussion

### 5.1 Use of CO gas during shutdown of D.R.I.

Generally rotary Kiln is heated up by LDO (Low density oil) Firing. LDO firing system is inserted through the CB (Central Burner) Pipe. When the LDO firing system is started, LDO is burnt and give coal firing temperature. The temperature is maintained at 500-600 deg Cel. at the Kiln outlet. After attaining the temperature mentioned above the injection fines coal is started from Kiln outlet side. Then after 1-2 Hours of time the Coarse Coal is started according to temperature. It is continued according to the schedule to reach the prescribed temperature. At last feed coal is started from Kiln inlet side up to maintain the feeding temperature. Then feeding of iron ore is started and continued. LDO is firing is continuing for some hour which depends upon the experience of engineers to maintain the temperature of outlet.

All the above work which is done by LDO is can be totally replaced by CO gas in the same procedure which is an ultimate product of Coke Oven. The only change in arrangements is the diameter of CO Gas pipe will be more than the diameter of LDO pipe.

During shutdown period the raw materials i.e. the iron ore, coal & dolomite etc. are not provided to us. So the operation of rotary Kiln is stopped according to schedule for maintenance work of the equipments for few days. If the shut down period is extended for a long period of time it may hamper the smooth condition of the equipment as well as the plant's economy. Keeping it in sight the following experimental projects can be applied.

### Experimental Data:

The data is recorded for the Month of December, 2014 and provided as below:

Table 1: Recorded data for the Month of December, 2014

Date	Avg.CO gas flow (M <sup>3</sup> /H)	Avg. Kiln outlet Temp (°C)	Avg. Kiln inlet Temp (°C)	Elbow duct Temp (°C)	WHRB Temp (°C)	Steam Generation (Ton/Hour)	Cost Benefit (Rupees) Rs.= 650x 1Ton steam
1	9800	27	27	1008	968	33	21450
2	9700	27	27	955	918	30	19500
3	9400	27	27	1008	968	33	21450
4	9500	27	27	978	938	30	19500
5	7000	27	27	965	945	32	20800
6	9700	27	27	1010	970	34	22100
7	9700	27	27	955	915	30	19500
8	9800	27	27	962	922	34	22100
9	7000	27	27	958	918	34	22100
10	9700	27	27	1008	968	33	21450
11	9600	27	27	960	920	30	19500
12	7000	27	27	990	950	31	20150
13	7000	27	27	1010	970	34	22100
14	7000	27	27	970	930	31	20150
15	9500	27	27	980	940	32	20800
16	9800	27	27	1000	960	31	20150
17	9900	27	27	1010	970	34	22100

18	10000	27	27	998	958	35	22750
19	9900	27	27	980	940	32	20800
20	9800	27	27	1010	970	34	22100
21	7000	27	27	1008	968	33	21450
22	9700	27	27	970	930	31	20150
23	10000	27	27	1000	960	35	22750
24	9900	27	27	980	940	32	20800
25	9700	27	27	1000	960	32	20800
26	7000	27	27	1010	970	34	22100
27	9900	27	27	1005	965	33	21450
28	9900	27	27	1010	970	34	22100
29	9800	27	27	1000	960	32	20800
30	9900	27	27	1008	968	33	21450
31	9900	27	27	1010	970	34	22100

Inferences from the above data table are made and shown in figure as follows:

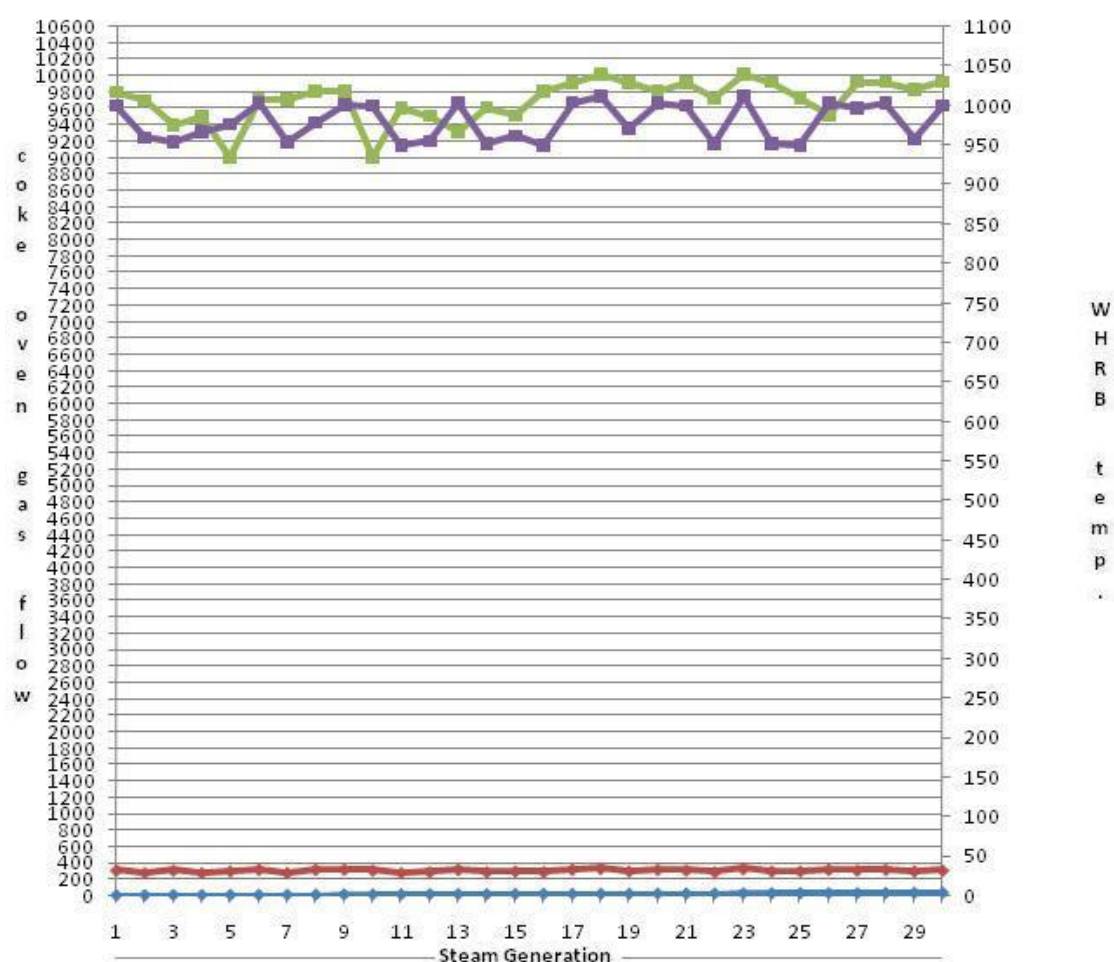


Figure 1: WHRB Temperature, CO gas flow, and steam generation for the above data table

## VI. Conclusion & Scope for future work

### 6.1 Conclusion

From the above data it is concluded that the CO gas that we are providing in this suitable arrangement is much profitable as it is desired for the plant's economy. Thus, the above methodology fulfils the targeted objectives [13].

While summarizing the end effects it has been observed possessing the following characteristics:

- Steam as well as power generation is possible.

- ii. It is a continuous process.
- iii. Zero pollution.
- iv. Less manpower is required.
- v. Less equipment is required.
- vi. One time investment.
- vii. Less maintenance is required.

## 6.2 Scope for future work

- i. Using cold ESP dust in ABC area, the temperature may be increased in WHRB as well as steam generation.
- ii. Using char (the waste or by-product of sponge iron plant), the temperature may be increased in WHRB as well as steam generation.

## References

- [1] Bandyopadhyay A., Ray A. K., Srivastava M. P., Subba Rao S. V. B., Prasad K. K., Bandyopadhyay P. K., Haque R. and Choudhary B. R., Selection of Coals for Rotary Kiln Sponge Iron Plant, Trans. Indian Institute of Metals, 40, (3), p. 209-218, 1987.
- [2] Biswas D. K., Asthana S. R. and Rau V. G., Some Studies on Energy Savings in Sponge Iron Plants, Trans. of ASME, 125, p. 228-237, 2003.
- [3] Elsenheimer G., and Serbent H., The Current Position of the SL/RN Process, Taking into Account Conditions in India, Int. Conf. on Alternative Routes on Iron and Steel under Indian Conditions, Jamshedpur, India, vol. 2, p. 105-110, 1988.
- [4] Jena S. C., Patnaik N. K. and Sarangi A., Heat and Mass Balance in Rotary Kiln Sponge Iron Making, Int. Conf. Alternative Routes on Iron and Steel under Indian Conditions, Jamshedpur, Jan. 11-13, p. 59-64, 1996.
- [5] P. John and B. Richelieu, "Carbon deposits: Formation, nature and characterisation," presented at the COMA/CRF Meeting, United Kingdom, 2006.
- [6] V. Zymala and F. Honnart, "Coke oven carbon deposits growth and their burning off," *ISIJ International*, vol. 47, pp. 1422-1431, 2007.
- [7] S. R. Turns, *An introduction to combustion concepts and applications*, 3rd ed. New York: McGraw Hill, 2012.
- [8] H. S. Caram and N. R. Amundson, "Diffusion and reaction in a stagnant boundary layer about a carbon particle," *Ind. Eng. Chem., Fundam.*, vol. 16, pp. 171-181, 1977.
- [9] F. Yi, J. Fan, D. Li, S. Lu, and K. Luo, "Three dimensional time dependent numerical simulation of a quiescent carbon combustion in air," *J. Fuel*, vol. 90, pp. 1522-1528, 2012.
- [10] T. H. Shih, W. W. Liou, A. Shabbir, Z. Yang, and J. Zhu, "A new k-e eddy-viscosity model for high reynolds number turbulent flows – model development and validation," *Computer Fluids*, vol. 23, pp. 227-238, 2012.
- [11] K. K. Kuo, *Principle of combustion*. New York: John Wiley and Sons, 1986.
- [12] P. Cheng, "Two-dimensional radiating gas flow by a moment method," *AIAA Journal*, vol. 2, pp. 1662-1664, 1964.
- [13] T. F. Smith, Z. F. Shen, and J. N. Friedman, "Evaluation of coefficients for the weighted sum of gray gases model," *J. Heat Transfer*, vol. 104, pp. 602-608, 1982.

**Harish C. Dalai** is presently serving as Manager, Quality Control Department at Bhusan Steels Ltd, India. He obtained his master's degree in Mechanical Engineering from Biju Patnaik University of Technology, India. He has more than 12 years of research & industry experience in India. His research interest includes quality and performance measurement.

**Dr. N C Nayak** obtained his Ph. D in the department of Industrial Engineering and Management and Master's degree in Mechanical Engineering both from Indian Institute of Technology, Kharagpur. He has over 22 years of teaching, research and industry experience in India. Presently he is serving as Associate Professor of Mechanical Engineering Dept. at IGIT Saranga. He has published a number of research papers in International and National Journals and Conferences. His research interest includes operations management, industrial engineering, composites and supply chain management.



## Text Detection in Video Using Haar Wavelet Transformation and Morphological Operator

Dinesh AnnajiKene<sup>1</sup>, Dr. D. J. Pete<sup>2</sup>

Department of Electronics and Telecommunication Engineering,  
DattaMeghe College of Engineering, Airoli, Navi Mumbai – 400708.  
University of Mumbai, India

**ABSTRACT:** This paper presents simple and efficient method for text detection, extraction and localization from video or static images using Haar wavelet and Morphological operator. Haar wavelet transform have its coefficients either 1 or -1, so that the operation speed of Haar wavelet transformation is fastest among all wavelets. The sub bands contain both text edges and non-text edges however the intensity of text edges is different that of the non-text edges. Instead of using Canny operator we used Sobal operator for edge detection because Sobal operator detect more edges than Canny operator when there is text information. Morphological operators are applied to edit or smoothing out the text region. Then detected text regions are further decomposed into character level. Then using some refinement the final text region are obtained.

**Keywords :** CC Based method, Texture based method, Edge based method, optical character recognition (OCR)

### I. INTRODUCTION

A brief history of Video Text detection:- The origin of video text detection research may be traced to document image analysis because of its core techniques in optical character recognition (OCR). Patent on OCR for reading aids for the blind and for input to the telegraph was filed in the Nineteen century and working models were demonstrated by 1916. However the field of document image analysis itself is only about 40 years old, OCR on specifically designed printed digits (OCR fonts) was first used in business in the 1950s. The first postal; address reader and the social security administration machine to read typewritten earnings reports were installed in 1965. Devices to read typeset material and simple hand printed forms came in to their own in 1980s, when the prices of OCR systems dropped by a factor of a 10 due to the advent of microprocessors bit mapped display and solid state scanners. The study of automatic text detection started about three decade ago. In the 1980-95, a lot of methods were proposed.[1]

Video content can be seen as two major categories, “Perceptual content” and “Semantic content”. Perceptual content includes attributes such as colour intensity, shape, texture and their temporal changes, While semantic content includes object, events and their relations. Among them text in images / videos is of particular interest as 1) It is very useful for understanding the content of an image 2) It is very easy to extract compared to other semantic content and 3) It is useful for application such as text based image search and automatic video logging. The semantic gap refers to the different interpretation and meaning of the extracted low level feature (e.g. texture, colour, shape etc.) by the uses with respect to applications. Text in video can be used to fill this gap because in many videos there is considerable amount of text, Video text can thus help to improve the effectiveness of content based image and video retrieval system [1]

Compared with the text in a typical document the text in a video frame is in much smaller quality. However these texts in video often give crucial information about media contents. They usually appears in the form of names, location, products, brands, score of the match, date & time etc. which are helpful information to understand the video contents. The text in images and videos can be superimposed on arbitrary background or embedded on the surfaces of the object in the scene with varying fonts size, colour, alignment, movement and lighting condition. Hence text detection and extraction are extremely difficult.

A large number of approaches such as Connected Components based, Texture based and other methods have been proposed. Some of these methods have already obtained impressive performances. A majority of text detection and extraction approaches in the literature are developed based on scanned document nature, although most of them can be adopted for video images detection and extraction. Text in video presents unique challenges over that in document images, due to many undesirable properties of video for text detection and extraction problem. Fortunately text in video usually persists for at least several seconds to give human viewer sufficient time to read it. This temporal nature of video is very valuable and can be well utilize for text detection, extraction and recognition in video.

## II. RELATED WORK

In order to show that the proposed method is effective and robust in terms of metrics and multi-oriented text lines detection, we have studied variety of related works. In the research book by PalaiahnakoteShivkumara, Chew Lim Tan, Wenyn Liu and Tong Lu, "Video Text Detection" A Research book published by Springer-Verlag London 2014, shows the variety of methods, operators and models for image as well as video text detection. In that book he analyse the minute details of Text Detection in Video and also shows some application oriented methods.[1] P. Shivkumara, TrungQuePhan and Chew Lim Tan in their paper New Fourier Statistical Features in *RGB* Space for Video Text Detection proposed Fourier statistical method for color images, text to convert in gray and then again in color for detection and extraction [2]. As well PlaiahnakoteShivkumara, TrungQuyPhan et al. represented gradient vector flow and grouping based method. [3].

P. Shivkumara, T.Q. Phan and C.L. Tan [3] in their paper A Laplacian Approach to Multi –Oriented Text Detection in Video represented a Laplacian method for multi-oriented text detection [4]. In which it shows that the performance of these methods is low because scene text poses many challenges compared to graphics text. Multi-oriented text has only been partially addressed where the algorithm is limited to caption text and a few selected directions. Recently, addressed this multi-oriented issue in based on Laplacian and skeletonization methods. However, this method still has room for improvement in the following respects: Recall, Precision and F-Measure. [4]

Chung-Wei Liang et.al. used DWT based text localization method in his paper, "DWT Based Text Localization". In which he used Haar wavelet transformation and Morphological operator along with AND operator.[5]

Neha Gupta et. Al. also used Haar Wavelet and Morphological operator in their paper, "Localization of Text in Complex Images using Haarwavlet transformation". For the experimental result they used complex background images as input.[6]

M. Naguet. Al. used Neural network along with wavelet and Morphological operator in their research paper, "Morphological Text Localization using Wavelet and Neural network". Their paper implemented Neural networks for recognition of text character from isolated text images and make it editable. [7]

Narsimha Murthy K N et. Al. in his research paper, "A Novel Method for Efficient Text Extraction from Real Time Images with Diversified Background using Haar Discrete Wavelet Transform and K-Means Clustering" shows that they used real time images for data input and get efficient text output using K-means clustering[8].

## III. PROPOSED SYSTEM

In order to show that the proposed method is effective and robust in terms of metrics and multi-oriented text lines detection, we have considered a variety of datasets which include images and videos of sports news, low contrast, different fonts and size, different orientation etc.

### Methodology

Many efforts have been made earlier to address the problems of text area detection, text segmentation and text recognition. Current text detection approaches can be classified into three categories:

The first category is connected component-based method, which can locate text quickly but have difficulties when text is embedded in complex background or touches other graphical objects.

The second category is texture-based, which is hard to find accurate boundaries of text areas and usually yields many false alarms in "text-like" background texture areas.

The third category is edge-based method. Generally, analyzing the projection profiles of edge intensity maps can decompose text regions and can efficiently predict the text data from a given video image clip.

Text region usually have a special texture because they consist of identical character components. These components contrast the background and have a periodic horizontal intensity variation due to the horizontal alignment of many characters. As a result, text regions can be segmented using texture feature.

### 3.1 Video Preprocessing

Automatic video text detection is extremely difficult so we need video preprocessing to reduce the complexity of the succeeding steps probability consisting of video text detection, localization, extraction, tracking, reconstruction and recognition.

### 3.2 Image Segmentation

In video image segmentation, after inputting an original videos frames image segmentation techniques are employed to extract all the pixels belonging to text. The aim of segmentation is to divide the pixels of each frame from a video clip in to two classes of regions, which do not contain text and region which contain text. A lot of techniques have been developed to perceive images, which in general consist of three layers (as shown in figure) of so called Image Engineering (I. E.), processing (low layer), analysis (middle layer) and understanding (high level). The objective of segmentation is to partition an image in to separated region which ideally composed to interested object and accordingly obtain a more meaningful representation of image. There are some general rules to be followed.

1. They should be uniform and homogenous with respect to specific characteristics.
2. Their interior should be simple enough and without too many small holes.
3. Adjacent regions should have significantly different values with respect to the characteristics on which they are uniform.
4. Boundaries of every segment should be simple, not ragged and must be spatially accurate.

Each image can be segmented in to multiple separated regions using two strategies namely, Bottom-Up & Top-Down segmentation.

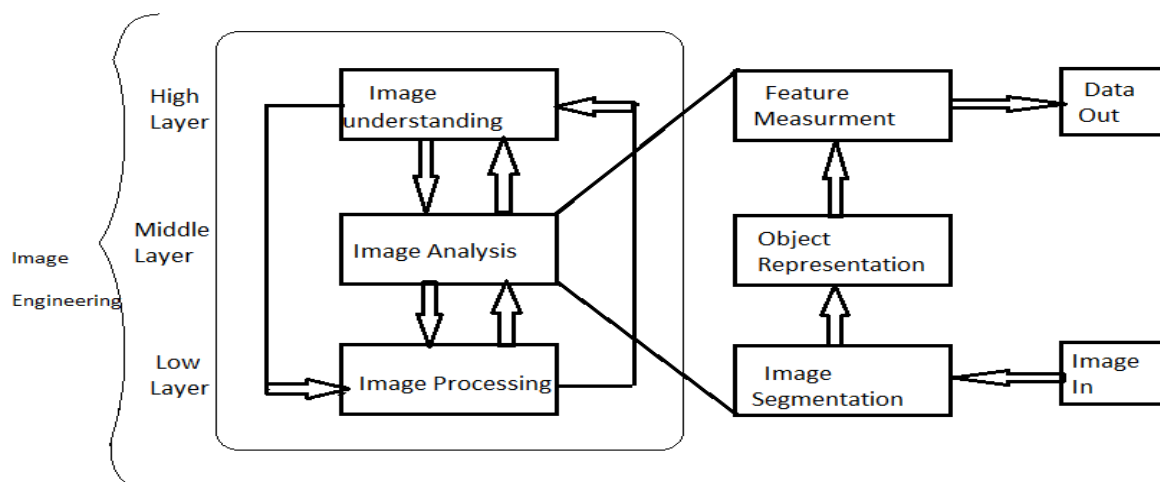


Fig. The Role of Image Segmentation

### 3.3 Pre-processing Operators

The aim of preprocessing operations for video text detection is an improvement of the image data by suppressing undesired degradation and simultaneously enhancing specific text relevant features. There are several preprocessing operators that are either enhance the image feature or suppress the information which is not relevant to video text detection.

#### a) Image Cropping and Local operator :

These are useful for brightness adjustment & contrast enhancement. Commonly used local operators are Multiplication & Addition, Another commonly used operator is Linear Blend operator, which is designed to cross-dissolve two video frames.

b) *Neighborhood operator :*

These operators are used to remove noise and sharpness the image detail. The neighborhood operators are

1. Linear Filter Operator
  - i) Average Filter
  - ii) Median Filter
2. Derivative operator
  - i) Robert operator
  - ii) Sobel operator
  - iii) Laplacian operator

c) *Morphological operator :*

Mathematical Morphology is a tool for extracting image component that are useful in the representation and descriptive of region shape, such as boundaries, skeleton and the convex hull. It is defined fundamental Morphological operation such as Dilation, Erosion, Majority, Opening and Closing to perform such operations. We often need, first convert colorful video frame in to a binary image which has only two elements of either a real foreground or a background complexity with respect to the others.

d) *Color Based Preprocessing :*

A color image is built of several color channels, each of them indicating the value of the corresponding channel. For example, an RGB image consist of three primary color channels of Red , Green and Blue, An HIS model has three intuitive color characteristics as Hue, Saturation and Intensity. These color representation are designed for specific devices and have no accurate definition for a human observer. Therefore color transformation is required to convert the representation of color to gray scale representation.

If the input image is a gray-level image, the image is processed directly starting at discrete wavelet transform. If the input image is colored, then its RGB components are combined to give an intensity image. The pictures are often in the Red-Green-Blue color space. Intensity image Y is given by:

$$Y = 0.299R + 0.587G + 0.114B \quad (1)$$

Image Y is then processed with 2-D discrete wavelet transform. The Y is actually value component of the Hue-Saturation-Intensity (HSI) color space. In stage the color image RGB is converted in to HSI color space, then value component is extracted from HSI color space using above expression.

The RGB to HSI transformation is

$$H = \arctan(\beta/\alpha) \quad (2)$$

$$S = \sqrt{\alpha^2 + \beta^2} \quad (3)$$

$$I = (R+G+B)/3 \quad (4)$$

$$\text{Where } \alpha = R - 1/2 (G + B) \quad , \quad \beta = \sqrt{3}/2 (G - B)$$

The noise of image is reduced by using a medium filtering that is applied on the gray scale image. After this filtering a major part of noise will be removed while the edges in the image are still preserved.

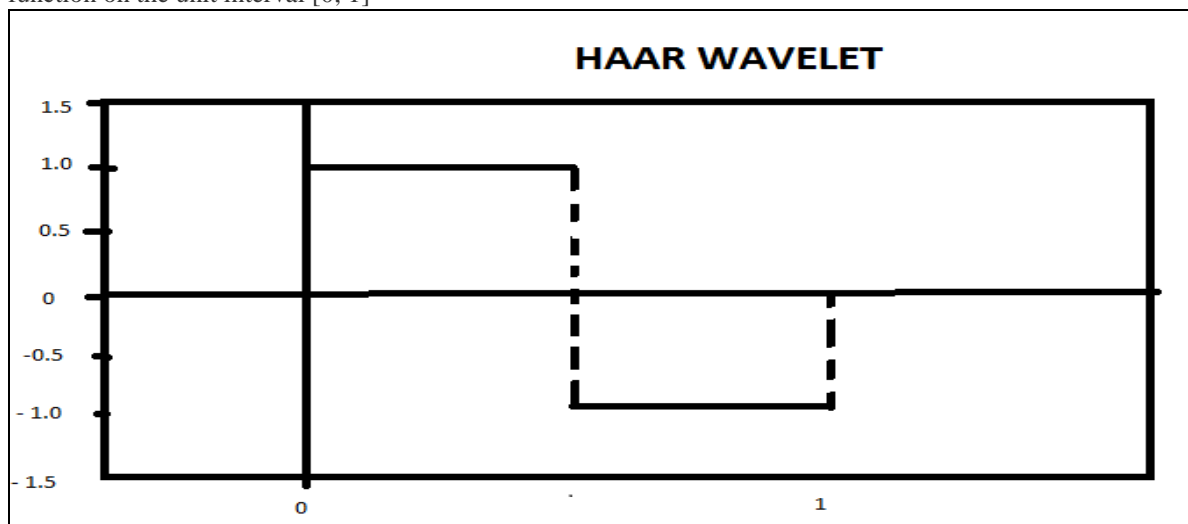
#### IV. WAVELET TRANSFORMATION

Digital image is represented as a two-dimensional array of coefficients, each coefficient representing the intensity level at that coordinate. Most natural images have smooth color variations, with the fine details being represented as sharp edges in between the smooth variations. Technically, the smooth variations in color can be termed as low frequency variations, and the sharp variations as high frequency variations.

The low frequency components (smooth variations) constitute the base of an image, and the high frequency components (the edges which give the details) add upon them to refine the image, thereby giving a detailed image. Hence, the smooth variations are more important than the details. Separating the smooth variations and details of the image can be performed in many ways. One way is the decomposition of the image using the discrete wavelet transform. Digital image compression is based on the ideas of sub-band decomposition or discrete wavelet transforms. Wavelets, which refer to a set of basic functions, are defined recursively from a set of scaling coefficients and scaling functions. The DWT is defined using these scaling functions and can be used to analyze digital images with superior performance than classical short-time Fourier-based techniques, such as the DCT. Shivkumar et.al. used 2-D Haar wavelet decomposition to directly detect video text based on three high frequency sub-band images of LH, HL and HH .after computing features for pixels, K means algorithm is applied to classify the feature vectors in to two cluster of background and text candidates.

## V. HAAR WAVELET

The Haar Wavelet is a sequence of rescaled “Square Shapes “ functions which together form a wavelet family or basis. Wavelet analysis is similar to Fourier analysis in that it allows a target function over an interval to be represented in terms of an orthogonal function basis. The Haar sequence is now recognized as the first known wavelet basis and extensively used as a teaching example. The Haar sequence was proposed in 1909 by Alfred Haar. Haar used these function to give an example of an orthogonal system for the space of square integrable function on the unit interval [0, 1]



The Haar wavelet's mother wavelet function  $\psi(t)$  can be described as

$$\psi(t) = \begin{cases} 1 & 0 \leq t < \frac{1}{2} \\ -1 & \frac{1}{2} \leq t < 1 \\ 0 & \text{otherwise} \end{cases}$$

Its scaling function  $\phi(t)$  can be described as

$$\phi(t) = \begin{cases} 1 & 0 \leq t < 1 \\ 0 & \text{otherwise} \end{cases}$$

#### A. HaarTransform :

The Haar transform is the simplest of the wavelet transform. This transform cross multiplies a function against the Haar wavelet with various shift and stretches like the Fourier transform cross multiplies a function against a sine wave with two phases and many stretches.

The Haar transform is derived from the Haar matrix. An example of a 4 x 4 Haar transformation matrix is shown below.

$$H_4 = \frac{1}{2} \begin{pmatrix} 1 & 1 & 1 & 1 \\ 1 & 1 & -1 & -1 \\ -\sqrt{2} & -\sqrt{2} & 0 & 0 \\ 0 & 0 & \sqrt{2} & \sqrt{2} \end{pmatrix}$$

#### Property

The Haar transform has following properties

- 1) No need for multiplications. It require only addition and there are many element with zero value in the Haar matrix, so the composition time is short , it is faster than Walsh transform whose matrix is composed of + 1 and – 1.
- 2) Input and output length are the same . however the length should be a power of 2  
i.e.  $N = 2^K$ ,  $K \in \mathbb{N}$
- 3) It can be used to analysis the localized feature of signals , Due to the orthogonal property of the Haar function the frequency components of input signal can be analyzed.

### VI. MORPHOLOGICAL OPERATION

Mathematical morphology is a tool for extracting image components that are useful in the representation and descriptive of region shape, such as boundaries, skeletons and the convex hull. It is defined two fundamental morphological operations, dilation and erosion, in terms of the union or intersection of an image with a translated shape called as structuring element. To perform such operations we often need first convert a colorful image which has only two elements of either a real foreground or a background complementary with respect to the other. Morphological operations often take a binary image and structuring element as input and combine them using a set operator (Insertion, Union, Inclusion, Complement). They process object in the input image based on characteristics of its shape which are encoded in the structuring element.

Usually the structuring element is sized 3 X 3 and has its origin at the center pixel. It is shifted over the image and at each pixel of the image its elements are compared with the set of the underlying pixels. If the two sets of elements match the condition defined by the set operator, the pixels underneath the origin of the structuring element is set to a pre-defined value (0 or 1). A Morphological operator is therefore defined by its structuring element and the applied set operator.

### VII. MOTION ANALYSIS

As a preprocessing technique motion vector analysis from temporal frames is believed helpful for video text detection. It produces time dependent information about the motion of both the foreground object and their background to provide hints for identifying text from consecutive video frames. More ever it potentially play a key role in detecting and tracking video text from multiple directions or with occlusions.

The major goals of motion analysis are to refine the text detection in terms of removing false alarms in individual frames interpolating the location of accidentally missed text character and words in individual frames and temporarily localizing the beginning and end of eachword as well as its spatial localization within each frame. Their method proposed for motion analysis is based on the comparison of region in successive frames and includes five typical steps.

1. *Text Tracking*: this step is responsible for tracking the already detected text along with the frames that constitute each text sequence targeting the formation of temporally related chains of characters. Each



character chain here represents the same characters during its existence in a collection of similar regions occurring in several continuous frames. Every time a character region is detected for the first time, a position is stored and a signature is computed for that character region by using the features of luminance, size and shape. Each frame contributes with one region classified as a character chain.

2. *Text Integration* :- this step groups the character chains in order to form word based on the spatial and temporal analysis of each character chain. Three temporal elements are adopted a) Temporal coexistence b) Duration and c) Motion. The chain not include in words at this phase are considered as noise and are discarded.
3. *Character Recovery* :- Video temporal redundancy is explored to complete the words with missing character as least for some frames e.g. due to noise or too textured background. In order to complete the words they are extended to the size of their biggest chain of character and the characters missing in the chains are recovered by means of temporal interpolation with motion composition. Thus by using temporal redundancy, the text detection for each frame is improved by completing the words with missing character for some frames
4. *Elimination of overlapped words*:- It is important to improve the performance for scene text usually, overlapping of words occurs when false words are detected e.g. due to shadow or three dimensional text. Every time two or more words overlap more precisely their bounding boxes overlap at least for one frame, the words with smaller area are discarded.
5. *Text Rotation* :- This steps perform the rotation of the text to the horizontal position in order to be recognized OCR system.

### VIII. RESULTS

The results of the work of first stage Localizer are computed in the following manner:

1. Created dataset with various Text images and videos
2. Colour images and frames of videos are converted in to Gray scale
3. Texture of text area analysed by Haar wavelet transformation
4. Localized the text region or segments using Connected Component method ( Bottom Up approach) and Sobal operator.
5. Used Morphological operator to edit the localized text region.
6. Resize the image .
7. Adjust Gray colour at extracting place with neighbours colour.
8. Label the connected component region.
9. Apply the bounding boxes.
10. Convert the image again back from gray to RGB scale by comparing colours of the starting image.
11. Display the result.

The results of the work of second stage Localizer are computed in the following manner:

1. After 1<sup>st</sup> localizer output, the detected text region further decomposed in character level using Connected Component and Morphological operator.
2. Applied the bounding box.
3. Display the result.

The results of the work of Third stage Localizer are computed in the following manner.

1. Eliminate the lines of bonding box.
2. Resize the text region using Connected Component major axis lenth& minor axis length, pixel index list.
3. Used again Morphological operator to edit the detected text .
4. Label the text region.
5. Display the result

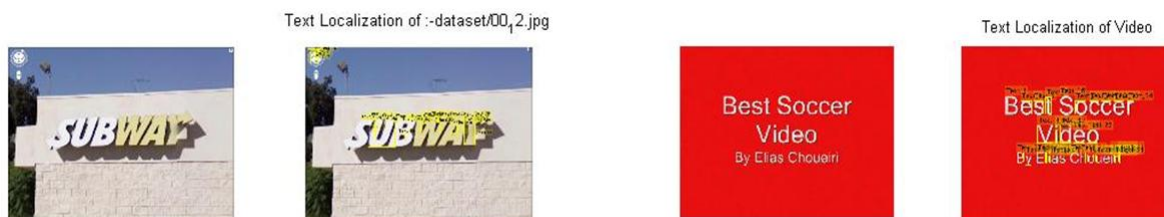
#### Result of Localizer 1

Result of image 1.1 Result of Video frame 1.1

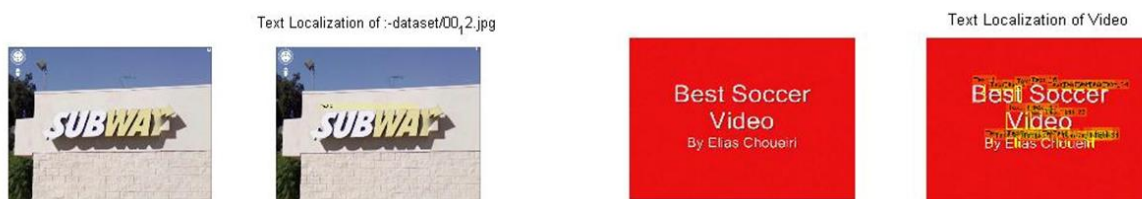


**Result of Localizer 2**

Result of image 2.1 Result of Video frame 2.1

**Result of Localizer 3**

Result of image 3.1 Result of Video frame 3.1

**IX. CONCLUSION & FUTURE SCOPE**

In this work, we present a relatively simple and effective algorithm for text detection and extraction in videos by applying DWT to the images. As it requires less processing time which is essential for real time application. Mostly all the previous methods fail when the character are not aligned well or when the characters are too small. They also results in some missing character when the character have very poor contrast with respect to the background. But this algorithm is not sensitive to image color or intensity, uneven illumination and reflection effects. This algorithm can be used in large variety of application fields such as vehicle license plate detection to detect number plate of vehicle [5], mobile robot navigation to text based land marks, object identification of various parts in industrial automation, analysis of technical papers with the help of charts, maps, and electrical circuits etc. this algorithm can handle both scene text images and printed documents. In future work we plan to exploit the colour homogeneity of text in video, temporal text detection from frame to frame, Multi-frame integration for image enhancement.

**X. REFERENCES**

- [1] PalaiahnakoteShivkumara, Chew Lim Tan, Wenyin Liu and Tong Lu, "Video Text Detection" *A Research book published by Springer- Verlag London* 2014.
- [2] P. Shivakumara, TrungQuyPhan and Chew Lim Tan, "New Fourier-Statistical Features in RGB Space for Video Text Detection", *IEEE Transactions on CSVT*, VOL. 20, NO. 11, pp 1520-1532., November 2010
- [3] PalaiahnakoteShivkumara and TrungQuyPhan, "Gradient Vector Flow and Grouping-based Method for Arbitrarily Oriented Scene Text Detection in Video Images". *IEEE Transaction on circuits and systems for video technology*, Vol.23, No.10, pp1729-1738, October 2013
- [4] P. Shivakumara, T. Q. Phan and C. L. Tan, "A Laplacian Approach to Multi-Oriented Text Detection in Video", *IEEE Transactions on Pattern Analysis and Machine Intelligence*, Vol.33, No.2, pp 412-419, February 2011
- [5] Chung-Wei Liang and Po-Yueh Chen, "DWT Based Text Localization", *International Journal of Applied Science and Engineering*, pp.105-116, 2004
- [6] Neha Gupta and V. K. Banga, "Localization of Text in Complex Images using Haarwavlet transformation" *International Journal of Innovative Technology and Exploring Engineering(IJITEE)*, Vol-1, Issue-6, pp 111-115, November 2012
- [7] M. Nagu, B. Raja Rao, "Morphological Text Localization using Wavelet and Neural network". *International Journal of Computer Science and Information Technology(IJCSIT)*, Vol-2(2), Issue-6, pp 891-896, 2011
- [8] Narsimha Murthy K N et. al., "A Novel Method for Efficient Text Extraction from Real Time Images with Diversified Background using Haar Discrete Wavelet Transform and K-Means Clustering" *International Journal of Computer Science issues (IJCSI)*, Vol-8, Issue-5, pp 235-245, 2011

## Strain Based Finite Element for Cylindrical Shell under Sinusoidal Loads

A. Mousa<sup>1</sup>, Ahmed E. Al-Juaidi<sup>2</sup>

<sup>1</sup>Department of Civil and Architectural Engineering, College of Engineering, University of Bahrain, Kingdom of Bahrain

<sup>2</sup>Civil and Environmental Engineering, Utah State University, Logan, Utah 84322, United States of America

**ABSTRACT:** A cylindrical triangular finite element is developed in this paper. The element has only five essential nodal degrees of freedom (Three general external degrees of freedom and two rotations) at each of the three corner nodes. The displacement fields of the element satisfy the exact requirements of rigid body modes of motion. Shallow shell formulation is used and the element is based on an independent strain assumption insofar as it is allowed by the compatibility equations. A cylindrical shell problem for which a previous solution exists is first analyzed using the new element to validate the program and to compare the results. The element is then used in the analysis of cylindrical shell subjected to uniformly distributed load varying sinusoidal along its length in addition to symmetric sinusoidal edge loads present along its longitudinal boundaries. The distribution of various components of stresses is obtained and the effect of radius-length ratio is also presented to give the designer an insight for the behavior of such structures.

**Keywords** -Strain-based, cylindrical triangular finite element.

### I. INTRODUCTION

Considerable attention has been given applying the finite element method of analysis to curved structures. The early work on the subject was presented by Grafton and Strome (1963) who developed conical segments for the analysis of shells of revolution. Jones and Strome (1966) modified the method and used curved meridional elements which were found to lead to considerably better results for the stresses.

Further research led to the development of curved rectangular as well as cylindrical shell elements (Connor *et al*, 1967; Bogner *et al*, 1967; Cantin *et al*, 1968 and Sabir *et al*, 1972). However, to model a shell of arbitrary or triangular shape by the finite element method, a triangular shell element is needed. Thus many authors have been occupied with the development of curved triangular shell elements and consequently many elements (Lindberg *et al*, 1970 and Dawe, 1975) resulting in an improvement of the accuracy of the results. However, this improvement is achieved at the expense of more computer time as well as storage to assemble the overall structure matrix.

Meanwhile, at the United Kingdom, a simple alternative approach has been used to the development of curved elements. This approach is based on determining the exact terms representing all the rigid body modes together with the displacement functions representing the straining of the element by assuming independent strain functions insofar as it is allowed by the compatibility equations.

This approach has successfully employed in the development of curved shell elements (Ashwell *et al*, 1971, 1972; Sabir *et al*, 1975, 1982, 1983, 1987; El-Erris, 1994, 1995 and Mousa, 1994, 1998, 2012). These elements were found to yield faster convergence with other available finite elements. The strain-based approach is employed in the present paper to develop a new triangular strain-based cylindrical element having only five degrees of freedom at each corner node.

The new element is first tested by applying it to the analysis of a clamped barrel vault for which a previous solution exists.

The work is then extended to the analysis of a cylindrical shell subjected to uniformly distributed load varying sinusoidal along its length and symmetric sinusoidal edge loads present along its longitudinal boundaries. The distribution of the various components of stresses is obtained to give designers an insight into the behavior of such structures.

## II. THEORETICAL CONSIDERATION OF THE DISPLACEMENT FUNCTIONS FOR THE NEW CYLINDRICAL ELEMENT

In a system of curvilinear coordinates, the simplified strain-displacement relationship for the cylindrical shell element shown in Fig. (1) can be written as:

$$\begin{aligned}\varepsilon_x &= \frac{\partial u}{\partial x} + \frac{w}{R}, \quad \varepsilon_y = \frac{\partial v}{\partial y}, \quad \gamma_{xy} = \frac{\partial u}{\partial y} + \frac{\partial v}{\partial x} \text{ and} \\ K_x &= \frac{\partial^2 w}{\partial x^2}, \quad K_y = \frac{\partial^2 w}{\partial y^2}, \quad K_{xy} = -2 \frac{\partial^2 w}{\partial x \partial y}\end{aligned}\quad (1)$$

Where  $u, v$  and  $w$  are the displacement in the  $x, y$  and  $z$  axes,  $\varepsilon_x, \varepsilon_y$  are the in-plane direct axial and circumferential strains and  $\gamma_{xy}$  is the in-plane shearing strain. Also  $K_x, K_y, K_{xy}$  are the mid-surface changes of curvatures and twisting curvature respectively and  $R$  is the principle radii of curvature.

Equation (1) gives the relationships between the six components of the strain and three displacement  $u, v$ , and  $w$ . Hence, for such a shell there must exist three compatibility equations which can be obtained eliminating  $u, v$  and  $w$  from equation (1).

This is done by a series of differentiations of equation (1) to yield the following compatibility equations:

$$\begin{aligned}\frac{\partial^2 \varepsilon_x}{\partial y^2} + \frac{\partial^2 \varepsilon_y}{\partial x^2} + \frac{\partial^2 \gamma_{xy}}{\partial x \partial y} + \frac{K_y}{R} &= 0 \\ \frac{\partial K_{xy}}{\partial x} - 2 \frac{\partial K_y}{\partial y} &= 0 \\ \frac{\partial K_{xy}}{\partial y} - 2 \frac{\partial K_x}{\partial x} &= 0\end{aligned}\quad (2)$$

To keep the triangular element as simple as possible, and to avoid the difficulties associated with internal and non-geometric degrees of freedom, the essential five degrees of freedom at each corner node are used, namely  $u, v, w, \frac{\partial w}{\partial x}, \frac{\partial w}{\partial y}$ . Thus, the triangular cylindrical element, to be developed has a total of fifteen degrees of freedom and  $15 \times 15$  stiffness matrix.

To obtain the rigid body components of the displacement field, all the strains, as given by equations (1), are set to zero and the resulting partial differential equations are integrated. The resulting equations for  $u, v$ , and  $w$  are given by:

$$\begin{aligned}u_1 &= -\frac{a_1 x}{R} - a_2 \left( \frac{x^2}{2R} \right) - \frac{a_3 xy}{R} + a_4 + a_6 y \\ v_1 &= -a_2 \left( \frac{x^2}{2R} \right) + a_5 - a_6 x \frac{\partial K_{xy}}{\partial y} - 2 \frac{\partial K_x}{\partial x} \\ w_1 &= a_1 + a_2 x + a_3 y\end{aligned}\quad (3)$$

Where  $u_1, v_1$ , and  $w_1$  are the rigid body components of the displacement fields  $u, v$ , and  $w$ , respectively, and are expressed in terms of the six independent constants  $a_1, a_2, \dots, a_6$ .

Since the element has fifteen degrees of freedom, the final displacement fields should be in terms of fifteen constants. Having used six for the representation of the rigid body modes, the remaining nine constants are available for expressing the straining deformation of the element. These nine constants can be apportioned among the strains in several ways, for the present element we take:

$$\begin{aligned}\varepsilon_x &= a_7 - \frac{1}{R} \left( a_{12} \frac{y^2}{2} + a_{13} x \frac{y^2}{2} + a_{14} \frac{y^3}{6} \right) \\ \varepsilon_y &= a_8 \\ \gamma_{xy} &= a_9 \\ K_x &= a_{10} + a_{11} xy \\ K_y &= a_{12} + a_{13} x + a_{14} y \\ K_{xy} &= a_{15} + [a_{11} x^2 + 2 a_{13} y]\end{aligned}\quad (4)$$

In which the un-bracketed independent constants terms in the above equations were first assumed. The linking bracketed terms are then added to satisfy the compatibility equation (2).

Equations (4) are then equated to the corresponding expressions, in terms of  $u, v$  and  $w$  from equations (1) and the resulting equations are integrated to obtain:

$$\begin{aligned} u_2 &= a_7x + \frac{a_9y}{2} + \frac{a_{10}x^3}{6R} + \frac{a_{11}x^4y}{24R} + a_{15}\left(\frac{x^2y}{4R}\right) \\ v_2 &= a_8y + \frac{a_9x}{2} - \frac{a_{11}x^5}{120R} - a_{15}\left(\frac{x^3}{12R}\right) \\ w_2 &= -\frac{a_{10}x^2}{2} - \frac{a_{11}x^3y}{6} - \frac{a_{12}y^2}{2} - \frac{a_{13}xy^2}{2} - \frac{a_{14}y^3}{6} - \frac{a_{15}xy}{2} \end{aligned} \quad (5)$$

The complete displacement functions for the element are the sum of corresponding expressions in equations (3) and (5). The rotation about the  $x$  and  $y$ -axes respectively, are given by:

$$\begin{aligned} \varphi_y &= -\frac{\partial w}{\partial x} = -a_2 + a_{10}x + \frac{a_{11}x^2y}{2} + \frac{a_{13}y^2}{2} + \frac{a_{15}y}{2} \\ \varphi_x &= -\frac{\partial w}{\partial y} = -a_3 + \frac{a_{11}x^3}{6} - a_{12}y - a_{13}xy - \frac{a_{14}y^2}{2} - \frac{a_{15}x}{2} \end{aligned} \quad (6)$$

The complete displacement functions are the sums of corresponding expressions from equations (3) and (5).

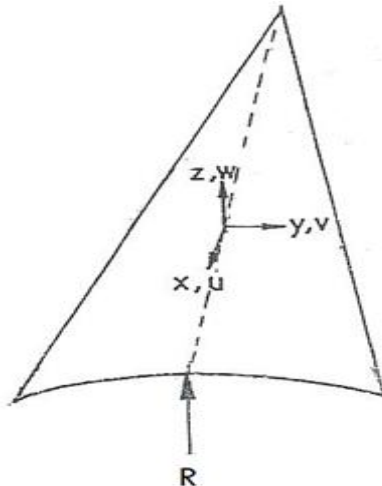


Fig. 1. Coordinate system for a triangular cylindrical shell element

Having derived the final expression for the displacement functions, it is now possible to obtain the elemental stiffness  $[K]$  for the cylindrical shell element in the usual manner using the following equations:

$$K = [C^{-1}]^T \left\{ \iint B^T B dx dy \right\} [C]^{-1} \quad (7)$$

where  $B$  and  $D$  are the strain and rigidity matrices, respectively, and  $C$  the matrix relating the nodal displacement to the constants  $a_1$  to  $a_{15}$ .  $B$  can be calculated from equations (1), (3), (4) and  $D$  is given by substituting the matrices  $B$  and  $D$  into equation (5). The integration within the bracketed terms of equation (5) are carried out explicitly and the rest are computed to obtain the stiffness matrix  $[K]$ .

### III. PATCH CONVERGENCE TEST

This test is to be considered which is frequently used to test the performance of the shell elements is that of Scordelis-Lo Roof having the geometry as shown in Fig. (2). The shell has the following dimensions and

material properties: thickness,  $t = 0.03$  m,  $R = 3$  m,  $L = 6$  m,  $\alpha = 40^\circ$ , modulus of elasticity,  $E = 3$  Pa, Poisson's ratio,  $\mu = 0.0$ , density,  $\rho = 0.625$  Pa. The straight edges are free while the curved edges are supported on rigid diagrams along their plan considering the symmetry of the problem only one quarter of the roof is analyzed.

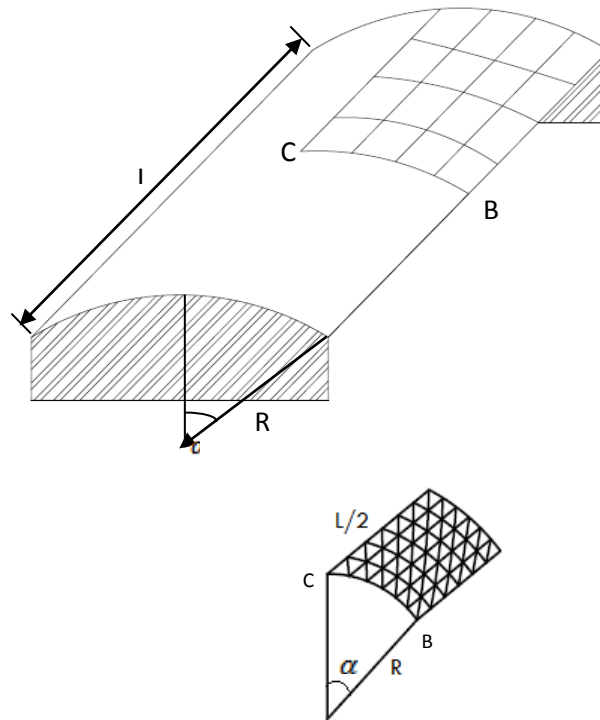


Fig. 2. Geometry and finite element mesh of the roof

The results obtained by the new present element for the vertical displacement at the midpoint B of the free edge and the center C of the roof are compared to other kinds of shells elements (Batoz *et al*, 1992 and Hamadi *et al*, 2000). The analytical solution of this problem is based on the shallow shell theory is given by Scordelis and Lo (1969). Convergence curves (Fig 3 and Fig 4) show that the convergence of the present element faster convergence than the other. Then the new present element would be more efficient to use it in the analysis of proposed cylindrical shell under loads.

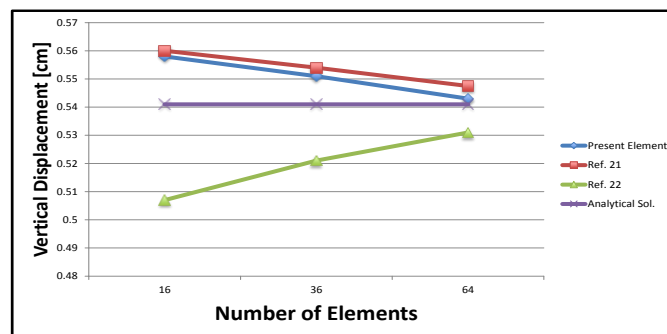
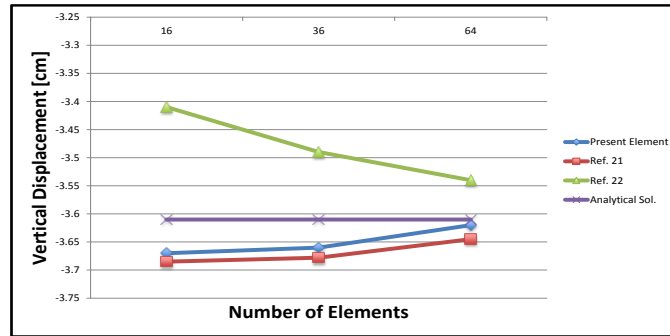


Fig. 3 Convergence curve for the deflection,  $w$ , at point C



Fig. 4 Convergence curve for the deflection,  $w$ , at point B

#### IV. PROBLEM CONSIDERED

An open barrel cylindrical shell is analyzed under uniform surface load varying sinusoidally in addition to the sinusoidal symmetric edge loads present along the longitudinal boundaries. The geometric properties of the shell is shown in Fig.(5). The shell has the following geometry and properties;  $L=26.67$  m,  $R=8$  m,  $\alpha = 45^\circ$ , thickness  $t=80$  mm,  $E=25 \times 10^6 \frac{kN}{m^2}$ ,  $\mu = 0.2$  and the applied load  $q = 3.25 \frac{kN}{m^2}$ , the distribution of this load is based on the following equation:  $q \sin\left(\frac{\pi x}{L}\right)$

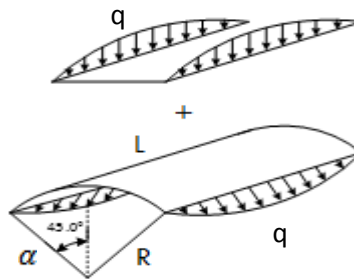
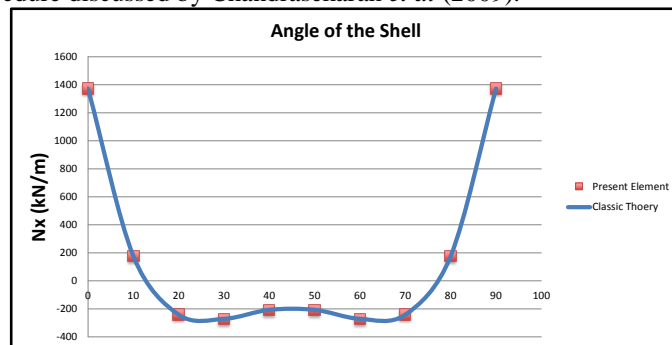
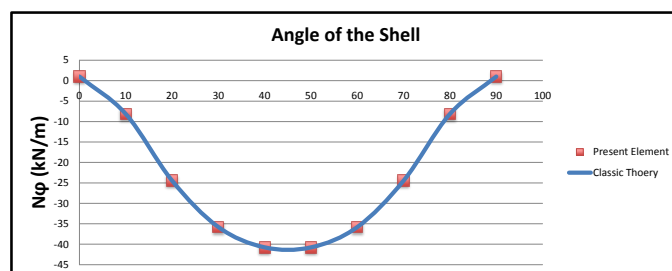
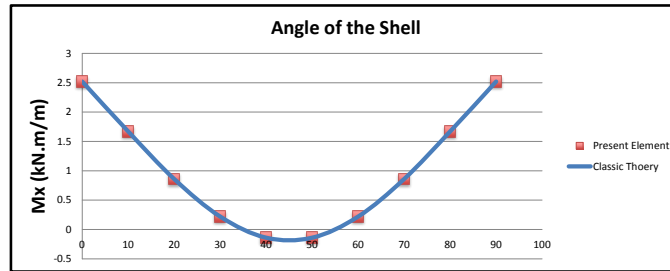
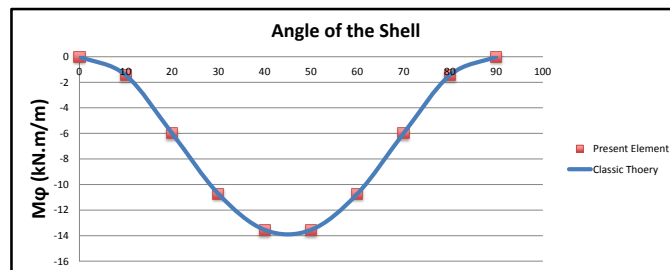
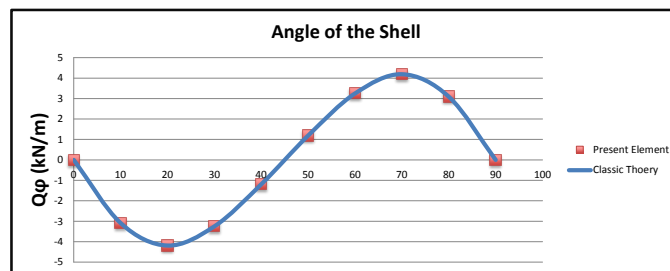


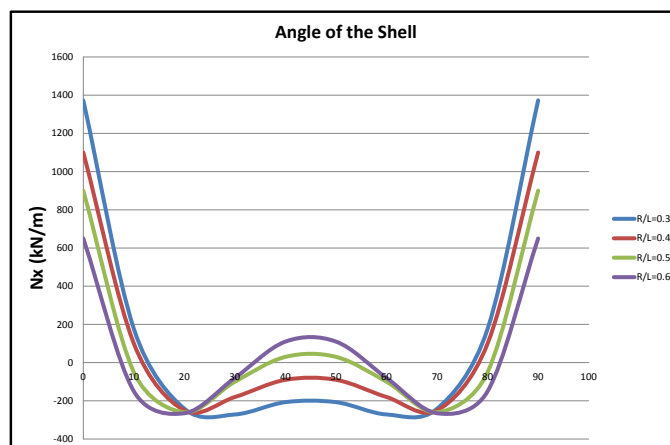
Fig. 5. Geometry and loads on the shell

Figs. (6-10) show the stress resultant for the problem considered. It is seen that the obtained results on the basis of the proposed present element very closely agree with these obtained from the analysis based on classic flexure theory procedure discussed by Chandrasekaran *et al* (2009).

Fig. 6 Axial stress resultant  $N_x$ , at distance  $L/2$ Fig. 7 Axial stress resultant  $N_\phi$ , at distance  $L/2$

Fig. 8 Bending stress resultant  $M_x$ , at distance  $L/2$ Fig. 9 Bending stress resultant  $M_\phi$ , at distance  $L/2$ Fig. 10 Stress resultant  $Q_\phi$ , at distance  $L/2$ 

The work is extended to study the effect of radius length ratio on behavior of the cylindrical shell problem. Figs. (11-15) show the stresses resultant for different radius length ratio ( $R/L = 0.3, 0.4, 0.5, 0.6$ ). It's clear that the various stress resultants are decreased by increasing the radius length ratio.

Fig. 11 Stress resultant  $N_x$ , at different radius length ratio

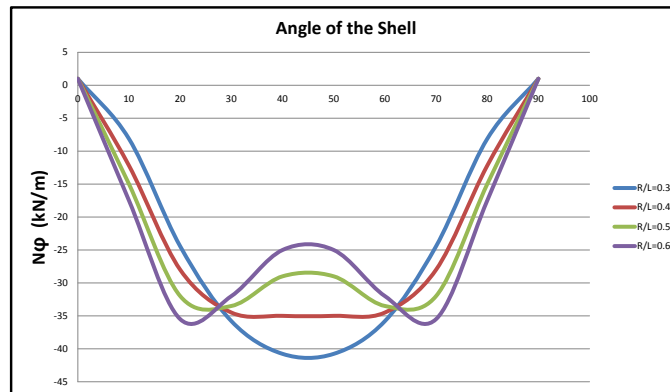


Fig. 12 Stress resultant  $N\phi$ , at different radius length ratio

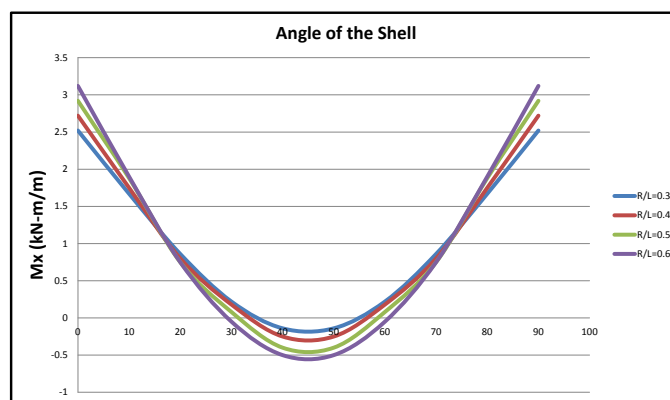


Fig. 13 Stress resultant  $M_x$ , at different radius length ratio

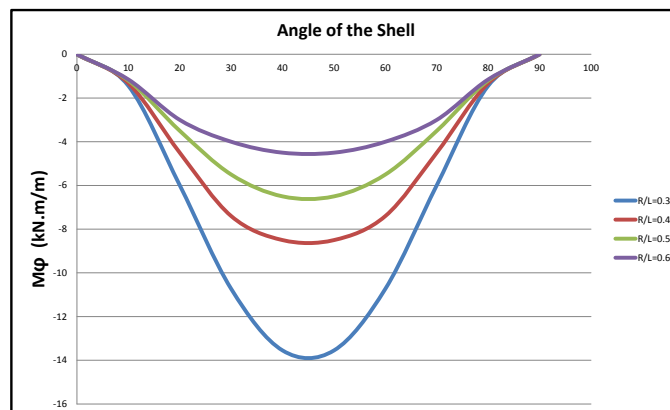


Fig. 14 Stress resultant  $M\phi$ , at different radius length ratio

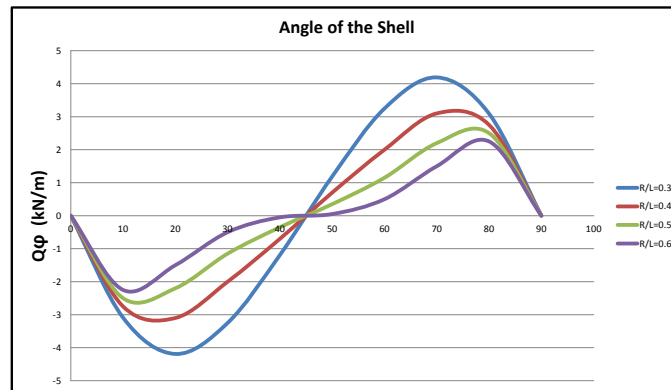


Fig. 15 Stress resultant  $Q\phi$ , at different radius length ratio

## V. CONCLUSION

A new triangular strain-based finite cylindrical element is developed using shallow shell formulation. The element has the essential five degrees of freedom at each corner node.

The developed triangular cylinder finite element is first applied to analysis of a clamped barrel vault. The results for the deflections is presented and shows that the developed element has a very good agreement results. This element is then used to analyze a cylindrical shell subjected to uniformly distributed load varying sinusoidal along its length and symmetric cylindrical edge sinusoidal load presented along its longitudinal boundaries.

The effect of the radius length ratio on the various stresses components is presented.

It's seen the various stresses components is decreased by increasing the radius length ratio. This gives the designers an insight for the behavior of such structures.

## REFERENCES

- [1] Grafton P.E. and Strome. D.R., Analysis of axisymmetric shells by the direct stiffness method AIAA. *J.1*.1963, 2342-2347.
- [2] Jones. R.E. and Strome. D.R., Direct stiffness method analysis of shells of revolution utilizing curved elements, AIAA. *J.(4)*.1966, 15159-1525.
- [3] Conner. J.J. and Brccbia, C., Stiffness matrix for shallow rectangular shell element, *J. Eng. Mech. Div. ASCE*.93. No EMS. 1967, 41-65.
- [4] Bogner. F.K. Fox. R.L. and Schmit. I. A., A cylindrical shell discrete element, *J. AIAA*. 5(4).1967, 745-750.
- [5] Cantin. G. and Clough. R. W., A curved cylindrical shell finite element, *AIAA J.16*. 1968, 1057-1062.
- [6] Sabir. A.B. and Lock A.C., A curved cylindrical shell finite element, *Int. J. Mech. Sci.14*. 1972, 125-135.
- [7] Lindberg. G.M. Cowper. G. R. and Olson. M.D., A shallow shell finite element of triangular shape, *Int. J. Solids Struct* 14.1970, 1133-1156.
- [8] Dawe. D.J., High order triangular finite element for shell and analysis, *Int. J. Solids Struct*.11.1975, 1097-1110.
- [9] Ashwell. D. G. Sabir. A. B. and Roberts T. M., Further studies in the application of curved finite element to circular studies, *Int. J. Mech. Sci.14*.1971, 507-517.
- [10] Ashwell. D. G. and Sabir. A. B., A new cylindrical shell finite element based on simple independent strain functions, *Int. J. Mech. Sci.14*.1972, 171-183.
- [11] Sabir. A. B., Stiffness matrices for general deformation (out of plane and in-plane) of curved beam members based on independent strain functions, *The Maths of Finite Elements and Applications II. Academic Press*.34.1975, 411-421.
- [12] Sabir. A. B. and Charchafchi. T. A., Curved rectangular and general quadrilateral shell element for cylindrical shells, *The Maths of Finite Elements and Applications IV. Academic Press*.1982, 231-238.
- [13] Sabir. A. B., Strain based finite for the analysis of cylinders with holes and normally intersecting cylinders, *Nuclear Eng. and Design* 76.1983, 111-120.
- [14] Sabir. A. B. Strain based shallow spherical shell element, *Proceedings Int. Conf. on the Mathematics of Finite Element and Applications*, Brunel University, 1987.
- [15] El-Erri, H. F., Behavior of hipped roof structures, *Proc. 2nd. MCE Eng. Con., CEI, Baghdad*, 1994.
- [16] El-Erri, H. F., Effect of eccentricity of crown and edge beams on the behavior of hipped roof structures, accepted for publishing in the journal of military college of engineering, Baghdad, 1995.
- [17] El-Erri, H. F., A general shell finite element with in-plane rotation, *J. Al-Muhandis of the University of Technology, Baghdad*, No. 130. 1997.
- [18] Mousa. A. I. and Sabir. A. B., Finite element analysis of fluted conical shell roof structures, *Computational structural engineering in practice. Civil Comp. Press*, ISBN 0-948748-30-X . 1994, 173-181.
- [19] Mousa. A. I., Finite element analysis of a gable shell roof, *Advances in Civil and Structural of Engineering Computing for Paretic civil-comp press*, 1998. 26-268.
- [20] Mousa A.I, Aljuadi A.E, Kameshki E. Dahman, N, New strain cylindrical rectangular finite element for the analysis of arch dam, *Canadians Journal on Environment, Construction and Civil Engineering, Canada*. 2012.
- [21] J. L. Batoz and G. Dhatt, Modelisation des structures par elements finis, Vol. 3: *Coques*, Eds Hemes, Paris, 1992.
- [22] D. Hamadi and M. T. Belarbi, Experimental and numerical analysis of an elliptical paraboloid shell structure, *The Eight Arab Structural Engineering Conference*, 21-23, pp 109-118, Cairo University Faculty of Engineering, 2000.
- [23] C. Scordelis and Lo, K. S., Computer analysis of cylindrical shells, *J. Amer. Concrete Institute*, Vol. 61, 1969, 539-561.
- [24] Chandrasekaran et al, Design aids for fixed support reinforced concrete cylindrical shells under uniformly distributed loads, *International Journal of Engineering Science and Technology*, Vol. 1, No. 1, 2009, 148-171.



## A study of propagation path-loss models

Nwaokoro Amaka Ann<sup>1</sup>, Emerole Kelechi Chukwunonyerem<sup>3</sup>

<sup>1,2</sup> (Department of Electrical and Electronics Engineering, Federal University of Technology, Owerri, Imo State, Nigeria)

**ABSTRACT :** An Empirical model is efficient and simple to use, as it is obtained from in-depth field measurement. The input data here are qualitative, though not very correct for area like dense urban area, rural area and others. On the other hand, Site-specific models are based on numerical methods and the finite difference time-domain (FDTD) technique. The input data here are very precise and in depth while Theoretical models are obtained from physical hypothetical assumption with inclusion of some moderate conditions. This can be seen when, for instance, considering the over-root top, the diffraction model here is obtained by the use of physical optics with the assumption of constant heights and buildings spacing.

**Keywords -** free, time, domain, path, propagation, cost, power

### I. FREE SPACE PROPAGATION MODEL

Free space propagation model assumes that there is no obstacle between the transmitter and receiver during signal propagation. The transmitter radiates signal to an infinite distance without any issue of signal absorption or reflection. If the transmitter propagates signal at 360° using a fixed power with an ever increasing sphere, then the transmitter will have a power flux of

$$P_d = P_t / 4\pi d^2 \quad 1$$

Where  $P_t$  is the power transmitted ( $\text{W/m}^2$ )

$P_d$  is the power obtained when the distance is  $d$  from antenna (1).

According to (2), free space propagation model shows that the signal received by the receiver decays with distance between the transmitter and receiver at a rate of 20dB/decade.

The path loss for free space model is given. Thus;

$$PL_{FSPL} = 32.45 + 20 \log_{10}(d) + 20 \log_{10}(f) \text{ [dB]} \quad 2$$

Where;

$f$  is the frequency in MHz

$d$  is the distance between transmitter and receiver km

(3), (4), (5).

### II. HATA PROPAGATION MODEL

The Hata model is a set of equation obtained on measurements and extrapolations taken from curves that are derived by Okumura. It is an empirical formula for graphical path loss. (1), (2).

Hata presented the prediction area into three divisions: Open, suburban and urban areas. This model is appropriate for frequency range of 150-1500 MHz (UHF) and for distance of 1km-20km. However, Hata model does not consider terrain profile like hills that are found between transmitter and receiver. (2)

In the words of (3), Hata model for calculation of path loss are used in three situations namely:

**Situation1:** Urban Hata pathloss

$$PL = 69.55 + 26.16 \log_{10}(f) - 13.82 \log_{10}(hb) + (44.9 - 6.55 \log_{10}(hb)) \log_{10}(d) + s - a(hm) \quad 3$$

**Situation 2:** Suburban Hata pathloss

$$PL = PL_{Urban} - 2((\log_{10} f / 28))^2 - 5.4 \quad 4$$

**Situation 3:** Rural Hata pathloss

$$PL = PL_{Urban} - 4.78 (\log_{10}(f))^2 + 18.33 \log_{10}(f) - 40.98 \quad 5$$

Where the MS (Mobile station) antenna correction factor for the entire above situation is:

$$a(h_m) = 1.11 \log_{10}(f) - 0.7 h_m - (1.56 \log_{10}(f) - 0.8) \text{ in dB} \quad 6$$



$f$  is the frequency in MHZ

$h_m$  is the height of the mobile antenna in meters

$h_b$  is the height of the base station antenna in meters (1), (3), (5)

### III. SUI MODEL

This stands for Stanford university Interim model. It is developed by Stanford University for frequency band of 2.5GHZ. In this model, the height of the base station antenna can be any value between 10m to 80m while that of the receiver can be between 2m to 20m based on (5).

The SUI model listed out three classes of terrain namely: terrain A, B, and C. According to (6) and (5), terrain A is suitable for dense urban locality, terrain B for hilly regions, while terrain C is appropriate for rural community with considerable vegetation. The authors also stated that the basic pathloss equation of the Stanford university interim model is thus:

$$PL = A + 10\gamma \log_{10}(d/d_0) + X_f + X_h + S \text{ for } d > d_0 \quad 7$$

Where,

$d$  is the distance between Base Station and Receiving antenna (m)

$d_0$  is 100 meters

$\lambda$  is wavelength in meters.

$X_f$  is the correction for frequency

$X_h$  is the correction for receiving antenna height in meters

$S$  is the correction for shadowing in dB

$\gamma$  Is the path loss exponent

(5) further stated that random variables can be taken as the path loss exponent  $\gamma$  while the weak fading standard should be derived. Hence, the parameter A, which is the Attenuation is presented as,

$$A = 20 \log_{10}(4\pi d_0/\lambda) \quad 8$$

$$\gamma = a - b h_b + (c/h_b) \quad 9$$

Where;

$h_b$  is base station antenna height which is between 10m to 80m.

Constant a, b, and c depend on the terrain type.

The value of  $\gamma$  is 2 for free space,  $3 < \gamma < 5$  for urban NLOS environment, and  $\gamma > 5$  for indoor propagation.

Also;

$$X_f = 6.2 \log_{10}(f/2000) \quad 10$$

$$X_h = -10.9 \log_{10}(h_f/2000) \quad 11$$

### IV. ECC-33 MODEL

The ECC-33 model stands for Electronic communication committee-33 model. ECC extrapolated the Okumura measurements and amended its assumption to closely depict a fixed wireless access system (7). This path loss model, otherwise known as ECC- 33 model, is suitable for suburban small urban areas and represented thus,

$$PL = PL_{fs} + PL_{bm} - G_b - G_m \quad 12$$

$$PL_{fs} = 92.4 + 20 \log_{10}(d) + 20 \log_{10}(f) \quad 13$$

$$PL_{bm} = 20.41 + 9.83 \log_{10}(d) + 7.894 \log_{10}(f) + 9.56(\log_{10}(f))^2 \quad 14$$

$$G_b = \log_{10}(h_b/200) \{13.98 + 5.8[\log_{10}(d)]^2\} \quad 15$$

$$G_m = [42.57 + 13.7 \log_{10}(f)][\log_{10}(h_m) - 0.585] \quad 16$$

Where,

$PL_{fs}$  is the free space path loss

$PL_{bm}$  is the basic median path loss

(3) (7)

### V. COST-231 PROPAGATION MODEL

This stands for Co-operative for Scientific and Technical research. It is an enhanced version of the Hata propagation model. That is, it employs suitable correction factors to improve the limitations of the Hata model.(1). Cost-231 model makes use of four variables in predicting propagation loss. The variables are Frequency, height of base station, height of receiver's antenna and distance between base station and receiver antenna (2).

The Cost hata Path loss equation is given by

$$PL(dB) = 46.3 + 33.9 \log(f_c) - 13.82 \log(h_b) - \alpha(h_m) + (44.9 - 6.55 \log(h_b)) \log_{10}(d) + c_M \quad 17$$

Where;

$c_M$  may be 0 for suburban city or 3 for metropolitan city (ogbulezie, et al., 2013)

## VI. LEE PROPAGATION MODEL

According to (3), this model predicts the pathloss in urban, suburban, rural and free space regions.

CASE 1:

$$\text{For Urban region} = 123.77 + 30.5 \log_{10}(d) + 10n \log_{10}(f/900) - \alpha_o \quad 18$$

CASE 2: for suburban region

$$PL = 99.86 + 38.4 \log_{10}(d) + 10n \log_{10}(f/900) - \alpha_o \quad 19$$

CASE 3: For Rural region

$$PL = 86.12 + 43.5 \log_{10}(d) + 10n \log_{10}(f/900) - \alpha_o \quad 20$$

CASE 4: For free space region

$$PL = 96.92 + 20 \log_{10}(d) + 10n \log_{10}(f/900) - \alpha_o \quad 21$$

Where n is an experimental value, say 3

$\alpha_o$  is the correction factor.

Hence;

$$\alpha_o = \alpha_1 + \alpha_2 + \alpha_3 + \alpha_4 + \alpha_5 \quad 22$$

Where;

$$\alpha_1 = (h_b/30.48)^2$$

$$\alpha_2 = (h_m/3)^k$$

$$\alpha_3 = (p_t/10)^2$$

$$\alpha_4 = (G_b/4)$$

$$\alpha_5 = G_m$$

Note k could be chosen to be 2

## VII. REGRESSION MODEL

Regression models are used to predict one variable from one or more other variables. (8). These models are very powerful tools that help scientists forecast about past, present or future activities through the use of information from past or present happenings. According to these authors, a regression model can be represented as shown in the equation below,

$$Y = b_o + b_1 \quad 23$$

$$b_1 = \frac{\sum (x_i - \bar{x})(y_i - \bar{y})}{\sum (x_i - \bar{x})^2} \quad 24$$

$$\begin{aligned} b_o &= \frac{1}{n} \left( \sum Y_i - b_1 \sum x_i \right) \\ &= \bar{y} - b_1 \bar{x} \end{aligned} \quad 25$$

Where;

Y is the dependent variable which is the attenuation represented as A

$x$  is the independent variable which is represented as  $D_d$

$b_o$  Is the intercept

$b_1$  is the slope calculated from equation (24) and (25).

In other words, equation (23) can be re-written as

$$A = b_o + b_1 D_d \quad 26$$

Where;  $D_d$  is the independent variable

Hence, equation (26) is used to calculate the empirical formular while equation (25) and (24) are used to determine the values of  $b_o$  and  $b_1$  in that order.

### VIII. LEAST SQUARE FORMULATION

According to (9), “Finer propagation models use partition- dependent attenuation factors, which assumes  $n=2$  free space path loss with additional path loss based on the objects that lie between the transmitter and receiver”. The author highlighted that for outdoor-to- indoor propagation environment, the object may consist of house exteriors, trees, wooded patches, plaster board walls, and so on. Then the path loss, for 1m free space at any given point, can be expressed by equation (27) below:

$$\text{Pathloss, } PL(d) = 20\log_{10}(d) + a \times x_a + b \times x_b + \dots \quad 27$$

Where;

$a, b, \dots$  are the quantities of each partition type between the receiver and transmitter.

$x_a, x_b, \dots$  are their respective attenuation values in dB. When the data at a known site is measured, the unknown in equation (27) are the individual attenuation factors  $X_a, X_b$  etc. One of the methods suggested for the computation of the attenuation factors is to reduce or minimize the mean- square error of measured versus predicted data.

In the words of the author, if  $P_i$  stands for the path loss with respect to 1m Free Space measured at the  $i$ th location, it then means that  $N$  number of measurement will give rise to the system of equation written:

$$P_1 = 20\log_{10}(d_1) + a_1 \times x_a + b_1 \times x_b \quad 28$$

$$P_2 = 20\log_{10}(d_2) + a_2 \times x_a + b_2 \times x_b \quad 29$$

$$P_N = 20\log_{10}(d_N) + a_N \times x_a + b_N \times x_b \quad 30$$

Putting this equation in a succinct form, that is using matrix notation.

$$\vec{A}\vec{x} = \vec{p} - 20\log_{10}(\vec{d}) \quad 31$$

Where;

$$\vec{p} = \begin{bmatrix} P_1 \\ P_2 \\ \vdots \\ P_N \end{bmatrix}$$

$$\vec{d} = \begin{bmatrix} d_1 \\ d_2 \\ \vdots \\ d_N \end{bmatrix}$$

$$\vec{x} = \begin{bmatrix} x_a \\ x_b \\ \vdots \\ x_z \end{bmatrix}$$

$$A = \begin{bmatrix} a_1 & b_1 \dots & z_1 \\ a_2 & b_2 \dots & z_2 \\ \vdots & \vdots & \vdots \\ a_N & b_N \dots & z_N \end{bmatrix} \quad 32$$

(9)

There are more measured points in  $P$  compared to the unknown in  $X$  in equation (31), hence, it cannot be solved immediately. Therefore, multiplying both sides of equation (31) by the transpose of  $A$  produces a tractable linear matrix equation.

$$A^T A \vec{x} = A^T [\vec{p} - 20\log_{10}(\vec{d})] \quad 33$$

This equation is termed the “normal equation”. Solving the normal equations - taking the proper precaution against ill- conditioned matrices simultaneously minimizes the mean square error with respect to all values in  $X$ . since these data represent large – scale path loss, which tends to a log – normal distribution, the mean –square error criterion, as well as mean and standard deviation comparisons are based on the dB values of path loss. (9) give the forecasts that match measurement with a non-zero mean and small standard deviation error.

### IX. PATHLOSS EXPONENT MODELS WITH AGGREGATE PENETRATION LOSS (APL)

“Adding penetration loss into the path loss exponent model increases its accuracy for outdoor –to- indoor propagation” (10). The method used in this model is to first estimate the strength of the signal received using

the outdoor in value. Following this is the addition of aggregate propagation loss (APL) to the outdoor result in order to obtain the indoor received power. The formula for this model is expressed in equation (34) below;

$$P_R = P_T + G_T + G_R + 20 \log_{10} \left[ \frac{1}{4\pi} \left( \frac{\lambda}{1m} \right) \right] - 10n_{out} \log \left( \frac{d}{1m} \right) - APL \quad 34$$

According to the authors, there is a difference between aggregate penetration loss and penetration loss of the partition - based model. Aggregate Penetration Loss (APL) stands for an average difference that exists between the indoor and outdoor path loss, not minding the location inside the house. It is worth to know that APL does not consider the particular number of wells or height above ground level. Also, the author defined partition based penetration loss as the difference in path loss between , two position or location that are positioned on the immediate inside and outside of the exterior wall.

## X. PARTITION-BASED OUTDOOR - INDOOR MODEL

(10) emphasized that pseudo deterministic methods do use the partition – based path loss model because the standard deviation (error) encountered in path loss by the use of exponent models for outdoor to indoor propagation could be enormous wide spread neighborhood use of a wireless network. The partition-based path loss model is expressed as equation (35) below;

$$P_R = P_T + G_T + G_R + 20 \log_{10} \left( \frac{\lambda}{4\pi d} \right) - \sum_{i=1}^N x_i \quad 35$$

$X_i$  is the value for attenuation of the  $i$ th obstruction that is intersected by the line drawn from the transmitter to the receiver point.

This outdoor obstruction could be a deciduous or coniferous tree, an area of terrain, a building and so on.

Also, the indoor obstruction is usually a wall. Partition-based- outdoor to indoor model can be extended to three dimensions by taking cognizance of the high and low blocking of trees.

These authors (10), revealed that the partition based outdoor-to-indoor model performs better when the transmitter-receiver (TR) separation is less than 50m and for more distant transmitters, once the surrounding area has just a few scatterers. When the number of the surrounding scatterers is on the high side, this result to the domination of multipath penetration which leads to the loss of physical significance of the partition-based model. This could happen, for instance, when the model try to forecast propagation through a building. One of the disadvantages of the partition-based model is that it requires a site-specific database with outdoor site characteristic and indoor floor plans. There is also the possibility that some of the application might require such a detail and extra accuracy, according to the authors.

## XI. CONCLUSION

Free space propagation model calculates pathloss in the absence of an obstacle during signal propagation. Based on field measurements, and plotted curve, the Hata model is used to calculate the Pathloss. In the SUI model, the height of the base station antenna varies between 10m to 80m while that of the receiver can be between 2m to 20m. The ECC-33 model extrapolates field measurements and amended its assumption to closely depict a fixed wireless access system. The Cost-231 model is an improvement on the Hata model by employing four variables to calculate pathloss

## References

- [1] Ubom, E. A, Idigo, V.E., Azubogu, A.C.O., Ohaneme, c.o., and Alumona, T.L. (2011). "Path loss Characterization of Wireless Propagation for South-South Region of Nigeria", International Journal of computer theory and Engineering, vol.3, N03.
- [2] Ayyapan, k. and dananyayan, p. (2014). PROPAGATION MODEL FOR HIGHWAY IN MOBILE COMMUNICATIONS JOURNAL, VOL. 3, N04.
- [3] Alsami, M.A, Arslan, T, Thompson, J. and Erdogan, A.T.(2011). Frequency Analysis of path loss models on wimax. Computer science and Electronic Engineering conference (CEEC).
- [4] Nwawelu, U.N., and Ahaneku, M.A.(2012). The Limitations of campus wireless Networks: A case study of university of Nigeria Nsukka (Lionet). International Journal of Networks and communication, 2(5);112-12
- [5] Rakesh, N. and Srivatsa, s.k.(2013). A STUDY ON PATH LOSS ANALYSIS FOR GSM MOBILE NETWORKS FOR URBAN, RURAL AND SUBURBAN REGIONS OF KARNATAKA STATE. International Journal of Distributed and parallel systems (IJDPS), vol.4, N01.
- [6] Jadhav, A.N and kale, s.s. (2014). Suburban Area pathloss propagation prediction and optimization using Hata model at 2375MHz. International Journal of Advanced Research in computer and communication Engineering, vol.3, issue 1.
- [7] Ogbulezie, J.C, onuu, M.U., Bassey, D.E and Etienam- Umoh, S. (2013). Site specific measurements and propagation models for GSM in three cities in northern Nigeria. American Journal of scientific and industrial Research.
- [8] Folaponmile, A and Sani, M.S. (2011). Empeirical model for the prediction of mobile radio cellular signal attenuation in harmattan weather. Information Technology Research Journal, vol 1(1)
- [9] Meng, Y.S, Lee, Y.H; and Ng, B.C (2009). STUDY OF PROPAGATION LOSS PREDICTION IN FOREST ENVIRONMENT. Progress in Electromagnetics Resaech B, vol. 17, pg 117-133.
- [10] Durgin, G., Rappaport, T.S and XU, H. (1998) Measurement and models for Radio pathloss and penetration loss in and Around Homes and Trees at 5.85GHz. IEEE Transaction on communications, vol.46, N011.

## Status and Perceptions of the Application of Building Information Modeling for Improved Building Projects Delivery in Nigeria

\*S.C Ugochukwu<sup>1</sup>, S.C Akabogu<sup>2</sup> and K.C Okolie<sup>3</sup>

<sup>1</sup>Department of Quantity Surveying, Nnamdi Azikiwe University, Awka, Anambra State, Nigeria.

<sup>2</sup>Works Department, Nnamdi Azikiwe University Teaching Hospital, Nnewi, Anambra State, Nigeria.

<sup>3</sup>Department of Building, Nnamdi Azikiwe University, Awka, Anambra State, Nigeria.

**ABSTRACT:** Building Information Modeling (BIM) is a new and innovative approach to building design, construction, and management. It is a cutting-edge, state of the art technology that is not only transforming, but improving the building delivery/production process in developed countries of the world. Sadly, Nigeria is yet to adopt this revolutionary technology in her construction industry. This study thus, sought to evaluate the present status of application of BIM in building projects in Nigeria, with a view to betoning its importance in improving the present state of building delivery in the country. This was effected by means of a field survey of building professionals in which their perceptions were analyzed, based on a structured questionnaire administration; in order to elicit their level of awareness of BIM application, determine their extent of participation in BIM projects, identify and rank the most suitable procurement method that encourages BIM application, the barriers to the application of BIM and the benefits of BIM application to building delivery in Nigeria. Results/Findings revealed that knowledge of BIM application among professionals is very poor (33%), participation/use of BIM in projects is non-existent, the collaborative method of procurement best supports BIM application, lack of awareness remains the major barrier to BIM application, while simultaneous access to project database by stakeholders is the highest ranked benefit of BIM application. The study concludes that Nigeria still has a long way to go in understanding, embracing and applying BIM to improve the traditional and stagnant state of her building delivery process. Hence, all hands should be on deck; the government, professional bodies, construction organizations and the academia to ensure that BIM becomes a priority with respect to legislations, training, research and use in the Nigerian building industry.

**Key Words:** Building Information Modeling, Building, Innovative technology, Nigeria, Project delivery.

### I. INTRODUCTION

The building construction industry has over the years witnessed revolutions in its production processes and operations [1] [2]. Building which is the core product of this industry floats in a stream of innovations, transformations and evolutions from its conception through its delivery (completion) processes. Building Information Modeling or BIM for short is one of these recent developments. According to [3], BIM is a new and innovative approach to building design, construction, and management that has changed the way industry professionals worldwide think about how technology can be applied to building design, construction, and management.

[4] surmises that the recent emergence of BIM constitutes one of the most exciting developments in building design, management, maintenance and operations. These advances have offered project teams a multi-sensory collaborative tools and opportunities for new communication structures. They have become powerful analysis and interdisciplinary decision-making tools [5], designed to represent and simulate existing or hypothetical buildings and settings. BIM thus, has far reaching consequences on building procurement [6].

BIM is a revolutionary technology and process that has quickly transformed the way buildings are conceived, designed, constructed and operated [7] [8]. The National Building Information Modeling Standards (NBIMS) committee of USA also defines BIM as follows: "BIM is a digital representation of physical and functional characteristics of a facility. A BIM is a shared knowledge resource for information about a facility forming a reliable basis for decisions during its life cycle; defined as existing from earliest conception to

demolition. A basic premise of BIM is collaboration by different stakeholders/professionals at different phases of the life cycle of a facility/Building to insert, extract, update or modify information in the BIM to support and reflect the roles of that stakeholder [9] [10].

[11] further reports that for each of the three major phases in the building life cycle—design, construction, and management—building information modeling offers access to the following critical information:

- Design phase - design, schedule, and budget information
- Construction phase - quality, schedule, and cost information
- Management phase - performance, utilization, and financial information.

The ability to keep this information up to date and accessible in an integrated digital environment gives architects, engineers, builders, and owners a clear overall vision of their projects, as well as the ability to make better decisions faster—raising the quality and increasing the profitability of projects (Building SMART, 2010). It supports the continuous and immediate availability of project design scope, schedule, and cost information that is high quality, reliable, integrated, and fully coordinated.

Several BIM tools are in existence [12][13][14]. Table 1 depicts some BIM authoring tools and their primary building functions. They include architectural, structural, electrical, mechanical and site work 3D modeling softwares. Some of these softwares are also capable of scheduling and cost estimation.

**Table 1:** BIM tools

Product Name	Manufacturer	Function
Cadpipe HVAC	AEC Design Group	3D HVAC Modeling
Revit Architecture	Autodesk	3D Architectural Modeling and parametric design.
AutoCAD Architecture	Autodesk	3D Architectural Modeling and parametric design.
Revit Structure	Autodesk	3D Structural Modeling and parametric design.
Revit MEP	Autodesk	3D Detailed MEP Modeling
AutoCAD MEP	Autodesk	3D MEP Modeling
AutoCAD Civil 3D	Autodesk	Site Development
Cadpipe Commercial Pipe	AEC Design Group	3D Pipe Modeling
DProfiler	Beck Technology	3D conceptual modeling with real time cost estimating.
Bentley BIM Suite (MicroStation, Bentley Architecture, Structural, Mechanical, Electrical, Generative Design)	Bentley Systems	3D Architectural, Structural, Mechanical, Electrical, and Generative Components Modeling
Fastrak	CSC (UK)	3D Structural Modeling
SDS/2	Design Data	3D Detailed Structural Modeling
Fabrication for AutoCAD MEP	East Coast CAD/CAM	3D Detailed MEP Modeling
Digital Project	Gehry Technologies	CATIA based BIM System for Architectural, Design, Engineering and Construction Modeling
Digital Project MEP	Gehry Technologies	MEP Design
Systems Routing	Graphisoft	3D Architectural Modeling
ArchiCAD	Graphisoft	3D MEP Modeling
MEP Modeler	Hydratec	3D Fire Sprinkler Design and Modeling
HydraCAD	M.E.P. CAD	3D Fire Sprinkler Design and Modeling
AutoSPRINK VR	M.E.P. CAD	3D Fire Sprinkler Design and Modeling
AutoSPRINK VR	Mc4 Software	Fire Piping Network Design and Modeling
FireCad	Mc4 Software	Fire Piping Network Design and Modeling
FireCad	Micro Application	3D Detailed MEP Modeling
CAD-Duct	Nemetschek	3D Architectural Modeling
Vectorworks Designer	QuickPen	3D Detailed MEP Modeling
Duct Designer 3D, Pipe Designer 3D	International	
RISA	RISA Technologies	Full suite of 2D and 3D Structural Design Applications
Tekla Structures	Tekla	3D Detailed Structural Modeling



Affinity Vico Office	Trelligence Vico Software	3D Model Application for early concept design 5D Modeling which can be used to generate cost and schedule data
Power Civil Site Design, Site Planning	Bentley Systems Eagle Point	Site Development Site Development

**Source:** Adopted from [15].

[16] submit that since its inception nearly 25 years ago, the presence of building information modeling (BIM) technology in Architecture/Engineering/Construction has revolutionized the way structures are built. From conception and design, to coordination and construction, the use of these intelligent computer imaging tools have opened avenues of communication and clarity previously unavailable to the industry [17] [18]. Though BIM technology systems have seen an increase in adoption and implementation in developed countries of the world, the ways in which these principles have been applied has remained stagnant in many developing countries, including Nigeria [19].

A 2010 study of BIM use on construction projects indicated that majority of surveyed participants used BIM for visualization, clash detection, and building design [20], relegating beneficial BIM capabilities to pre-construction and prefabrication activities with little to no regard for field applications. These limitations toward the use of BIM in the planning and completion of site work also mirrors a knowledge gap in the Nigerian building industry.

The Nigerian building industry is yet to fully embrace the adoption of BIM to enhance or improve her building projects delivery. [19]. In fact, the Nigerian building industry is notoriously conservative and slow to change. Her traditional procurement and building delivery methods have largely remained the same for decades.

Building construction is undoubtedly a team work. It has been acknowledged worldwide that the process of building an edifice is the collaborative responsibility of various professionals/stakeholders and integration of the various phases/stages of a project to offer best quality products. The traditional building design is largely reliant upon two-dimensional drawings (plans, elevations, sections etc.). This denies having a virtual information model of the building project from the design team (Architect, Engineers, Builders, Surveyors, etc); (where each professional adds discipline-specific data to the single shared model) to the main contractor and subcontractors and then on to the owner/operator. This scenario gives rise to loss of information which occurs when a new team takes ownership of the project. The present system of building process (traditional method) in Nigeria restricts communication to work in one direction only.

This research work seeks to proffer solution to the information-share, communication and collaboration problems among stakeholders/professionals across the various phases/stages (Design, Construction and Management) of building construction projects in Nigeria. The study is expected to provide effective tools for the Nigerian building industry to operate successively in this competitive economy. It will help to enhance collaboration and communication among stakeholders, ensure clarity, quality, facilitate take-offs and estimating, visualization of alternative solutions and options, reduce fabrication cost and errors. It will also aid in the decision process by providing a virtual playground through which project teams can test and evaluate multiple sequencing and scheduling alternatives for cost and/or feasibility of building production.

This study aims to evaluate the present status of application of BIM in building projects in Nigeria, with a view to betoning or emphasizing its importance, in order to improve the present state of building delivery in Nigeria. The following objectives are the premise for achieving this aim:

- i. To assess the level of awareness of Nigerian building professionals of the concept/application of BIM
- ii. To determine the extent of participation or use of BIM by Nigerian building professionals.
- iii. To identify and rank the most suitable building procurement method that encourages the application of BIM in Nigeria.
- iv. To identify and rank the barriers to the application/use of BIM for building delivery in Nigeria.
- v. To identify and rank the benefits of BIM application to building construction projects in Nigeria.

## II. METHODOLOGY

The study employed the survey design. According to [21], survey design is one in which group of people or items considered being representative of the entire group are studied by collecting and analyzing data from them. [22] asserts that describes survey research describes the situation as it is. It describes the characteristics, behaviours, attitudes and opinions of the population based on the data gathered from the sample. Similarly, [23] submits that the survey approach is concerned with a generalised result when data is abstracted from a particular sample or population.

For the study, a survey of expert opinion on major issues of concern with respect to the knowledge, use, application, benefits and barriers of BIM in Nigerian building projects was conducted. A well structured

questionnaire was designed and administered to building professionals: Architects, Engineers, Quantity Surveyors, Builders, Estate Surveyors and Town-Planners the survey was in construction companies/firms, ministries and parastatals within Anambra and Enugu states of Nigeria who have a good network, base of operation and solid reputations in execution of building projects throughout the country. They were selected by means of a simple random sampling.

A total number of one hundred and fifty five (155) copies of the questionnaire were distributed out of which one hundred and thirty five (135) representing 87.1% were duly completed and returned (*see table 2*). A total of twenty (20) copies were either not returned or were inadequate for analysis.

**Table 2:** Respondents (professionals) composition and questionnaire response

Professional affiliation	Number of copies of questionnaire administered	Number returned	Number not returned
Architects	45	38	7
Engineers	60	52	8
Builders	25	24	1
Quantity Surveyors	12	9	3
Estate Surveyors	5	5	0
Town planners	8	7	1
<b>Total</b>	<b>155</b>	<b>135</b>	<b>20</b>

## 2.1 Data Analysis Procedure

The data collected was analysed using the mean score method and ranking, a descriptive statistical tool. Some of the questions in the questionnaire involved assessing some issues or indices of BIM application on a four (4) point Likert's scale. Some responses were also presented in frequency and expressed in simple percentages.

The mean score for each factor is calculated by summing up the scores assigned to it by respondents and then, the rank for each factor is assigned. It is computed using the following equation:

$$(1) \quad MS = \frac{\sum_{i=1}^4 a_i \cdot n_i}{\sum_{j=1}^N x_j} \times 100$$

Where  $x_j$  = sum of the  $j$ th factor;  $j$  = the factors 1,2,3,4,...,N;  $N$  = total number of factors or issues examined;  $a_i$  = constant expressing the weight given to the  $i$ th response:  $i = 1, 2, 3, 4$

for a response of 'strongly agreed'

$$a_1 = 4$$

for a response of 'agreed'

$$a_2 = 3$$

for a response of 'disagreed'

$$a_3 = 2$$

for a response of 'strongly disagreed'

$$a_4 = 1$$

$n_i$  = the variable expressing the frequency of the  $i$ th response,  $n_1$  = the frequency of 'very high' response,  $n_2$  = the frequency of 'high' response,  $n_3$  = the frequency of 'medium' response,  $n_4$  = the frequency of 'low' response.

### III. DATA PRESENTATION AND ANALYSIS

#### 3.1 Awareness of Nigerian building professionals of the concept/application of BIM

Table 3 shows the responses of building professionals with respect to their awareness of the existence of BIM.

**Table 3:** Level of awareness of Nigerian building professionals of BIM

Response	Frequency	Percentage
Yes	91	67%
No	44	33%
<b>Total</b>	<b>135</b>	<b>100%</b>

From table 3, 91 respondents representing 67% of the total respondents know about BIM while 44 respondents representing 33% of the total respondents don't know or have never heard of BIM.

#### 3.2 Participation of Nigerian building professionals in BIM

Table 4 shows the responses of building professionals with respect to the extent of their participation or involvement in BIM projects.

**Table 4:** Extent of participation/use of BIM by building professionals in Nigeria.

Response	Frequency	Percentage
Yes	0	0%
No	135	100%
<b>Total</b>	<b>135</b>	<b>100%</b>

As shown in table 4, none of the respondents have participated in a building project in Nigeria where BIM was applied.

#### 3.3 Procurement methods that best promote the application of BIM in Nigeria.

Table 5 shows the opinions and ranking of Nigerian building professionals with respect to the type of procurement that best encourages the use of BIM.

**Table 5:** Ranking of the procurement methods that promote /accommodate the application of BIM in Nigeria.

S/N	Procurement methods	SA 4	A 3	D 2	SD 1	Mean score	Rank
1	Collaborative(relational)	86	42	7	0	3.59	1
2	Management (Packaged)	65	58	12	0	3.39	2
3	Design and construct (Integrated)	25	52	47	11	2.67	3
4	Traditional (Separated)	0	15	85	35	1.85	4

From table 5 above, the traditional method of procurement ranked below 2.50 and was the least in the rank, which means the respondents disagreed that this method promotes the application of BIM while the rest methods ranked well above 2.5 which means that the respondents are in agreement that these methods promote the application of BIM. However, the number one ranked variable was collaborative procurement methods.

#### 3.4 Barriers to the application of BIM in the building delivery process in Nigeria.

**Table 6:** Ranking of the barriers to the application or use of BIM in building delivery in Nigeria.

S/N	Barriers	SA 4	A 3	D 2	SD 1	Mean score	Rank
1	Lack of awareness of BIM among stakeholders	90	45	0	0	3.67	1
2	Frequent power failure and poor internet connectivity	61	72	2	0	3.44	2
3	Lack of skilled BIM trained staff	78	30	26	1	3.37	3
4	Lack of industrial standards	64	58	10	3	3.36	4
5	Cost of training and high cost of software	42	65	21	7	3.05	5

6	Lack of clients demand of BIM in their projects	35	54	20	26	2.73	6
7	Lack of new amended condition of contract and procurement method	26	40	62	7	2.63	7

From table 6, all the variables (barriers) tested ranked well above 2.50. This is corroboration to the fact that the respondents are in agreement with all the listed variables. However, the number one ranked variable was lack of awareness of BIM among the stakeholders while the least ranked variable was lack of new amended condition of contract and procurement method.

### 3.5 Benefits of the application of BIM to the building delivery process in Nigeria.

**Table 7:** Ranking of the benefits of BIM application to building delivery in Nigeria.

S/N	Benefits	SA	A	D	SD	Mean score	Rank
1	Simultaneous access to project database by all stakeholders.	125	10	0	0	3.93	1
2	Project visualization	123	12	0	0	3.91	2
3	Robust information	121	14	0	0	3.90	3
4	Quality communication	112	23	0	0	3.83	4
5	Project documentation	96	32	5	2	3.64	5
6	Clash detection	71	54	10	0	3.45	6
7	Multi-dimensional integration	75	41	12	7	3.36	7
8	Digital facilities management	64	55	10	6	3.31	8
9	Auto-quantification	52	68	9	6	3.23	9
10	Time and cost reduction	45	36	39	15	2.82	10

From table 7, all the variables (benefits) tested, ranked well above 2.50. This means that the respondents are in agreement with all the listed variables. However, the number one ranked variable was simultaneous access to project database by all stakeholders while the least ranked variable was time and cost reduction.

## IV. CONCLUSION AND RECOMMENDATIONS

### 4.1 Conclusion

There is no gainsaying the fact that the benefits of applying BIM to the building delivery process are innumerable. Sadly, the Nigerian building industry is yet to fully acknowledge, embrace and adopt this new technology. Application of BIM as an information system in the building construction industry is really a reengineering factor to the sub-sector. Improved profitability in the building construction business and more successful delivery of projects to clients are benefits of applying BIM in the industry. The factors responsible for late delivery of projects, overruns cost estimate, risk management, safety and even compromise in quality are grossly taken care of by the application of BIM. The management of construction industry is also in a better position with BIM.

BIM approach to project design and construction simplifies workers jobs. The application of BIM is very suitable and useful for all sizes and types of construction projects; simple or complex, small or big construction projects. From the design stage to the completion, BIM provides smooth flow of information with effective organizational and control structures within the project construction team and the management of the facility through the life cycle of the facility. The application of BIM is economical and easy. It is a solution to some of the problems facing the industry and thus, leading to improvement, enhanced technical and general management of construction projects and addressing some strategic issues in the sector. The total control of cost estimates, prompt delivery of projects and quality are the most important key performance indicators in construction.

The use of BIM in the construction industry results to; clients' satisfaction, zero defects in projects, predictability in terms of cost and time of projects, productivity and efficiency. Presently, construction industries using the BIM have experienced improved performance and are achieving higher goals in benchmarking and realizing their best practices. No doubt that BIM can now be considered and adopted as another dimension to the overall contributory agenda aimed at modernizing project construction by re-engineering the industry. It is therefore pertinent to emphasize, that by applying BIM in Nigerian construction industry, successful projects implementation and delivery will be assured.

#### 4.2 Recommendations

Based on the foregoing findings of the study, the following corrective propositions are advanced:

- The federal government of Nigeria through the legislative arm should enact laws, making the application of BIM in building projects a necessity. There should be proof of a company's competency in using BIM during the bidding process in order to qualify for tendering and award for any building contract.
- Professional bodies such as the Nigerian Institute of Quantity Surveyors(NIQS), Nigerian Institute of Building(NIOB), Nigerian Institute of Architects(NIA) and the Nigerian Society of Engineers(NSE), that are vested with the responsibilities of overseeing the activities of professionals and building construction works in Nigeria all have major roles to play. They should make BIM a priority to all professionals to learn and put to use.
- Construction companies in Nigeria should embark on training and re- training of their staff so that new skills and construction methods like BIM and virtual reality can be acquired to impact positively on the construction industry at large.
- Construction companies and relevant government agencies and parastatals in Nigeria should procure all necessary software for BIM and virtual reality to facilitate the learning and use of BIM for application in construction projects in the country.
- Research study should be routinely conducted by academics or concerned individuals and organizations to establish the extent to which BIM is known and applied in building projects in Nigeria.

#### REFERENCES

- [1] J. Egan, *Rethinking Construction* (London, UK: CIB, 1998).
- [2] J. Egan, *Accelerating Change: Strategic forum for construction* (London, UK: CIB, 2002).
- [3] S. Azhar, Building Information Modeling: Trends, benefits, risks and challenges, *ASCE Journal of Leadership and Management in Engineering*, 11 (3), 2011, 241-252.
- [4] Y. Ayarici, F. Khosrowshahi, A.M. Ponting, and S. Mihindu, (2009). Towards implementation of Building Information Modeling in the construction industry. *Proc. Fifth International Conference on Construction in the 21st Century (CITC-V)-Collaboration and Integration in Engineering, Management and Technology*. May 20-22, Istanbul, Turkey, 2009.
- [5] S. Fox, and J. Hietanen, Interorganizational use of building information models: potential for automation, informational and transformational effects, *Construction Management and Economics*, 25(3), 2007, 289-296.
- [6] S. Azhar, W. A. Carlton, D. Olsen, and I. Ahmad, Building Information Modeling for sustainable design, *Journal of Automation in Construction* (Special issue on Building Information Modeling and changing construction practices), 20 (2), 2011, 217-224.
- [7] B. Hardin, *Building Information Modeling and Construction Management* (Indianapolis: Wiley Publishing, 2009).
- [8] H. Yah, and P. Damian, Benefits and barriers of Building Information Modelling. *Proc. 12th International Conference on Computing in Civil and Building Engineering*, Beijing, China, 2008.
- [9] D. A. Harris, *National Building Information Modeling Standard*. (1st ed., 2007).<http://www.buildingsmartalliance.org/index.php/nbims>.
- [10] NBIMS, *National Building Information Modeling Standard*, 2010. [http://www.wbdg.org/pdfs/NBIMSV1\\_p1.pdf](http://www.wbdg.org/pdfs/NBIMSV1_p1.pdf)
- [11] N. M. Aziz, and H. Salleh, A readiness model for IT investment in the construction Industry, *African Journal of Business Management*, 5 (7), 2011, 2524-2530.
- [12] G. Elvin, *Tablet and wearable computers for integrated Design and construction*, 2003.<http://www.comitproject.org.uk>
- [13] G. Elvin, *Integrated practice in architecture: mastering design-build, fast-track, and Building Information Modeling* (N.J, USA: John Wiley & Sons, 2007).
- [14] W. Kymmell, *Building Information Modeling: Planning and managing projects with 4D CAD and simulations* (USA: McGraw Hill, 2008).
- [15] Autodesk, *Improving building industry results through integrated project delivery and Building Information Modeling*, 2008. [http://images.autodesk.com/adsk/files/bim\\_and\\_ipd\\_whitepaper.pdf](http://images.autodesk.com/adsk/files/bim_and_ipd_whitepaper.pdf)
- [16] G. Van-Nederveen, and F. Tolman, Modelling multiple views on buildings, *Automation in Construction*, 1-3, 1992, 215-224.
- [17] C. M. Eastman, *Building product models: Computer environments, supporting design and construction* (Boca Raton: CRC Press, 1999).
- [18] R. Howard, *Computing in construction: Pioneers and the future* (Woburn, Massachussets, USA: Butterworth-Heinemann, 2008).
- [19] S. Ibrahim, and I. M. Bishir, Review of the use of Building Information Modeling (BIM) in the Nigerian Construction Industry, *Journal of Environmental Sciences and Policy Evaluation*, 2 (2), 2012, 18 – 26.
- [20] D.K. Smith, and M.Tardif, *Building Information Modeling: A strategic implementation guide for Architects, Engineers, Constructors, and Real Estate asset managers* (NJ, USA: John Wiley and Sons, 2009).
- [21] B.G. Nwogu, *Educational research: Basic issues and methodology* (Ibadan, Nigeria: Wisdom Publishers Ltd, 1991).
- [22] J.C. Nnadozie, *Research method in education* (Awka, Nigeria: Nnamdi Azikiwe University, 1989).
- [23] S.G. Naoum, *Dissertation research for construction students* (2nd ed., London: Butterworth-Heinemann, 2007).